UNIVERSITY OF CAPE TOWN
IYUNIVESITHI YASEKAPA • UNIVERSITEIT VAN KAAPSTAD

FUTURE WATER

Concentrating human urine by evaporation

Department of Civil Engineering
University of Cape Town
March 2021

Dissertation submitted in fulfillment of the requirements for the degree

MSc Civil Engineering

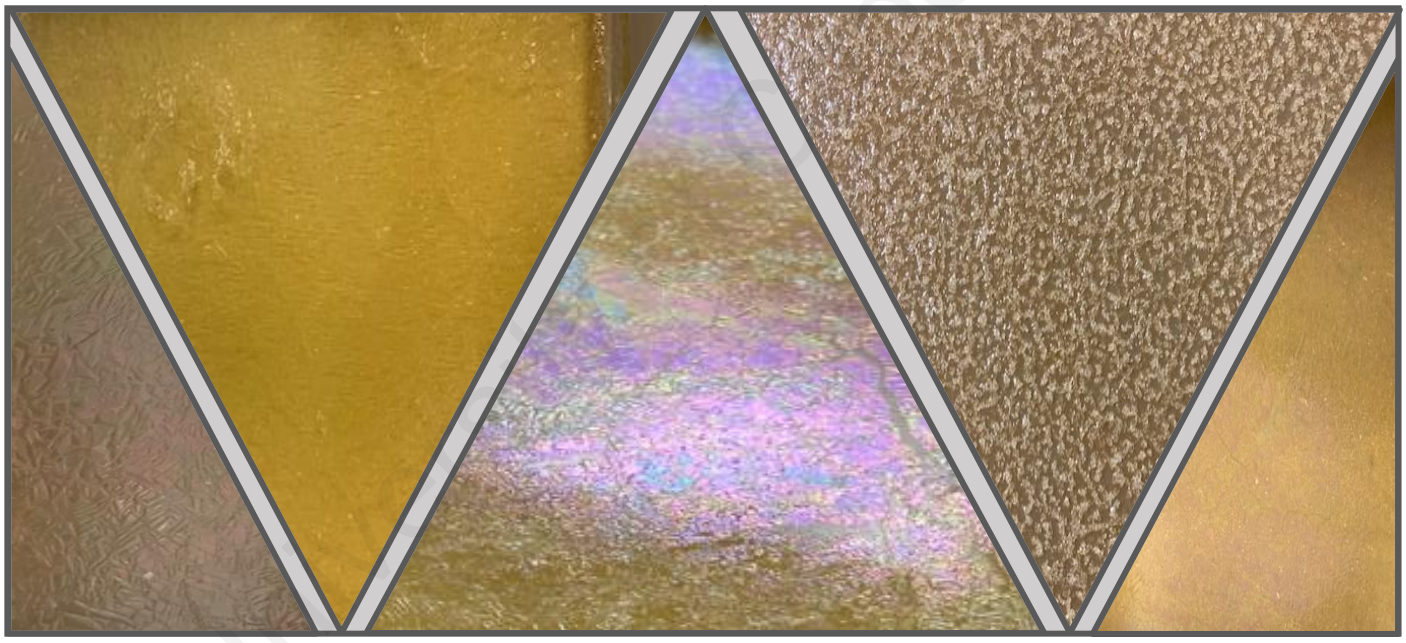

Prepared by:
Amy Hislop

Supervised by:
Dr Dyllon Randall

Plagiarism Declaration

I know that plagiarism is wrong. Plagiarism is to use another's work and pretend that it is one's own.

I have used the Harvard convention for citation and referencing. Each contribution to, and quotation in, this dissertation from the work(s) of other people has been attributed, and has been cited and referenced.

This dissertation is my own work.

I have not allowed, and will not allow, anyone to copy my work with the intention of passing it off as his or her own work.

Signature HSLAMY001

Date 2021/02/11

Acknowledgements

Through completing this thesis, many individuals were involved throughout the process and contributed towards the final deliverable. It was a pleasure to meet and work with each individual and the extra help, input and encouragement was greatly appreciated and never went unnoticed. I would like to mention and thank some of the many people involved in the process of completing this dissertation.

Firstly, to the entire Water Quality Team, **Caitlin Courtney, Daniel de Oliveria, Hlumelo Marepula, Mwana Mwane, Rhonda Hyde, Tarie Mufunde and Vuhkheta Mukhari**. It was a pleasure to be surrounded by such an enthusiastic group of young people. I am sure that each of you have a bright and exciting future waiting for you and that you will go out and have a positive influence on the world around us.

To **Njabulo Thela**, thank you for looking after all of the students working in the laboratory and making sure that we have the chemicals and equipment as needed. Thank you for always listening to queries, helping with setting up equipment and answering questions. Thank you to **Hector Mafungwa**, for being in the laboratory for assistance and showing me around when I was lost or needed any assistance.

To **Dr. Nico Fischer** from the catalysis department. I am extremely grateful for your help, input and time that was put into the XRD analysis for this dissertation. Thank you for having good advice, discussing results in a way that was understandable and also being proactive when running into problems with the analysis.

To **Jared** and **Tim** from Apex Scientific, although there were times when it did not seem, I am grateful for all that you did to make sure that the equipment in the laboratory was fixed and working as it should be. Thank you for keeping me updated and trying your best to repair the chamber as quickly as possible.

I would also like to thank my family for their patience during lockdown when I was working on my dissertation from home. I am also grateful that they have supported my decision to study further and been encouraging throughout.

Lastly, thank you to my supervisor **Dr. Dyllon Randall** for all his time and input into this dissertation. Thank you for motivating me and remaining positive and proactive when things seemed tough. Thank you for the continuous and rapid feedback on any work submitted. I am extremely grateful to have been a part of your research group in the Water Quality laboratory and to have been exposed to exciting aspects of your ongoing research. Despite the climate created by the COVID-19 pandemic, thank you for still coming onto campus to monitor my progress and have discussions when needed.

Synopsis

The current size of the global population was estimated to be 7.7 billion people in 2019. This is expected to increase to 9.7 billion people by the year 2030. To supply sufficient food for this growing population, the use of synthetic fertilizers has become a widely adopted agricultural practice. These fertilizers, rich in nitrogen, phosphorus and potassium (NPK) nutrients, ensure rapid and adequate food supply. However, the use of synthetic fertilizers is not sustainable. This is due to nitrogen (N) being derived from synthetic ammonia (NH_3) produced via the energy intensive Haber-Bosch process. The phosphorus (P) in synthetic fertilizer is also mined from non-renewable phosphate rock.

Similarly, a large population size leads to the inevitable generation of waste effluents collectively known as wastewater. Currently, wastewater is transported to and treated in traditional wastewater treatment facilities to ensure that nutrients in the wastewater are removed. This ensures that when the treatment plant effluent is released back into bodies of natural water, these bodies of water are not polluted. However, the cost associated with the treatment of wastewater and the maintenance of such facilities is high. As a result, less affluent countries have not been able to adequately maintain wastewater treatment facilities.

One component of the wastewater that is treated in such facilities includes black water. This contains urine, faeces and other excreta that are flushed down the toilet. Although human urine contributes approximately 1% by volume, to the total wastewater generated, this urine contains approximately 80%, 56% and 63% of the total N, P and K found in domestic wastewater, respectively.

In addition, traditionally black water is flushed down a toilet and enters the wastewater system, but a large portion of the global population do not have access to flushing toilets and clean drinking water. Furthermore, traditional flushing toilets use significant amounts of clean water, which in water scarce regions is a waste of an otherwise precious resource. These two ideas combined drives the need to rethink the current sanitation and wastewater practices. Rethinking current sanitation and traditional wastewater treatment practices encompasses a more wholistic approach towards achieving global sustainability – this approach considers resource recovery and reuse.

As urine is rich in the same NPK nutrients required in synthetic fertilizers, it has been proposed to separate and collect this urine through source separating toilets, and more recently, waterless urinals. Before re-use, the urine should be treated and turned into a urine-based fertilizers or other products. The nutrients contained in the collected urine can be recycled back into the environment while simultaneously reducing the need for synthetic fertilizers.

Separating urine from wastewater also lowers the N and P concentration entering the traditional wastewater treatment plants. This results in a wastewater stream that has a more favorable C:N:P nutrient ratio for conventional wastewater treatment. This lowers the volume requirement of the wastewater treatment plant, allowing for treatment with a relatively short sludge age. A shortened sludge age corresponds to a smaller requirement in plant volume, with lowered infrastructure and associated maintenance costs on the treatment plant.

The use of waterless urinals not only allows for the removal of urine from wastewater, but also minimizes the clean water traditionally used when flushing urinals. From previous studies, it was shown 11 g of solid fertilizer could be harvested from 1 kg of urine collected in the urinal.

The literature showed a diverse range of urine treatment and concentration options with evaporation being the most common. The experiments conducted in previous literature differed to the experiments in this thesis due to the chosen operating conditions (pH, temperature, humidity etc.) as well as the type of urine studied (fresh, hydrolyzed and stabilized). Furthermore, few studies focused on maximising the recovering of all key nutrients (N, P and K). Therefore, this study aimed to investigate these aspects through experiments and simulations.

The purpose of this dissertation was to further understand the fertilizer produced from human urine. More specifically, this dissertation aimed to experimentally determine the urine stabilization technique that gave the highest N, P and K nutrient recoveries at a water removal interval of 100%. This dissertation also aimed to determine the effect of water removal on the solids formed when using the preferred urine stabilization method of calcium hydroxide dosing. From this, a comparison between experimental and theoretical results was presented.

It was also desired to use theoretical simulations to determine the influence of urine composition on the preferred stabilization process and similarly, the influence of temperature on the preferred stabilization process. The final aim of this dissertation was to determine the energy consumed when evaporating water from urine stabilized through the preferred stabilization process.

To further study the solid fertilizer produced from human urine, a series of experiments and simulations were conducted. Firstly, six synthetic urine solutions and three real urine solutions, each stabilized using different treatment techniques, were evaporated. The success of each stabilization treatment was assessed in terms of the measured NPK recovery in the urine solution. Once the preferred urine stabilization method was chosen from the NPK experiments, this urine stabilization method was used when evaporating urine solutions. Urine solutions were evaporated to water removals of 50%, 75% and 100% respectively. At each water removal percentage, the total mass of solids formed was measured, as well as the N, P and K concentrations in these resulting solids. Experimental results were compared to the theoretical results which were obtained from thermodynamic simulations.

A further comparison was drawn by comparing the evaporation of synthetic and real $Ca(OH)_2$ stabilized urine solutions. $Ca(OH)_2$ stabilized synthetic urine solutions included both a solution with excess (unfiltered) $Ca(OH)_2$ as well as a filtered synthetic urine solution. The reason an excess Ca(OH)2 stabilized synthetic urine solution was included in the comparison was to compare the influence of excess $Ca(OH)_2$ on the pH of the urine solution. Thermodynamic simulations predicted that a urine solution with excess $Ca(OH)_2$ was predicted to have a greater buffering capacity against CO_2 compared to a filtered urine solution. A comparison was also drawn between the three urine solutions by studying the mass of remaining solution over time, as well as the scale formed in the synthetic and real urine solutions.

A final experimental aspect considered urea hydrolysis in solution between temperatures of 40°C to 70°C, at a relative humidity of 40%. Urea solutions were evaporated at different temperature conditions in a climate chamber to determine the extent of urea hydrolysis . These experiments were evaporated for 95 hours. Urea hydrolysis experiments were repeated at 40°C and 70°C. However, these experiments were stopped once 100% of the water was removed from solution, shortening the evaporation time to 53 hours for the 70°C experimental run.

Using a fixed urine composition, additional thermodynamic simulations were run. One set of simulations varied evaporation temperature and the second set of simulations varied stabilized urine composition by introducing four additional stabilized urine streams. From the simulated results, the total mass of solids as well as the mass of NPK solids were used to determine the influence of temperature and composition on the chosen stabilized urine solution.

The results from the thermodynamic simulations were further processed using a basic mass and energy balance to develop a first estimate of the energy input associated with the evaporation process. This estimate was done independently for both varied temperature and varied composition conditions.

From the experimental procedure, it was determined that $Ca(OH)_2$ stabilized human urine was the preferred urine stabilization treatment as this urine solution had a nitrogen recovery of 109%. As P and K components of each urine solution were non-volatile, the preferred urine stabilized treatment was chosen by considering the solution with the highest N recovery. Although acetic acid and citric acid stabilized synthetic urine solutions has N recoveries of 103% and 93.5% respectively, it was decided that stabilizing with $Ca(OH)_2$ power is a better stabilization method. This decision was made considering the precise dosing required when acidifying urine. This method would require additional equipment such as a dosing pump, compared to $Ca(OH)_2$ stabilization which requires no dosing equipment. Urine stabilization with $Ca(OH)_2$ required only the pre-addition of sufficient $Ca(OH)_2$ powder to the urine solution.

Using $Ca(OH)_2$ stabilized synthetic urine, simulations were compared to experimental results at 50%, 75% and 100% water removal. It was found that the simulations did not compare well with experimental results. A total of 18.8 g of solids were predicted to form at 100% water removal. Experimentally 22 g solids were formed. Additionally, at 75% water removal a peak in N, P and K recovery was experimentally observed but this was not observed in the simulation results.

Reasons for this deviation include the loss of ammonia to the atmosphere due to ammonia volatilization, which were not accounted for in thermodynamic simulations. The loss of urea due to urea hydrolysis was also not accounted for in OLI where experimentally 8.12% urea loss was observed at 70°C.

When considering the influence of temperature on the solids formed in $Ca(OH)_2$ stabilized urine, the simulations showed a decrease in solids with an increase in temperature. Furthermore, a change in urine composition showed that the mass of solids that formed

depended on whether the quantity of ions that are present in major salts, increased or decreased in solution.

Lastly, when using the simulation results to determine the input energy requirement associated with the process, it was seen that the overall input energy requirement increases with an increase in evaporating temperature. However, a changing urine composition did not have a significant effect on the overall energy input. When costing this energy requirement, a urine-based fertilizer could be produced via the evaporation process at a cost of 0.63 R kg^{-1}. When compared to available synthetic fertilizers, which are sold for between 13.17 and 24.53 R kg^{-1}, there appears to be a good business case for urine-based fertilizer production.

Considering the information presented in this dissertation, it was recommended that future work consider investigating the rate of urea hydrolysis at further different operating temperatures and evaporation rates. Additionally, when considering $Ca(OH)_2$ stabilized synthetic and real urine, $Ca(OH)_2$ stabilized synthetic urine was a good proxy to $Ca(OH)_2$ stabilized real urine. However, there were slight discrepancies, especially in terms of evaporation rates. Therefore, it is recommended that all the different stabilization methods used in this dissertation that were based on synthetic urine, be tested also with real urine.

It was also recommended that the thermodynamic simulations account for urea hydrolysis, NH_3 volatilization and the formation of $CaCO_3$ during evaporation in future work. Finally, it was recommended that the solid fertilizer formed after complete water removal by evaporation be tested to determine its applicability to growing different crops, as well as to determine how this fertilizer compares to commercial and synthetic fertilizers.

Table of Contents

List of Figures

List of Tables

Glossary

Term	Definition
Acidification	Lowering the pH of a substance below a pH of 6, by adding acid
Amorphous	Non-crystalline solid, lacking crystal structure
Biomass	Organic material, material that is derived from living organisms such as animals or plants
Contamination	Presence of an impurity that may be harmful or unwanted
Convective evaporation	Evaporation occurring due to the bulk movement of surrounding air, can be due to the presence of a fan
Dosing	Feeding or adding a chemical in a small quantity
Enthalpy	Property of a thermodynamic system, sum of the internal energy of the system and the product of the system's pressure and volume
Eutrophication	Plant growth stimulated by excess nitrogen and phosphorus in a body of water, leading to the depletion of dissolved oxygen
Haber-Bosch	Artificial nitrogen fixation process to produce ammonia
Microbial community	Groups of microorganisms sharing a common living space and interacting in different ways
Micronizing mill	A crushing device used to crush and reduce the average diameter of solid particles in a sample
Ore grade	Indicator of quality and mineral content of ore
Passive evaporation	Evaporation that occurs alone without the aid of moving air or an external energy source being provided
Photo spectrometry	Using transmission of light and wavelengths that are specific to materials, as a means to quantitatively measured that material
Preferred orientation	Stronger tendency for the crystals in a solid or powder to be positioned in a certain lattice structure
Relative humidity	Moisture content of the atmosphere. Expressed as a percentage that can be retained by the atmosphere
Solute	Solid dissolved in liquid medium (solvent)
Speciation	Distribution of a chemical species between different forms
Stabilization	Process to prevent urea hydrolysis. pH can be raised above pH 11 or lowered below pH 4 to ensure that urine has been stabilized
Ureolysis	Breakdown of urea into ammonia and carbonate ions
Waste valorization	Industrial process to reclaim value from waste streams

Nomenclature

Abbreviation/Symbol	Meaning
$	Dollar
CFA	Central African Frank
COD	Chemical oxygen demand
EFC	Eutectic freeze crystallization
kWh	Measure of energy (kW per h)
NPK	Nitrogen, phosphorus and potassium nutrients
OLI	Name of wastewater software used in simulation procedures in this thesis
PHREEQC	pH redox equilibrium (C++ language)
R	Rand
SAICE	South African Institution of Civil Engineers
TKN	Total Kjeldahl Nitrogen
TOC	Total Organic Carbon
TSG	ThermoScientific Gallery
USGS	United States Geological Survey
WW	Wastewater
WWTP	Wastewater treatment
XRD	X-Ray Diffraction

Chapter 1. Introduction

Marin Brown, a sustainability consultant at Fairsnape, expressed the importance of rethinking wastewater to ensure long-term sustainability. This would require one to consider decentralizing wastewater assets, emphasizing the value of resources in our wastewater, as well as turning to new technologies to help change current systems (McClelland, 2017). Rethinking wastewater in terms of resource recovery, and decentralizing wastewater assets through source separating toilets, provides the backbone for the research conducted throughout this dissertation.

1.1 Research background

Daily activities such as industry and agriculture, lead to the inevitable generation of various types of wastewater. This not only contains the effluent from agricultural or industrial activities, but may also contain effluent from commercial activities such hospitals and businesses, diverted storm water as well as domestic effluent (UN-water, 2017). Domestic effluent is created through the generation of a variety of household waste streams. Examples of such are greywater and blackwater. Greywater consists of the effluent from the kitchen sink, bath and shower, while blackwater contains the effluent from flushing toilets which includes human faeces, urine and any other excreta (Corcoran, 2010).

When addressing the generation and treatment of blackwater, it is important to note the contribution of human urine to the nutrient load of domestic wastewater. Human urine contributes approximately 1% of the volume of domestic wastewater (Höglund, 2001). Although this may seem insignificant, this volume of 1% contains roughly 80%, 5 % and 63% of the total nitrogen (N), phosphorus (P) and potassium (K) found in domestic wastewater respectively (Höglund, 2001). Thus, the majority of these important nutrients in wastewater are derived from human urine.

Waste streams need to be treated to remove these nutrients to comply with strict legislation regarding the quality of wastewater effluent discharges (Randall and Naidoo, 2018). There is stringent legislation especially in terms of P concentration, not only in South Africa but globally (Randall and Naidoo, 2018). In South Africa the phosphate discharge legislation is 10 mg L^{-1} for general phosphate emissions (Sikosana et al., 2017). This stringent legislation is vital to prevent the pollution of bodies of water caused by excessive nutrient loads through a process known as eutrophication (Samer, 2015). When released, an excess of key nutrients, mainly N and P present in wastewater, promote the excessive growth of algal and photosynthetic biomass in bodies of water. This is known as eutrophication. The composition of the existing biological community within the body of water is altered through the process eutrophication as this additional nutrient-stimulated plant growth depletes dissolved oxygen present in the water. This plant growth also limits solar energy penetrating the body of water (Glibert, 2012).

To prevent the process of eutrophication, wastewater needs to be treated to ensure safe effluent quality before discharge to the surrounding environment. When treating wastewater, it needs to be collected and transported via piping networks, to wastewater treatment plants. The purpose of these treatment plants is to achieve the targeted removal of key nutrients, in particular N, P and chemical oxygen demand (Randall and Naidoo, 2018)

contained in wastewaters to reach safe effluent discharge quality. This effluent should have a lowered nutrient content, thus preventing the unwanted release of these nutrients into the ecosystem.

Because it is vital to preserve water quality in the environment, wastewater needs to be treated in such a manner that prevents the discharge of these key nutrients which would pollute the natural environment. In a South African context, the National Government is responsible for ensuring that aquatic environments and sources of water, are protected at a nationwide level against this form of pollution (Toxopeus, 2017). This responsibility is performed through the implementation of local municipalities. It is their role to provide sanitation services and infrastructure for wastewater removal and treatment, to local communities throughout South Africa. Through the implementation of this infrastructure, waste such as human excreta, can be transported to treatment facilities whereby it is treated in a contained system to prevent harmful release to the environment (Toxopeus, 2017).

Although significant wastewater infrastructure has been built in the 21st century, not only South Africa, but the world, has been challenged with a water quality crisis (UN-water, 2017). This crisis stems from a population which is increasing in size. This growing population corresponds to increased commercial and industrial activities, the increased release of household effluents as well as an increasing demand for food production (UN-water, 2017). To promote crop growth to ensure adequate food production, the agricultural sector turned to the use of synthetic fertilizers (Randall et al., 2016).

Crop growth is promoted by providing the necessary NPK nutrients required to enhance plant growth. To do so, synthetic ammonia (NH_3) is used to create nitrogen rich synthetic fertilizers (Randall et al., 2016). This synthetic ammonia made is via the energy intensive Haber- Bosch process. The Haber-Bosch process used for fertilizer production is responsible for approximately 1-2% of the world's global energy consumption (Kyriakou et al., 2020).

This process also generates approximately 1.44% of the global carbon dioxide (CO_2) emissions (Kyriakou et al., 2020). Further environmental pollution is caused due to the runoff associated with the use of synthetic fertilizers. This not only introduces excess nitrogen into the environment, but also corresponds to a loss in applied nitrogen. This needs to be compensated for by applying additional fertilizer, which has an additional cost implication (Randall et al., 2016).

Beyond the process of eutrophication, the above-mentioned water quality crisis has been further emphasized through the observed deterioration in natural water quality (Edokpayi et al., 2017; UN-water, 2017). This deterioration is not due to a failure of the current wastewater treatment systems, but rather due to the high cost and capacity relationship associated with this conventional treatment option and infrastructure required for wastewater treatment (Randall et al., 2016; UN-water, 2017).

The capacity of treatment facilities is dependent on a country's wealth, or level of the country's income (Sato et al., 2013). More affluent counties have an estimated treatment capacity of 70%, compared to a capacity of 8% found in poorer countries (Sato et al., 2013). Additionally , high treatment costs have led to maintenance difficulties especially in poorer

countries, creating lowered treatment reliability. This agrees with the findings of the United Nations in their 2017 World Water Report that found that only 20% of the globally produced wastewater receives adequate treatment (UN-water, 2017). Further challenges to the current sanitation system include universal access to said wastewater infrastructure (Toxopeus, 2017). This is particularly relevant in South Africa where some of the population are still utilizing buckets for toilets (Toxopeus, 2017). Through this, it becomes clear that there is an urgent need to rethink current wastewater practices. Such rethinking needs to close the loop between nutrients synthetically created for agricultural use, and the rich source of nutrients already present in human urine as mentioned above.

Through rethinking wastewater systems, one can develop innovative solutions to create a paradigm shift in modern sanitation systems (Randall and Naidoo, 2018). The focus of these solutions needs to incorporate two important aspects. The first to reduce nutrients in wastewater effluents to meet safe effluent discharge levels and legislative levels. Secondly, solutions need to prevent the future accumulation of nutrients in a body of water (Randall and Naidoo, 2018).

To prevent an excess of nitrogen and phosphorus from being released with the treated effluent containing domestic wastewaters, these nutrients can instead be recovered from human urine if collected separately from domestic wastewater (Larsen, 2020). This urine can be separated through the introduction and use of a source separating urinal (Larsen, 2020) or toilet. By removing urine from wastewater, the nutrient load of wastewater is reduced. A lowered nutrient load simplifies the wastewater treatment process (Jimenez et al., 2015). This simplification also corresponds to a simplified treatment plant design with lower volume requirements and a reduction in treatment and maintenance costs (Jimenez et al., 2015). By addressing this urgent need with innovative sanitation solutions, the concept of waste valorization is introduced. Waste valorization is defined as an industrial activity that aims to reuse or recycle a waste stream previously deemed to have no further value (Kabongo, 2013). As highlighted in 2018 by Randall et al*.,* considering the size of the global population, the use of fertilizers in agriculture to secure food production, and the cost of treating nutrient rich urine, the possibility of introducing waste valorization from wastewater becomes a relevant research topic (Randall and Naidoo, 2018).

1.2 Research problem statement

Human urine consists of various inorganic and organic constituents that can be recovered and reused, dissolved in approximately 96% water (Sakthivel and Chariar, 2013). Urine needs to be collected and transported to facilities for further processing, whereby the nutrients, such as nitrogen and phosphorus, can then be recovered. Concentrating the collected urine, through the removal of water, reduces the overall volume of urine required to be transported and handled and thus the cost.

Evaporation is one suggested method for water removal. Although previous studies have investigated forced convective evaporation of water from human urine, very little is known about the chemical composition and quantities of compounds formed in the remaining urine solution during the evaporative process using different types of pre-treatment.

1.3 Research aims and objectives

This project aimed to identify and quantify compounds formed experimentally during passive evaporation while simultaneously predicting what happens using a thermodynamic model.

Information obtained from simulation procedures was used to validate experimental work. Both experimental and simulation results were then used to build a higher-level understanding and mass balance around the compounds formed during the evaporation process. Through this, the proposed research aimed to address several research objectives, guided by the abovementioned research problem statement. The project had the following research objectives:

1. Experimentally determine what the preferred urine stabilization technique is at 100% water removal in terms of N, P and K nutrient recovery;
2. Determine the effect of different water removals on solid formation using the preferred urine stabilization method, specifically:
    a. The mass of total solids and major component (N, P and K) recovered at three different water removals (50%, 75% and 100%);
    b. A comparison between the experimental results and thermodynamically predicted results (pH profile, mass of solids and type of solids formed).
3. Determine the influence of urine composition on the preferred stabilization process;
4. Determine the influence different operating temperatures have on the preferred stabilization process;
5. Determine the energy consumption when evaporating water from urine stabilized through the preferred stabilization process at different water removal intervals, as well as operating temperature conditions.

1.4 Hypothesis

Through experimental and simulation procedures it was postulated that the removal of water would result in different solids precipitating out of solution. This allows for these nutrients to be recovered from the formed solid phase. Stabilizing human urine with an acid or based will result in a higher recovery of nutrients during evaporation at low temperatures (< 40°C) and high or low pH (>11 for base stabilization and <4 for acid stabilization) because both chemical and enzymatic urea degradation is prevented at these conditions.

It was further postulated that different compounds, compared to the initial compounds contained in fresh human urine, were expected to form during the water removal processes. This was attributed to either the degradation or volatilization of certain compounds such as urea and NH_3, when fresh urine was left for long periods of time or evaporated in an open system. The addition of acid or base to the solution for stabilization also introduced the chemical building blocks for the formation of new solids during the water removal step.

1.5 Scope and limitations of research

Experimental and simulation procedures were used to study urine evaporation. Three different types of urine were used in experimental analysis: fresh urine and the two types of stabilized urine, both considering two methods of stabilization each. One type was stabilized

through dosing with basic salts ($Ca(OH)_2$ and MgO), the second type was acidified using acetic and citric acid, respectively. Due to the COVID 19 pandemic, there was limited collection of human urine. Hence, a synthetic urine solution was used in place of the human urine for most experiments. When human urine was used, this urine was collected from the researchers in the Water Quality Laboratory at the University of Cape Town (UCT). The donations within the research group were anonymous and hence the diversity of the donor group was unknown for this study. Only the chosen water removal intervals at each temperature and humidity condition as specified in Table 9 was used in the experimental aspects of this study.

Chapter 2. Literature Review

2.1 Introduction

In 2019 the global human population was approximately 7.7 billion people (United Nations et al., 2019). To supply sufficient food to feed this population, the use of synthetic agricultural fertilizers has become common practice. These agricultural fertilizers contain large amounts of nitrogen (N) to support plant growth and in turn, food production (Larsen, 2020). This current population size, coupled with the global demand for vital nutrients such as nitrogen (N), phosphorus (P) and potassium (K), contained in synthetic fertilizers, has created an urgent need to address the use of these key nutrients from a sustainability perspective. One suggestion is to recover and reuse key nutrients from a nutrient rich waste stream, such as human urine. Recovering and utilizing these key nutrients from waste sources eliminates the need to mine or produce such nutrients synthetically (Randall and Naidoo, 2018).

Human urine is a waste stream not only rich in N, but also in K and P nutrients. This means human urine should no longer be viewed as a waste stream, but rather a potential stream to supply key nutrients through resource recovery. Traditionally, human urine has been a component in wastewater, which historically has been treated in traditional wastewater treatment facilities.

However, as the focus on human urine begins to shift, there is less emphasis on solely treating this stream as a component of traditional wastewater, and a greater emphasis on separating this stream to enable harvesting and reuse of said key nutrients (NPK) (Randall and Naidoo, 2018). Separating urine from other human excreta through source separation has been presented as a more sustainable innovation to traditional wastewater treatment practices (Kakimoto et al., 2019). This innovation includes the separation, storage and treatment of source separated urine to allow for the harvesting and recycling of valuable nutrients into usable products, such as agricultural fertilizers (Randall and Naidoo, 2018).

To better understand the abovementioned concept of resource recovery from human urine, one needs to investigate the overall concept of wastewater, as well as the challenges faced when using traditional wastewater treatment plants.

2.2 Wastewater and traditional treatment methods

Wastewater is generated through the daily functioning of society. There are four major activity classes which contribute to this inevitable generation of wastewater, namely agricultural, commercial, domestic and industrial sectors (UN-water, 2017). Each of these sectors contribute to the generation of wastewater, rich in unused nutrients of both organic and inorganic nature.

As the overall NPK nutrient content in human urine was highlighted above, one can focus on the domestic wastewater category. Domestic wastewater contains blackwater which consists of human excreta, including human urine, and greywater (UN-water, 2017). The flushing of toilets, bathing and kitchen sink usage contributes to this greywater component (UN-water, 2017).

Of the total volume of generated domestic wastewater, human urine is estimated to be approximately 1% of this volume (Randall et al., 2016). Although this may seem insignificant, human urine in itself is nutrient dense, containing around 80% N, 56% P and 63% K contained in domestic wastewater as a whole (Höglund, 2001).

Beyond these nutrients from human urine, additional nutrients are present in wastewater from other activities, such as farming. These nutrients need to be removed from wastewater via a wastewater treatment plant. If not removed, untreated wastewater enters the environment in its nutrient rich form. This may cause pollution or contamination in an ecosystem. Some of these species commonly found in wastewaters and few common examples of these species are (UN-water, 2017):

1. Nutrients required for plant growth (N, P and K);
2. Pathogens (Viruses and bacteria);
3. Heavy metals (Copper, lead and zinc);
4. Organic compounds that induce pollution (Pesticides, biodegradable organic compounds);
5. Micropollutants (Pharmaceuticals, cosmetic and cleaning materials).

These species all contribute to the overall composition of wastewater. The nutrient content of wastewater especially P, may lead to pollution of water bodies through the process of eutrophication, if released untreated (Samer, 2015). The process of eutrophication is a natural process, occurring slowly and naturally in nature. However, the release of nutrient rich, untreated wastewater may accelerates the rate at which this process occurs (de Jonge and Elliott, 2001).

When left untreated and released, the excess of key nutrients, mainly N and P present in wastewater, promote the excessive growth of algal and photosynthetic biomass in bodies of water. The composition of the biological community within the body of water is altered through eutrophication as the additional nutrient-stimulated plant growth depletes dissolved oxygen present in the body of water. This plant growth also limits solar energy penetrating the body of water (Glibert, 2012).

To avoid the eutrophication of aquatic environments such as lakes, the overall objective of conventional wastewater treatment facilities aims to achieve an overall nutrient removal from influent wastewater (Larsen, 2020). There are a variety of different treatment plant designs and options, Each of these options differ in design, efficiency and cost, however all aim to reduce the nutrient load of incoming wastewater to release an effluent meeting discharge regulations (UN-water, 2017). These treatment facilities use the concept of activate sludge to treat incoming wastewater (UN-water, 2017).

However, current wastewater treatment methods, such as conventional sewers and treatment plants, although shown to be highly effective methods, have still led to an observed deterioration in water quality due to poor management and insufficient capacity (UN-water, 2017). This was apparent in the 2017 World Water Report published by the United Nations. In this report it was found that most cities do not have sufficient wastewater management systems due to infrastructure that is either outdated or non-existent (UN-water, 2017).

Current sanitation systems are unsuccessful from both an environmental, as well as from a humanitarian perspective due to a lack of capacity, budget or technical expertise. This means that current sanitation systems are often unable to meet water quality discharge requirements(Larsen, 2020). One of the biggest challenges associated with the unsatisfactory performance of these current wastewater treatment methods, is largely attributed to the high cost and capacity associated with such systems as highlighted in Section 2.3.2 (Larsen, 2020; Sato et al., 2013).

This is further emphasized by (Boyer and Saetta, 2019) where the limitation of modern wastewater treatment plants is discussed. Modern wastewater treatment plants aim to protect the health of a population and prevent environmental harm. These modern plants collect grey and blackwater streams and transport these streams to a central processing facility. At these facilities, secondary wastewater treatment is implemented (Boyer and Saetta, 2019). This step removes nutrients and pathogens from the waste and aims to decrease the biological oxygen demand of the waste (Boyer and Saetta, 2019). These facilities do not focus on the recovery of nutrients from waste. Additionally, these treatment plants also do not focus on the removal of trace components from the waste stream, such as pharmaceuticals. These components are instead released in the effluent (Boyer and Saetta, 2019). Considering the lack of nutrient recovery, and the release of trace components into the environment through effluent release, the use and sustainability of modern wastewater treatment infrastructure does lead to concern. This is amplified when one considers the number of wastewater treatment plants that are approaching the end of their design life and will need to be replaced or changed to make these operations more sustainable (Boyer and Saetta, 2019).

When treating wastewater, the high nutritional content of human urine highlighted above, sparks interest and creates potential to explore more innovative sanitation solutions through the concept of waste valorization (Randall et al., 2016). Nitrogen and phosphorus nutrients can be recovered from urine and recycled into useable products such fertilizers, or even as a raw material source for bio-bricks (Lambert and Randall, 2019). Such innovative solutions aim to address the shortfalls and challenges of the current system. These challenges are discussed in greater detail in the section to follow.

2.3 The current challenge

With the abovementioned 7.7 billion people in the world, food security and associated agriculture has become an area under major focus and scrutiny (Randall and Naidoo, 2018). A large population size will create the demand for a large amount of food. This in turn creates the demand for the use of synthetic fertilizers within the agricultural industry. These fertilizers are associated with the mining and synthetic production of necessary components, as summarized in Figure 1.

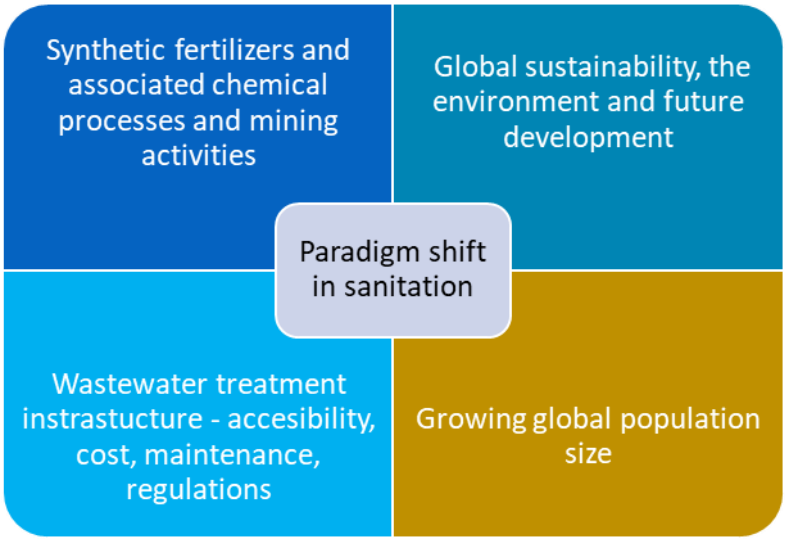

Figure 1. Four major challenges faced when dealing with a large population and traditional wastewater infrastructure. These challenges are leading to sanitation research and innovation to arrive at more sustainable solutions.

2.3.1 Synthetic fertilizers

Synthetic fertilizers were created to provide a range of nutrients to nourish soil to enhance plant growth. These fertilizers contain a rich variety of nutrients which can be classified into either primary, secondary or micro-nutrient groups (Bennett, 1997). Primary nutrients are essential for plant growth and are required in the greatest capacity. These nutrients include nitrogen, phosphorus and potassium, making up the nutrient group referred to as NPK in this report (Bennett, 1997).

The nitrogen used in synthetic fertilizers, is commonly in the form of ammonia (NH_3) which is synthesized through the Haber Bosch process (Smil, 2001). This process involves a series of reaction steps to react hydrogen and nitrogen in equal ratios (Bennett, 1997). Nitrogen is sourced from the surrounding atmosphere, whereas hydrogen can come from a variety of sources such as water, coal or natural gas to name a few (Bennett, 1997). The Haber Bosch process requires high operating temperatures between 1000 and 1500°C (Bennett, 1997). As a result, this causes the process to be energy intensive, contributing approximately 1-2% to the total global energy consumption (Kyriakou et al., 2020).

However, synthetic fertilizers not only contain this synthesized ammonia, but also sources of potassium and phosphorus, in the form of phosphoric acid. Phosphorus is sourced through the mining of rock phosphorus (Bennett, 1997). The mined rock is finely ground and digested with sulfuric acid at a moderate temperature (Bennett, 1997). This results in the formation of phosphoric acid and waste gypsum. The waste gypsum is separated using filtration and is then washed and subsequently disposed of (Bennett, 1997).

As with most mined resources, the availability and grade of phosphorus rock has been diminishing with the increasing demand for these resources (Randall and Naidoo, 2018). A lower grade of phosphorus rock corresponds to greater extraction costs, and increased

wastage to the environment. This wastage may include gypsum, heavy metals as well as radioactive materials (Randall and Naidoo, 2018).

Furthermore, as discussed by Randall and Naidoo, the use of synthetic fertilizers not only creates wastage but also the potential for further water pollution (Randall and Naidoo, 2018). This form of pollution occurs when the applied fertilizer is lost due to run off and causes eutrophication in bodies of water. The ammonia in applied fertilizers also converts back to nitrogen in the form N_2 and is subsequently lost to the surrounding atmosphere. Although this is not a form of harmful pollution, this lost nitrogen is costly from a financial perspective. Additional fertilizer (nitrogen) will be required to compensate for the previous losses (Randall and Naidoo, 2018).

An additional important consideration regarding the use of synthetic fertilizers is the environmental impact created due to the associated industrial processes to produce the required synthetic chemicals. A variety of acids may be used in these production processes, such as the above-mentioned sulfuric acid (Bennett, 1997). These processes also have associated waste streams, for example the washed gypsum.

Although synthetic fertilizers are effective, it needs to be considered that there are environmental concerns associated with their production and use, as highlighted above. These environmental concerns lead to questions regarding the sustainability in continuing to use such fertilizers.

2.3.2 Sustainable development and the environment

To address the overarching theme of sustainability in terms of how water resources are used (Figure 1), the United Nations (UN) adopted the 17 Sustainable Development Goals. These goals are set to be achieved by 2030 (United Nations, 2020). These goals focus on human rights and quality of life, as well as create a holistic approach in which sustainable development can be achieved around the world.

The sixth sustainable development presented in the set of goals, aims to achieve global access to clean water and proper sanitation systems (United Nations, 2020). The reason this was deemed an essential goal is because approximately 70% of the global population is not connected to a sewerage removal system (Van Drecht et al., 2009). To further emphasize the importance of sanitation and the value of water resources, 785 million people do not have access to a source of clean drinking water (WHO, 2019). Two billon people are still drinking water contaminated with feces (WHO, 2019). This is further amplified with the prediction that by 2025 half of the global population will be faced with living in water scarce regions (WHO, 2019).

By definition, the word sanitation refers to the provision of adequate facilities and associated services to ensure that human excreta, from toilet through to treatment and disposal, is safely managed (WHO, 2021). In a South African context, wastewater treatment facilities and sanitation systems are under great pressure. While 82% of South African households have access to either flushing toilets with a sewerage/septic tank system (Statistics South Africa, 2017), or a pit toilet, 3.1% of South African households do not have access to any form of sanitation or utilize buckets as toilets (Toxopeus, 2017). Although this figure decreased from

12.6% in 2002 to 3.1% in 2019, these improved statistics do not give any indication of what condition the available sanitation systems and infrastructure is in (Toxopeus, 2017).

To get an idea around the condition that these available systems are in, the South African Institution of Civil Engineers (SAICE) reviewed sanitation systems in urban and other areas. Urban sanitation systems were given a C minus rating. Sanitation systems in other areas were given an E rating (SAICE, 2017). This highlighted that although under stress, South Africa's sanitation and wastewater systems are still satisfactorily functional in metropolitan areas. However, with a C minus rating, these systems are seen to be stressed at peak conditions and are going to require substantial maintenance in the foreseeable future (SAICE, 2017). However, in rural areas, this is not the case. An E rating corresponds to a system that is found to be completely unfit for purpose (SAICE, 2017). In rural areas such systems are a threat to public health and safety as these systems have failed or pose a high risk of potential failure. South Africa is not the only country in such a predicament.

In general, many low- and middle-income countries have not properly invested in wastewater treatment plants to adequately remove nutrients from wastewater to promote long-term water quality. This can be seen through the overall global phosphorus and nitrogen removal levels of 20% and 10% being achieved respectively (Larsen, 2020). These low levels of nutrient removal correspond to high nutrient content in the effluent of treatment plants which is subsequently released into the environment. Although this has been highlighted as a present environmental concern, in the future this concern may be amplified due to a continuously growing population and continued release of nutrient-rich wastewater effluent.

2.3.3 The growing population

By 2030 the global population is expected to have increased to 9.7 billion people (United Nations et al., 2019). With an increase in population size, one not only needs to consider the current condition of wastewater infrastructure important as in Figure 1, but also the increase in the volume of wastewater required to be treated. These potentially increasing volumes of untreated wastewater create a challenging reality that a nation may have to cater for. Environmental emissions of nitrogen and phosphorus in the effluent from wastewater treatment facilities, is expected to increase in years to come due to this population growth (Larsen, 2020). Larsen expressed that it is not possible for a country to cope with these increasing emissions through the construction of new wastewater infrastructure (Larsen, 2020). However, the author does express that one way to face this challenge and minimize the risk of treatment facility failure, is to lessen the load on existing wastewater treatment facilities. This would require a nation to adopt innovative sanitation methods such as dry toilets with the facility to separate and transport human urine to onsite storage facilities (Larsen, 2020). Stored urine can then be collected for further processing such as nutrient recovery (Chipako and Randall, 2020a).

2.4 The potential solution: Urine source separation and further processing

Separating urine from other human excreta at the source of production, is referred to as source separation. This potential solution encompasses all the above-mentioned aspects in Figure 1, which challenge the current sanitation system not only in South Africa but globally.

2.4.1 Source separation

The large-scale implementation of source separation will reduce municipal infrastructure costs yet will require a large initial investment from a domestic/household level (Larsen, 2020). This is due to the installation of modified source separation toilets, as well as associated storage facilities and new piping networks. The source separated toilet decentralizes wastewater assets creating a shift in the management of wastewater and associated systems (Larsen, 2020). However, this may be more feasible in smaller towns, compared to larger cities due to the installation costs required.

For example, in some peri-urban and rural communities in Durban, the eThekwini Water and Sanitation Department installed urine diverting dry toilets (Udert et al., 2016). This was a pilot study and was rolled out in such areas as this form of sanitation provided a form of sanitation to areas which previously did not have adequate sanitation. Additionally, the installation of traditional sewers would have been costly due to the hills in these areas. This was the main reason traditional sanitation infrastructure could not be provided to these areas (Udert et al., 2016).

Once installed, the structure of the toilet is modified to allow for source separation. This is done by introducing two compartments in the toilet bowl – one compartment located in the front, for urine collection through a small hole, and a second located at the back for remaining fecal matter (Hellström et al., 1999). The collected urine can then be diverted from the relevant collection compartment to small scale central holding tank for short-term storage before mass collection (Hellström et al., 1999).

An addition to the concept of source separated toilets includes the innovative waterless urinal. These urinals allow for a significant reduction in water usage while still allowing for the separation and collection of concentrated urine at the source of production (Chipako and Randall, 2019). Source separated toilets are costly due to the associated piping retrofitting requirements that are needed to accommodate the collected urine. The reduction in water usage also resulted in solids blockages in this piping system. However, the proposed waterless urinal design by Flanagan and Randall eliminated these issues (Flanagan and Randall, 2018).

When used, the urinal can produce fertilizer at approximately 11 g per kg of urine (Flanagan and Randall, 2018). By recovering nutrients in the form of a saleable fertilizer, Randall and Flanagan estimated that 1000 urinals could generate an income from a waste stream at $85 per day (Flanagan and Randall, 2018).

The produced fertilizer both in the liquid and solids phases, rich in nitrogen, phosphate, calcium, magnesium, and potassium, provides an alternative to the synthetic fertilizers currently used in agricultural practices. This method of fertilizer production is also much less energy intensive when compared to synthetic fertilizers (Flanagan and Randall, 2018). The fertilizer produced from the waterless urinals was shown to be an effective fertilizer when compared to synthetic fertilizer and other kinds of available fertilizers used commercially (Meyer et al., 2018).

When comparing the use of human urine as a fertilizer, to the use of synthetic fertilizers in the cultivation of snap beans, it was concluded that urine could be applied as an alternative

fertilizer (Pandorf et al., 2019). This would result in savings in both energy and water, while simultaneously improving sanitation. This study also showed that the nutrients in human urine were available in a form that could be utilized by plants (Pandorf et al., 2019).

To understand why waterless urinals and associated source separation has been suggested as an alternative method to the current wastewater treatment system, one needs to understand the effect that this may have on existing infrastructure. This effect was studied using a biological nutrient removal (BNR) system (Jimenez et al., 2015). Varied amounts of urine were removed from the wastewater entering the BNR system to simulate various source separation situations and associated nutrient loads. With decreasing amounts of urine in influent wastewater, it was found that the concentrations of ammonia in the effluent wastewater was unchanged (Jimenez et al., 2015). The effluent nitrate concentration however, decreased due to the lowered influent concentration (Jimenez et al., 2015). Urine removal from wastewater also decreased the effluent phosphorus concentration in the BNR system (Jimenez et al., 2015). As with nitrogen, this is due to the lower influent phosphorus entering the facility.

Considering source separation, the loss of nitrogen from wastewater becomes relevant from a climate change perspective. At wastewater treatment plants nitrogen is partially transformed into nitrous oxide (N_2O) gas in a nitrifying treatment plant (Larsen, 2020). N_2O is a greenhouse gas which has a global warming potential 298 times greater than that of CO_2. The nitrification process requires an energy input to produce an energy-rich sludge as an output. This traditional nitrifying process has long sludge age (Larsen, 2020). In reducing the nitrogen in wastewater through the removal of urine, both the N_2O emissions from the treatment plant and the energy intensity of the nitrification process, can be reduced. This was found to result in the treatment plant producing energy instead of requiring an energy input (Larsen, 2020).

Furthermore, the removal of urine (rich in nitrogen and phosphorus) from municipal wastewater, results in wastewater that has an approximately favorable C:N:P ratio for conventional activated sludge processes (Larsen, 2020). This allows for a simpler wastewater treatment plant that can adequately treat remaining the wastewater with a relatively short sludge age (Larsen, 2020). A shortened sludge age corresponds to a smaller requirement in plant volume, with less infrastructure and associated maintenance costs on the treatment plant.

2.4.2 Urine handling after source separation

Once urine has been collected through source separation, one can use human urine as a fertilizer to ensure nutrients are actively recycled (Hellström et al., 1999). Urine is suited to provide the primary nutrients required in synthetic fertilizers as it contributes to an estimated 80% N , 56% P and 63% K contained in domestic wastewater as a whole (Höglund, 2001). Urine also shows a lower risk of containing pathogens and heavy metals, compared to feces (Rose et al., 2015).

However, such practice will result in increased transportation of urine from the storage tanks to the required agricultural site. As urine is mainly in the liquid form, the weight and volume

of the urine to be transported becomes a limiting factor (Chipako and Randall, 2020a). The urine transportation will also have a negative impact on the environment if conducted on a large scale and long term basis (Hellström et al., 1999; Larsen, 2020). When collecting and 'processing' urine, the technology and infrastructure for extensive urine source separation and collection in urban environments does not currently exist. This is partially due to the challenge presented in having to transport these large volumes of urine. As urine has a high-water content, one can mitigate these challenges by reducing the volume of urine required to be transported. This can be achieved by subjecting urine to a chosen water removal process (Hellström et al., 1999). Examples of such methods are discussed under Section 2.7. These water removal processes result in the concentration of human urine. The collected and concentrated urine can subsequently then be transported to treatment and processing facilities.

2.5 Human urine

The success of source separation and urine nutrient recycling is driven by the composition of human urine. An individual can produce between 0.8 and 1.5 liters of urine per day (Feineigle, 2011). This urine contains approximately 95% water (Feineigle, 2011). The remaining 5% is primarily composed of the abovementioned primary nutrients (N, P and K), as well as trace elements and other micronutrients (Feineigle, 2011).

Due to various external factors, the composition of N, P and K nutrients excreted from the body in the form of urine, may vary between 85-90%, 50-80% and 80-90% respectively (Larsen and Gujer, 1996). Although quantities of these nutrients vary between individuals, the Counsel for Scientific and Industrial Research (CSIR) published values indicating the expected yearly nutrient excretion per individual (Richert et al., n.d.). This was calculated in 2008 for rural households in Limpopo, South Africa and is shown in Table 1.

Table 1. Average annual quantities of N, P and K nutrients excreted per person in human urine. Excretion quantities are shown for individuals in South Africa and West Africa in kg/person/year.

Nutrient	Quantity in South Africa (kg/person/y)	Quantity in West Africa (kg/person/y) [1]
Nitrogen	3.65	2.8
Phosphorus	0.35	0.45
Potassium	1.26	1.3

The above quantities may seem insignificant when not considered within the correct context. To truly realize the economic value in the recovery and reuse of these excreted nutrients, an additional column has been included in Table 1. This presents information for nutrient quantities excreted in the urine from West African countries using FAO statistics [2].

2.5.1 Economic value of urine

The economic value of these excretions in Table 1 can be assessed by considering the monetary value of these excretions in comparison to the cost of synthetic fertilizers. Firstly, the average size of a family in Niger, a country in West Africa, was found to be nine people

[1] Values calculated using FAO statistics (see www.FAO.org)

(Richert et al., n.d.). This leads to an average family annually producing 25.2, 3.2 and 6.2 kg N, P and K respectively, as seen in Table 2.

Table 2. Major nutrients in urine excreted by an Individual and a family of nine in comparison to the nutrients found in 100 kg of a combination of commonly used synthetic fertilizers. Values taken from estimations in the year 2010.

Nutrient	Quantity in West Africa (kg/person/y) [2]	Quantity per family of 9 (kg/family/y)	Quantity in fertilizer combination (kg/100 kg fertilizer)
Nitrogen	2.8	25.2	27.0
Phosphorus	0.45	4.05	3.2
Potassium	1.3	11.7	6.2

Secondly, 50 kg urea and 50 kg of NPK fertilizers are a commonly used combination of fertilizers in West Africa. The nutrient content of such combination is shown on the right most of Table 2. When compared to the annual average family's nutrient excretions, the average family excretes nutrients approximately equivalent to two 50 kg bags of fertilizer. The potential value in recycling nutrients contained in human urine as a fertilizer, has sparked much interest in West Africa. In reality, the average family in such rural areas, would not be able to afford to buy two 50 kg bags of fertilizer as this would cost more than R2400 [2] (Richert et al., n.d.).

As an example, this economic assessment can be further extended to a country like Burkina Faso which relies heavily on fertilizers manufactured from imported nutrients (Richert et al., n.d.). Table 3 provides a comparison between the value of nutrients imported and the value of nutrients excreted in human urine.

[2] A total cost of $80 was estimated for 2010. It is expected to be greater 10 years later due to inflation. An inflation rate of 6% was used to determine the value in 2020. This was $143. An average annual exchange rate of R 16.47/$ from 2020 was used to covert currencies [Annual Average Exchange Rates (nedbank.co.za)].

Table 3. Comparison in the value of imported and excreted nutrients in Burkina Faso, West Africa for the year 2010

Imports			
Nutrient	**Total imports per year (1000 kg/year)**	**Unit cost of single nutrient fertilizer (R/kg)** [3]	**Total cost of imported nutrients (million R)**
Nitrogen	22600	12.7	287
Phosphorus	8800	30.3	267
Potassium	14800	13.2	195
Total	-	-	**749**
Excretions			
Nutrient	**Total excretions per year (1000 kg/year)**	**Unit cost of single nutrient fertilizer (R/kg)** [3]	**Value of excreted nutrients (million R)**
Nitrogen	38000	12.7	483
Phosphorus	5780	30.3	175
Potassium	19700	13.2	260
Total	-	-	**918**

It must be noted from the above that the cost of imported nutrients may be 10% inflated due to the price of single nutrient fertilizers being more expensive due to their nature (Richert et al., n.d.). Despite this, Table 3 still provides evidence that the recovery and reuse of nutrients in human urine, has a clear business case particularly in rural or poverty-stricken areas. Such areas not only require agricultural assistance but also innovative ideas to allow for the accessibility to an improvement of basic sanitation systems as discussed in Section 2.3. Not only in West Africa, but also on a global level, the value in recovering these nutrients is further emphasized (Larsen, 2020). Typical global annual nutrient estimates from human urine are shown in Table 4 [4].

Presented quantities are estimated using a global population size of 7.5 billion people (Larsen, 2020), which in turn is used to estimate the market value of the recovered nutrients should they be reused in a fertilizer product (World Bank, 2015).

Table 4. Annual global quantity and estimated market value of nutrients contained in human urine (Larsen, 2020)

Nutrient	**Annual quantity (Mt/year)**	**Annual market value (R/year)**
Nitrogen	25	218 billion [5]
Phosphorus	1.8	
Potassium	5.5	

[3] Prices were quoted in CFA. Average annual exchange rate of CFA 68.7/R in 2010 was used [www.exchangerates.org].

[4] Values may vary between sources, values estimate on a global population size of 7.5 billion people

[5] Value estimated from 2014 fertilizer price, which was considerably low (Larsen, 2020). Annual average exchange rate used at R 10.9 [www.businesstech.co.za]

Nutrients such as nitrogen mentioned in Table 4, are derived from the various different compounds such as urea, that make up the overall nutrient rich solution, known as human urine. The typical composition of this urine can be determined, although found to vary between individuals due to numerous different factors.

For example, personal diet and fluid intake (mainly water) are major factors that may cause variation in urine composition amongst individuals (Rose et al., 2015). Fluid intake also has a direct correlation to the amount of urine produced (Rose et al., 2015). Further factors such as body size, amount of exercise or excessive sweating, may affect the quantity, as well as the composition of urine produced amongst individuals.

2.5.2 Chemical composition of urine

Several previous studies have been conducted to determine the composition of fresh human urine. The findings of these studies have been summarized into a list of 158 chemical compounds, and can be found in the Bioastronautics Data Book at NASA (Putnam, 1971). Figure 2 outlines the broad categories into which these chemical compounds have been grouped.

Figure 2. Major categorization of human urine into six major overall nutrient groups (Putnam, 1971).

A notable study conducted by Putnam investigated the composition of human urine (Putnam, 1971). This study focused on the chemical, physical, engineering and concentrative properties of human urine between the temperatures of 21.1 and 60°C, with a solute concentration range from 4 to 90% solutes (which corresponds to 10 - 96% water content) (Putnam, 1971). The application of this work mainly applied to space missions. Urine concentration methods allowed for the extraction of drinkable water from human urine. This allowed for lighter equipment requirements as well as the minimization of waste (Putnam, 1971). Putnam's work had a slightly different perspective to this study as he focused mainly on water recovery from urine with the intention of reusing water instead of the NPK nutrients in human urine. However, the composition and properties of human urine still apply despite the difference in research perspective.

The work of Putnam used analytical procedures to measure the Total Organic Carbon (TOC), Total Kjeldahl Nitrogen (TKN), pH and total dissolved solids in concentrated urine to list 68 chemical compounds which constitutes approximately 99% of the solutes found in human urine (Putnam, 1971). Putnam acknowledged that there are 158 known chemical compounds in human urine. However, of the 158 chemical compounds, these 68 listed compounds had individual concentrations above 10 mg L^{-1} and resulted in a significant total solute concentration of 36800 mg L^{-1} (Putnam, 1971). The remaining 90 unlisted chemical compounds resulted in a less significant solute concentration of around 250 mg L^{-1} (Putnam,

1971). Putnam then further condensed this list from 68 to 42 significant chemical compounds to represent a summarized version of the typical composition of human urine (Putnam, 1971).

2.5.3 Significant solutes in human urine

Putnam's condensed list of 42 urine constituents from the original 158 chemical compounds, was not suggested to replace human urine but instead was suggested for the use in engineering calculations and design applications (Putnam, 1971). This condensed list proved to be a significantly accurate representation, as well as more convenient for most engineering analyses as these compounds account for 98% of the total solutes found in human urine (Putnam, 1971).

From Figure 2, Putnam further refined the classification of the compounds in human urine as shown in Table 5 (Putnam, 1971). This classification can be broken down further to include the carbon, nitrogen, hydrogen, oxygen and organic sulfur content of each major category, as shown in Table 5.

Table 5. Major categorization of human urine into major nutrient groups, according to the study conducted by David Putnam in 1971. Major categories are quantified and can be further broken down to include the relevant elemental contribution. Carbon, nitrogen, oxygen, hydrogen and organic sulfur contents of each major category are shown (Putnam, 1971) [6].

	Category				
Contribution	**Inorganic salts**	**Urea**	**Organic compounds**	**Organic ammonium salts**	**Total**
Total (mg L^{-1})	14 200	13400	5370	4130	37100
Carbon (mg C L^{-1})	100	2680	2470	1630	6880
Nitrogen (mg N L^{-1})	0	6250	1210	659	8120
Oxygen (mg O L^{-1})	1880	3570	1230	1580	8260
Hydrogen (mg H L^{-1})	7	893	347	266	1510
Organic sulfur (mg S L^{-1})	0	0	134	0	134

2.5.4 Typical concentrations of compounds in fresh human urine

The typical composition of common constituents in fresh human urine are presented in Table 6. To account for this variation, typical concentration ranges, when available, are shown in Table 6.

[6] Table adapted from NASA contractor report Putnam (Putnam, 1971)

Table 6. Summary of expected concentration of major constituents making up the overall composition of fresh human urine taken from various sources of literature. In some cases, concentration ranges were available and is shown below.

Constituent name	Concentration/range (mg L^{-1})	Source
Ammonia	386	(Kakimoto et al., 2019)
	480	(Rose et al., 2015; Tilley, 2008)
	300	(Tilley et al., 2008)
Calcium	30-390	(Putnam, 1971)
	230	(Rose et al., 2015)
	32	(Jana et al., 2012)
	70	(Tilley et al., 2008)
Chloride	5640	(Putnam, 1971)
	1870-8400	(Rose et al., 2015)
Creatinine	311-2150	(Kakimoto et al., 2019)
Magnesium	20-205	(Putnam, 1971)
	120	(Rose et al., 2015)
	70	(Tilley et al., 2008)
Phosphate	143	(Putnam, 1971)
	205	(Jana et al., 2012; Rose et al., 2015; Tilley, 2008)
	450	(Tilley et al., 2008)
	760	(Rose et al., 2015)
Potassium	750-2160	(Putnam, 1971)
	966–1446	(Beler-Baykal et al., 2004)
	1200	(Jönsson et al., 1997)
Sulfate	2080	(Putnam, 1971)
Urea	11600-13400	(Kakimoto et al., 2019)-(Putnam, 1971)
	21400	(Jönsson et al., 1997)
	10000	(Otterpohl et al., 2003)
Uric acid	901	(Kakimoto et al., 2019)
	152-859	(Jen, 2002)

From Table 6, ammonia, creatinine, urea and uric acid in fresh human urine are expected to collectively result in a total nitrogen content of 6300 mg-N L^{-1} (Kakimoto et al., 2019). Furthermore, from Figure 2 there are a variety of organic acids contained in fresh human urine. These can be further categorized, and the concentration of the relevant acids can be seen in Table 7.

Table 7. Typical concentration of organic acids found in fresh human urine (Kakimoto et al., 2019)

Organic acid	Total concentration (mg L^{-1})
Acetic acid	218
Ascorbic acid	225
Butyric acid	24.1
Formic acid	39.7
Lactic acid	190
Malic acid	12.7
Propionic acid	177.2
Valeric acid	23.9

The compounds listed in Table 6 and Table 7 exist as dissolved constituents in the fresh human urine solution. However, when this urine is stabilized in a certain manner (see Section 2.6), or concentrated through water removal processes for example, some of these compounds may undergo solid forming reactions. Any resulting solids may potentially be recovered should they prove to be useful or valuable. There is limited information on the chemical composition of solids formed during concentrative processes, however known information regarding solids formed during urine stabilization processes is available and is presented below.

2.5.5 Solid forming reactions

Udert et al*.,* studied biologically induced precipitation in urine when collected in no-mix toilets using fresh urine. The results from this study showed only the formation of hydroxyapatite (HAP, $Ca_{10}(PO_4)_6(OH)_2$), magnesium ammonium phosphate (struvite/MAP, $NH_4MgPO_4{\cdot}6H_2O$) and calcium carbonate (calcite, $CaCO_3$) solids only (K.M. Udert et al., 2003). As this study used fresh urine, the pH range for this study was between 6 and 8.

When left untreated, fresh urine may begin to hydrolyze (Section 2.6.1). During the hydrolysis process there is the potential for solid forming reactions different to those in fresh urine. Hydrolysis results in the enhanced formation and precipitation of solid calcite, HAP and struvite. This solid formation is enhanced due to an increase in the ammonia concentration and increase in pH associated with the urea hydrolysis process (Kai M. Udert et al., 2003).

To ensure the maximum recovery of nutrients from human urine during evaporation, one may choose to stabilize urine prior to evaporation. Urine stabilization refers to preventing the breakdown of urea due to the presence of enzymes (Randall et al., 2016). This degradation process is referred to as urea hydrolysis and is discussed in further detail under Section 2.6.1. Urine stabilization against enzymatic degradation requires the addition of chemicals to alter the pH of the urine solution. This results in the inhibition enzyme activity.

Dosing with $Ca(OH)_2$ (Section 2.6.3) is one potential stabilization technique to prevent urea hydrolysis. If followed, there is the potential for solid calcium phosphate to form in the stabilized urine solution (Randall et al., 2016). These solids, present in various forms such as apatite, can be removed from the solution and repurposed as a fertilizer (Rittmann et al., 2011). When stabilizing fresh urine with 10 g L^{-1} $Ca(OH)_2$, the pH of the urine solution is above 11. At such a high pH, it is expected that apatite and struvite solids precipitate out of the urine solution (Nriagu and Moore, 2012). Experimentally Randall et al*.,* showed that $Ca(OH)_2$

stabilization resulted in complete magnesium and phosphate precipitation from the urine solution. However unlike the findings of Udert et al., in fresh urine only $CaCO_3$ and $Ca(OH)_2$ solids were identified (Randall et al., 2016) in the $Ca(OH)_2$ stabilized urine solution. No calcium phosphate solids or struvite patterns were detected. Simulation results for $Ca(OH)_2$ stabilized urine from Randall et al., did indicate that a calcium phosphate precipitate in the form of hydroxyapatite (HAP) should have been present however amorphous calcium phosphate solids are not easily detectable when using XRD (Randall et al., 2016).

As mentioned, various solids may precipitate out of fresh urine, stabilized urine and hydrolyzed urine. The type of solids precipitated depends on the type of urine. Each type of urine exists at different pH conditions and these conditions govern the solids that precipitate out of the urine solutions. At high pH conditions, spontaneous precipitation of phosphorus rich solids occurs (Chipako and Randall, 2020b). This precipitation is caused by the solid-forming reaction between the naturally occurring magnesium and calcium ions with phosphate ions found in urine due to a supersaturation of these ions (Etter et al., 2014).

With an increase in urine pH, struvite and HAP are the most commonly formed magnesium and calcium precipitates respectively (Kai M. Udert et al., 2003). When there is no ammonium present in solution, struvite-K ($KMg(PO_4)\cdot 6H_2O$) may also form and precipitate out of the urine solution (Wilsenach et al., 2007).

As urea hydrolyzes, ammonium NH_4^+ ions are produced. These ions increase the pH of the solution resulting in the formation of the above-mentioned solids (Chipako and Randall, 2020b). Fresh urine has a pH between 6 and 7. Once urea is completely hydrolyzed, the pH of the fresh urine solution changes to approximately 9.25. The pH at which struvite begins to precipitate is around a pH of 7 to 8. HAP precipitation occurs at slightly higher pH values (Chipako and Randall, 2020b). Considering this, pH is the deciding factor on the solids that will precipitate out of the urine solution and this needs to be considered when deciding on the urine stabilization method (Chipako and Randall, 2020b).

2.5.6 Technologies for nutrient recovery from human urine

Different urine management technologies were studied in Durban, South Africa, after observing that urine left in a soak pit was causing environmental pollution. These technologies focused on rather recovering the nutrients from urine instead of allowing the nutrients to cause pollution (Udert et al., 2015). One technology for nutrient capture and recovery focused on struvite precipitation. This is a simple and rapid process to capture phosphorus in human urine, in a solid form (Udert et al., 2015). However, nutrients such as nitrogen and potassium, will remain in the effluent and pathogens will also not be treated or removed from the urine (Udert et al., 2015). Struvite precipitation would hence have to be used in conjunction with an additional treatment processes to minimize environmental pollution and any hygiene risks. The second nutrient recovery technology focused on a combination of nitrification and distillation processes (Udert et al., 2015). This technology is more complicated than the simple struvite precipitation technology, but all major nutrients are recovered from urine (Udert et al., 2015). The final nutrient recovery technology used electrolysis. This technology can be applied to small scale, on-site urine treatment processes. This technology did not recover nitrogen, rather nitrogen was removed from the solution. Chlorinated products were also formed, posing a health risk (Udert et al., 2015).

2.6 Urine stabilization

Fresh (unstabilized) urine, which may hydrolyze if not treated, could be collected daily for subsequent treatment and resource recovery (Larsen, 2020). However, Larsen strongly advised against this due to the strong possibility of high costs associated with such logistics (Larsen, 2020). Fresh urine needs to be stabilized to prevent the loss of nitrogen due to urea hydrolysis. Urine stabilization also addresses potential odor issues and mitigates environmental concern due to emissions of volatized ammonia gas generated during urea hydrolysis, which may become more problematic on a larger scale (Larsen, 2020). To combat these abovementioned issues, fresh urine can be stabilized through either acidification or dosing with a basic salt. Both acidification and dosing are discussed below.

2.6.1 Urea hydrolysis

Suggested urine stabilization methods aim to prevent the process of urea hydrolysis (also called ureolysis) (Kai M. Udert et al., 2003). Urea hydrolysis results in the breakdown of urea, the compound in which majority of the nitrogen contained in human urine can be found (Randall and Naidoo, 2018). The urea hydrolysis process becomes an important consideration when considering nitrogen recovery from urine.

Urea hydrolysis can occur in two ways, chemically or enzymatically (Randall et al., 2016). Enzymatic urea hydrolysis occurs when urea is broken down enzymatically to form ammonia and bicarbonate ions in the presence of the enzyme called urease ((Hellström et al., 1999; Kai M. Udert et al., 2003)). Enzymatic urea hydrolysis can be described by Equations (***1*** and 2 (Hellström et al., 1999). These equations show the formation of free ammonia, ammonium as well as bicarbonate ions (which may form carbon dioxide) (Hellström et al., 1999; Randall et al., 2016). These reactions induce an increase in the pH level of the solution (Kai M. Udert et al., 2003) which results in the precipitation of struvite among other minerals from the urine solution (Flanagan and Randall, 2018).

$$\mathrm{CON_2H_4} + 3\mathrm{H_2O} \rightarrow 2\mathrm{NH_4^+} + \mathrm{HCO_3^-} + \mathrm{OH^-} \quad \textbf{(1)}$$

$$\mathrm{NH_4^+} + \mathrm{OH^-} \leftrightarrow \mathrm{NH_3\,(aq)} + \mathrm{H_2O} \quad \textbf{(2)}$$

Free ammonia can be converted to volatile ammonia as shown by the equilibrium reaction in Equation 3 (Hellström et al., 1999). When this volatile ammonia is lost, a corresponding amount of nitrogen is lost, decreasing the amount of nitrogen available for recovery (Randall et al., 2016).

$$\mathrm{NH_3\,(aq)} \leftrightarrow \mathrm{NH_3\,(g)} \quad \textbf{(3)}$$

Enzymatic hydrolysis can occur at temperature and pH conditions as shown by the shaded region on the bottom left of Figure 3 (Randall et al., 2016).

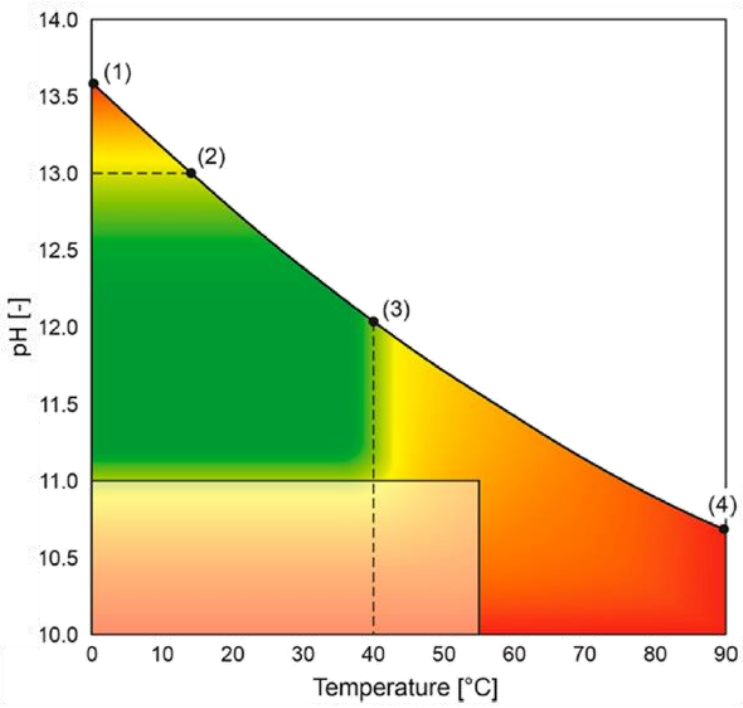

Figure 3. Graphical regions of observed urea losses in human urine at different temperature and pH operating conditions when stabilized using $Ca(OH)_2$. Red colouring corresponds to a high urea loss. Orange and yellow colouring correspond to medium and moderate urea losses, respectively. Green colouring indicates the lowest urea loss. The shaded rectangle in the bottom left corner depicts the area in which enzymatic urea hydrolysis was found to happen. The solid black line represents the found pH saturation curve. This figure was taken from the paper published by Randall et al., describing a novel method to stabilize human urine with $Ca(OH)_2$ (Randall et al., 2016).

As mentioned, there is a second avenue for urea hydrolysis, this is in the form of chemical hydrolysis. Chemical urea hydrolysis is possible when operating at an excessively high pH (>13) and temperatures (Warner, 1942). At an increased temperature, the rate of ureolysis has been observed to increase (Hellström et al., 1999). Furthermore, when working at high pH values during calcium dosing, chemical urea hydrolysis needs to be considered (Randall et al., 2016).

This form of hydrolysis is evident when considering Figure 3 (Randall et al., 2016). In Figure 3, the red, orange and yellow regions depict regions corresponding to high losses of urea, with red being the highest and yellow the lowest (Randall et al., 2016). These regions are observed at high pH levels, on the top left of Figure 3, as well as at high temperature conditions as seen on the bottom right of Figure 3. This form of urea hydrolysis also results in ammonia and carbon dioxide formation (Warner, 1942).

Urea hydrolysis occurs both enzymatically and thermally. However, at temperatures close to 40°C, enzymatic urea hydrolysis is much more prevalent compared to the other mechanisms of degradation (Simha et al., 2020). Enzymatic urea hydrolysis can be prevented by changing the pH of the fresh urine solution and as a result, stabilizing the solution. The chosen pH conditions aim to inhibit urea hydrolysis by operating at a pH that inhibits urea hydrolysis.

The optimal pH for Helicobacter pylori bacteria that produce the enzyme urease is 6.8 to 8.7 (Mobley and Hausinger, 1989). The activity of this bacterium is irreversibly inhibited at a pH below 3.5 and a pH greater than 8.6 (Rektorschek et al., 1998). Hence, the pH can either be raised to a pH >11 through dosing with basic salts such as $Ca(OH)_2$, $Mg(OH)_2$ or MgO (Simha et al., 2021), and alkalinizing the urine solution. The pH can also be lowered to a pH <3 through acidifying the urine. Urine acidification may use a variety of acids such as acetic or citric acid.

Additionally, De Paepe et al., used an electrochemical cell to increase the pH of fresh urine to a pH between 11 and 12 (De Paepe et al., 2020). Raising the pH through this method also resulted in a stabilized urine solution without acidification or alkalinizing of the urine solution. This was beyond the scope of this project. However, both urine acidification and alkalinization for stabilization are explored.

2.6.2 Acidification of urine

The first option to stabilize urine includes the addition of an acid to fresh urine. By acidifying fresh urine, the pH of the solution is decreased to a pH <3.5, beyond the point at which urease activity can occur. Hanærus et al., proposed that 26 mmol L^{-1} sulfuric acid (H_2SO_4) would inhibit urease activity (Hanaerus et al., 1996). Hellström et al., studied the addition of either acetic or sulfuric acids to stabilize urine. It was suggested that a single initial dose of 60 meq of either acid be used for a storage time of approximately 210 days without significant urea degradation (Hellström et al., 1999). However, in this investigation sulfuric acid proved superior to acetic acid as after 222 days, acetic acid stabilization resulted in significant urea hydrolysis (Hellström et al., 1999).

Similarly, Ray et al., investigated the inhibitory ability of various chemicals especially acids namely acetic, citric and sulfuric acid as well as vinegar, in the stabilization of fresh urine (Ray et al., 2018). When acidifying urine for stabilization, measurements of conductivity and pH were used as a proxy to determine whether urea hydrolysis was occurring in the studied stabilized urine solutions.

When conductivity and pH measurements were maintained in solution, urea hydrolysis was assumed to be inhibited as the conductivity and pH readings were stable (Ray et al., 2018). Ray et al., deemed vinegar, citric and acetic acids the most suitable due to lowered safety concern, low cost and high availability (Ray et al., 2018). However, from the investigation results, citric acid was seen to be superior in maintaining these proxy measurements (Ray et al., 2018). This was followed by acetic acid, vinegar and finally sulfuric acid (in order of decreasing suitability for urine stabilization) (Ray et al., 2018).

Ray et al., also investigated the use of acetic acid stabilization in waterless urinals (Saetta and Boyer, 2017). As fresh urine was present in waterless urinals, this urine hydrolyzed due to the presence of urease. This led to the precipitation of solids, which clogged pipes, and the volatilization of NH_3 gas which was associated with a bad odour. To prevent this, after each urination event a dosage of 2.5 mL 2500 meq L^{-1} acetic acid was added to the waterless urinal to inhibit urea hydrolysis (Saetta and Boyer, 2017). This lowered the pH of the urine and aimed to minimize the precipitation of calcium and magnesium rich solids.

Ray et al., used conductivity and pH to determine whether acetic acid had prevented urea hydrolysis (Saetta and Boyer, 2017). Conductivity increased in the urinal and associated storage tank, without acetic acid treatment. However, when treated with acetic acid, the conductivity in the second urinal and associated storage tank increased to a lesser extent. Combined with the pH results, it was shown that acetic acid could prevent urea hydrolysis in the waterless urinals studied (Saetta and Boyer, 2017).

As enzymatic urea hydrolysis is due to the bacterial community present in urine, the effect of acetic acid on the bacterial communities in human urine was investigated by Saetta et al. This was the first study to identify the microbial community in waterless urinals, as well as the effect of acetic acid on this community (Saetta et al., 2020). It was proposed by Saetta et al., that the addition of acetic acid alters the microbial communities through the introduction of carbon contained in acetic acid (Saetta et al., 2020). When the urine solution is at a pH lower than the pK_a value of acetic acid (4.75), the acid diffuses into the microbial cells. These cells have an internal pH greater than the pK_a of 4.75. Inside the cell, acetic acid loses protons through the process of deprotonation (Saetta et al., 2020). This begins to lower the internal pH of the cell. The acetic acid continues to accumulate within the cell until the cell dies (Trček et al., 2015). Conversely, if the pH of urine is greater than the pK_a of acetic acid, acetic acid loses protons in the urine solution and resulting acetate becomes a source of carbon for the microbial community (Saetta et al., 2020).

Saetta et al., found that when using acetic acid to stabilize urine, the diversity of the microbial community decreased compared to unstabilized urine. The acidified urine showed that the bacteria present belonged to the Enterobacterial class (Saetta et al., 2020). These results for acidified urine agreed with the bacterial classes predominantly found in fresh urine, even though the samples taken from acidified urine were taken two to three weeks after initial urine collection (Saetta et al., 2020). This finding showed that through acetic acid addition, the bacterial community had not begun to change into the diversified bacterial community found in hydrolyzed urine. Through acidification, the stabilized urine had a microbial community that showed closer resemblance to the community found in fresh urine (Saetta et al., 2020).

However, there are potential disadvantages associated with acidification as a method of urine stabilization. Should this stabilization method be required on-site, this method could be dangerous if large volumes of strong acids need to be handled or used to make more dilute acids required for urine dosing (Randall et al., 2016). In addition, acidification requires exact acid dosing and pumping which is accompanied with additional equipment requirements (Randall et al., 2016). Both Ray et al., and Saetta et al., showed that when acidifying urine with acetic acid, the frequency of acid dosing influences the rate of urea hydrolysis (Ray et al., 2018; Saetta et al., 2020). An alternative to acidification is alkalinization. This involves dosing urine with basic salts. These salts increase the pH of the urine solution due to the presence of hydroxide (OH^-) ions.

2.6.3 Alkalinization of urine

When alkalizing human urine, a pH >10 is used to stabilize the urine solution to prevent the loss of nitrogen from the solution. This alkalinization can be achieved by dosing urine solutions with different alkalizing media or salts. The pH of the urine is increased and thus

urea hydrolysis is prevented by inhibiting the activity of urease producing bacteria, allowing for nutrient recovery from the stabilized urine solution.

In a study by Simha et al., different alkalizing media were studied at temperatures of 50°C and 60°C. These temperatures were used as often processes have waste heat sources (Simha et al., 2020). These heat sources could be used to remove water from the stabilized urine to allow for the recovery of NPK nutrients. Simha et al., used $Ca(OH)_2$ and wood ash as alkalizing agents either alone or mixed with a substrate (biochar, wheat bran or desert soil). Wood ash was used as this is a widely available waste product from the Scandinavian region (Simha et al., 2020). Lime (CaO) was also studied as an alkalizing agent due to its low cost. The chosen alkalinizing agents[7] were added to a urine solution, which was evaporated at 50°C and 60°C (Simha et al., 2020). The nitrogen recovery from these solutions was then assessed to determine the suitability of each agent or combination thereof.

Each of the media studied resulted in different nitrogen recoveries at each temperature. It was seen that not all of the media could maintain the solution pH above a pH of 10 throughout urine evaporation. As a result, a greater nitrogen loss was observed in these solutions. When the pH of the solution could not be maintained, this was due to the solution absorbing CO_2 and forming carbonic acid (Simha et al., 2020).

To alkalinize urine Senecal et al., suggests the use of chemicals such as lime, or waste wood ash. Lime is used to raise the pH of acidic soils containing clay, so that there is a greater availability of phosphorus for plant growth (Senecal et al., 2018). Hence using lime in urine to prevent urea hydrolysis while concentrating urine, allows for a fertilizer to be produced containing nutrients in urine as well as a minimal loss in nitrogen. This is a more balanced fertilizer which would contain all the nutrients required for plant growth (Senecal et al., 2018).

Senecal et al., investigated the hygienic aspect associated with urine alkalinization. Fresh urine was alkalized using wood ash and evaporated at 42°C until the pH of the solution reached a pH <10.5 (Senecal et al., 2018). The alkalized urine was then inoculated with feces containing five different pathogens. This mimicked fecal cross-contamination that may occur in source separated toilets (Senecal et al., 2018). Some of the inoculated solution was left at 20°C and the rest was left at 42°C, and open to the atmosphere. At 20°C bacteria and bacteriophage pathogens were decreased beyond detection limit (Senecal et al., 2018). The World Health Organization (WHO) recommends a target of a $\log_{10}$ reduction in pathogen detection. From the investigation of Senecal et al., a $3\log_{10}$ reduction in pathogens in alkaline urine could be reached in 325 days when stored at 20°C and 9.2 days when stored at 42°C. This showed that a safe urine-based fertilizer rich in NPK nutrients could be produced through the use of wood ash as an urine alkalinization medium (Senecal et al., 2018).

Wood ash was one of the alkaline media selected by Senecal et al., due to its initial high pH (<12.5), as well as high surface area which allowed for faster urine evaporation processes (Senecal et al., 2018). However, $Ca(OH)_2$ has also been shown to increase the initial pH of urine above a pH of 12 and inhibit urease activity to allow for the dehydration of urine (Randall et al., 2016).

[7] Alkalinizing agents used were lime, ash, soil-lime, char-lime and bran wheat-ash combinations.

An alternative method for stabilizing urine is by adding $Ca(OH)_2$ to increase the pH of the solution (Randall et al., 2016). However, careful consideration needs to be taken with regards to temperature, to prevent chemical urea hydrolysis at high temperature and high pH conditions (Randall et al., 2016). There are three potential calcium compounds that may be applicable for calcium dosing, namely calcium carbonate, calcium hydroxide and calcium oxide ($CaCO_3$, $Ca(OH)_2$ and CaO respectively) (Randall et al., 2016). These compounds are considered due to their lower cost (Muster et al., 2013) as well as present use of CaO and $Ca(OH)_2$ as disinfectants in sanitary situations (Strande and Brdjanovic, 2014). During stabilization with $Ca(OH)_2$, calcium phosphate forms a precipitate that can be recycled in fertilizer products (Rittmann et al., 2011).

PHREEQC, a thermodynamic computer simulation package, was used to determine the resulting pH value due to dosing with each of the three suggested salts, at different levels of salt concentration (Randall et al., 2016). From the simulation results, it was clear that $CaCO_3$ was unsuited for calcium dosing. This resulted in a too low pH level of 7.2, still within the optimal range of pH levels for urease activity (Randall et al., 2016). Both CaO and $Ca(OH)_2$ resulted in a pH increase to a value of 12.5, inhibiting urease activity (Randall et al., 2016). As CaO forms $Ca(OH)_2$ when placed in solution, Randall et al., concluded dosing fresh urine with $Ca(OH)_2$ sufficiently stabilizes the urine (Randall et al., 2016).

When dosing with $Ca(OH)_2$ the design curve for urea hydrolysis and saturation pH in Figure 3 becomes relevant. This curve shows loss of urea due to urea hydrolysis as a function of pH and temperature. Urea loss is quantified using the color spectrum starting from minimal urea loss indicated by green shading to significant urea loss in red shading. The black curve acting as a boundary to the colored region, is known as the saturation line.

This saturation line is the upper boundary on the chart and represents the saturation pH of the solution (Randall et al., 2016). When at a specific temperature and adding $Ca(OH)_2$ to the urine solution, one will reach a point where the solution is saturated in $Ca(OH)_2$, at this point the pH of the solution is expected to fall on this saturation line at the corresponding temperature (Randall et al., 2016). No matter how much more $Ca(OH)_2$ is added to the solution, the pH of the solution will not change as no more $Ca(OH)_2$ can be dissolved due to saturation conditions. This saturation pH does not depend on the composition of human urine, but depends on the amount of $Ca(OH)_2$ added to the human urine in the stabilization step (Randall et al., 2016).

Using salt solubility and saturation for a chosen urine composition, PHREEQC was then used to determine the amount of $Ca(OH)_2$ required for adequate dosing to saturate the solution (Randall et al., 2016). A $Ca(OH)_2$ dose of 4.3 g L^{-1} was determined (Randall et al., 2016). However, due to variance in urine composition to ensure that the urine solution was saturated with $Ca(OH)_2$ an amount of 10 g L^{-1} was recommended in practice (Randall et al., 2016).

Not only $Ca(OH)_2$ but a variety of alkaline media could potentially be used in dosing to increase the pH of fresh urine, namely calcium/magnesium oxides and hydroxides salts as well as ash

(Randall et al., 2016). In contrast to acidification above, such alkaline media show several advantageous traits:

- Lowered risk of pathogens being present in the stored urine at much higher pH conditions (Eriksen et al., 1996; Pancorbo and Overman, 1988).
- These alkaline media are used in common practice to neutralize acidic soil hence improving soil quality while simultaneously delivering calcium/magnesium to the soil as essential growth nutrients (Shaul, 2002).
- Calcium/magnesium precipitates form with phosphate at high pH values, creating an avenue for phosphate removal (Randall et al., 2016).

2.7 Methods available for urine concentration

As human urine is mainly composed of water (Rose et al., 2015), removing such water through a chosen method, allows for significant volume reduction as well as the recovery of nutrients that precipitate out of solution. By removing water, the volume of the now stabilized urine decreases, leading to a reduction in the cost of transporting the urine (Randall et al., 2016). A second effect of urine dehydration is an increase in the salinity of the remaining urine, causing a decrease in enzymatic urea hydrolysis through the inactivity of enzyme urease (Hotta and Funamizu, 2008).

Water removal increases the concentration of the nutrients which are to be recovered and reused in products such as fertilizers. This can be achieved through a variety of different technologies or methods.

2.7.1 Freeze concentration and eutectic freeze crystallization

Water may be recovered from a saline solution through the formation of ice, when using freeze concentration (Rahman et al., 2006; Randall and Nathoo, 2018). It is desired that the ice formed is free of any impurities so that when melted, pure water can be obtained. The remaining impurities are concentrated in the liquid phase (Rahman et al., 2006).

This method of water removal has been used in the desalination of seawater due to the low energy intensity associated with this concentrative method (Chang et al., 2016). This is due to the thermodynamics associated with ice formation. The latent heat of fusion for ice formation is one seventh of the heat of vaporization to form water vapor (Rahman et al., 2006). One major disadvantage of freeze concentration is the resulting brine solution that is created due to the removal of water from the saline solution (Rahman et al., 2006).

Eutectic freeze crystallization(EFC) is an extension to the concept of freeze concentration (Rahman et al., 2006). The concept of EFC aims to remove water in the form of ice, from solution. This results in a concentrated solution which causes the simultaneous crystallization of salts from the solution. In removing water and salt in this manner, a concentrated brine solution can be further treated (Rahman et al., 2006).

An example of a binary system (containing two components C1 and C2) during EFC has been adapted and is shown in
Figure ***4*** as a visual aid to the method explanation (Schmidt, 2007). Figure 4 only considers the thermodynamics of the binary system during EFC and not the kinetics of the system though (Randall et al., 2012). When using EFC as a method for water removal, the kinetics of the

system would also need to be considered. If more of C2 is added to C1 an inverse proportionality between molecular weight fraction and melting temperature is observed (Schmidt, 2007). The higher the molecular weight fraction of C2, the lower the melting temperature. If more C2 is added to the mixture, there is a region in which C1 starts to form solid crystals and C2 does not (Schmidt, 2007). The eutectic point of the solution is reached when the minimum melting temperature of the solution is reached at a specific molecular weight fraction of each component. This point is defined as the point whereby any further decrease in temperature will cause C2 to solidify as well as C1 (Schmidt, 2007).

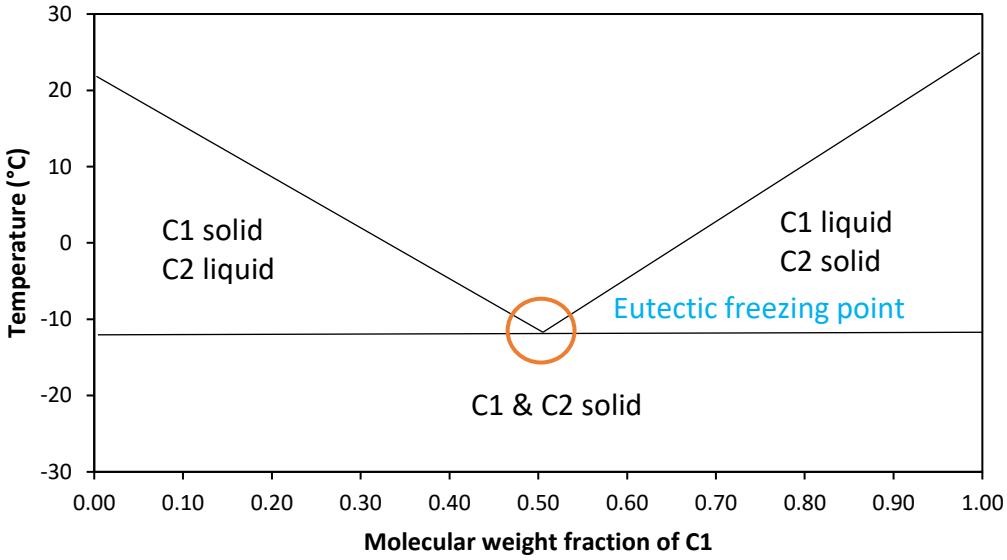

Figure 4. Visual representation of eutectic freeze crystallization using two components C1 and C2.

Although a binary system is used in Figure 4, the eutectic freezing point can be applied to a multi-component system such as human urine (Schmidt, 2007). It has been proposed to subject the urine solution to lowered temperatures at which various nutrient-rich salts can form and be recovered from the solution (Chipako and Randall, 2020b). In theory, this method has been estimated to achieve 99% nitrogen recovery at a temperature of -30°C (Randall and Nathoo, 2018).This low temperature requirement creates design challenges.

As freeze concentration would be a more efficient process when applied to pre-concentrated urine, Randall and Nathoo proposed a dual-process method (Randall and Nathoo, 2018). Firstly, reverse osmosis (RO) is used to preconcentrate the urine, then the brine from the RO process is further concentrated by freeze concentration (Randall and Nathoo, 2018).

2.7.2 Reverse osmosis/Membrane processes

To concentrate urine through a reverse osmosis (RO) membrane process, the regular osmotic process is reversed. This means that solutes are forced to move from a solution of lower concentration, to a solution of higher concentration (Rao, 2011). This is achieved through implementing an external pressure to create a driving force opposing the natural diffusion of the solutes across a membrane (Rao, 2011).

When using a RO system, the membrane operates under high pressure to produce a filtrate that is predominantly water. The majority of the remaining salts are collected in the small volume of rejected concentrates and forms a brine solution. The difficulty posed by the disposal of the RO brine formed, is a major disadvantage of using RO technologies (Tian et al., 2016). However, if used for water removal from a saline urine solution, theoretically only the water molecules should be able to penetrate and pass through the RO membrane. As a result, the remaining salts are concentrated in a brine solution. This highly concentrated solution could instead be applied as a liquid fertilizer to avoid having to dispose of the concentrated brine solution (Ek et al., 2006). However, RO membranes typically have a rejection rate of >99% for monovalent elements, but some of the salts are able to pass through the membranes.

Ek et al., also investigated nitrogen recovery from urine using RO. The same nitrogen recovery of 95% was found when using a membrane for water removal, as well as during evaporation (Ek et al., 2006). However, when compared to evaporation, a volume reduction of 80% was achieved (Ek et al., 2006). In addition, RO was found to be less than half the cost of the studied evaporation process, with a third of the energy requirement per cubic meter of urine required to be processed (Ek et al., 2006).

Reverse osmosis is not the only membrane process that is available for use. There are other methods such as forward osmosis (Zhang et al., 2014), membrane distillation and electrodialysis (Chipako and Randall, 2020b).

2.7.3 Evaporation

Evaporation allows for the removal of water from a solution, when a source of heat turns liquid water into water vapor through increasing the temperature (Antonini et al., 2012). A distillation step may follow this evaporation step to result in drinkable water from collected water vapor (Udert and Wächter, 2012).

Table 8. Advantages and disadvantages of water removal by evaporation

Advantages	Disadvantages
Least complex water removal method (Antonini *et al.*, 2012)	Loss of approximately 93% ammonia-bound nitrogen (due to urea hydrolysis), unless performed in a closed environment or use of pre-evaporation ammonia stripping to recover nitrogen (Bethune, 2015)
Observed 95% water removal and nitrogen recovery when under vaccuum conditions at 30°C (Table 8) (Ek *et al.*, 2006)	Can be energy intensive depending on chosen heat source (Antonini *et al.*, 2012)

As seen inTable 8, there are numerous challenges faced when using evaporative techniques for water removal. A major area of concern are the ammonia emissions, if evaporation of water from urine were to be performed on a large scale (Chipako and Randall, 2020b).

However, in evaporative experiments Ek et al., achieved a high water removal with high nitrogen recovery using hydrolyzed urine (Ek et al., 2006) (Table 9). This is contrasted with membrane distillation techniques which have been shown to achieve the same high nitrogen recovery, with a lower water removal (Chipako and Randall, 2020b).

As mentioned in Table 8, this also may be an energy intensive process. However, evaporation can be performed passively, without an active heat source present to lower the energy demand. In 2016, Bethune et al., studied the passive evaporation of urine obtained through source separation in dry toilets (Table 9). The urine was evaporated in urine evaporation systems (UES) specifically designed for optimal airflow (Bethune et al., 2014). In the UES design, trays of urine were housed in a wooden chamber. The sides and back of this chamber were closed, leaving the front of the chamber open to air flow. A fan and chimney were installed on the back wall of the chamber to draw air into the chamber and across the surface of the tray containing urine (Bethune et al., 2014). It was found that the increased and optimized air flow correlated to increased rates of evaporation in comparison to one of their previous studies from 2014 (Bethune et al., 2014).

In a different study, Bethune et al., found that after undergoing evaporation, highly concentrated urine produced a dark-colored brine solution, of high salinity (Bethune, 2015). This solution subsequently dried, leaving odorless residual solids composed of majority Na, Cl, N, P and K elements (Bethune et al., 2014). Bethune et al., also noted that approximately 90% of the initial free nitrogen (NH_4^+/NH_3) in solution was lost due to ammonia volatilization (Bethune, 2015).

This volatilization resulted in a significant loss of nitrogen as discussed above. This decreased the quantity of nitrogen relative to the amount of potassium and phosphorus in both the remaining brine solution and residual solids formed due to evaporation (Bethune, 2015).

By optimizing airflow in the UES as mentioned above, Bethune et al., found that increased rates of evaporation could reduce the time available for ammonia to volatize to gas. This in turn was expected to decrease the amount of nitrogen lost during the overall passive evaporation process (Bethune et al., 2014).

As previous studies on urine evaporation have been conducted at a variety of conditions, Table 9 summarizes some of the notable studies as well as findings and suggestions from these studies. Evaporation is the chosen method of water removal investigated in this study.

Table 9. Summary of urine evaporation experiments, experimental conditions and major findings and suggestions.

Summary of experimental conditions	Major findings and suggestions	References
Passive evaporation of urine obtained from waterless source separation toilets. Urine evaporated in vertically stacked trays 1 cm apart; with electrical conductivity and pH measured during evaporation. A constant temperature of 20°C and fluctuating humidity between 20% and 22% was used. Holes were drilled at alternating ends of trays so urine would flow across trays and drip down by gravity. Composition of solid product analyzed after evaporation.	Salinity increased over and evaporation rate decreased over time. Dark highly saline brine solution produced before completely drying to solid product; solid product with no odor, composed of Na, Cl, N, P and K; decreased N compared to P and K in both brine and solid product; Nitrogen loss due to NH_3 volatilization (90% initial NH_4/NH_3 lost). Observed pH 9.2 showed advanced urea hydrolysis occurred.	(Bethune, 2015)
Solar thermal evaporation in no mix sanitation system over 26 days leaving behind solid phase fertilizer. Diluted urine collected from sanitation system in University Can To Vietnam for 100 males in 10 bathrooms. 50 L undiluted urine collected directly from 100 males in neighboring dormitory. Both diluted and undiluted urine was completely hydrolyzed. Urine fed into thermal still, temperature increased due to convection and greenhouse effect. pH, total P and N, and electrical conductivity measured.	Temperatures ranged from 45°C to 62°C in thermal still during maxima, dropped to 25°C during night. 360 g solid fertilizer produced in 26 days and 2 m^2 thermal still area using hydrolyzed urine. Fertilizer mainly composed NaCl and nearly 2% P and N. Fertilizer sustained biomass. Acidified urine achieved improved nutrient contents in fertilizer and greater biomass yields when tested. Achieved using thermal energy so no requirement for technologies, workforce or energy intensive processes.	(Antonini et al., 2012)

Table 9 continued. Summary of urine evaporation experiments, experimental conditions and major findings and suggestions.

Second experiment with acidified urine to assess pH and nitrogen loss Two batches diluted urine; one dosed with H_2SO_4 (96%, 27.8 mL L^{-1} urine) and the other with H_3PO_4 (89%, 31.5 mL L^{-1} urine) After 20 days thermal evaporation solids produced and analyzed		(Antonini et al., 2012)
Hydrolyzed urine evaporated in vacuum. Temperature initially 30°C to prevent volatilization during evaporation, increased during evaporation.	95% N, 100% P and 99% K recovery with 95% water removal achieved during evaporation of urine.	(Ek et al., 2006)
Open cycle evaporation- urine processes integrated with cabin air-conditioning and humidity control, additional urine evaporator and air heater required. Fan circulates cabin air through a heater which encounters a wick evaporator. Urine is fed into wick evaporator where water vapor is formed from the urine, concentrating the urine. Water is then filtered and pumped for storage and reuse in aircraft. Urine used in wick immediately treated with 2.57 gm/L H_2SO_4 and 0.63 CrO_3 and slowly pumped into wick as needed	Easy to recover ~ 100% of water in urine using this evaporation system compared to single water recovery technique. Only water that remains unrecovered is the water trapped within the formed solids or water that is attracted to the evaporation wick material	(Putnam and Thomas, 1969)

2.8 Gaps and opportunities in literature

When concentrating fresh urine through reverse osmosis or the abovementioned freeze concentration method, there is very little research and knowledge currently available on such processes (Chipako and Randall, 2020b). This limits the available information regarding the process efficiencies.

Through consulting the literature this is not only relevant to these methods, but also to evaporative techniques. It is apparent that there is opportunity for further research around evaporation to determine what compounds are formed and in what quantities. This will allow for a better understand and economic position in the valorisation of waste contained in human urine.

The first step for this research lies in source separation as emphasized by Larsen. Larsen expresses that currently there are limited technology and institutional facilities available to allow for the success of extensive source separation of urine in urban areas (Larsen, 2020). After source separation the next area of major importance regards the understanding around the removal of water from the recovered urine. This will minimize the difficulty associated with the transportation of urine before treatment and processing (Larsen, 2020).

This thesis focused on the use of urine as an alternative to synthetic fertilizers. However, it must be noted that this is not the only application. With further research, concentrated urine may be the source of urea required to make bio-bricks and other material (Lambert and Randall, 2019).

Chapter 3. Materials and methods

The overall objective of this thesis was to determine the preferred urine stabilization method for maximum recovery of N, P and K nutrients during evaporation. Once the preferred stabilization method was known, this work then determined the independent effect of different amounts of water removal, urine composition and operating temperature on the solids formed during evaporation.

To answer the key objectives of this thesis, a series of simulations and experiments were conducted to collect the relevant information. These simulations and experiments are related to the key objectives and are summarized in Table 10.

Table 10. Summary of aims and objectives with the corresponding simulation and experimental conditions.

Aim	Simulation/Experiment	Simulation/Experimental conditions			
1. Experimentally determine what the preferred urine stabilization technique is at 100% water removal in terms of major nutrient recovery (N, P and K). Compare experimental recovery to simulated recovery to determine how realistic such thermodynamic predictions are.	E1 – 9	**Urine type and treatment**	**Real urine**	**Treatment dosage**	**pH**
			Fresh	-	6.8
			Hydrolyzed	1 mL urease/L for 48 hrs	9
			$Ca(OH)_2$ stabilized	10 g $Ca(OH)_2$/L	12.5
		Urine type and treatment	**Synthetic urine**	**Treatment dosage**	**pH**
			Fresh (U1a)	-	6.3
			Hydrolyzed (U1h)	1 mL urease/L for 48 hrs	9
			$Ca(OH)_2$ stabilized (U1b)	10 g $Ca(OH)_2$/L	12.5
			MgO stabilized	1.5 g MgO/L	10
			Acetic acid stabilized	35 mL 0.5 M acid/L	3
			Citric acid stabilized	5 mL 0.5 M acid/L	3
		Temperature: ~25°C (ambient) **Humidity:** Ambient **Water removal:** 100%			
	S23 – S31 [8]	**Temperature:** 25°C			
2. Determine the mass of total solids and major component (N, P and K) recovery at three different water removals (50%, 75% and 100%). Compare experimental results to simulation results.		**Urine type:** filtered $Ca(OH)_2$ stabilized synthetic urine **Temperature:** 40°C **Humidity:** 40%			
	E19/S2	**Water removal:** 50%			
	E20/S2	**Water removal:** 75%			
	E18/S2	**Water removal:** 100%			

[8] Simulation entries are indicated by grey shading and experimental entries are indicated by no shading. For all simulation conditions, humidity conditions were irrelevant and water removal intervals from 0% to 100% were used, unless otherwise stated.

Table 10 continued. Summary of aims and objectives with the corresponding simulation and experimental conditions.

Aim	Simulation/Experiment	Simulation/Experimental conditions
3. Determine the effect of urine composition on solids formed in $Ca(OH)_2$ stabilized urine at a fixed temperature.	S12	**Temperature:** 40°C **Urine type:** $Ca(OH)_2$ stabilized synthetic, varied composition **Urine composition:** U1b, U2b, U3b, U4b and U5b (see Table 12 for values)
4. Determine the effect of temperature on the solids formed in $Ca(OH)_2$ stabilized urine.	S2	**Urine type:** $Ca(OH)_2$ stabilized synthetic urine (U1b) **Temperature:** 20°C to 70°C
5. Use this information to determine the energy requirement to evaporate $Ca(OH)_2$ stabilized urine	S2 S10 – S15	**Cost calculation:** Based on operating temperature **Cost calculation:** Based on urine composition (See 3 and 4 above for temperature and urine conditions)

3.1 Simulation tools, procedure, and required input information

The simulations in Table 10 were performed using the Stream Analyzer software component associated with OLI Studio version 10 software. Output simulation data was then transferred into Microsoft Excel and further interpreted or compared to the relevant experimental results (see Chapter 4).

OLI Studio software is a simulation tool based on theoretical thermodynamics. OLI software enables users to study the aqueous chemistry and electrolytic chemical processes that are predicted to occur in aqueous systems. The OLI Stream Analyzer component is the main interface of OLI software (OLI Systems, 2018). This Stream Analyzer component was used for all urine evaporation simulations conducted throughout this thesis and going forward, will be referred to as 'OLI'. As a tool, OLI was used to perform thermodynamic calculations for the specified system. Calculations aimed to determine various thermophysical properties for a system, such as how chemical species will distribute in solution, understanding various phase equilibria situations, and molar flows or mass balances for a system. OLI also described additional thermodynamic qualities for a system such as density, heat capacity and enthalpy. The overall simulation procedure is given in Appendix A.1. This simulation procedure, as well as experimental work, relied on the composition of fresh urine shown in Table 11.

Table 11. Composition of fresh urine (U1a) taken from Randall et al., 2016. All values represent the measured component, measured in g m^{-3}. In the case of nitrogen, measurements were converted to the relevant units and values as required for use in OLI simulations. These converted values are quoted in red text. Values used in OLI simulations are quoted in bold text.

Measurement	**Units**	**U1a** (Randall et al., 2016)	**U2a** (Rose et al., 2015)	**U3a** (K.M. Udert et al., 2003)	**U4a** (Kai M. Udert et al., 2003)	**U5a** (Etter et al., 2014)
TIC	g m^{-3}	28	-	-	-	-
Urea	**g urea m^{-3}**	**11625.9**	**16300**	**16200**	**18800**	**9550**
PO_4-P	**g m^{-3}**	**260**	**472**	**743**	**559**	**388**
NH_3-N	g m^{-3}	436	465	476	386	-
NH_4^+	**g NH_4^+ m^{-3}**	**561.8**	**599**	**613**	**497**	**564**
Dissolved COD	g m^{-3}	6400	8440	-	8150	7660
Cl^-	**g m^{-3}**	**4430**	**5140**	**3900**	**5230**	**6620**
SO_4^{-2}	**g m^{-3}**	**825**	**2075**	**1540**	**1350**	**878**
Na^+	**g m^{-3}**	**2510**	**2780**	**2760**	**3730**	**3240**
K^+	**g m^{-3}**	**469**	**1680**	**2190**	**2250**	**1870**
Ca^{+2}	**g m^{-3}**	**132**	**111**	**184**	**168**	**89.2**
Mg^{+2}	**g m^{-3}**	**57**	**95.0**	**94.8**	**121**	**45.4**
pH	**-**	**6.3**	**6.2**	**6.2**	**6**	**5.6**
Temperature	**°C**	**25.0**	**25.0**	**25.0**	**25.0**	**25.0**
Charge imbalance	%	-1.12	-5.24	2.95	7.25	3.05

3.1.1 $Ca(OH)_2$ stabilized urine (b) composition from initial fresh urine (a) composition

As suggested by Randall et al., fresh urine can be stabilized using a $Ca(OH)_2$ dosage of 10 g L^{-1} (Randall et al., 2016). After dosing and stabilizing fresh urine, an intermediate filtration step could follow in laboratory-based experiments. This intermediate filtration step removes precipitates which form during the stabilization process prior to evaporative processes (Randall et al., 2016). Such precipitates are mainly composed of Mg^{+2} and PO_4^{-3} components, as well as excess Ca^{+2} (Randall et al., 2016).

Using the initial fresh urine compositions, $Ca(OH)_2$ stabilized urine compositions were simulated including the intermediate filtration step. This was simulated by using the steps outlined in Figure 20 (Appendix A.1) below. A detailed step-by-step example whereby U1a is stabilized with $Ca(OH)_2$ in OLI is presented in Appendix A.1 (see Figure 22) . Resulting filtered $Ca(OH)_2$ stabilized urine compositions for the five fresh urine compositions, are listed in Table 12.

It was also desired to investigate the effect of an unfiltered $Ca(OH)_2$ stabilized solution during water removal processes. To simulate this stream in OLI, the abovementioned $Ca(OH)_2$ stabilization methodology was followed. However, instead of only selecting the liquid phase (step 6, Appendix A.1), all phases were included when adding the $Ca(OH)_2$ dosed stream. This stream was then used in the relevant simulations as done with other streams discussed.

Table 12. Composition of $Ca(OH)_2$ stabilized urine. Values represent the measured component, measured in g m^{-3}. In the case of nitrogen, measurements were converted to the relevant units and values as required for use in OLI simulations. These converted values are quoted in red text. Values used in OLI simulations are quoted in bold text.

Measurement	**Units**	**U1b** (Randall et al., 2016)	**U2b** (Rose et al., 2015)	**U3b** (K.M. Udert et al., 2003)	**U4b** (Kai M. Udert et al., 2003)	**U5b** (Etter et al., 2014)
TIC	g m^{-3}	28	-	-	-	-
Urea	**g urea m^{-3}**	**11625.9**	**16300**	**16200**	**18800**	**9550**
PO_4-P	**g m^{-3}**	**260**	**472**	**743**	**559**	**388**
NH_3-N	g m^{-3}	436	465	476	386	-
NH_4^+	**g NH_4^+ m^{-3}**	**561.8**	**599**	**613**	**497**	**564**
Dissolved COD	g m^{-3}	6400	8440	-	8150	7660
Cl^-	**g m^{-3}**	**4430**	**5140**	**3900**	**5230**	**6620**
SO_4^{-2}	**g m^{-3}**	**825**	**2075**	**1540**	**1350**	**878**
Na^+	**g m^{-3}**	**2510**	**2780**	**2760**	**3730**	**3240**
K^+	**g m^{-3}**	**469**	**1680**	**2190**	**2250**	**1870**
Ca^{+2} (unfiltered)	g m^{-3}	5541	5520	5594	5577	5498
Ca^{+2} (filtered)	**g m^{-3}**	**1465**	**1490**	**1325**	**1414**	**1482**
Mg^{+2}	**g m^{-3}**	**57**	**95.0**	**94.8**	**121**	**45.4**
pH	**-**	**6.3**	**6.2**	**6.2**	**6**	**5.6**
Temperature	**°C**	**25.0**	**25.0**	**25.0**	**25.0**	**25.0**
Charge imbalance	%	-1.12	-5.24	2.95	7.25	3.05

3.1.2 Hydrolyzed urine (h) composition from initial fresh urine (a) composition

Like urine stabilized with $Ca(OH)_2$, the composition of hydrolyzed urine streams needed to be derived from the compositions of the fresh urine streams that were available. To do so, it was assumed that all urea in the fresh urine solutions would have degraded through urea hydrolysis, to form CO_3^{-2} and NH_4^+ ions (See Appendix A.1) (Kai M. Udert et al., 2003). This degradation was based purely on perfect stoichiometric conversions, assuming negligible loss of components through volatilization. Example calculations and the composition of hydrolyzed urine solutions are shown in Appendix A.1.

3.1.3 Additional simulation input specifications: temperature and water removal

The last two remaining input variables that needed to be specified in the OLI simulations were the survey temperature, as well as the required water removal intervals over which the composition survey was to be run.

As the effect of temperature on urine evaporation was a point of interest in this thesis, survey temperatures between 20°C and 70°C were used. A step size of 10°C between these two temperature boundaries was used when studying the effect of temperature with a fixed urine composition. Appendix A.1 contains a detailed discussion on the water removal intervals while using survey compositions in this thesis.

3.1.4 Simulation structure and complete summary of required input information

After determining the abovementioned input specifications, OLI simulations could be generated, and results collected for analysis. Following the abovementioned overall simulation structure in Figure 20 (Appendix A.1), the overall simulation section was structured following one of the two paths. Figure 23 and Figure 24 (Appendix A.1) outline the basic overall structure for the two simulation paths studied using OLI simulations.

3.1.4.1 Fixed urine composition and varied temperature simulations

The first simulation path (Figure 23 Appendix A.1) was concerned with studying the effect of varied temperature on the type of individual solids formed, the distribution of N, P and K nutrients, as well as the energy requirements associated with such water removal processes when using a fixed composition for the chosen type of urine. This was repeated for each of the three types of urine using a fixed initial composition i.e. U1a, U1b, and U1h.

3.1.4.2 Fixed temperature and varied urine composition simulations

The second simulation path outlined using Figure 24 Appendix A.1, was the inverse of the first simulation path. This path studied the effect of five different urine compositions, for the chosen type of urine, at a fixed simulation temperature. The same output variables as collected in the first simulation path, were collected for the second path. For example, this was done at 20°C for U1a, U2a, U3a, U4a and U5a. These simulations were then repeated for temperatures from 20°C to 70°C for all three types of urine.

As numerous simulations following one of the two above paths were conducted, Table 13 summarizes performed simulations by number. The input specifications used in simulations is also summarized in Table 13.

Table 13. Complete summary of simulation numbers and simulation input specifications used for OLI simulations in this work

Simulation number (S)	Simulation path	Thermodynamic framework	Urine composition/s	Temperature (°C)		Water removal (%)	Step size
				Composition	Simulation		
1	1	MSE with H_3O^+ ion	U1a	25	20-70	0-100	50 steps
2			U1b (filtered)				
3			U1h				
4, 5, 6, 7, 8, 9	2	MSE with H_3O^+ ion	U1a-U5a	25	20, 30, 40, 50, 60 ,70	0-100	50 steps
10, 11, 12, 13, 14, 15			U1b-U5b (filtered)				
16, 17, 18, 19, 20, 21			U1h-U5h				
22	1	MSE with H_3O^+ ion	U1b (unfiltered)	NA	40	0-100	50 steps
23	1	MSE with H_3O^+ ion	E1[9]	NA	25	0-100	50 steps
24			E2				
25			E3				
26			E4				
27			E5				
28			E6				
29			E7				
30			E8				
31			E9				

[9] For all urine compositions with an E composition refer to Section 0 below

3.2 Output from OLI simulations

From the generated OLI simulations, various aspects of the available results were collected as output variables. The aspects of the collected results are listed below:

Required information collected from simulations

1. Mass of total solids formed as a function of water removal;
2. Predicted mass and identity of individual solids expected to form in solution during water removal;
3. Phase distribution, on a mass and molar basis, as a function of water removal;
4. Element balance in each of the phases present, as a function of water removal (particularly for elements N, P and K);
5. Solution enthalpy as a function of water removal.

3.2.1 Interpreting simulation results: Yield definition

From the collected information, one major aspect of analysis concerned the calculation of the yield of solids formed as a function of water removal. At different conditions, the studied urine solution may have already been saturated with certain compounds prior to any water removal and hence resulted in an apparent large mass of total solids. However, when disregarding these compounds, the mass of solids that formed during water removal was seen to be smaller than initially anticipated. Hence, the yield of solids formed was a parameter that was calculated to quantify the total amount of solids formed universally between all simulations.

As the definition of yield may vary, the way yield was calculated when interpreting simulation results, is defined using Equation (**4** below. As certain solids may have been present prior to water removal processes, the yield definition was based on a principle of difference as indicated below:

$$Yield\ (\%) = \frac{Mass\ of\ solids\ for\ interval_i}{Maximum\ mass\ of\ solids} \times 100 \quad \textbf{(4)}$$

$$Mass\ of\ solids\ for\ interval_i = Mass\ of\ solids\ at\ interval_{end\ i} - mass\ of\ solids\ at\ interval_{start\ i} \quad \textbf{(5)}$$

$$Maximum\ mass\ of\ solids = Mass\ of\ solids\ at\ 100\%\ removal - mass\ of\ solids\ at\ 0\%\ removal \quad \textbf{(6)}$$

3.3 Additional considerations for OLI modelling

When using OLI as a simulation tool, there were additional considerations that needed to be considered when specifying input variables for each OLI simulation. The first consideration was the individual solids that were predicted to form.

3.3.1 Expected solid phases

OLI contains an extensive database of solid compounds from which thermodynamic predictions are made. OLI additionally allows for these predicted solids to be refined through the selection of solids realistically expected to form. This prevents unrealistic solids predictions to be eliminated from the simulation results.

To be consistent with previous research, as well as allow for this realistic consideration of solids expected to form, a previous study published in 2016 by Randall et al., was used as a basis for the list of possible solids. The list of solids expected to form when evaporating water from human urine, was presented in a study in Table 1 by Randall et al., 2016. These expected solids are summarized in Table 25 found in Appendix A.1.

Table 25 was used when selecting potential solids expected to form. This simulation step was done for all simulations and could be done under advanced chemistry, in the chemistry tab found on the main OLI interface.

3.3.2 Temperature and humidity considerations

Additionally, OLI could not incorporate and account for humidity in simulations. Therefore it was assumed that all OLI simulation results were obtained at the specified input simulation temperature and at a very low humidity.

Conversely, temperature could be specified in OLI simulations. Simulations were run from a temperature of 20°C to a temperature of 70°C, in 10°C intervals. Considering Figure 3, this temperature range covers all regions over which urea hydrolysis could potentially be observed or avoided. At any temperature over 70°C, it is expected that urea hydrolysis would occur chemically at a rapid rate due to the high operating temperature (Randall et al., 2016). Due to this, exceeding 70°C was deemed unnecessary for this thesis.

3.3.3 Urea hydrolysis

Lastly, at temperatures greater than 40°C significant chemical urea hydrolysis has been observed (Randall et al., 2016). This was not accounted for in OLI simulations. Hence, a series of urea hydrolysis experiments were run at elevated temperatures to quantify the hydrolysis occurring. Temperatures from 40°C to 70°C at a fixed relative humidity were investigated.

3.4 Experimental methods and materials

A second aspect to this thesis was the element of experimental work. Experimental work was limited due to the COVID-19 pandemic and various limitations to the experimental work is discussed under the various methodologies below. Although limited, experimental methods outlined under Section 3.4, focused primarily on urine treatment techniques and the evaporative process, as well as validating OLI modelling from the discussed computational methods from above. This is shown in Figure 25 (Appendix A.2).

When investigating urine treatment, the best treatment technique was determined by studying the recovery of major nutrients namely N, P and K, associated with various different treatment types. Treatment types included no treatment (fresh and hydrolyzed urine) or stabilization. Either alkalinization ($Ca(OH)_2$ or MgO) or acidification (acetic acid or citric acid) were used as stabilization techniques. The detailed treatment methods followed are discussed under Sections 3.5.1 to 3.5.5.

From Figure 25 in Appendix A.2, the experimental work concerned with the validation of OLI modelling, involved a series of sub-experiments. These sub-experiments focused on identifying the individual solids formed during evaporation, quantifying urea hydrolysis at elevated temperatures, and considering the scale formed when evaporating urine solutions.

3.5 Urine stabilization techniques

3.5.1 NPK recovery experiments

To determine the best urine stabilization treatment technique for water removal processes, nine different urine solutions were evaporated. The recovery of major nutrients N, P and K was measured at the end of evaporation processes and this was used to determine the best stabilization method. A list of the nine urine solutions is given below:

1. Real fresh urine
2. Real $Ca(OH)_2$ stabilized urine
3. Real hydrolyzed urine
4. Synthetic fresh urine
5. Synthetic hydrolyzed urine
6. Base addition 1: $Ca(OH)_2$ stabilized synthetic urine
7. Base addition 2: MgO stabilized synthetic urine
8. Acid addition 1: acetic acid stabilized synthetic urine
9. Acid addition 2: citric acid stabilized synthetic urine

Fresh and hydrolyzed urine (1, 3, 4 and 5) did not follow a urine treatment/stabilization method. Fresh urine needed to be used within 24-48 hours of collection to avoid urea hydrolysis. Conversely, hydrolyzed urine had been left to allow urea to degrade or hydrolyze. To speed up this degradation process, urease was added to the relevant urine solutions prior to evaporation. Additionally, four treatments to stabilize urine solutions were considered. Two treatment methods investigated acidifying urine solutions, and the other two methods considered urine stabilization through the addition of a base.

Previously when conducting experimental work, human urine was collected from the male bathroom in New Engineering Building at the University of Cape Town. This collection was done in accordance with the relevant ethical considerations. The COVID-19 pandemic meant that urine could no longer be collected in this way. Hence, an alternative synthetic urine stream was developed and mixed for use in the experimental work. Small quantities of human urine could be collected due to a limited number of additional researchers present in the Water Quality Laboratory. This allowed for real urine to be used in a limited number of experimental runs.

3.5.2 Real urine

3.5.2.1 Proposed urine collection

When collecting human urine, a novel nutrient recovery urinal was used as the waterless urinal to collect real human urine (Flanagan and Randall, 2018). This urinal was placed in a male bathroom in the New Engineering Building, allowing for anonymous urine donations.

3.5.2.2 Proposed urine stabilization

For all three real urine experimental runs, the same fresh urine was used. As mentioned above, when using fresh urine (1), the collected fresh urine needed to be used within 24-48 hours. When collecting $Ca(OH)_2$ stabilized urine (2), there was no time limit to when the urine needed to be used, provided the collection container was sealed. However, when collected, 10 g L^{-1} $Ca(OH)_2$ was added to the collected fresh urine straight after collection to eliminate urea hydrolysis. This was mixed for 15 minutes prior to filtering the then stabilized solution using filter paper with a pore size of 1.2 µm (Munktell Filtrek™, Bärenstein, Germany).

In the case of hydrolyzed human urine (3), the required volume of the collected fresh urine was taken and set aside for hydrolysis to occur. This urine was placed in a Schott bottle and dosed with 1 mL Jack Bean urease (U1875- 25 mL, Sigma Aldrich, Germany) per liter of fresh urine. The Schott bottle was sealed and placed on a shaker at 150 rpm for 48 hours. This process ensured that the urea content of the fresh urine was readily degraded resulting in a hydrolyzed urine solution.

3.5.3 COVID-19 adjusted urine collection and handling procedure

Urine collection methods outlined above, were altered due to the climate created by the COVID-19 pandemic. The large-scale collection of human urine on campus was no longer a viable option. As a result, experimental work largely focused on the use of synthetic urine, with the fresh synthetic urine recipe outlined below.

In using synthetic urine, the initial urine composition across all experiments was kept constant. In addition, the composition of synthetic urine could be matched to the input urine composition used in OLI simulations, thus allowing for greater consistency as well as a better comparison between experimental and theoretical results.

3.5.4 Synthetic urine

To produce a source of synthetic fresh urine (4), chemical salts were dissolved in deionized water, according to an adjusted recipe. A recipe from the VUNA handbook for fresh synthetic urine, was used as the basis for the fresh synthetic urine used throughout this thesis (Etter et al., 2014). This recipe was adjusted to use the chemical salts available in the Water Quality Laboratory, as well as to match the major ion concentrations of U1a above (Table 11). The VUNA recipe and adjustment calculations are outlined in Appendix A.2.

3.5.4.1 Fresh synthetic urine

After following the synthetic fresh urine recipe in Table 27 Appendix A.2, the solution was well mixed and the pH of the solution was measured.

When treating urine using different treatment techniques, the above method for synthetic fresh urine was always followed. The resulting synthetic fresh urine solution was then treated according to the relevant urine treatment procedures as specified below.

3.5.4.2 Hydrolyzed synthetic urine

To obtain a solution of synthetic hydrolyzed urine (5), synthetic fresh urine was mixed according to Table 27 (Appendix A.2). Before hydrolyzing the synthetic urine, the composition of the fresh synthetic urine solution was measured in the ThermoScientific Gallery (TSG) (ThermoFisher Scientific, Massachusetts, United States) using the pre-experimental sampling procedures below. Jack bean urease (U1875- 25 mL, Sigma Aldrich, Germany) was then added to the synthetic fresh urine solution. A dosage of one milliliter urease (Sigma Aldrich, Germany) per liter of synthetic fresh urine, was used. The flask was sealed with parafilm and left for a period of 96 hours to allow for the complete degradation of urea. The flask was left on a shaker at 70 rpm for this time period.

After this period, before experimentation began, the composition of the hydrolyzed synthetic urine was measured using the TSG. It was expected that the urea content of the synthetic urine would be minimal due to the presence of added urease. As a result of the urea degradation, the ammonia concentration of the synthetic urine was expected to have increased to 7550 mg L^{-1} as in U1h (Appendix A.2). However, this was not the case as over time the parafilm had perforated and as a result ammonia was lost through volatilization.

Similar to hydrolyzed synthetic urine, stabilized urine was obtained through treating the synthetic fresh urine solution. Prior to stabilization, the composition of the synthetic fresh urine solution was measured in the TSG using pre-experimental sampling techniques. The composition of the stabilized urine solution was then re-measured using the TSG, using the post experimental/stabilization sampling techniques (see Appendix A.2).

Urine stabilization treatment techniques included dosing with basic salts ($Ca(OH)_2$ and MgO) to operate at a pH greater than 8.6, and acidification. Acetic and citric acid dosing was used to stabilize urine to a pH below 3.5.

3.5.4.3 Stabilized synthetic urine ($Ca(OH)_2$ and MgO)

When stabilizing urine with $Ca(OH)_2$, a pH greater than 11 was desired (Randall et al., 2016). To ensure that the pH of the solution did not change, it was desired to add an amount of the chosen base to the solution, that would result in reaching the saturation pH of the solution. For a safety factor, slightly more than the exact saturation amount was added to each solution.

Using the composition of U1a in OLI, saturation pH curves for both stabilization treatments were generated. A pH of 12.5 was used for $Ca(OH)_2$ treatment and a pH of 10 was used for MgO treatment (Appendix A.2). These pH values minimized the potential chemical urea hydrolysis.

When stabilizing with $Ca(OH)_2$, a dosage of 10 g L^{-1} $Ca(OH)_2$ (CAL005-5 kg, Kimix Chemicals and Lab supplies cc., Eppingdust) was used. This was mixed well for 15 minutes, before filtering the synthetic solution using a 1.2 µm pore size filter paper (Munktell Filtrek™,

Bärenstein, Germany). The initial $Ca(OH)_2$ stabilized synthetic urine (6) composition was determined using the TSG. TheMgO Stabilization treatment followed the same methodology. However, in this case a dosage of 1.5 g L^{-1} MgO (342793-1 kg, Sigma Aldrich, Germany) was used instead to obtain the initial MgO stabilized synthetic urine solution (7).

3.5.4.4 Stabilized synthetic urine (acetic acid and citric acid)

A second treatment route is to stabilize urine through acidification. The addition of an acid lowers the pH of the urine solution beyond the pH at which the enzyme urease can operate to degrade urea. As mentioned above, a pH below 3.5 would inhibit urease activity, However, a slightly lower pH value of 3 was chosen to ensure that the urine was adequately stabilized.

For both urine stabilization with acetic (8) and citric (9) acid, the method of urine treatment was the same. The first step was to make 0.5 M solutions of both acetic and citric acid. For acetic acid stabilization, 14.4 mL of glacial acetic acid (>99% purity) (1018302500-2.5 L, Merck, Germany) was added to 500 mL of deionized water. To create a 0.5 M citric acid solution 52.5 g of citric acid monohydrate ($C_6H_8O_7.H_2O$) (CIA020-500g, Kimix Chemicals and Lab supplies cc., Eppingdust) was dissolved in 500 mL deionized water.

Four liters of fresh synthetic urine was mixed in a flask and placed on a magnetic stirrer plate. Slowly, 0.5 M acid was added to the synthetic fresh urine in fixed volumes of one milliliter at a time. The solution was continuously gently mixed, and the pH of the solution was continuously monitored. The volume of acid added to the solution was recorded, and acidification of the fresh synthetic urine was terminated once the pH of the solution settled at a pH 3. At this point the acidified urine was ready for the experimental run (See general NPK method below).

3.5.5 General NPK experimental method

The nine treated urine solutions discussed above, were mixed or collected, and treated according to the abovementioned methodologies. Each urine solution was then filtered using 1.2 µm filter paper (Munktell Filtrek™, Bärenstein, Germany).

To repeat each experimental run in triplicate, three evaporation trays were cleaned using a water wash, followed by an acid wash and then two deionized water rinses. The trays were dried and then the empty masses of each tray were measured and recorded using the balance (PS 4500.X2.M, RADWAG, Poland). A 1 L measuring cylinder was used to measure the required volume of urine solution as shown below. The measured volume was added to a tray and the full mass of the tray was remeasured and recorded as the starting full mass. This step was repeated for the remaining two trays.

It was noted that a smaller volume of real urine was used for fresh, hydrolyzed and $Ca(OH)_2$ stabilized urine experimental runs. This lowered volume was used because the fresh urine used in all three experimental runs was kept the same. The fresh urine was treated accordingly to obtained $Ca(OH)_2$ stabilized and hydrolyzed urine solutions. For synthetic urine solutions, a volume of 0.95 L, compared to 1 L was used as a portion of the initial urine solution was retained for analyzing the initial composition of the solution.

The pH of each solution in the three trays was measured and recorded before starting the experimental run. The pH was measured using a flat-tipped pH probe (3 M KCl, Metrohm, Switzerland). Each full tray was placed under a 2.4 W fan which blew air directly onto the tray below. This is shown in the experimental set-up illustrated in Figure 26 (Appendix A.2).

The mass of each tray was measured daily, and the trays were left until these mass reading did not change. This meant that the maximum amount of water was removed through evaporation from each tray and the trays were as close as possible to 100% water removal.

Table 14. NPK solution and experiment number for the nine urine solutions studied during NPK experiments. The volume and treatment for each urine solution is summarized below.

Experiment number	NPK solution	Pre-evaporation filtration	Volume (L)	Treatment description
E1	1	1.2 µm filtration	0.5	NA; fresh urine used within 24-48 hours of collection
E2	2		0.3	10 g L^{-1} $Ca(OH)_2$ added to fresh urine straight after collection, mixed for 15 minutes prior to filtration
E3	3		0.3	1 mL urease L^{-1} fresh urine, added straight after collection, left for 48 hours on shaker at 150 rpm in sealed Schott bottle
E4	4	1.2 µm filtration	0.95	NA, synthetic fresh urine
E5	5			1 mL urease L^{-1} fresh synthetic urine, added and left for 96 hours on shaker at 70 rpm in flask sealed with parafilm
E6	6			10 g L^{-1} $Ca(OH)_2$ added to fresh synthetic urine mixed for 15 minutes prior to filtration
E7	7			1.5 g L^{-1} MgO added to fresh synthetic urine mixed for 15 minutes prior to filtration
E8	8			35 mL L^{-1} 0.5 M acetic acid added to fresh synthetic urine
E9	9			5 mL L^{-1} 0.5 M citric acid added to fresh synthetic urine

3.5.5.1 Theoretical NPK comparison simulations

Experimental NPK results were compared to OLI predicted NPK results. This was done by conducting additional NPK OLI simulations (Table 13). NPK simulations used the measured initial urine composition in terms of major ion concentrations at 25°C. The measured urine compositions can be found in Appendix C. Figure 23 (Appendix A.2) was used as the OLI simulation path for NPK simulations, however temperature was not varied in this case.

OLI simulations were run to simulate a 100% water removal using a composition survey. The results from the composition survey were copied into Microsoft Excel and analyzed to obtain the NPK recovery, in the same manner experimental NPK recoveries were calculated.

3.6 Understanding OLI simulations

The second aspect of experimental work aimed to further understand OLI simulations for urine evaporation, as well as validate the results obtained through the above simulation methodologies. This aspect of experimental work focused on aspects of simulations that needed further understanding, such as urea hydrolysis, and the suitability in using a synthetic urine stream. This experimental work also investigated the validity of OLI results by comparing the actual total solids formed versus the simulation prediction sand compared the types of solids that formed.

3.6.1 Urea hydrolysis

To quantify the urea hydrolysis that occurred experimentally, a series of urea solutions were evaporated at temperatures from 40°C to 70°C, with a 10°C step size. As chemical urea hydrolysis has been predicted to be present at temperatures greater than 40°C, it was deemed unnecessary to study lower temperatures of 20°C and 30°C (Randall et al., 2016). Additionally, as temperature and humidity would have an impact on the kinetics of evaporation, the urea hydrolysis experiments were conducted in a climate chamber (TH3 PE 100, Jeio Tech, Koera) at a low fixed humidity, controlled at 40%. All urea hydrolysis experiments, discussed below, are summarized in Table 15.

Table 15. Summarized urea hydrolysis experiments with experiment number, experimental conditions and initial solution composition used in experimental runs.

Experiment number	Solution	Experimental conditions			
		Temperature (°C)	Humidity (%)	Water removal (%)	Time (h)
E10	10 g urea in 500 mL	40	40	~100	95
E11		50			
E12		60			
E13		70			
E14		40			95
E15		70			40

3.6.1.1 Set time period urea hydrolysis experiments

Set time urea experiments (E10-E13) were conducted for a fixed time period of 95 hours. This was fixed as it was assumed that a higher temperature would result in a faster water removal.

However, this may not have allowed the urea in solution sufficient time to hydrolyze. Hence, for an accurate comparison, the only variable changed in the first set of urea hydrolysis experiments was the temperature at which the urea solution was evaporated.

Urea hydrolysis experiments were performed in triplicate, using three separate labelled trays. Three separate urea solutions were made by dissolving 10 g urea (U1250-5 kg, Merck, Germany) in 500 mL deionized water in three separate volumetric flasks respectively. The mass of urea added to each solution was recorded, and each solution was mixed well for 25 minutes using a magnetic stirrer. While mixing the urea solutions, the three small trays were rinsed well with deionized water and dried. Once dried, the mass of each small empty tray was measured using the balance (PS4500.X2.M, RADWAG, Poland) and recorded as the empty tray mass.

Each respective urea solution was added to the relevant tray and the mass of the full tray and solution was measured and recorded. All trays were then carefully added to the climate chamber at relevant temperature and humidity conditions. When all trays were in the chamber, the timer was started for a run time of 95 hours.

After 95 hours, the trays were removed from the chamber and the mass of each tray and the solid urea remaining, was measured using the same balance (PS4500.X2.M, RADWAG, Poland). The difference in the amount of urea initially added to each tray, and the amount of urea remaining, allowed one to quantify the extent of urea hydrolysis occurring at 40°C, 50°C, 60°C and 70°C over a set period of time.

3.6.1.2 Varied time urea hydrolysis experiments

A second element to urea hydrolysis experiments was introduced when there was a small extent of hydrolysis observed at 40°C and 70°C, despite the drying times varying greatly. The 40°C solution took 95 hours to reach 100% water removal. However, the 70°C solution had reached 100% water removal after 40 hours despite being left for the full period of 95 hours.

The above experiments as outlined above, were repeated at 40°C (E14) and 70°C (E15). However, during these experimental runs, one of the three trays was placed on top of the balance (PS4500.X2.M, RADWAG, Poland) inside the chamber. The mass of the solution and tray was measured over time and the experimental run was terminated at the point when the solution reached approximately 100% water removal. This point was determined when the mass of the solution and tray no longer was changing over time. When repeating the two above experimental runs, the time for which the solution was left to evaporate varied and was not set at 95 hours as above.

In addition to urea hydrolysis, the second aspect to understanding the OLI simulations was to understand how the use of a synthetic urine stream (used in simulations) would compare to human urine. The use of synthetic urine did not consider various other organic compounds normally present in human urine, other than urea. To allow for a comparison to be drawn the following methodologies outline below were followed.

3.6.2 Real versus synthetic urine

Three liters of real human urine were collected using the COVID-19 adjusted method discussed in Section 3.5.2.1. A small sample of fresh urine was taken to determine the initial

fresh urine composition using the ThermoScientific Gallery (TSG) (ThermoFisher Scientific, Massachusetts, United States). Samples were prepared using pre-experimental sampling techniques.

The collected urine was then stabilized with 10 g L^{-1} $Ca(OH)_2$, to ensure minimal urea degradation (E16). The stabilized human urine was filtered using 1.2 µm filter paper, and initial composition samples were prepared for analysis in the TSG using post-experimental/stabilization sampling techniques. Filtering the stabilized urine removed excess $Ca(OH)_2$ and any precipitated that had form.

Similarly, three liters of synthetic fresh urine was mixed according to the adjusted recipe in Table 27 (Appendix A.2). The composition of this fresh urine was measured using pre-experimental sampling techniques. After this, the synthetic fresh urine was stabilized using a $Ca(OH)_2$ dosage of 10 g L^{-1} and filtered to 1.2 µm Post-experimental/sampling techniques (Appendix A) were then used to measure the final $Ca(OH)_2$ stabilized synthetic urine composition.

3.6.2.1 Stabilized urine ($Ca(OH)_2$ not in excess)

Three trays were washed with water, then 0.08 M HCl. This was followed by two de-ionized water rinses. The trays were then dried, and the mass of the empty trays was taken using the balance (PS4500.X2.M, RADWAG, Poland) and recorded. One liter of the filtered $Ca(OH)_2$ stabilized human urine was added to each tray. The mass and initial pH of each full tray was recorded using the balance and flat-tipped pH probe (3 M KCl, Metrohm, Switzerland) respectively. The three trays were then placed into the chamber (TH3 PE 100, Jeio Tech, Korea) at 40°C and a controlled 40% relative humidity to evaporate the solutions to approximately 100% removal.

Tray one was placed on the balance which was placed inside the chamber. The mass of this tray was measured over time. This information was recorded on the computer connected to the balance every ten minutes, throughout the duration of the experiment. The flat-tipped pH probe was also placed into tray one, to log the pH of this tray every ten minutes to correspond to the recorded mass data.

The experiment was run until all water was removed from urine added to each tray (100% removal). This was the point at which the mass reading remained unchanged. At this point, the chamber was stopped. The mass of each tray was taken using the balance and recorded. This allowed for the total mass of solids formed to be determined as follows:

$$Mass\ solids = Remaining\ solids\ and\ tray\ mass - Initial\ empty\ tray\ mass \quad \textbf{(7)}$$

The solids formed were then dissolved in deionized water to use the elemental analysis procedure described below. The above experimental procedure was repeated using the filtered synthetic $Ca(OH)_2$ stabilized synthetic urine (E18).

3.6.2.2 Stabilized urine ($Ca(OH)_2$ in excess)

Similar to experiment E16 outlined above, an additional experiment using $Ca(OH)_2$ stabilized urine was run. The methodology for this experiment was identical to that of E16 above with one step omitted - the pre-evaporation filtration step. This meant that the collected human urine was dosed with 10 g L^{-1} $Ca(OH)_2$ and not filtered prior to evaporation. Excess $Ca(OH)_2$ and any solids precipitates were not removed from the solution and were recovered with the final solids post-evaporation. Experimental conditions for human and synthetic $Ca(OH)_2$ urine are summarized in Table 16.

Table 16. Summarized experimental conditions used when evaporating real and synthetic stabilized urine solutions in the climate chamber (TH3 PE 100, Jeio Tech, Korea).

Experiment number	Type of urine	Experimental conditions			
		Temperature (°C)	Humidity (%)	Water removal (%)	Pre-evaporation filtration
E16	$Ca(OH)_2$ stabilized human (no excess)	40	40	~100	1.2 µm
E17	$Ca(OH)_2$ stabilized human (excess)				-
E18	$Ca(OH)_2$ stabilized synthetic				1.2 µm

3.7 OLI model validation

The final aspect of experimental work was to validate the OLI simulation results. The first set of validation experiments below aimed to validate OLI results by determining the experimental mass of total solids. The second set of validation experiments aimed to identify the individual solids formed experimentally. Experimental results were then compared to OLI predictions.

3.7.1 Validation of total solids formed as a function of water removal

The experimental total mass of solids formed was used as a proxy to validate simulation results. The predicted total mass of solids as well as NPK recovery at the three water removal intervals studied, was taken from S2 (Table 13) above. These theoretical predictions were compared to the experimental results measured when evaporating synthetic urine.

The total mass of solids formed experimentally was determined through stabilizing 4 L of synthetic fresh urine, with $Ca(OH)_2$ as discussed above. This stabilized urine was filtered to 1.2 µm (Munktell Filtrek™, Bärenstein, Germany). The composition of fresh and initial stabilized urine was determined as done in above experimental work. Three trays were prepared as done in NPK experimental runs.

The mass of each dry tray was measured and recorded using a balance (PS4500.X2.M, RADWAG, Poland). One liter of filtered synthetic $Ca(OH)_2$ stabilized urine was added to each tray using a 1000 mL measuring cylinder. The masses of the full trays were then measured and recorded.

Each of the three trays were carefully transferred into the climate chamber (TH3 PE 100, Jeio Tech, Korea). One tray was placed on top of the balance which was placed inside the climate chamber. This allowed for the mass of the tray to be recorded over time, every ten minutes. Additionally, as discussed above, a flat-tipped pH probe (3 M KCl, Metrohm, Switzerland) was also placed into the tray that was placed on the balance. The chamber was set to run at 40°C and a relative humidity of 40%.

The recorded mass data was monitored, and the experimental run was terminated when the desired water removal of 50% was met. The remaining solution was filtered to 0.45 µm, using a filter paper of known mass (635492, 47 mm diameter, MF-Millipore™, Darmstadt, Germany). The wet filter paper with solids, was placed on a watch glass of known mass. This was then placed in the oven (Model 267 80 L digital oven, Apex Scientific, South Africa) at 30°C and left for 24 hours to dry.

The mass of the dry filter paper and watch glass was then remeasured, and the total mass of dry solids could be determined using Equation (**8)**.

$$Mass\ solids = Final\ mass\ filter\ paper\ and\ watch\ glass - Initial\ mass\ filter\ paper - Initial\ mass\ watch\ glass \quad \textbf{(8)}$$

The above methodology was repeated for 75% water removal. However, as shown in Table 17, the results from E18 above were used for 100% water removal.

Table 17. Experimental conditions used in $Ca(OH)_2$ stabilized synthetic urine evaporation experiments for three different water removal intervals

Experiment number	Type of urine	Experimental conditions		
		Temperature (°C)	Humidity (%)	Water removal (%)
E19	Synthetic $Ca(OH)_2$ stabilized	40	40	50
E20				75
E18 (**Table *16***)				100

3.7.1.1 Identification of individual solids formed during water removal processes

The final experimental aspect of identifying the individual solids formed had to be approached in a step-wise manner. This meant that a series of matrix solutions were evaporated one after the other, each time adding a new component to the solution. Matrix solutions as well as the amount of each salt dissolved in solution are summarized in Table 18.

Table 18 was used to create OLI simulations corresponding to each solution matrix. Simulations contained the same initial salts, in the same quantities. The simulations were run to 100% water removal using a composition survey. At this point, the individual solids formed were noted. These results were compared to experimental results obtained through evaporating the above solutions.

To create the solutions to be evaporated, the required mass of each compound, shown in Table 18, was measured and dissolved in a 1 L volumetric flask with de-ionized water. The

solution was mixed well on a magnetic stirrer for 15 minutes. As in these experiments, only the final solids formed was of importance, no initial or final compositions were measured using the ThermoScientific Gallery (TSG) (ThermoFisher Scientific, Massachusetts, United States). Additionally, the volume of solution added to evaporation trays was also insignificant.

An evaporation tray was cleaned using tap water, acid and de-ionized water as above, and dried. Approximately 500 mL of the mixed solution was then poured into the dry tray. The tray was then placed into an oven (Model 267 80 L digital oven, Apex Scientific, South Africa) at 30°C for 120 hours. This ensured that the solution had completely evaporated and only the solid phase was left in the tray.

This solid phase was scraped and crushed and then transferred into a labeled sample container. This was repeated for all seven solutions and the collected samples were sent for XRD (x-ray diffraction) analysis. When initially analyzing solution matrix 5, XRD results showed many undefined phases present. To combat this, solids from matrix 5 were mixed with an organic phase. The chosen organic phase had to be compatible with material of the cup in the micronizing mill, but also could not allow the solids to dissolve. The compatible organic used was 99.5% anhydrous cyclohexane (227048-250 mL, Sigma Aldrich, Germany). After extensive milling the sample was dried and then reanalyzed using XRD analysis. This procedure, as well as all XRD analysis, was performed by the Catalysis Department at UCT.

Table 18. Solution matrices for XRD analysis experiments. The identity of the salt used in each solution is shown first. The quantity of each salt dissolved in one litre de-ionized water, is then shown below this

Experiment number	Matrix	Salt					
		1	2	3	4	5	6
E21	**1**	KCl	$Ca(OH)_2$				
		0.894 g	10 g				
E22	**2**	KCl	Na_2SO_4	$Ca(OH)_2$			
		0.894 g	1.220 g	10 g			
E23	**3**	KCl	Na_2SO_4	NaH_2PO_4	$Ca(OH)_2$		
		0.894 g	1.220 g	0.329 g	10 g		
E24	**4**	KCl	Na_2SO_4	NaH_2PO_4	$MgCl_2$	$Ca(OH)_2$	
		0.894 g	1.220 g	0.329 g	0.223 g	10 g	
E25	**5**	KCl	Na_2SO_4	NaH_2PO_4	$MgCl_2$	$NaCl$	$Ca(OH)_2$
		0.894 g	1.220 g	0.329 g	0.223 g	6.327 g	10 g
E26	**6**	$CO(NH_2)_2$	$Ca(OH)_2$				
		11.626 g	10 g				
E27	**7**	KCl	NH_4Cl	$Ca(OH)_2$			
		0.894 g	1.666 g	10 g			

3.8 Analytical methods used in experimental procedures

When performing the above experimental work, various analytical measures were used when measuring the composition of urine solutions. These methods are presented and described below.

3.8.1 Measurement of major ion concentrations using the ThermoScientific Gallery

The ThermoScientific Gallery (TSG) (ThermoFisher Scientific, Massachusetts, United States) was used to measure the composition of urine solutions in terms of the concentration of major ions in solution. The TSG is a discrete analyzer that works on the principle of photospectrometry to analyze samples. The concentration of ammonia, calcium, chloride, magnesium, potassium, phosphate and sulfate ions, as well as urea dissolved in solution, could be obtained through the use of the TSG. When preparing samples for the TSG, samples needed to be filtered to 0.45 µm using a syringe filter to prevent blockages. Samples needed to be manually diluted according to the TSG test limits. Further TSG dilutions were also required in some cases. These limits are outlined in Appendix A.2. Manual dilutions were performed during sampling procedures which are outlined below.

3.8.1.1 Sampling procedures - Elemental analysis of solids

As an alternative to XRF analysis, the major ion concentrations of the resulting solids were determined by dissolving a known mass of solids in a known volume of deionized water. The concentration of this solution was measured in the TSG and used, along with a mass correction ratio, to determine to composition of solids.

3.8.1.2 External analysis for Na^+ and K^+ ions

As both pre- and post-experimental sampling techniques could not measure Na^+, samples were sent to Bemlab for external Na^+ analysis. Additionally, at times the Gallery reading for K^+ was unreliable. A potential reason for this was due to interference from other ions. This meant that samples sent to Bemlab for analysis, were tested for both Na^+ and K^+ concentrations. Additional sampling procedures are outlined in Appendix A.2.

3.8.1.3 X-ray Diffraction (XRD) analysis for individual solids identification

XRD analysis was done by Associate Professor Nico Fischer in the Catalysis Department in the Chemical Engineering Building at the University of Cape Town. Solid samples were scraped to the center of evaporation trays, and well mixed and crushed to ensure the most homogenous sample. Samples for XRD, remaining in the evaporation trays, were then dried at 30°C in the oven for a period of two days to ensure complete water removal. Dried samples were carefully poured into clean two milliliter centrifuge tubes and labelled. Centrifuge tubes were sealed to prevent contamination and then sent for XRD analysis.

XRD analysis was performed on a D8 Advance diffractometer (Bruker, Germany) equipped with a position-sensitive detector (LYNXEYE) in Bragg Brentano geometry. Power to the copper anode was set at 35 kV and 40 mA. The diffraction patterns were acquired in the 2Θ range of 20° to 120° (1/d = 0.19 to 0.97 Å-1) using a step size of 0.017° and with a time per step of 0.84 seconds. The total scan time amounts to 1 h 57 min, The diffraction pattern was compared to reference data files reported in an ICDD database (PDF-4+, released in 2020).

Chapter 4. Results and discussion

From the review of literature, a wide range urine treatment options were available, with evaporation often being used to concentrate human urine. However, the experiments from these studies often differed in terms of operating conditions used (pH, temperature, humidity etc.) as well as the type of urine studied(fresh, hydrolyzed and stabilized). Furthermore, few studies focused on maximizing the recovering of all key nutrients (N, P and K). Therefore, this study aimed to investigate these aspects in more detail and for a wider range of conditions.

Using a combination of the abovementioned simulation and experimental results, a better understanding of the overall urine evaporation process was obtained in this thesis. This understanding encompassed urine stabilization techniques with a major focus on the NPK recovery associated with different urine stabilization techniques. Experimental results further considered the accuracy of OLI modelling as well as a first estimate of the energy consumption associated with the urine evaporation process.

The first aspect of experimental work aimed to determine the preferred urine stabilization technique at 100% water removal. The preferred technique was determined through the NPK nutrient recoveries obtained When using different urine stabilization techniques.

4.1 Urine stabilization techniques and NPK nutrient recovery

As explored in Chapter 2, human urine is rich in the major nutrient components found in synthetic fertilizers. These components are nitrogen (N), phosphorus (P) and potassium (K). Utilizing different urine stabilization techniques such as $Ca(OH)_2$ dosing, has been shown to improve the recovery of such nutrients in the final solids that form during evaporative processes (Randall et al., 2016; Simha et al., 2020).

NPK experimental work explored urine stabilization techniques to determine the more favourable stabilization technique. Six synthetic (S) urine solutions and three human (H) urine solutions were studied in terms of major nutrient recoveries. The N, P and K recoveries obtained in the synthetic and human urine solutions is shown in Figure 5.

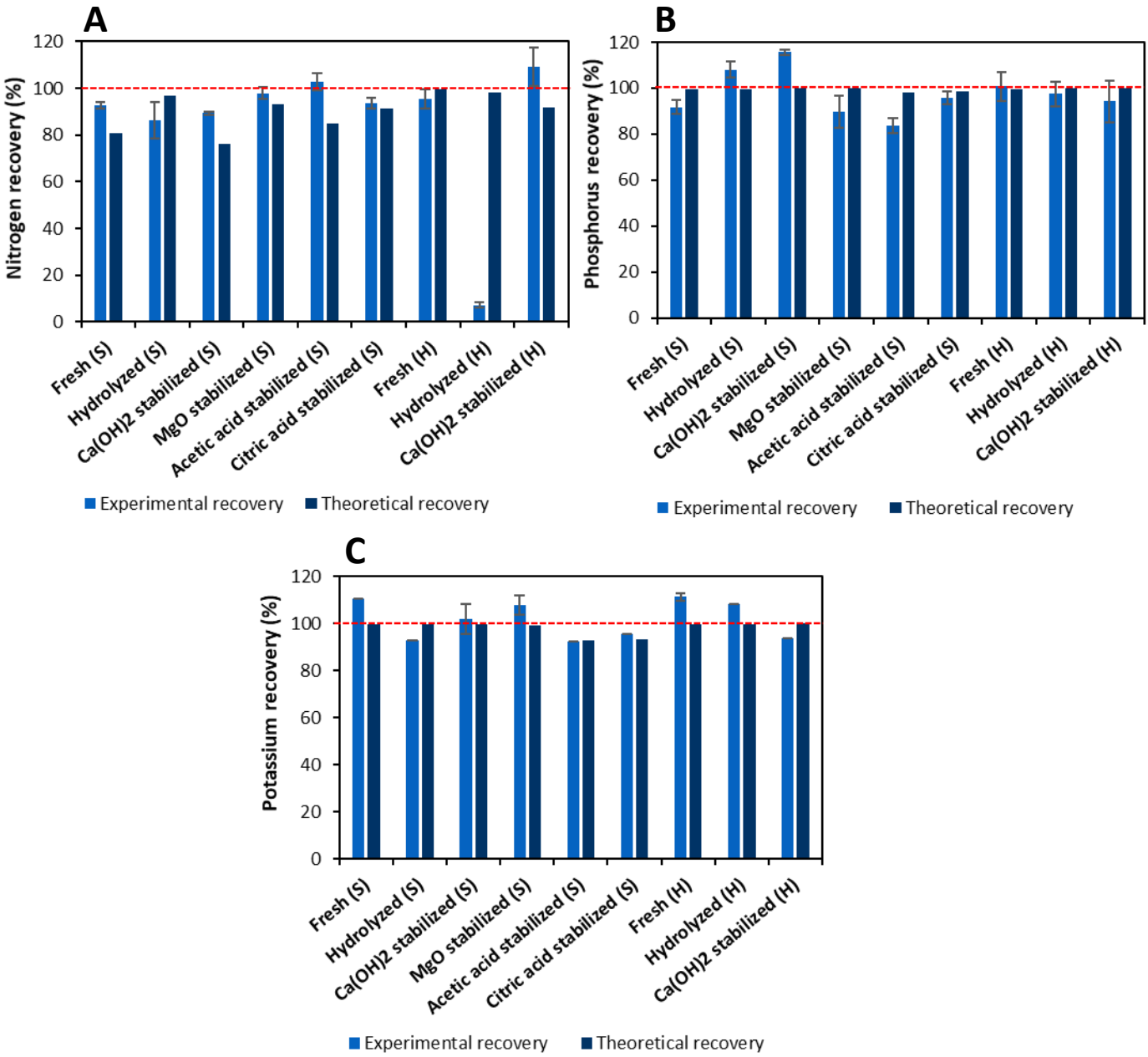

Figure 5. NPK recoveries for the nine studied urine solutions. Synthetic urine solutions are indicated as (S) and human urine solutions are indicated as (H). Experimentally, urine solutions were evaporated at room temperature and ambient humidity conditions. Experimental results were used to determine experimental recoveries. Theoretical results were obtained from NPK OLI simulations. Simulations were conducted at 25°C. The red dotted line indicates 100% recovery. **(A)** shows nitrogen recovery in the nine solutions. Likewise, **(B)** and **(C)** show the phosphorus and potassium recoveries, respectively.

Nitrogen recoveries achieved in the nine urine solutions is shown in Figure 5A. It was expected that fresh urine solutions would have low nitrogen recoveries as these solutions were not stabilized. As a result, loss of nitrogen due to urea hydrolysis was expected. However, Figure 5A shows that fresh synthetic urine had a nitrogen recovery of 92.7%. Fresh real urine had a higher nitrogen recovery of 95.7%. These fresh solutions may have evaporated over a short time period and as a result there was insufficient time for the expected urea hydrolysis to occur.

Similarly, in Figure 5A, synthetic hydrolyzed urine did not present a large loss in nitrogen with a nitrogen recovery of 86.2%, which was unexpected. If urine solutions were left unstabilized, the urea content in the solution began to hydrolyze, resulting in both the real and synthetic hydrolyzed urine solutions. This unexpected finding may have been due to the absence of the urease-producing bacteria, that are usually ubiquitous in the environment, due to the short time period that the synthetic solution was evaporated over. The absence of such factors would have resulted in very slow or negligible urea hydrolysis. If the synthetic solution were evaporated over a longer time period, it is expected that urease-producing bacteria will be present, and a greater extent of hydrolysis and corresponding nitrogen loss may be observed.

Hydrolyzed real urine did however show a decreased nitrogen recovery as expected. This could be attributed to the fact that real urine did contain the added Jack Bean urease which caused urea hydrolysis to occur. A low nitrogen recovery of 7.17% was observed in the hydrolyzed real urine solution in Figure 5A. This demonstrated loss of nitrogen was more prevalent in real hydrolyzed urine compared to synthetic hydrolyzed urine solutions.

To minimize this loss of nitrogen from urine, urine solutions could be treated through various stabilization techniques. These techniques alter the pH of the solution into a region at which the activity of enzyme urease was inhibited (Rektorschek et al., 1998). From Figure 5, these techniques included either acidification or the addition of basic salts. The loss of nitrogen through urea hydrolysis, could also be prevented through the rapid evaporation of fresh urine under sterile conditions. This decreased the time over which enzymatic urea hydrolysis could occur. Over time, urease producing bacteria could accumulate in the urine evaporation system and may cause enzymatic urea hydrolysis observed in fresh urine. Sterile conditions included well-cleaned evaporation trays and equipment.

The first urine stabilization method studied was $Ca(OH)_2$ stabilization. Figure 5A shows synthetic $Ca(OH)_2$ stabilized urine to have a nitrogen recovery of 89.3% and real $Ca(OH)_2$ stabilized urine to have a higher nitrogen recovery of 109%. The lower nitrogen recovery associated with the synthetic urine solution was due to the volatilization of NH_3 from the urine solution due to the high pH achieved through $Ca(OH)_2$ dosing. Initially the $Ca(OH)_2$ stabilized synthetic urine contained 8.25% of the total nitrogen in solution as NH_4^+. Compared to $Ca(OH)_2$ stabilized real urine, which contained 5.03% of the total nitrogen in solution was NH_4^+.

In the $Ca(OH)_2$ stabilized synthetic urine, all NH_3 volatized from the solution. However, in the $Ca(OH)_2$ stabilized real urine, only 80% of the NH_3 initially present, volatized. This resulted in some NH_3 being retained in the total nitrogen in the solids formed through evaporating $Ca(OH)_2$ stabilized real urine. Of the final nitrogen retained in $Ca(OH)_2$ stabilized real urine, 0.66% of the NH_3 in the total nitrogen was retained.

Theoretical nitrogen recoveries for $Ca(OH)_2$ stabilized synthetic and real urine solutions were 76.1% and 91.6% respectively. Both urine solutions predicted no NH_3 recovery in the final solids formed. For $Ca(OH)_2$ stabilized real urine, this led to the lowered nitrogen recovery when compared to the experimental recovery of 109%.

The NH_3 initially present in solution was predicted to be in the vapor phase at 100% water removal. This realistically would be lost to the surrounding environment. The additional loss in nitrogen was associated with the urea recovery predicted in OLI. This was predicted to be 82.2% and 99.0% for synthetic and real $Ca(OH)_2$ stabilized urine solutions. Experimentally, this was 95.6% for $Ca(OH)_2$ stabilized synthetic urine and 113% for human urine.

From the remaining stabilized synthetic solutions, acetic acid had the highest nitrogen recovery (103%), followed by MgO stabilized synthetic urine (97.8%) and citric acid stabilized urine (93.5%). $Ca(OH)_2$ stabilized synthetic urine had the lowest nitrogen recovery of 89.3%. However, when considering all stabilized urine solutions studied, $Ca(OH)_2$ stabilized real urine had the highest nitrogen recovery (109%).

When comparing experimental and theoretical results in Figure 5A, the nitrogen recovery in hydrolyzed real urine, did not closely agree with the experimental results. However, the results for the remaining eight urine solutions showed some agreement between experimental and theoretical results. The nitrogen recoveries in hydrolyzed synthetic and fresh real urine solutions, were over-estimated when compared to the theoretical results. When compared to experimental results, theoretical results for fresh, MgO, acetic acid and citric acid stabilized synthetic urine solutions were underestimated.

Theoretical predictions for hydrolyzed real urine showed a nitrogen recovery of 98.3%, compared to experimental results with a recovery of 7.17%. This major discrepancy was due to a limitation in the OLI model. OLI does not account for atmospheric nitrogen losses by volatilization. Experimentally, urea degrades to form NH_3 which volatizes and is lost to the surrounding environment. As OLI cannot account for this, nitrogen from the NH_3 formed due to urea hydrolysis, is recovered in solids at 100% water removal. This led to the much higher theoretical nitrogen recovery in Figure 5A. This was also observed for hydrolyzed synthetic urine although this was not as extreme due to the lower extent of urea hydrolysis observed in this solution.

The theoretical recovery in acetic acid was under-estimated at 85.2%, compared to the experimental observation of 102%. This under-estimation was attributed to an experimental urea recovery of 104% (compared to 85.0% theoretically predicted) and an experimental NH_3 recovery of 92.0% (theoretical recovery 87.0%). Citric acid stabilization showed a similar trend whereby theoretical results under-estimated the experimental results. Theoretical nitrogen recovery was 91.2% in citric acid stabilized synthetic urine, compared to an experimental recovery of 93.6%. Although, unlike acetic acid results, citric acid stabilized synthetic urine did not show as large a discrepancy between experimental and theoretical recoveries. Urea recovery was experimentally determined to be 92.0% and theoretically predicted to be 92.7%. NH_3 recovery was 93.7% experimentally and predicted to be 91.5% using OLI.

For MgO stabilized urine, a 97.9% nitrogen recovery was measured and theoretically a nitrogen recovery of 93.2% was predicted. Like the hydrolyzed urine solutions above, OLI simulations could not account for NH_3 volatilization as theoretically 81.5% NH_3 was recovered yet experimentally only 7.88% NH_3 was recovered at 100% water removal. Additionally, 94.1% urea was theoretically recovered, compared to an experimental urea recovery of 105%. This

difference in urea recoveries led to a higher experimental nitrogen recovery compared to OLI predictions.

Fresh synthetic urine showed an under-estimation in theoretical recovery (80.8%) compared to the experimental recovery (92.7%). Experimentally, 89.8% urea was recovered, compared to a theoretical prediction of 87.1%. The NH_3 recovery differed greatly between experimental and theoretical results. Experimentally, a high NH_3 recovery of 132% was measured. Theoretically, a low NH_3 recovery of 3.31% was predicted. This discrepancy may be attributed to the thermodynamic predictions in OLI as NH_3 was not predicted to be present in the final solids formed but rather in the vapor phase. However, the NH_3 was trapped in the experimentally formed solids and hence detected when performing final solids analysis.

Similarly, Figure 5B and Figure 5C show the experimental and theoretical phosphorus and potassium recoveries, respectively. Both phosphorus and potassium will not volatize from the initial urine solutions and as a result, it was expected that experimental recoveries close to 100% be achieved (Simha et al., 2020).

When performing the experimental work, urine solutions were filtered to 1.2 µm, prior to undergoing evaporative processes. This filtration step may have removed phosphorus solids that form as precipitates due to stabilization processes (Chipako and Randall, 2020b). To recover the phosphorus removed from solution when filtering, one would need to retain the filtered solids obtained from the pre-evaporation filtration step. These solids will be rich in phosphorus. Alternatively, one could evaporate urine solutions without pre-evaporation filtration. In this case, the final solids formed would contain all the phosphorus initially present in the fresh urine as this is not removed from the solution via filtration.

From Figure 5B, experimental phosphorus recovery for the nine urine solutions was high for all solutions, as expected. Acetic acid had the lowest experimental phosphorus recovery of 83.6%. This was followed by MgO stabilized urine with the second lowest experimental recovery of 89.7%. Experimental phosphorus recoveries above 90% were obtained for the seven remaining urine solutions, with $Ca(OH)_2$ stabilized synthetic urine with the highest recovery (116%).

As it was expected that close to 100% of the phosphorus in solution should be recovered, the lowered experimental recovery of phosphorus in acetic acid had to be attributed to the experimental solids analysis. During the evaporation of acetic acid stabilized urine, the final solids formed would have incorporated phosphorus. These solids may not have been completely dissolved in the final solution used to analyze the elemental composition of the final solids formed. As a result, these solids were filtered out when preparing solutions for the Gallery. This led to the lowered experimental phosphorus recovery of 89.7%.

When comparing experimental phosphorus recoveries to theoretical phosphorus recoveries, the theoretical recoveries were close to 100% for all urine solutions as expected. As discussed above, phosphorus is not able to volatize and as a result 100% of the initial phosphorus in solution should be recovered at 100% water removal.

For the NPK analysis in terms of urine treatment techniques, the final major nutrient recovery studied was potassium recovery. From Figure 5C shows both the experimental and theoretical potassium recoveries form the nine urine solutions.

Like the phosphorus in urine, potassium does not volatize. Hence it was hypothesized that the potassium present in each urine solution would be recovered in the final solids at 100% water removal. As seen in Figure 5C this was the case for most experimental and theoretical potassium recoveries in the urine solutions studied.

Theoretical potassium recoveries in acetic and citric acid stabilized urine were slightly lower than 100% (92.9% and 93.6% respectively). These theoretical results showed agreement with experimental recoveries. Experimental potassium recovery in acetic and citric acid stabilized urine solutions was 92.6% and 95.8% respectively.

The remaining theoretical potassium recoveries ranged from 99.7% to 100%, as expected. Experimentally, a greater range was observed in potassium recoveries. Experimental recoveries ranged between 92.6% and 112%. This greater range may have been introduced due to loss in potassium solids due to experimental analysis. When solids were transferred from evaporation trays to the final solutions mixed in volumetric flasks, some residual potassium may have remained in evaporation trays. Additionally, as observed with phosphorus, the solids containing potassium may have been removed through filtration when preparing Gallery samples, lowering potassium recoveries slightly. Additionally, under-diluting Galley samples or residual potassium in sampling flasks may have raised potassium recoveries.

Potassium concentration presented difficulties when being measured in the Gallery. For this reason, samples were sent to an external lab for analysis to determine the potassium concentration. When possible, the potassium concentration was analyzed in the Gallery. This could be done in triplicate and error bars were determined in Figure 5C. However, when potassium could not be measured in the Gallery, one sample from each experiment was sent for external analysis. As only one sample per experiment was sent for external analysis, error bars for these experiments could not be determined.

When conducting the above NPK experiments, the pH of each urine solution was also measured in conjunction with nutrient recoveries. The pH measurements over time could be used to determine when urea hydrolysis may have occurred in the solution. The results for synthetic (S) urine and human (H) urine solutions are shown below in Figure 6.

The pH of synthetic fresh urine remained fairly constant over time (Figure 6A). The pH of the synthetic fresh urine solution then dropped rapidly after 80 hours, near the completion of the experimental run. Similarly, for the pH profile of synthetic urine stabilized with $Ca(OH)_2$,the pH of this urine solution remained close to a pH value of 12, although over time, this pH did decrease slightly. The elongated period at which the urine solution was kept above a pH of 11, indicated that the urine solution was well stabilized, and therefore the risk of urea hydrolysis occurring was minimal (Randall et al., 2016). As with fresh synthetic urine, the pH of the urine stabilized with $Ca(OH)_2$ dropped rapidly after approximately 100 hours of evaporation as the experimental run neared 100% water removal.

Synthetic urine stabilized with MgO did not present the same pH trend to that of urine stabilized with $Ca(OH)_2$. The pH of MgO stabilized synthetic urine presented a continual decrease in pH from the initial value of 10.3, to a final value of 5.15. MgO stabilization initially avoid the optimal pH for urease activity (pH 6.8-8.7) (Rektorschek et al., 1998). However, after 20 hours of evaporation, this pH region was no longer avoided. This showed that MgO stabilization did not provide the same stabilization effectiveness as seen with $Ca(OH)_2$.

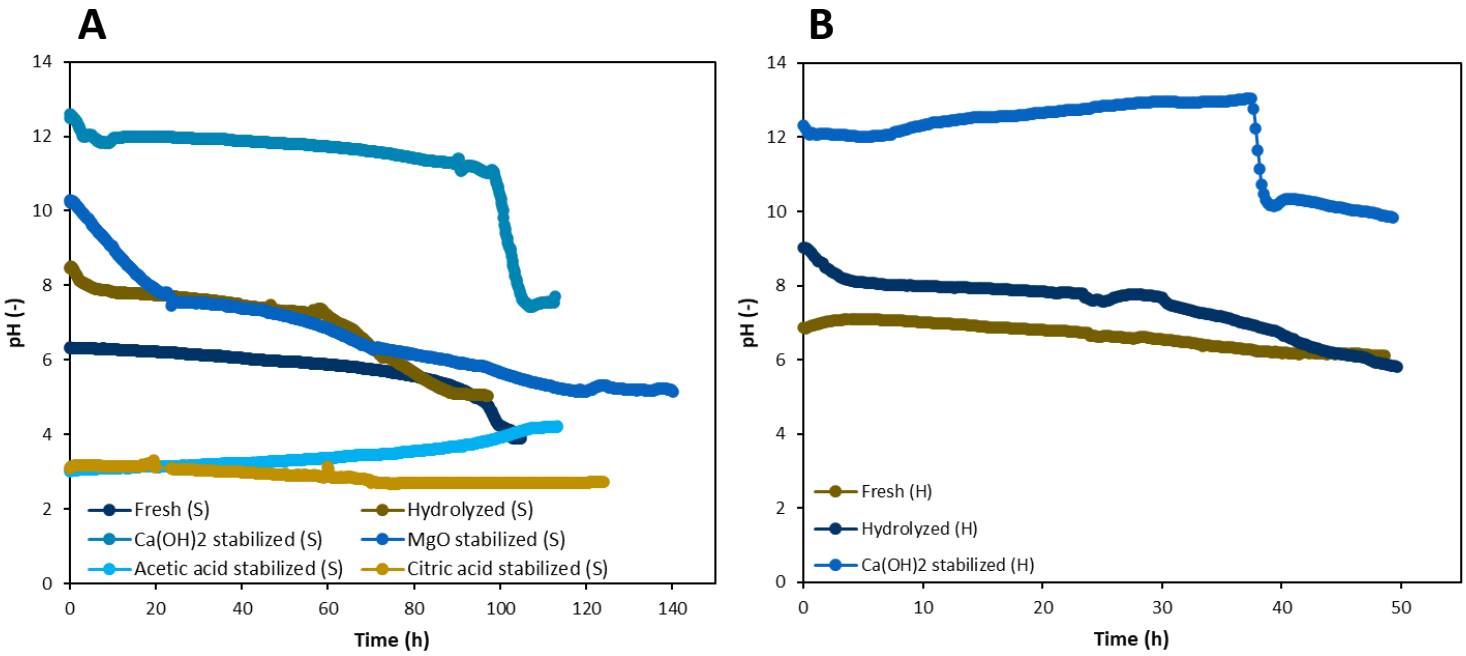

Figure 6. pH profiles for the nine NPK urine evaporation experiments. **(A)** shows the pH profiles for the six synthetic urine solutions (S). **(B)** shows the pH profiles for the three human urine solutions (H).

Alternatively, acidification of urine was also used as a method to stabilize synthetic urine solutions. Both acetic and citric acid addition were considered. Figure 6A shows both acidification stabilization treatments started at an initial pH of 3. Acetic acid stabilization showed an increase in pH over time while citric acid showed a decrease in pH over time. Final pH levels of 4.23 and 2.99 were observed with acetic acid and citric acid dosing respectively. Both acid stabilization treatments ensured the pH of synthetic urine solutions were maintained below the optimal pH for urease activity.

Like the synthetic urine solutions shown in Figure 6A, the pH data collected over time for fresh and hydrolyzed real urine (Figure 6B) fell within the optimal pH range for urease activity. As observed for synthetic $Ca(OH)_2$ stabilized urine, the pH data for real human urine stabilized with $Ca(OH)_2$ shows promise as a stabilization technique because a high pH above 11 is maintained for almost 40 hours during water removal processes.

When stabilizing urine with acid, acid had to be carefully added to the solution while the pH was continuously measured. This ensured that the urine was acidified to an exact pH of 3. If more, or less acid was added to the urine, the urine would not have been acidified to a pH of

3. If less acid was added, the pH of the urine solution would be greater than 3, and this may pose the risk of falling in the pH region at which optimal urease activity is supported.

Alternatively, acidification could still be used to stabilize urine. However, in doing so a pH controller and dosing pump would be required to ensure accurate acidification to the correct pH. Compared to $Ca(OH)_2$ stabilization, this equipment and maintenance thereof, is an additional cost which is not required when adding $Ca(OH)_2$ powder for urine stabilization.

$Ca(OH)_2$ stabilization allows for a much more accurate stabilization method because when the solution is saturated with $Ca(OH)_2$ the solution will be at the saturation pH of the solution. For urine, this pH is above a pH of 11. When at a pH greater than 11, urease activity is inhibited. Hence, this urine stabilization technique is more accurate and simpler when compared to urine acidification.

From NPK experimental results urine stabilization through $Ca(OH)_2$ addition is concluded to be the preferred urine stabilization treatment technique. This urine treatment technique during the water removal process, both experimentally and via simulations, was studied in greater detail. The results from this study are presented below.

4.2 Effect of water removal on solids formation in $Ca(OH)_2$ stabilized urine

Considering urine stabilized through $Ca(OH)_2$ addition, the first experimental aspect was to determine the suitability of OLI predictions compared to experimental results. Once a comparison between these two results was drawn, the accuracy of OLI modelling for urine evaporation could be determined.

4.2.1 Comparison of experimental and theoretical mass of total solids and major nutrient recoveries

Experimentally, synthetic $Ca(OH)_2$ stabilized urine was evaporated to three water removal intervals (50%, 75% and 100%). The mass of total solids formed, as well as the NPK composition of these solids, was measured. The NPK composition of solids formed was given relative to the initial amount of each nutrient in solution. These experimental results were compared to OLI predictions. Figure 7 below shows experimental results (Figure 7A) and theoretical predictions (Figure 7B).

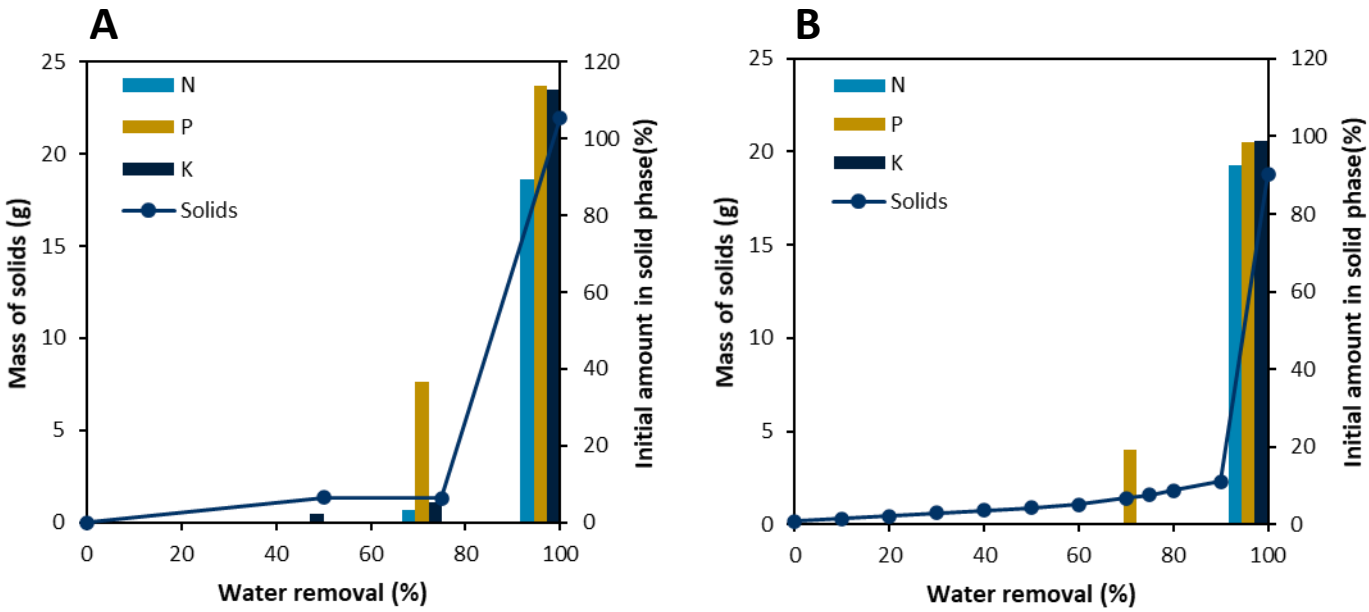

Figure 7A. Experimental mass of total solids formed and the recovery of NPK nutrients in synthetic $Ca(OH)_2$ stabilized urine (U1b). Urine was evaporated at 40°C and 40% realtive humidity. **Figure 7B**. Theoretical mass of total solids formed and recovery of NPK nutrients in synthetic $Ca(OH)_2$ stabilized urine (U1b). Theoretical results were obtained at a simulation temperaure of 40°C. NPK recoveries were calculated using the amount of nutrient present in intial stabilized urine prior to evaporation.

The experimental results (Figure 7A) did not compare well to the theoretical OLI predictions shown in Figure 7B. In both Figure 7A and Figure 7B, majority of the mass of total solids formed at higher water removal intervals (>80%). However, in Figure 7A this occurred experimentally before 80% water removal. In Figure 7B this was predicted to occur closer to 90% water removal. Additionally, a peak in phosphorus recovery at 75% water removal, is observed in Figure 7A. This phosphorus peak (37% initial phosphorus in solution is recovered in the solid phase) is accompanied by nitrogen (3.06% of initial amount in solution) and potassium (5% of initial amount in solution) recoveries, with majority of the remaining nutrient recovery occurring at 100% water removal. Theoretical predictions in OLI showed a phosphorus peak showing 19% of the initial phosphorus in solution was present in the solid phase, yet the nitrogen and potassium recoveries experimentally associated with this peak were not predicted in OLI.

These differences observed between experimental and theoretical results may be attributed to limitations in the OLI software. These limitations are associated with urea hydrolysis and ammonia volatilization. Such limitations lead to deviations, especially in the mass of total solids, between Figure 7A and Figure 7B.

4.2.2 Comparison of experimental and theoretical OLI results

The mass of total solids formed in Figure 7 was used as a proxy to compare and determine the overall accuracy of OLI simulations. Figure 7A shows at 100% water removal, 22 g of total solids was formed. In contrast, OLI predicted that 18.8 g of solids would be formed (Figure 7B). Experimental results measured 16.9% more total solids than the predicted mass. At 50%

water removal, the experimental results showed 49.3% more total solids, and at 75% water removal, the experimental results showed 18.9% less total solids than predicted.

From this finding, the accuracy of OLI predictions compared to experimental results increased with an increase in water removal. Although the accuracy increased, the mass of total solids measured experimentally and predicted using OLI still showed a significant difference.

When comparing experimental results (Figure 7A) to results for the OLI modelling (Figure 7B), a second aspect of comparison aimed to compare the individual solid species formed theoretically and experimentally. Once this comparison was made, the limitations to OLI modelling could be further explored to investigate the observed deviations.

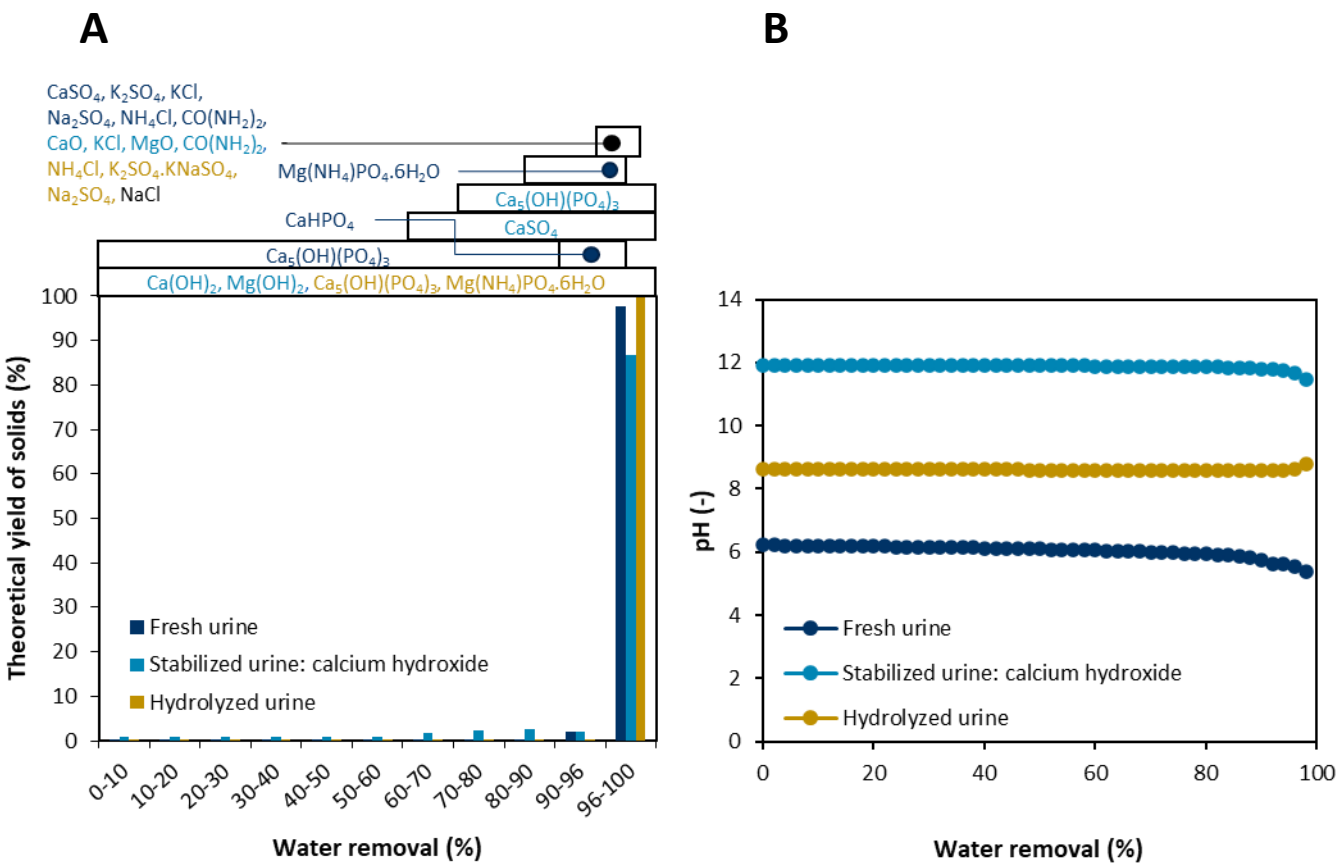

Figure 8. shows the modelling results of U1 obtained from OLI simulations. These modelling results are based on the same urine composition (U1), a temperature of 40°C and a dosage of 10 g L^{-1} for calcium hydroxide for the urine stabilization. For the hydrolyzed urine it was assumed that all the urea was converted into ammonium (NH_4^+) and carbonate ions (CO_3^{2-}). **(A)** shows the theoretical yield of solids that form during the removal of water from fresh, hydrolyzed, and stabilized urine at 40°C. Stabilized urine refers to urine dosed with calcium hydroxide. The type of major solids that theoretically form for each type of urine is also shown above. The black rectangles correspond to the water removal intervals at which these solids theoretically form. The colour of the text corresponds to the type of urine the in which these solids are predicted to form. Black text with no colour coding means that these solids formed in all types of urine. Most solids form after 96% water removal. **(B)** shows the theoretical pH profiles for the three different types of urine.

Figure 8A shows the individual solid species predicted to form in all three types of urine using the results from OLI simulations (synthetic U1a, U1b and U1h). Although below in Figure 8A

theoretical results are shown for three types of urine, experimentally only the individual solids formed in $Ca(OH)_2$ stabilized urine (U1b) were determined using XRD analysis.

From the yield of total solids shown in Figure 8A, majority of the individual solid species are predicted to form at a water removal interval greater than 96%. From Figure 8A, the predicted solid species from U1b include CaO, $Ca(OH)_2$, $Ca_5(OH)(PO_4)_3$, $CaSO_4$, KCl, MgO, $Mg(OH)_2$ and $CO(NH_2)_2$.

To validate the theoretical results shown in Figure 8A, XRD matrix experiments discussed in Section 3.7.1.1 were conducted. The XRD results from each solution identified the individual solid species that had formed experimentally. These experimental results are shown in Table 19.

From Table 19, the overall initial composition of urine was experimentally built by considering a series of seven matrix solutions. After evaporating each solution, the resulting solids were sent for XRD analysis and the following solution was expanded by adding one more chemical salt. This process was continued in a step wise manner, until the overall $Ca(OH)_2$ stabilized synthetic urine stream was evaporated and the solids sent for analysis.

From these experimental XRD results, MgO and $Mg(OH)_2$ solid phases were not detected in any matrix solutions. From OLI predictions, these species were present in very small amounts (< 0.001 g L^{-1}). These small quantities may not have been able to be detected during XRD analysis. Additionally, $CaCO_3$ was detected experimentally yet not predicted theoretically. This is because OLI simulations do not consider the surrounding air which realistically contains CO_2. This CO_2 reacts with the $Ca(OH)_2$ in solution to form CO_3^{-2} through reaction (**9)** (Simha et al., 2018). The CO_3^{-2} can then react with the available calcium to form $CaCO_3$.

$$CO_2 + H_2O \leftrightarrow H_2CO_3 \leftrightarrow HCO_3^- + H^+ \leftrightarrow CO_3^{-2} + 2H^+ \quad \textbf{(9)}$$

Lastly, the experimental results in Table 19 were limited when the matrix solutions were too complicated for accurate XRD analysis. This was observed with solutions 4 and 5. During XRD analysis, the individual solids formed experimentally could not be described accurately with the available extensive XRD database. After troubleshooting, one possible suggestion for this difficulty was that preferred orientation was occurring in these more complicated solutions (Ruiz-Agudo et al., 2013).

Preferred orientation may occur in samples when solid crystals form, these crystals form in sheets (Ruiz-Agudo et al., 2013). When forming these sheets, the crystals may grow in a certain manner, lying in a certain optical plane known as 'preferred orientation'. Depending on the orientation in which the crystals grow, XRD may not be able to detect the identity of the crystal as this orientation may not be the orientation listed in the XRD database for that crystal.

To eliminate this preferred orientation occurring, an organic phase in a micronizing mill may be used. The chosen organic phase needs to allow for the grinding of the solids, without dissolving the solids, or destroying the sample cup. In the case of this thesis, cyclohexane was

used. The cyclohexane was added to the formed solids and milled for an extended period of time.

Table 19. XRD matrix solution results. XRD results include the solid species identified for each XRD solution. Solution 5 was analyzed twice. The second time included the use of cyclohexane in a micronizing mill. Milled sample is indicated using an asterisk. The initial salt and amount of this salt dissolved in solution is indicated for reference.

Solution	Initial salt and amount of salt in solution					
1	KCl 0.894 g	$Ca(OH)_2$ 10 g				
2	KCl 0.894 g	Na_2SO_4 1.220 g	$Ca(OH)_2$ 10 g			
3	KCl 0.894 g	Na_2SO_4 1.220 g	NaH_2PO_4 0.329 g	$Ca(OH)_2$ 10 g		
4	KCl 0.894 g	Na_2SO_4 1.220 g	NaH_2PO_4 0.329 g	$MgCl_2$ 0.223 g	$Ca(OH)_2$ 10 g	
5	KCl 0.894 g	Na_2SO_4 1.220 g	NaH_2PO_4 0.329 g	$MgCl_2$ 0.223 g	$NaCl$ 6.327 g	$Ca(OH)_2$ 10 g
6	$CO(NH_2)_2$ 11.626 g	$Ca(OH)_2$ 10 g				
7	KCl 0.894 g	NH_4Cl 1.666 g	$Ca(OH)_2$ 10 g			

	Solid species identified in final solids formed
1	$Ca(OH)_2$ $CaCO_3$ KCl
2	$Ca(OH)_2$ $CaCO_3$ KCl CaO $NaCl$ $KNaS_2O_7$ K_2SO_4
3	$Ca(OH)_2$ $CaCO_3$ KCl CaO $NaCl$ $KNaS_2O_7$ K_2SO_4
4	Solution too complex
5	Solution too complex
5*	$CaCO_3$ $CaSO_4$ KCl $NaCl$
6	$Ca(OH)_2$ $CaCO_3$ $CO(NH_2)_2$
7	XRD not possible

The XRD results shown in Table 19 for solution 5* were conclusive after including the above milling step. Although the results for solution 5* completed the set of experimental results, this result also proved that preferred orientation was occurring in solutions. Using the completed set of results in Table 19 above, one could identify the individual solid species formed in $Ca(OH)_2$ stabilized synthetic urine experimentally.

Solutions 4 and 7 in Table 19 do not have conclusive XRD results as solution 4 was very similar to solution 5. The only difference between the two solutions was that solution 5 had the addition of NaCl to make up the correct Cl^- concentration to match U1b. Hence, solution 5 was milled with cyclohexane and it was assumed that the results for solution 4 if milled, would be like that of solution 5*. Solution 7 could not be analyzed in XRD analysis as the NH_4Cl added to solution resulted in the final solids formed absorbing too much moisture to allow for XRD analysis to occur.

Comparing theoretical predictions and experimental results, theoretical predictions gave a good comparison to the experimental results. The differences between theoretical and experimental results could be identified and explained.

A further limitation to OLI modelling is the loss of ammonia due to volatilization. Ammonia volatilization refers to the loss of nitrogen from solution due to the formed ammonia gas (NH_3) escaping to the environment. This can be prevented by retaining the NH_3 in the form of NH_4^+ ions in solution.

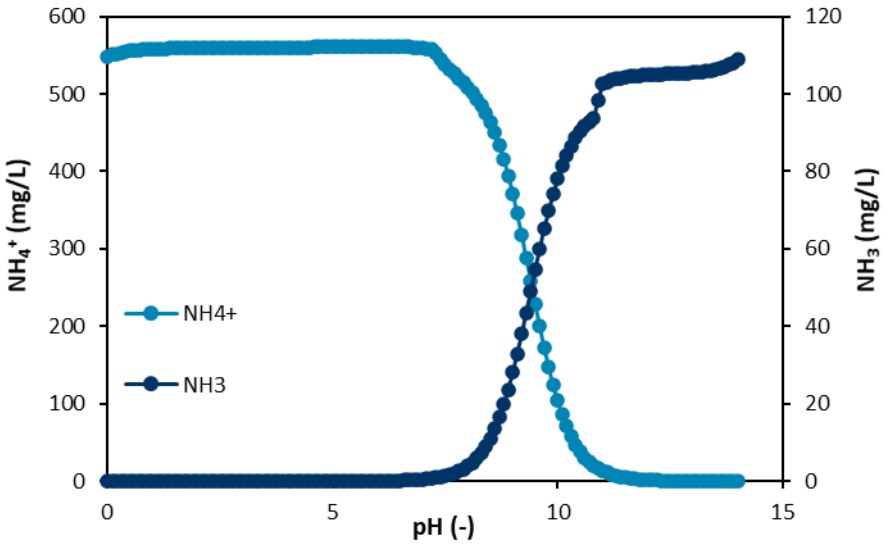

Figure 9. Ammonia (NH_3) and ammonium (NH_4^+) speciation curve. Speciation curve was generated using OLI software.

$Ca(OH)_2$ stabilized urine has a pH greater than 10. At this point on the speciation curve (Figure 9), ammonia is more likely to exist in the form of NH_3 compared to aqueous NH_4^+ ions. The NH_3 forms a vapor which escapes and is lost to the surrounding atmosphere. Although this speciation between NH_3/NH_4^+ is predicted in OLI simulations, the actual loss of gaseous NH_3 to the atmosphere is not accounted for in OLI simulation results. As there is a loss of nitrogen from solution, there is less nitrogen to be recovered from the solution. This is observed

experimentally (Figure 7A). However, this is not accounted for in in simulation results (Figure 7B). This can be seen in the difference in nitrogen recoveries between Figure 7A and Figure 7B where the results in Figure 7A shows a lower recovery compared to Figure 7B.

To determine whether OLI simulations could account for chemical urea hydrolysis due to working at elevated operating temperatures, the amount of solid urea formed as a function of water removal, was studied at temperatures between 40°C and 70°C (Figure 10). As shown in red on Figure 10, an initial amount of 10 g L^{-1} urea was dissolved in solution. With an increase in water removal, more solid urea began to precipitate out of solution. At 100% water removal, it was predicted that 100% of the initial 10 g L^{-1} urea would be recovered for all temperatures studied. This indicated that OLI simulations did not account for chemical urea hydrolysis, as expected.

Figure 10 further indicated the high solubility associated with urea. This can be observed within the high water removal region in which one needs to operate to recover solid urea from solution. From Figure 10, this region is between 99.3% and 100% water removal when operating at 40°C. This region was predicted to narrow with an increase in operating temperature.

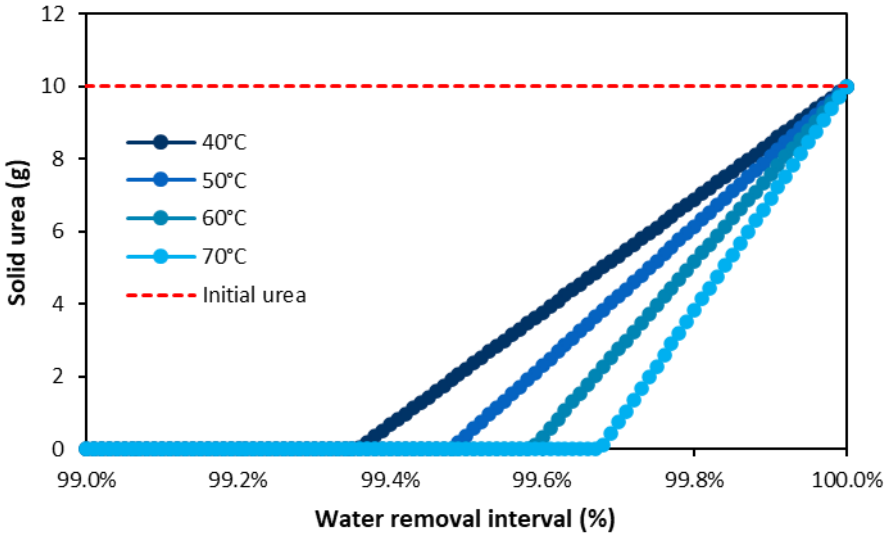

Figure 10. Total mass of urea in the solid phase as a function of water removal, for four different operating temperatures. Mass of solid urea formed is obtained from OLI simulations, using an initial 10 g L^{-1} urea. Red line shows initial urea in solution.

Using the results from the urea hydrolysis experiments shown in Figure 11A and Figure 11B, it was experimentally shown that chemical urea hydrolysis increased with an increase in operating temperatures.

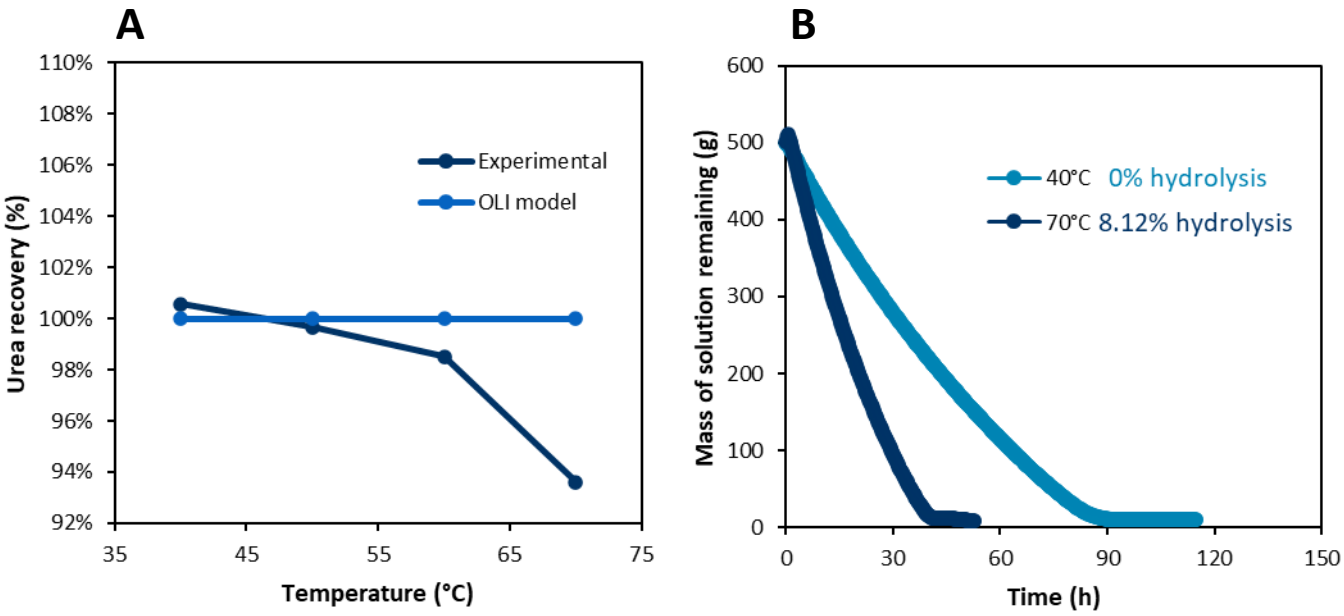

Figure 11A. Experimental and theoretical urea recovery at 100% water removal after a fixed time of 95 hours. Theoretical urea recovery is predicted using OLI simulation data. **Figure 11B.** Experimentally determined extent of urea hydrolysis and rate of evaporation. Experimental runs not completed for a fixed time period. Experiment terminated at 100% water removal.

Initially, Figure 11A showed a 93.6% urea recovery at 70°C. This corresponded to 6.4% urea hydrolysis. Results in Figure 11A were obtained by evaporating urea solutions at the chosen temperature for a fixed time period of 95 hours, the rate of urea hydrolysis was further investigated in Figure 11B.

When studying a water and urea solution, it has been shown that urea decomposes readily at elevated temperatures or in the presence of urease, when in the aqueous phase. Hence increasing evaporation rates to reduce the time spent in the aqueous phase, should limit the extent of urea hydrolysis. This is done by operating at higher temperatures. However, not only would this higher operating temperature be more costly from an energy requirement perspective, but it may increase the potential for chemical urea hydrolysis to occur (Randall et al., 2016).

In Figure 11B, 100% of the water was removed from the urea solutions by evaporation at both 40°C and 70°C. A higher operating temperature (70°C) reduced the evaporation time when compared to an operating temperature of 40°C. However, at 40°C, negligible chemical urea hydrolysis was observed, and at 70°C 8.12% chemical urea hydrolysis was observed during the evaporation process.

Although operating at an elevated temperature of 70°C, will speed up the evaporative processes, there is the risk of chemical urea hydrolysis occurring (Randall et al., 2016). From Figure 11B it can however, be seen that operating at 70°C shortened the evaporation time to reach 100% water removal, by 42.3 hours. This improved the evaporation time by 55.5% but resulted in a urea loss of 8.12%. When considering large scale urine processing operations, this significant time saving may be outweighed by this loss of solid urea.

4.2.2.1 Comparison between real and synthetic $Ca(OH)_2$ stabilized urine

The final aspect considered in the OLI/experimental work comparison, was the suitability of using of a synthetic urine stream. In OLI simulations, a $Ca(OH)_2$ stabilized urine stream (U1b) was used. Experimentally, salts were dissolved in deionized water to match U1b. However, when creating this synthetic urine stream, the only major organic species considered was urea although there are many other organic species in human urine such as creatinine and creatine (Putnam, 1971). To determine whether the use of a synthetic urine stream was a good approximation in both simulations and experiments, real and synthetic $Ca(OH)_2$ stabilized urine solutions were studied. These two urine solutions were compared using similar evaporation rates. The pH profiles of the urine solutions during evaporation were also monitored.

Both the synthetic and human $Ca(OH)_2$ urine solutions were filtered prior to evaporation. A third solution was also investigated. This solution was a synthetic urine solution, stabilized with $Ca(OH)_2$ and not filtered prior to evaporation. By adding the unfiltered $Ca(OH)_2$ stabilized synthetic urine solution to the study, the $Ca(OH)_2$ in solution was in excess compared to the filtered synthetic $Ca(OH)_2$ solution studied. It was hypothesized that having such an excess in $Ca(OH)_2$ would increase the buffering capacity of the stabilized synthetic urine solution. This meant that the pH of the unfiltered solution would be maintained at the saturation pH for a longer period of time during water removal processes, compared to the filtered synthetic urine solution. All three solutions were evaporated at 40°C and 40% relative humidity in a controlled climate chamber.

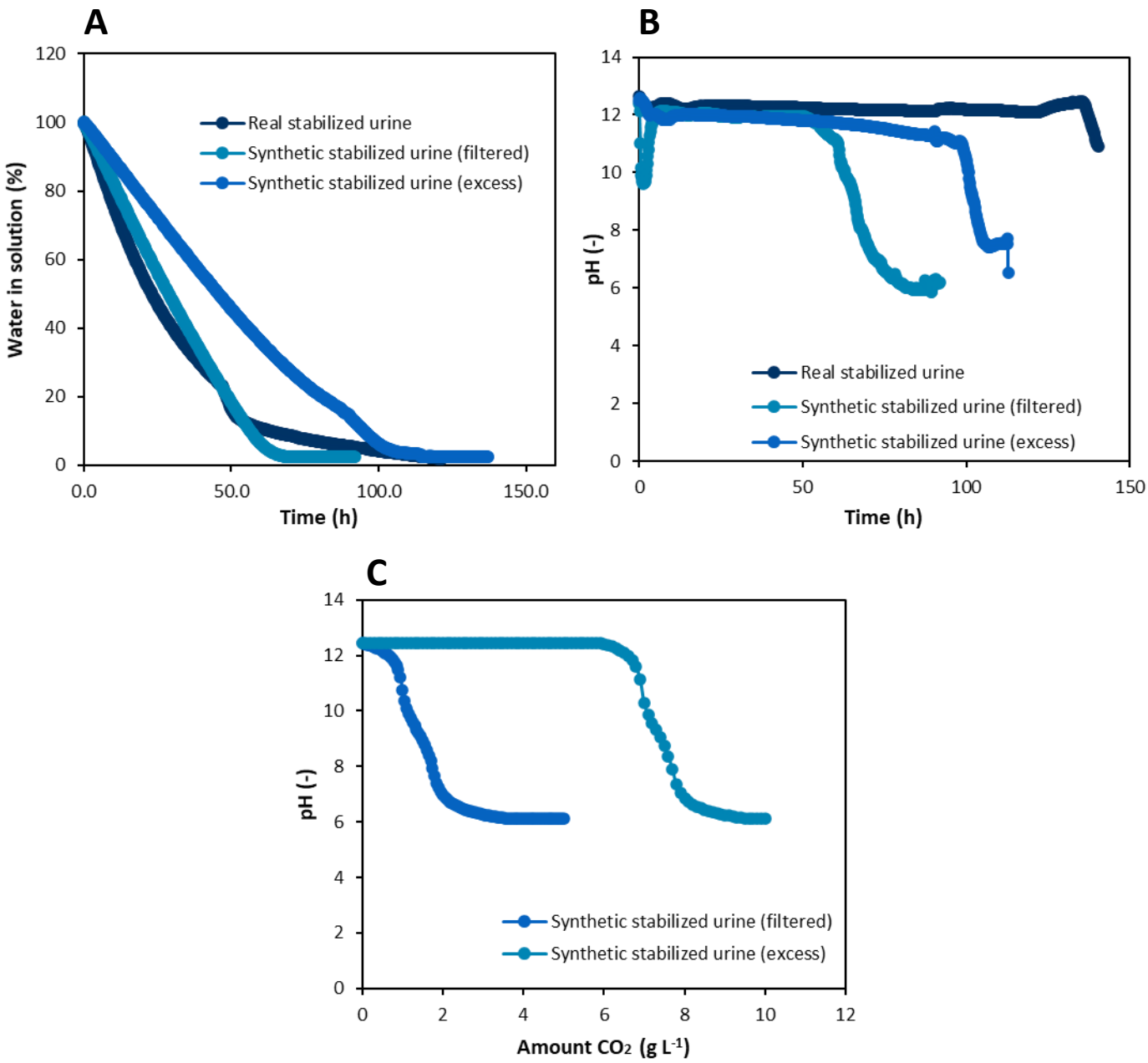

Figure 12. Comparison of synthetic and real stabilized urine solutions. **(A)**. Shows the evaporation rate of $Ca(OH)_2$ stabilized synthetic and real urine solutions. Synthetic urine solutions include unfiltered (excess $Ca(OH)_2$) and filtered solutions. The real urine solution was filtered prior to evaporation processes. **(B)** shows the corresponding pH profiles for all three urine solutions. **(C)** shows the buffering capacity of U1b to CO_2 as determined using OLI simulations.

Comparing the evaporation rate of all three solutions from Figure 12A, the two synthetic urine solutions show a smoother rate compared to real urine. The evaporation rate of $Ca(OH)_2$ real urine showed a change in rate at 47.5 hours. Filtered synthetic urine showed the best comparison to the evaporation rate of real human urine. Unfiltered synthetic urine showed the longest evaporation rate in Figure 12A. This could have been attributed to the excess $Ca(OH)_2$ forming more $CaCO_3$ scale compared to the scale formed in filtered synthetic urine. The presence of more $CaCO_3$ scale resulted in greater hindrance to the evaporation of water from the solution.

However, although there was an observed deviation in evaporation rates between the three solutions, scale was formed on the surface of all three solutions. This scale is shown in Figure 13. The scale sample taken from filtered $Ca(OH)_2$ stabilized urine was sent for XRD analysis and the results confirmed that this scale was $CaCO_3$. The scale observed in Figure 13C was acidified to determine if the same $CaCO_3$ scale was formed in real human urine. Known masses of the scale in Figure 13D were combusted to determine whether this scale was composed of organic compounds. However, the mass before and after combustion remained unchanged. This showed that the scale had no organics present. Upon acid addition this scale sample also fizzed slightly indicating release of CO_2 which would happen if the solid was a carbonate compound.

Figure 13. Comparison of scale formed in syntehtic and real $Ca(OH)_2$ stabilized urine solutions. **(A)** Scale formation observed on the surface of a filtered $Ca(OH)_2$ stabilized synthetic urine solution and sample of this scale is shown in **(B).** Similarly, **(C)** shows the scale formation observed on the surface of filtered $Ca(OH)_2$ stabilized real human urine and sample of this scale in **(D).**

From Figure 12B the pH of real urine behaves differently to that of synthetic urine solutions. Figure 12B shows that throughout the evaporation process, the pH of the urine solution was maintained close to a pH of 12 with $Ca(OH)_2$ stabilization. Near the end of the evaporative process (>130 hours) the pH of real human urine rapidly decreased to a final pH of 10.9. However, in the case of synthetic urine solutions, this pH decrease was more substantial. A final pH of 6.19 and 6.52 was measured in filtered and unfiltered $Ca(OH)_2$ stabilized urine solutions, respectively.

As both synthetic urine solutions did not incorporate any organic compounds other than urea, the absence of such organics may have contributed to this difference between real human and synthetic urine solutions. In addition, Figure 12C shows the amount of CO_2 from the surrounding atmosphere that can be absorbed into the $Ca(OH)_2$ stabilized urine solution as a function of the pH of the solution. This is shown for both filtered and unfiltered stabilized urine solutions. From Figure 12C both synthetic urine solutions, when at a fixed pH, can absorb the same amount of CO_2, the unfiltered solution however is buffered better against a change in pH compared to the filtered solution.

Figure 12C shows that an unfiltered $Ca(OH)_2$ stabilized solution can absorb a much greater quantity of CO_2 before a change in solution pH occurs, compared to the filtered $Ca(OH)_2$ stabilized solution. When considering experimental results, the pH of filtered synthetic urine remains steady during water removal processes, as does the pH of unfiltered synthetic urine in Figure 12B. As predicted in OLI simulations, the decrease in pH of unfiltered synthetic urine occurs after that of filtered synthetic urine. This may be attributed to the information in Figure 12 C showing that although the two solutions can absorb the same amount of CO_2 at a fixed pH, the unfiltered solution has a better buffering capacity. This means that this solution can cope with more CO_2 before a pH change is observed in the solution.

4.3 Effect of urine composition on solids formation for $Ca(OH)_2$ stabilized urine at a fixed temperature

The effect of urine composition for synthetic urine stabilized with $Ca(OH)_2$ in terms of the total mass of solids formed, as well as the mass of major nutrients formed was determined using simulations at 40°C. Figure 14 shows the variance in major ions for different urines stabilized with $Ca(OH)_2$. After stabilizing fresh urine solutions with 10 g L^{-1} $Ca(OH)_2$, a pre-evaporation filtration step was included prior to the water removal step. This filtration step results in the removal of phosphorus and magnesium ions from the initial fresh urine solutions (Figure 14).

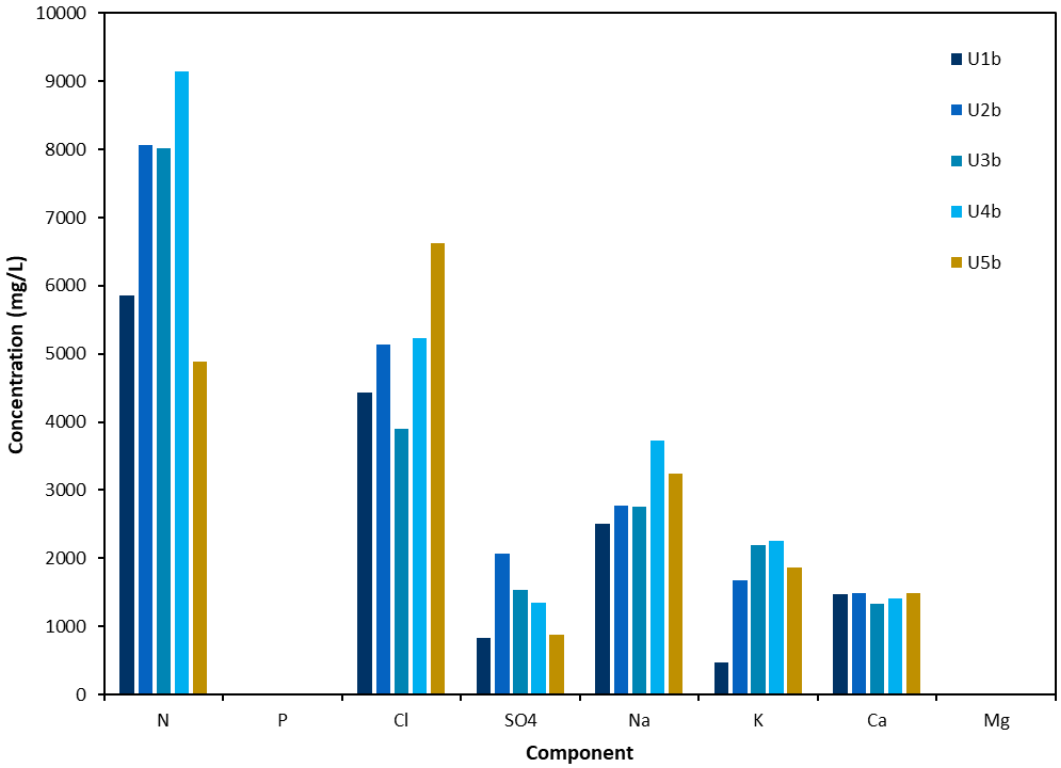

Figure 14. Initial composition for five different urine samples stabilized with $Ca(OH)_2$. Composition is given in terms of major ion concentrations. In all cases, a pre-evaporation filtration step was used. This can be seen from the negligible phosphorus and magnesium concentrations after filtration. These five different urine samples were used as a simulation input to determine the effect of urine composition on the mass of solids and major nutrients during water removal processes at a fixed temperature of 40°C.

From the initial urine samples that were stabilized with $Ca(OH)_2$, U4b, U2b and U3b contain the highest nitrogen concentration. This is attributed to the high initial urea content of these stabilized urine solutions. Additionally, U5b, along with U2b, U3b and U4b, contain high concentrations of Na^+ and Cl^- ions. From OLI simulations, urea and NaCl were the two major solids formed when removal of all the water by evaporation. As the abovementioned urine solutions, contain large amount of urea and Na^+ and Cl^- ions, it would make sense that these would contribute to the largest mass of solids formed during water removal processes for U4b.

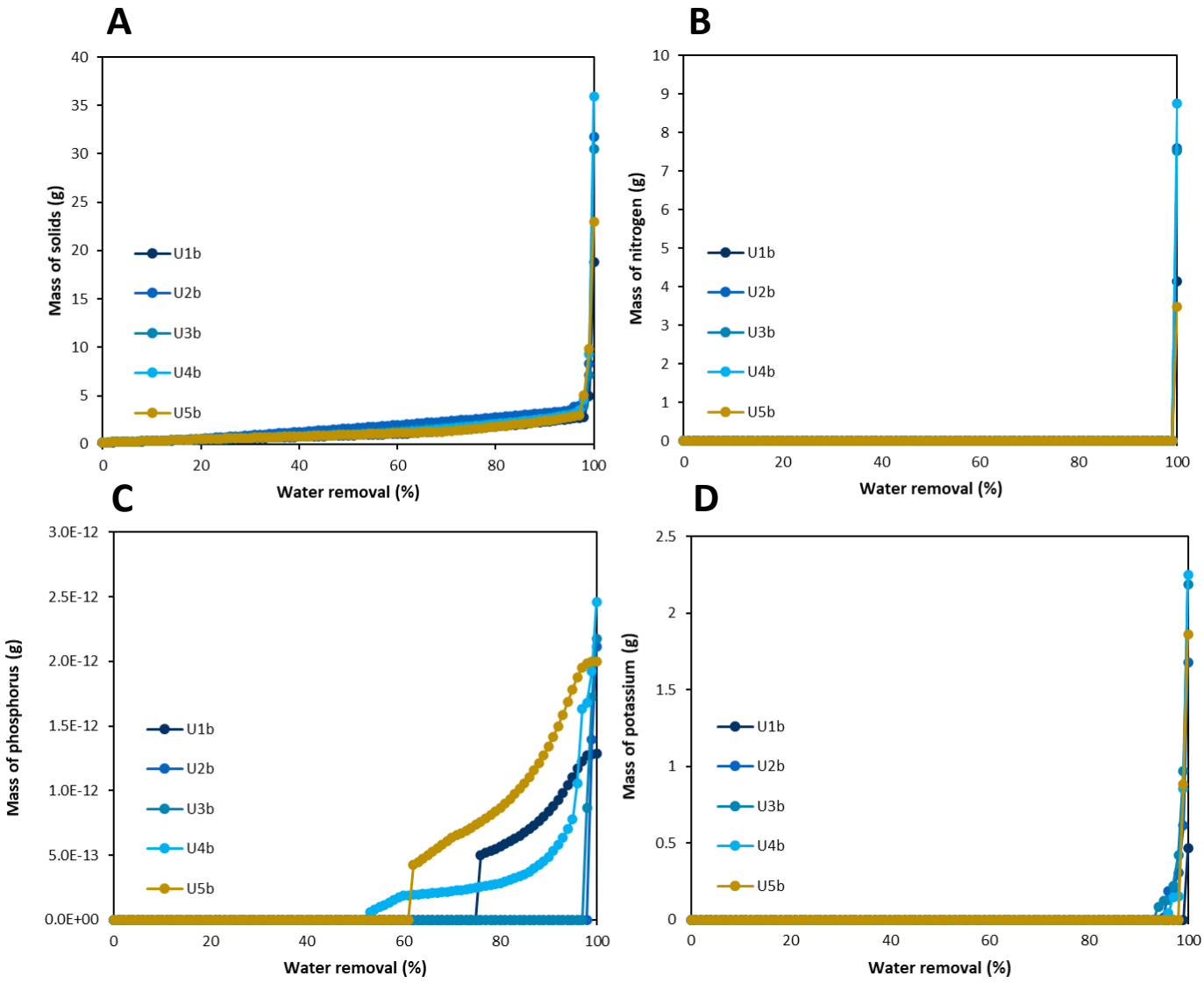

Figure 15. Mass of total solids and major nutrients formed as a function of water removal for urine stabilized with $Ca(OH)_2$ at a fixed temperature of 40°C. Water removals between 0% and 100% were studied using OLI simulations. **(A)** shows the total mass of solids formed, **(B)** shows the total mass of nitrogen formed, **(C)** shows the total mass of phosphorus formed, and similarly **(D)** shows the total mass of potassium formed as a function of water removal for a fixed composition. A pre-evaporation filtration step was used in simulations. This is particularly relevant in **(C)** as the amount of phosphorus recovered at 100% water removal is negligible but would be higher if no pre-filtration were used.

Figure 15A validated this hypothesis showing the effect of a high initial urea content in $Ca(OH)_2$ stabilized urine. U4b in Figure 15A was shown to form the greatest mass of total

solids. Figure 15A also shows U2b and U3b forming the second and third highest mass of total solids. This information corresponded to the mass of nitrogen solids formed as shown in Figure 15B.

However, in the case of U1b and U5b, the influence of Na^+ and Cl^- ions on the total mass of solids formed, was introduced. Figure 14 shows U5b to have a greater potential to form a greater mass of NaCl compared to U1b, although U1b has a higher potential to form urea solids. The higher urea concentration in U1b was not great enough to outweigh the potential to form NaCl solids in U5b. As a result, U5b was predicted to form a greater mass of total solids compared to U1b.

Figure 15A shows the mass of total solids formed at 40°C during water removal processes for five different $Ca(OH)_2$ stabilized urine compositions. Figure 15B shows the mass of nitrogen solids formed from these five stabilized solutions during water removal processes at 40°C. Similarly, Figure 15C and Figure 15D shows the mass of phosphorus and potassium solids formed during evaporation from the five $Ca(OH)_2$ stabilized urine solutions at 40°C.

From Figure 15A, the majority of the total solids were formed at water removals greater than 96%. However, from water removals above 60%, a gradual increase in total solids was observed. This increases rapidly after 96% water removal with a significant mass of total solids present from 90% water removal. This is similar to the mass of potassium solids formed as shown in Figure 15D. Figure 15B shows that majority of nitrogen solids are formed close to 100% water removal. The information in Figure 15 indicated that if one desires to recover major nutrients (N, P or K) from urine as solids, one needs to operate at high levels of water removal (between 96% and 100%).

The results shown in Figure 15C consider a pre-evaporation filtration step; simulations also included this 'filtration' step . This meant urine was evaporated straight after the stabilization process without removing any precipitates that may have formed during the stabilization process. This step has a major impact on the mass of phosphorus solids, and the point at which these solids can be recovered. When comparing Figure 15C and Figure 16, solid phosphorus appears even at 0% water removal. This is due to phosphorus precipitates forming during the stabilization process.

From the initial composition of $Ca(OH)_2$ stabilized urine in Table 12, Figure 16 shows that theoretically 100% of the initial phosphorus in solution forms solid calcium phosphate during the stabilization process, prior to water removal processes occurring. This is observed for all stabilized urine solutions, regardless of the urine composition. The amount of calcium phosphate that forms between the five urine solutions differs according to the initial amount of phosphate present in solution. For example, U3b contains the most initial phosphate in solution and in Figure 16, is shown to form the most solid phosphate during water removal.

If it is desired to achieve high phosphorus recovery at 100% water removal, then omitting the pre-evaporation filtration step may be required to achieve this. Evaporating the stabilized solution as is, will achieve high phosphorus recovery as the phosphorus will be present in the final solids formed. However, if one desires to recover phosphorus independently of water

removal and other solids formed, a pre-filtration step could be used to remove and recover phosphorus solids from the solution prior to the evaporation processes and solids formation.

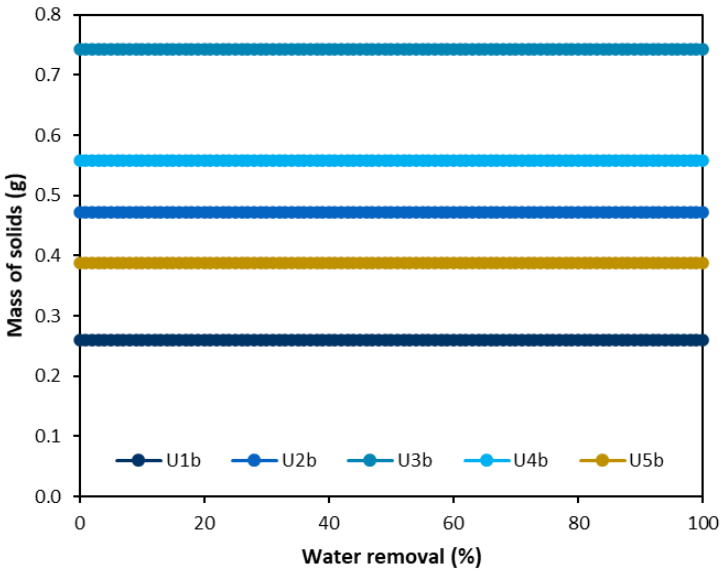

Figure 16. Total mass of phosphorus formed as a function of water removal for five different urine solutions stabilized with $Ca(OH)_2$,without a pre-evaporation filtration step. Fresh urine solutions were stabilized with 10 g L^{-1} $Ca(OH)_2$ and thereafter the water was removed. The mass of solids formed was obtained from OLI simulations at a fixed temperature of 40°C.

4.4 Effect of operating temperature on solids formation for $Ca(OH)_2$ stabilized urine

The effect of operating (evaporation) temperature on total solids formed as well as N, P and K solid formation was studied using OLI simulations. However, when studying the effect of operating temperature, the urine composition was fixed. Urine composition U1b was used in simulations, while the operating temperatures were varied between 20°C and 70°C.

Figure 17A shows the mass of total solids formed when U1b was evaporated at different operating temperatures between 20°C and 70°C. Figure 17B shows the mass of nitrogen solids formed from U1b between these operating temperatures from 20°C to 70°C. Similarly, Figure 17C and Figure 17D shows the mass of phosphorus and potassium solids formed during evaporation as a function of temperature (20°C to 70°C) in U1b.

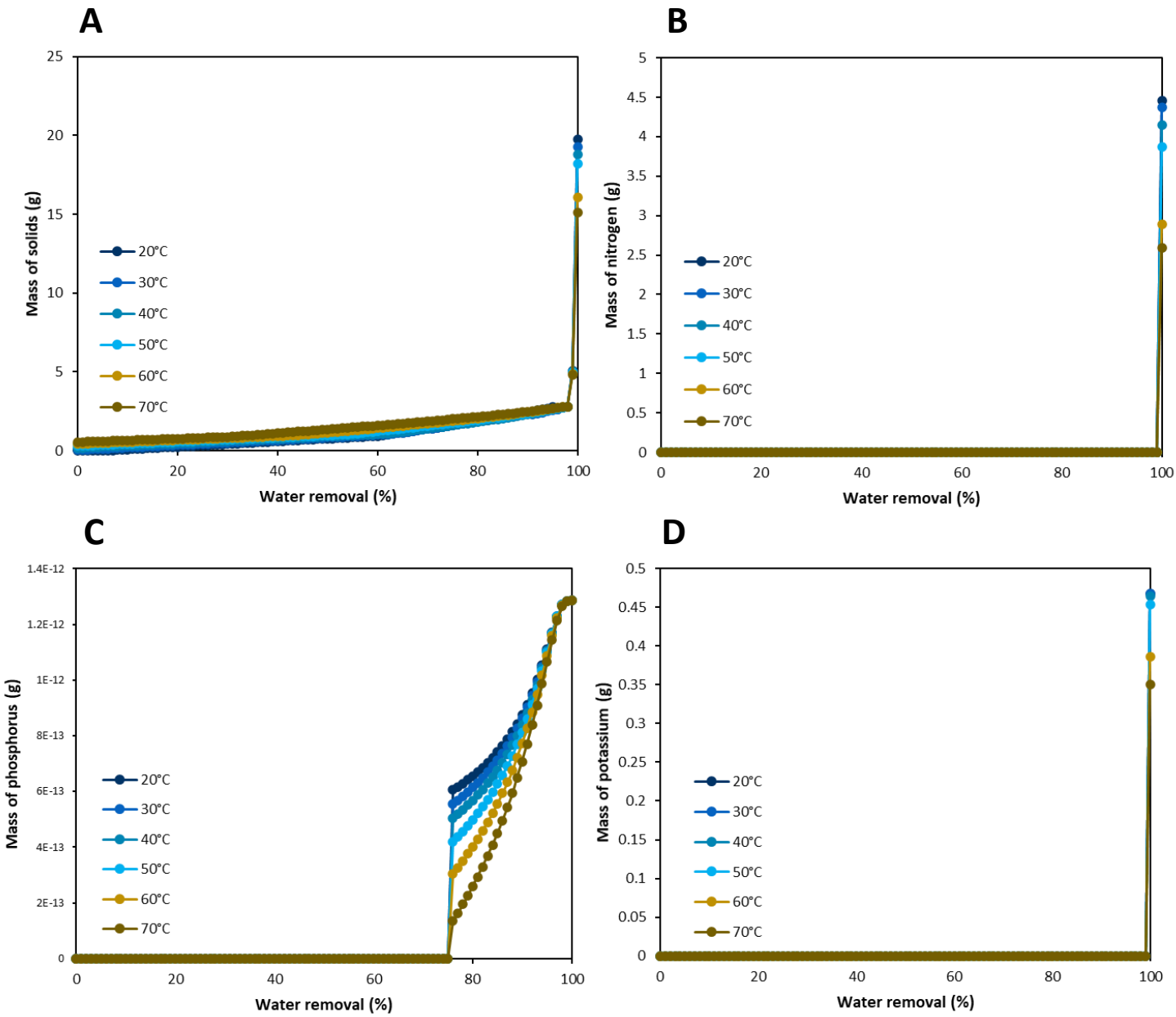

Figure 17. Mass of total solids and major nutrients formed as a function of water removal and temperature for $Ca(OH)_2$ urine (U1b). Water removals between 0% and 100% were studied using OLI simulations. Additionally, water removal at temperatures between 20°C and 70°C were investigated. **(A)** shows the total mass of solids formed. **(B)** shows the total mass of nitrogen formed. **(C)** shows the total mass of phosphorus formed, and similarly **(D)** shows the total mass of potassium formed as a function of water removal for a fixed composition of U1b. A pre-evaporation filtration step was used in simulations. This is particularly relevant in **(C)** as the amount of phosphorus recovered at 100% water removal is negligible.

Simulation results in Figure 17 showed a similar trend to that of Figure 15. Majority of the total solids were formed at water removals greater than 96%. However, in Figure 17A, there was an observed decrease in total solids formed, with an increase in operating temperature. Figure 17B and Figure 17D showed that solid N and K compounds, can be recovered at water removal intervals close to 100%. Both N and K solid formation is predicted to decrease with an increase in operating temperature. This agreed with the trend in the mass of total solids shown in Figure 17A.

OLI modelling does not account for urea hydrolysis. Additionally, simulation results showed that at 100% water removal, the remaining urea, not in the solid phase, was present in the liquid phase. This is not possible as at 100% water removal, only solid and vapor phase should be present. Theoretically no water would be present to allow salts to exist in solution (or the aqueous phase). Hence, the results in Figure 17B, used the mass of solid urea (as g-N) at 100% water removal, noting the inaccuracy of the OLI model.

The observed decrease in mass of nitrogen solids formed with an increase in operating temperature can be explained by considering the solubility trend for urea. The solubility of urea increases with an increase in temperature (Appendix B.1). This means that with an increase in temperature, more urea was predicted to remain in the liquid phase in OLI simulations. In conjunction with the abovementioned inaccuracy of OLI in predicting a liquid urea phase at 100% water removal, the trend in Figure 17B is explained.

However, realistically an increase in operating temperature was expected to result in a decrease in the mass of solid nitrogen compounds formed. This was expected due to chemical urea hydrolysis, which occurs at an increased rate when at temperatures above 40°C (Randall et al., 2016).

In Figure 17D, the major potassium solid formed in in the urine stabilized with $Ca(OH)_2$ is KCl. The solubility trend for KCl is similar to that of urea mentioned above (Appendix B.1). The solubility of KCl increases with an increase in temperature. Like that of urea solids, major potassium solids KCl decrease with an increase in operating temperature. This results in an increasing KCl liquid phase with an increase in operating temperature, even at 100% water removal. However, as above, this liquid phase is not an accurate prediction at 100% water removal. Additionally, potassium does not degrade or vaporize at elevated temperatures unlike urea. Hence, it was expected that the same mass of potassium solids should be recovered at 100% water removal regardless of operating temperature. This was not predicted in Figure 17D, showing that a portion of potassium was remaining in the liquid phase even at 100% water removal. This portion of liquid phase potassium increased with an increase in operating temperature.

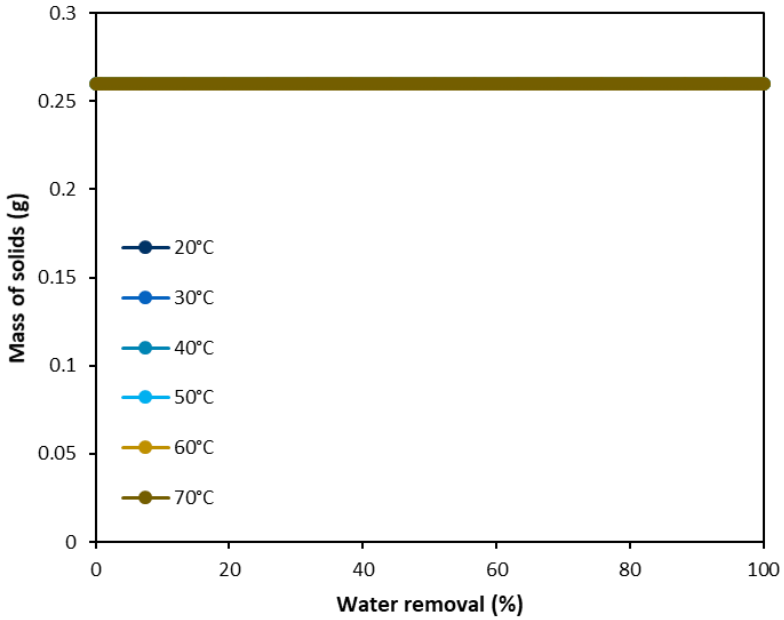

Figure 18. Total mass of phosphorus formed as a function of water removal temperature for a fixed $Ca(OH)_2$ stabilized urine composition, without a pre-evaporation filtration step. After stabilization with 10 g L^{-1} $Ca(OH)_2$, urine was immediately subjected to water removal processes. Mass information was obtained from OLI simulations.

Although the mass of phosphorus solids formed in Figure 17C is negligible due to a pre-evaporation filtration step, Figure 17C shows that the total mass of phosphorus solids formed at 100% water removal is the same, regardless of operating temperature. When omitting the pre-evaporation filtration step, Figure 18 shows that theoretically, 100% of the initial phosphorus in the urine solution will precipitate out of solution with the $Ca(OH)_2$ stabilization process. This precipitation occurs prior to any water removal processes and is independent of operating temperature.

4.5 Energy consumption associated with water removal from $Ca(OH)_2$ stabilized urine at varied operating temperatures and stabilized urine compositions.

To develop a first estimate of the input energy requirement associated with the urine evaporation process, it was assumed that 1000 L (1 m^3) of urine was evaporated per day. The results from the OLI simulations were then collected and processed using the cost calculations explained in Appendix B.2. However, OLI did not account for the initial heat required to raise the solution from the inlet temperature (25°C) to the operating temperature.

To determine the amount of initial energy required to heat urine solutions from the inlet to the required outlet (evaporation) temperature, basic mass and energy balances were manually computed. As calculations were done by hand, it was assumed that the urine solution was composed of 97.9 wt% water and 2.15 wt% NaCl, as discussed in the costing method in Appendix B. This assumption was made as urine is majority water. Furthermore, once evaporated, it was observed that the major salt that formed was NaCl. Complicating the mass balance with additional solids did not drastically influence the mass and energy balance as the contribution from these compounds was much less than the contribution from water.

The input heating requirements to raise the temperature from the inlet to the required outlet temperatures, for both water (Table 35 Appendix B.2) and NaCl (Table 36 Appendix B.2) are shown below. In the case of Figure 19A, operating temperatures varied, but in Figure 19B this was fixed at 40°C while the urine composition varied.

The initial energy required to heat solutions to evaporation temperatures determined through the addition of results in Table 35 and Table 36 (both found in Appendix B.2), was added to the heating requirement associated with the change in enthalpy during water removal processes. This change in enthalpy was calculated using OLI simulations. The total energy associated with the water removal process as a function of evaporation temperature is shown in Figure 19A. This was done using a fixed $Ca(OH)_2$ stabilized urine composition (U1b). Similarly, the same costing process was followed in Figure 19B, where the evaporation temperature was fixed at 40°C, and the composition of $Ca(OH)_2$ stabilized urine was varied.

In Figure 19, each input energy requirement curve starts at 0 kWh m^{-3} urine and increases vertically, before increasing exponentially. This vertical increase in input energy requirement prior to any water removal, represents the initial energy input required to reach the evaporation temperature. In Figure 19A this increases with an increase in temperature as a greater energy input is required to reach the higher operating temperature. When operating at 20°C, a negative energy input (energy removal) is required as evaporation is occurring at a temperature 5°C lower than the inlet temperature of the solution. In Figure 19B, the vertical increase in input energy is the same for all five urine solutions as the evaporation temperature (40°C), is the same for each solution.

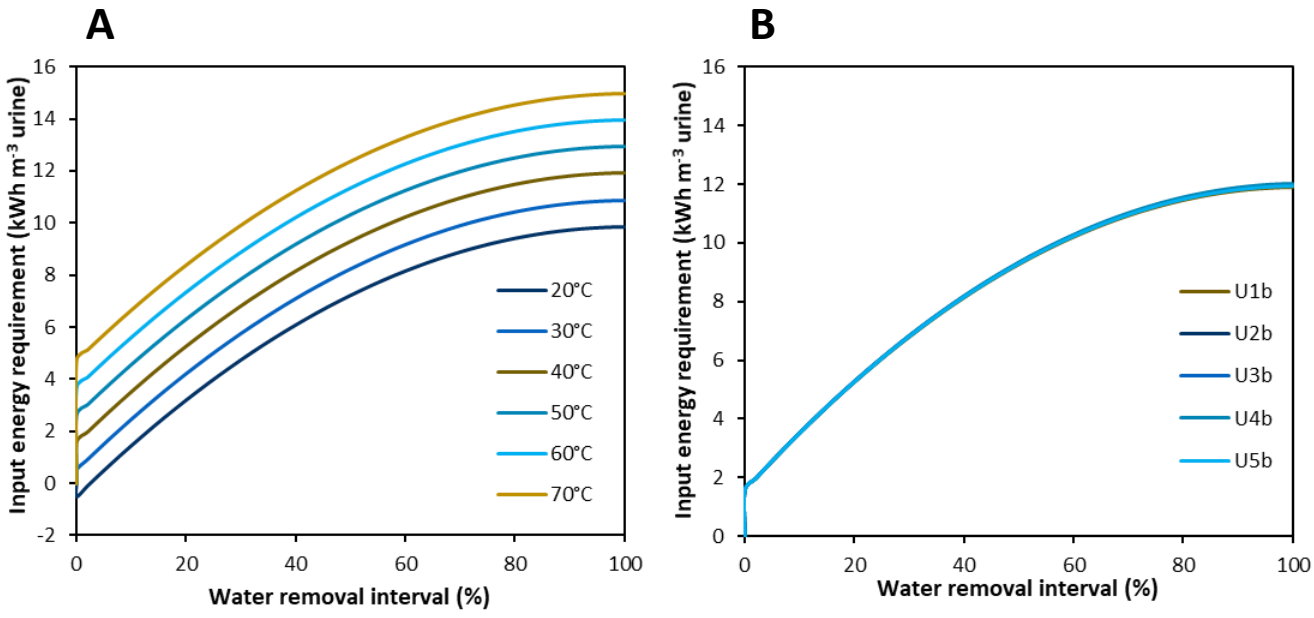

Figure 19. Input energy requirement associated with $Ca(OH)_2$ stabilized urine as a function of operating temperature and composition. The energy requirement is given in kWh per m^3 urine per day. **(A)** shows the input energy requirement for fixed $Ca(OH)_2$ stabilized urine composition (U1b) was used when performing costing calculation at temperatures between 20°C and 70°C. **(B)** shows the input energy requirement associated with $Ca(OH)_2$ stabilized urine of five different urine compositions. Costing in **(B)** was calculated at a fixed temperature of 40°C.

Figure 19 shows a similar trend in input energy requirements. With an increase in water removal, there is an exponential increase in input energy input requirement. This is explained through the way energy requirements were calculated.

Calculations were performed on a cumulative basis. Meaning that if one requires to evaporate a urine solution from 0% to 100% water removal at 40°C, the input energy requirement at 100% removal considers all previous input energy requirements. Additionally, if the 40°C solution is at 20% water removal and a water removal of 80% is desired, the input energies at 20% and 80% can be determined from Figure 19A. Subtracting these two values will then determine the amount of energy input required to reach the desired 80% water removal.

Furthermore, Figure 19A shows that the higher the evaporation temperature, the greater the input energy requirement. However, Figure 19B shows that urine composition has no effect on the input energy requirement. If this is applied to an industrial situation, this may mean that regardless of the urine composition, which naturally will vary, the input energy requirement should remain constant.

Although there is an increase in energy input requirement when operating at higher temperatures, these higher temperatures will increase evaporation rates, lowering the time required for water removal processes. Although there is a greater potential for urea hydrolysis to occur, these higher operating temperatures would allow for a faster processing time.

The aim of the basic costing was to create figures that could be used as basic design charts. When considering the evaporation process, one would be able to use the chart to read off the input energy requirement associated with evaporating water from urine stabilized $Ca(OH)_2$ at a specific process temperature. This energy requirement in kWh per m^3 urine, could then be correlated to an energy cost using the relevant municipal energy tariffs.

Eskom electricity tariffs in 2020 were set at 116.72 c kWh^{-1} [10]. Using this tariff, it was estimated that U1b would require 11.91 kWh of energy to reach 100% water removal at 40°C. This results in a cost of R 13.90 to evaporate one m^3 of stabilized urine to recover the nutrients in the stabilized urine in the solid form.

Experimental results in Figure 7A showed that a total of 22 g L^{-1} solids were obtained when evaporating stabilized urine to 100% water removal. When evaporating 1 m^3 urine, this corresponds to 22 kg m^{-3}. Using the cost of R13.90, the solids formed during urine evaporation could be used as a fertilizer with an associated energy cost of 0.63 R kg^{-1}. The selling prices of synthetic fertilizers was between 0.8 and 1.49 $ kg^{-1} in Africa in 2020. This correlates to 13.17 and 24.53 R kg^{-1} using an average exchange rate of 16.47 R $\$^{-1}$ for 2020[11], which is much higher than the energy cost of 0.63 R kg^{-1}. This shows that, compared to synthetic fertilizers, the research into evaporating urine and using the resulting solids as a fertilizer is potentially a cost effective alternative and should be further studied to ensure successful implementation and widespread acceptance and use.

[10] Tariffs and charges (eskom.co.za)
[11] Annual Average Exchange Rates (nedbank.co.za)

Chapter 5. Conclusion and recommendations

This thesis focused on the recovery of all three key nutrients (N, P and K) contained in human urine by evaporation at pH and temperature conditions which differed to experimental conditions used in previous studies. The type of urine studied, also differed to the types of urine studied in the available literature. In the final chapter of this dissertation, the major findings and key results of this thesis are summarized in Section 5.1. This chapter then ends the dissertation by considering recommendations and improvements to incorporate into future work.

5.1 Summary of key findings and results

Nine different urine solutions were studied in terms of NPK recoveries. This was used to determine the best urine stabilization treatment methodology. Hydrolyzed real urine had the lowest nitrogen recovery (7.17%) due to the addition of urease enzyme which was responsible for urea hydrolysis. Both acetic and citric acid had reasonable nitrogen recoveries of 103% and 93.5%, respectively. Both phosphorus and potassium components were non-volatile, and as a result, the decision for the best urine stabilization treatment method had to be made on the nitrogen recovery achieved in the urine solution.

Considering the pH of each urine solution, it was noted that MgO stabilization did not maintain the pH of the urine solution above a pH of 10 to ensure that urea hydrolysis was prevented. Additionally, both acetic and citric acid as well as $Ca(OH)_2$ stabilization methods were seen to maintain the pH of the urine solutions below a pH of 3.5 and above a pH of 11 respectively, ensuring that the risk of urea hydrolysis was eliminated. Based on these findings, it was concluded that $Ca(OH)_2$ stabilization was the most suitable method of urine stabilization. This method of urine stabilization had the highest nitrogen recovery when used to stabilize real urine (109%). Calcium hydroxide stabilization also helped buffer the pH of the solution. This stabilization method was also preferred due to its simplicity of not requiring dosing equipment.

Using the preferred method of stabilization ($Ca(OH)_2$ stabilized urine), experimental and OLI simulations were compared to determine the accuracy of the theoretical predictions. It was concluded that the OLI simulations did not accurately predict experimental observations. At a 75% water removal, the experimental results showed a recovery in N, P and K respectively. Simulations only predicted a recovery in N at 75% water removal. Furthermore, at a 100% water removal, the experimental results showed a total of 22 g solids had formed, while simulations predicted 18.8 g solids.

A comparison was drawn between the individual solid species predicted to form using OLI simulations, and the experimental solids identified using XRD analysis. Most major salts predicted to form were identified. However, salts such as CaO, MgO and $Mg(OH)_2$, were not identified experimentally. These salts were predicted to be present in small quantities and as a result may not have been detected by XRD. $CaCO_3$ was detected experimentally but not predicted thermodynamically. It was concluded that this solid phase was present due to the reaction of $Ca(OH)_2$ with CO_2 from the surrounding atmosphere. This was not accounted for in OLI simulations.

Further reasons for these discrepancies were explored. Firstly, it was observed that OLI simulations did not account for urea hydrolysis. Experimentally, urea hydrolysis was observed at temperatures greater than 40°C to 70°C. It was observed that operating at 70°C could decrease evaporation time to reach 100% water removal by 55.5%. However, this was accompanied by 8.12% urea hydrolysis.

Furthermore, OLI simulations did not account for the loss in NH_3 due to the volatilization of this gas into the surrounding atmosphere. This was not only observed when comparing OLI results to experimental results for $Ca(OH)_2$ stabilized urine but was also observed when comparing NPK experimental results to the theoretical results.

A final comparison was drawn between real and synthetic urine solutions. Both solutions experimentally showed the formation of a scale which may hinder evaporation rates. The scale formed in the synthetic urine solution was identified as $CaCO_3$ through XRD analysis. The scale formed in real $Ca(OH)_2$ urine was also concluded to be $CaCO_3$ as a sample of this scale fizzed upon the addition of acid. Additionally, when subjected to combustion, there was no change in mass in the scale sample.

OLI simulations were then used to determine the effect of temperature and composition on the solids formed in $Ca(OH)_2$ stabilized urine. It was observed that a change in urine composition influences the solids formed. Different urine compositions introduced different concentrations of ions into solution and as a result, different compounds formed from these ions. Increasing temperature resulted in a decrease in the solids formed. When considering the major solids that form (KCl, NaCl and urea), an increase in solubility with an increase in temperature was observed. Hence OLI predicted these compounds to be in the liquid phase at 100% water removal. This was concluded as impossible because, at 100% water removal, only the solid and vapor phase should be present.

Lastly, these simulations were used to determine the input energy requirement required to evaporate 1 m^3 $Ca(OH)_2$ stabilized urine per day. An increase in evaporation temperature required an increased energy input to reach the higher temperature. However, urine composition had minimal effect on the input energy requirement. When costing this energy requirement, a urine-based fertilizer could be produced via the evaporation process with an energy cost of 0.63 R kg^{-1}.This cost does not consider additional costs such as labour, catalysts, storage, transport and $Ca(OH)_2$ though. When compared to available synthetic fertilizers, which are sold for between 13.17 and 24.53 R kg^{-1}, the potential for such urine-based fertilizers was highlighted.

5.2 Recommendations for future work

Based on this work, the following recommendations are made:

1. As urea hydrolysis may be prevented through evaporating a urine solution in a short time period, it is recommended that the rate of urea hydrolysis at different operating temperatures, as well as operating times (corresponds to evaporation rates) be investigated.

2. Additionally, when considering $Ca(OH)_2$ stabilized synthetic and real urine, $Ca(OH)_2$ stabilized synthetic urine was a good proxy to $Ca(OH)_2$ stabilized real urine. However, there were slight discrepancies, especially in terms of evaporation rates. Therefore, it is recommended that all the different stabilization methods used in this dissertation based on synthetic urine, be tested also with real urine.
3. As shown in experimental results, OLI simulations do not account for urea hydrolysis, NH_3 volatilization and the formation of $CaCO_3$ scale on the surface of the urine solution during evaporation. To improve the accuracy of OLI simulations and suitability to urine evaporation work, it is recommended that these experimental findings be considered and incorporated when using OLI as a simulation tool in future work.
4. The final recommendation for this dissertation is to test the solid fertilizer formed after complete water removal by evaporation. This fertilizer should be tested to determine its applicability to growing different crops, as well as to determine how this fertilizer compares to commercial and synthetic fertilizers.

Reference list

Antonini, S., Nguyen, P.T., Arnold, U., Eichert, T., Clemens, J., 2012. Solar thermal evaporation of human urine for nitrogen and phosphorus recovery in Vietnam. Sci. Total Environ. 414, 592–599. https://doi.org/10.1016/j.scitotenv.2011.11.055

Beler-Baykal, B., Bayram, S., Akkaymak, E., Cinar, S., 2004. Removal of ammonium from human urine through ion exchange with clinoptilolite and its recovery for further reuse. Water Sci. Technol. 50, 149–156. https://doi.org/10.2166/wst.2004.0371

Bennett, G.E., 1997. Waste minimization and cost reduction for the process industries. J. Hazard. Mater. 53, 236–237. https://doi.org/10.1016/S0304-3894(96)01858-4

Bethune, D.N., 2015. A Novel Urine Evaporation and Collection System for Dry Toilets (Civil Engineering Graduate program). University of Calgary, Alberta.

Bethune, D.N., Chu, A., Ryan, M.C., 2014. Passive evaporation of source-separated urine from dry toilets: a lab study. J. Water Sanit. Hyg. Dev. 4, 654–662. https://doi.org/10.2166/washdev.2014.058

Boyer, T.H., Saetta, D., 2019. Opportunities for Building-Scale Urine Diversion and Challenges for Implementation. Acc. Chem. Res. 52, 886–895. https://doi.org/10.1021/acs.accounts.8b00614

Chang, J., Zuo, J., Lu, K.-J., Chung, T.-S., 2016. Freeze desalination of seawater using LNG cold energy. Water Res. 102, 282–293. https://doi.org/10.1016/j.watres.2016.06.046

Chipako, T.L., Randall, D.G., 2020a. Investigating the feasibility and logistics of a decentralized urine treatment and resource recovery system. J. Water Process Eng. 37, 101383. https://doi.org/10.1016/j.jwpe.2020.101383

Chipako, T.L., Randall, D.G., 2020b. Urine treatment technologies and the importance of pH. J. Environ. Chem. Eng. 8, 103622. https://doi.org/10.1016/j.jece.2019.103622

Chipako, T.L., Randall, D.G., 2019. Urinals for water savings and nutrient recovery: a feasibility study. Water SA 45, 266–277. https://doi.org/10.4314/wsa.v45i2.14

Corcoran, E. (Ed.), 2010. Sick water? the central role of wastewater management in sustainable development: a rapid response assessment. Arendal, Norway.

de Jonge, V.N., Elliott, M., 2001. Eutrophication, in: Steele, J.H. (Ed.), Encyclopedia of Ocean Sciences (Second Edition). Academic Press, Oxford, pp. 306–323. https://doi.org/10.1016/B978-012374473-9.00047-3

De Paepe, J., De Pryck, L., Verliefde, A.R.D., Rabaey, K., Clauwaert, P., 2020. Electrochemically Induced Precipitation Enables Fresh Urine Stabilization and Facilitates Source Separation. Environ. Sci. Technol. 54, 3618–3627. https://doi.org/10.1021/acs.est.9b06804

Edokpayi, J.N., Odiyo, J.O., Durowoju, O.S., 2017. Impact of Wastewater on Surface Water Quality in Developing Countries: A Case Study of South Africa. Water Qual. https://doi.org/10.5772/66561

Ek, M., Bergström, R., Bjurhem, J.-E., Björlenius, B., Hellström, D., 2006. Concentration of nutrients from urine and reject water from anaerobically digested sludge. Water Sci. Technol. 54, 437–444. https://doi.org/10.2166/wst.2006.924

Eriksen, L., Andreasen, P., Ilsøe, B., 1996. Inactivation of Ascaris suum eggs during storage in lime treated sewage sludge. Water Res. 30, 1026–1029. https://doi.org/10.1016/0043-1354(95)00258-8

Etter, B., Udert, K.M., Gounden, T., 2014. VUNA – Scaling Up Nutrient Recovery from Urine 8.

Feineigle, M., 2011. Urine: Closing the NPK Loop [WWW Document]. Permac. Res. Inst. URL https://www.permaculturenews.org/2011/11/27/urine-closing-the-npk-loop/ (accessed 4.22.20).

Flanagan, C.P., Randall, D.G., 2018. Development of a novel nutrient recovery urinal for on-site fertilizer production. J. Environ. Chem. Eng. 6, 6344–6350. https://doi.org/10.1016/j.jece.2018.09.060

Glibert, P.M., 2012. Ecological stoichiometry and its implications for aquatic ecosystem sustainability. Curr. Opin. Environ. Sustain. 4, 272–277. https://doi.org/10.1016/j.cosust.2012.05.009

Hanaerus, A., Hellström, D., Johansson, E., 1996. Conversion of urea during storage of humane urine. Vatten 52, 263–270.

Hellström, D., Johansson, E., Grennberg, K., 1999. Storage of human urine: acidification as a method to inhibit decomposition of urea. Ecol. Eng. 12, 253–269. https://doi.org/10.1016/S0925-8574(98)00074-3

Höglund, C., 2001. Evaluation of microbial health risks associated with the reuse of source-separated humna urine.

Hotta, S., Funamizu, N., 2008. Inhibition factor of ammonification in stored urine with fecal contamination. Water Sci. Technol. 58, 1187–1192. https://doi.org/10.2166/wst.2008.349

Jana, B.B., Rana, S., Bag, S.K., 2012. Use of human urine in phytoplankton production as a tool for ecological sanitation. Water Sci. Technol. 65, 1350–1356. https://doi.org/10.2166/wst.2012.044

Jen, J., 2002. Simultaneous determination of uric acid and creatinine in urine by an eco-friendly solvent-free high performance liquid chromatographic method. Talanta 58, 711–717. https://doi.org/10.1016/S0039-9140(02)00377-6

Jimenez, J., Bott, C., Love, N., Bratby, J., 2015. Source Separation of Urine as an Alternative Solution to Nutrient Management in Biological Nutrient Removal Treatment Plants. Water Environ. Res. 87, 2120–2129. https://doi.org/10.2175/106143015X14212658613884

Jönsson, H., Stenström, T.-A., Svensson, J., Sundin, A., 1997. Source separated urine-nutrient and heavy metal content, water saving and faecal contamination. Water Sci. Technol., Sustainable Sanitation 35, 145–152. https://doi.org/10.1016/S0273-1223(97)00192-3

Kabongo, J.D., 2013. Waste Valorization, in: Idowu, S.O., Capaldi, N., Zu, L., Gupta, A.D. (Eds.), Encyclopedia of Corporate Social Responsibility. Springer, Berlin, Heidelberg, pp. 2701–2706. https://doi.org/10.1007/978-3-642-28036-8_680

Kakimoto, T., Shibuya, H., Suzuki, H., Hotta, S., Funamizu, N., 2019. Components of Pure Fresh Human Urine and Their Fate in Storage Process, in: Funamizu, N. (Ed.), Resource-Oriented Agro-Sanitation Systems: Concept, Business Model, and Technology. Springer Japan, Tokyo, pp. 123–137. https://doi.org/10.1007/978-4-431-56835-3_9

Kyriakou, V., Garagounis, I., Vourros, A., Vasileiou, E., Stoukides, M., 2020. An Electrochemical Haber-Bosch Process. Joule 4, 142–158. https://doi.org/10.1016/j.joule.2019.10.006

Lambert, S.E., Randall, D.G., 2019. Manufacturing bio-bricks using microbial induced calcium carbonate precipitation and human urine. Water Res. 160, 158–166. https://doi.org/10.1016/j.watres.2019.05.069

Larsen, T.A., 2020. Urine Source Separation for Global Nutrient Management, in: O'Bannon, D.J. (Ed.), Women in Water Quality, Women in Engineering and Science. Springer International Publishing, Cham, pp. 99–111. https://doi.org/10.1007/978-3-030-17819-2_6

Larsen, T.A., Gujer, W., 1996. Separate management of anthropogenic nutrient solutions (human urine). Water Sci. Technol., Water Quality International '96 Part 2 34, 87–94. https://doi.org/10.1016/0273-1223(96)00560-4

McClelland, J., 2017. Why seeing the value of wastewater is vital for a sustainable future [WWW Document]. Raconteur. URL https://www.raconteur.net/sustainability/why-the-value-of-wastewater-is-vital-for-a-sustainable-future (accessed 4.1.20).

Meyer, G., Frossard, E., Mäder, P., Nanzer, S., Randall, D.G., Udert, K.M., Oberson, A., 2018. Water soluble phosphate fertilizers for crops grown in calcareous soils – an outdated paradigm for recycled phosphorus fertilizers? Plant Soil 424, 367–388. https://doi.org/10.1007/s11104-017-3545-x

Mobley, H.L., Hausinger, R.P., 1989. Microbial ureases: significance, regulation, and molecular characterization. Microbiol. Mol. Biol. Rev. 53, 85–108.

Muster, T.H., Douglas, G.B., Sherman, N., Seeber, A., Wright, N., Güzükara, Y., 2013. Towards effective phosphorus recycling from wastewater: Quantity and quality. Chemosphere 91, 676–684. https://doi.org/10.1016/j.chemosphere.2013.01.057

Nriagu, J.O., Moore, P.H., 2012. Phosphate Minerals. Springer Science & Business Media.

OLI Systems, Inc., 2018. A guide to using OLI Analyzer.

Otterpohl, R., Braun, U., Oldenburg, M., 2003. Innovative technologies for decentralised water-, wastewater and biowaste management in urban and peri-urban areas. Water Sci. Technol. J. Int. Assoc. Water Pollut. Res. 48, 23–32.

Pancorbo, O.C., Overman, A.R., 1988. Poliovirus Retention in Soil Columns after Application of Chemical- and Polyelectrolyte-Conditioned Dewatered Sludges. APPL Env. MICROBIOL 54, 6.

Pandorf, M., Hochmuth, G., Boyer, T.H., 2019. Human Urine as a Fertilizer in the Cultivation of Snap Beans (*Phaseolus vulgaris*) and Turnips (*Brassica rapa*). J. Agric. Food Chem. 67, 50–62. https://doi.org/10.1021/acs.jafc.8b06011

Putnam, D.F., 1971. Composition and concentrative properties and human urine (NASA Contractor Report No. NASA CR-1802). NASA, Huntington Beach, California.

Putnam, D.F., Thomas, E.C., 1969. Recovery of Potable Water from Human Urine. Aerosp. Med. 40, 736–739.

Rahman, M.S., Ahmed, M., Chen, X.D., 2006. Freezing-Melting Process and Desalination: I. Review of the State-of-the-Art. Sep. Purif. Rev. 35, 59–96. https://doi.org/10.1080/15422110600671734

Randall, D.G., Krähenbühl, M., Köpping, I., Larsen, T.A., Udert, K.M., 2016. A novel approach for stabilizing fresh urine by calcium hydroxide addition. Water Res. 95, 361–369. https://doi.org/10.1016/j.watres.2016.03.007

Randall, D.G., Naidoo, V., 2018. Urine: The liquid gold of wastewater. J. Environ. Chem. Eng. 6, 2627–2635. https://doi.org/10.1016/j.jece.2018.04.012

Randall, D.G., Nathoo, J., 2018. Resource recovery by freezing: A thermodynamic comparison between a reverse osmosis brine, seawater and stored urine. J. Water Process Eng. 26, 242–249. https://doi.org/10.1016/j.jwpe.2018.10.020

Randall, D.G., Nathoo, J., Genceli-Güner, F.E., Kramer, H.J.M., Witkamp, G.J., Lewis, A.E., 2012. Determination of the metastable ice zone for a sodium sulphate system.

Chem. Eng. Sci., 18th International Symposium on Industrial Crystallization 77, 184–188. https://doi.org/10.1016/j.ces.2011.12.022
Rao, S.M., 2011. Reverse Osmosis. Resonance 16, 1333–1336. https://doi.org/10.1007/s12045-011-0151-8
Ray, H., Saetta, D., Boyer, T.H., 2018. Characterization of urea hydrolysis in fresh human urine and inhibition by chemical addition. Environ. Sci. Water Res. Technol. 4, 87–98. https://doi.org/10.1039/C7EW00271H
Rektorschek, M., Weeks, D., Sachs, G., Melchers, K., 1998. Influence of pH on metabolism and urease activity of Helicobacter pylori. Gastroenterology 115, 628–641. https://doi.org/10.1016/S0016-5085(98)70142-8
Richert, A., Gensch, R., Jönsson, H., Stenström, T.-A., Dagerskog, L., n.d. Practical Guidance on the Use of Urine in Crop Production 69.
Rittmann, B.E., Mayer, B., Westerhoff, P., Edwards, M., 2011. Capturing the lost phosphorus. Chemosphere, The Phosphorus Cycle 84, 846–853. https://doi.org/10.1016/j.chemosphere.2011.02.001
Rose, C., Parker, A., Jefferson, B., Cartmell, E., 2015. The Characterization of Feces and Urine: A Review of the Literature to Inform Advanced Treatment Technology. Crit. Rev. Environ. Sci. Technol. 45, 1827–1879. https://doi.org/10.1080/10643389.2014.1000761
Ruiz-Agudo, E., Kudłacz, K., Putnis, C.V., Putnis, A., Rodriguez-Navarro, C., 2013. Dissolution and Carbonation of Portlandite [Ca(OH)2] Single Crystals. Environ. Sci. Technol. 47, 11342–11349. https://doi.org/10.1021/es402061c
Saetta, D., Boyer, T.H., 2017. Mimicking and Inhibiting Urea Hydrolysis in Nonwater Urinals. Environ. Sci. Technol. 51, 13850–13858. https://doi.org/10.1021/acs.est.7b03571
Saetta, D., Zheng, C., Leyva, C., Boyer, T.H., 2020. Impact of acetic acid addition on nitrogen speciation and bacterial communities during urine collection and storage. Sci. Total Environ. 745, 141010. https://doi.org/10.1016/j.scitotenv.2020.141010
SAICE, 2017. SAICE Infrastructure report card for South Africa. South African Institute for Civil Engineering, South Africa.
Sakthivel, R., Chariar, V., 2013. Waterless Urinals: A Resource Book. IIT Delhi & VVF for UNICEF & Stockholm Environment Institute, New Delhi, India.
Samer, M., 2015. Biological and Chemical Wastewater Treatment, in: Wastewater Treatment Engineering. Egypt. https://doi.org/10.5772/61250
Sato, T., Qadir, M., Yamamoto, S., Endo, T., Zahoor, A., 2013. Global, regional, and country level need for data on wastewater generation, treatment, and use. Agric. Water Manag. Complete, 1–13. https://doi.org/10.1016/j.agwat.2013.08.007
Schmidt, J.M., 2007. Urine processing for potable water recovery (Doctor of Philosophy). Purdue University, Indiana.
Senecal, J., Nordin, A., Simha, P., Vinnerås, B., 2018. Hygiene aspect of treating human urine by alkaline dehydration. Water Res. 144, 474–481. https://doi.org/10.1016/j.watres.2018.07.030
Shaul, O., 2002. Magnesium transport and function in plants: the tip of the iceberg. Biometals 15, 307–321. https://doi.org/10.1023/A:1016091118585
Sikosana, M.K.L.N., Randall, D.G., Von Blottnitz, H., 2017. A technological and economic exploration of phosphate recovery from centralised sewage treatment in a transitioning economy context. Water SA 43, 343. https://doi.org/10.4314/wsa.v43i2.17

Simha, P., Friedrich, C., Randall, D.G., Vinnerås, B., 2021. Alkaline Dehydration of Human Urine Collected in Source-Separated Sanitation Systems Using Magnesium Oxide. Front. Environ. Sci. 8. https://doi.org/10.3389/fenvs.2020.619901

Simha, P., Lalander, C., Nordin, A., Vinnerås, B., 2020. Alkaline dehydration of source-separated fresh human urine: Preliminary insights into using different dehydration temperature and media. Sci. Total Environ. 733, 139313. https://doi.org/10.1016/j.scitotenv.2020.139313

Simha, P., Senecal, J., Nordin, A., Lalander, C., Vinnerås, B., 2018. Alkaline dehydration of anion–exchanged human urine: Volume reduction, nutrient recovery and process optimisation. Water Res. 142, 325–336. https://doi.org/10.1016/j.watres.2018.06.001

Smil, V., 2001. Enriching the Earth: Fritz Haber, Carl Bosch, and the Transformation of World Food Production. MIT Press.

Statistics South Africa, 2017. Statistical release (Statistical release No. P0318). Stats SA, South Africa.

Strande, L., Brdjanovic, D., 2014. Faecal Sludge Management: Systems Approach for Implementation and Operation. IWA Publishing.

Tian, X., Wang, G., Guan, D., Li, Jiuyi, Wang, A., Li, Jin, Yu, Z., Chen, Y., Zhang, Z., 2016. Reverse osmosis brine for phosphorus recovery from source separated urine. Chemosphere 165, 202–210. https://doi.org/10.1016/j.chemosphere.2016.09.037

Tilley, E., 2008. Compendium of sanitation systems and technologies. Swiss Federal Institute of Aquatic Science and Technology (Eawag), Dübendorf.

Tilley, E., Atwater, J., Mavinic, D., 2008. Recovery of Struvite from Stored Human Urine. Environ. Technol. 29, 797–806. https://doi.org/10.1080/09593330801987129

Toxopeus, M., 2017. The state of sanitation and wastewater treatment services in South Africa [WWW Document]. Helen Suzman Found. URL https://hsf.org.za/publications/hsf-briefs/the-state-of-sanitation-and-wastewater-treatment-services-in-south-africa (accessed 4.3.20).

Trček, J., Mira, N.P., Jarboe, L.R., 2015. Adaptation and tolerance of bacteria against acetic acid. Appl. Microbiol. Biotechnol. 99, 6215–6229. https://doi.org/10.1007/s00253-015-6762-3

Udert, K.M., Buckley, C.A., Wächter, M., McArdell, C.S., Kohn, T., Strande, L., Zöllig, H., Fumasoli, A., Oberson, A., Etter, B., 2015. Technologies for the treatment of source-separated urine in the eThekwini Municipality. Water SA 41, 212–221. https://doi.org/10.4314/wsa.v41i2.06

Udert, K.M., Etter, B., Gounden, T., 2016. Promoting Sanitation in South Africa through Nutrient Recovery from Urine. GAIA - Ecol. Perspect. Sci. Soc. 25, 194–196. https://doi.org/10.14512/gaia.25.3.12

Udert, Kai M., Larsen, T.A., Biebow, M., Gujer, W., 2003. Urea hydrolysis and precipitation dynamics in a urine-collecting system. Water Res. 37, 2571–2582. https://doi.org/10.1016/S0043-1354(03)00065-4

Udert, K.M., Larsen, T.A., Gujer, W., 2003. Biologically induced precipitation in urine-collecting systems. Water Supply 3, 71–78. https://doi.org/10.2166/ws.2003.0010

Udert, K.M., Wächter, M., 2012. Complete nutrient recovery from source-separated urine by nitrification and distillation. Water Res. 46, 453–464. https://doi.org/10.1016/j.watres.2011.11.020

United Nations, 2020. 17 goals to transform the world for persons with disabilities [WWW Document]. URL https://www.un.org/development/desa/disabilities/envision2030.html (accessed 2.24.20).
United Nations, Department of Economic and Social Affairs, Population Division, 2019. World population prospects Highlights, 2019 revision Highlights, 2019 revision.
UN-water, 2017. Wastewater management. A UN-Water analytical brief (Analytical brief). United Nations.
Van Drecht, G., Bouwman, A.F., Harrison, J., Knoop, J.M., 2009. Global nitrogen and phosphate in urban wastewater for the period 1970 to 2050: N AND P IN URBAN WASTE WATER. Glob. Biogeochem. Cycles 23, n/a-n/a. https://doi.org/10.1029/2009GB003458
Warner, R.C., 1942. The Kinetics of the Hydrolysis of Urea and of Arginine. J. Biol. Chem. 142, 705–723.
WHO, 2021. Sanitation [WWW Document]. World Health Organ. URL http://www.who.int/topics/sanitation/en/ (accessed 2.24.20).
WHO, 2019. Drinking-water [WWW Document]. WHO. URL https://www.who.int/news-room/fact-sheets/detail/drinking-water (accessed 2.11.21).
Wilsenach, J.A., Schuurbiers, C.A.H., van Loosdrecht, M.C.M., 2007. Phosphate and potassium recovery from source separated urine through struvite precipitation. Water Res. 41, 458–466. https://doi.org/10.1016/j.watres.2006.10.014
World Bank, 2015. Commodity markets outlook. Quaterly outlook.
Zhang, J., She, Q., Chang, V.W.C., Tang, C.Y., Webster, R.D., 2014. Mining Nutrients (N, K, P) from Urban Source-Separated Urine by Forward Osmosis Dewatering. Environ. Sci. Technol. 48, 3386–3394. https://doi.org/10.1021/es405266d

Appendices

Appendix A.1: Supplementary methodologies and example calculations

Overall simulation procedure

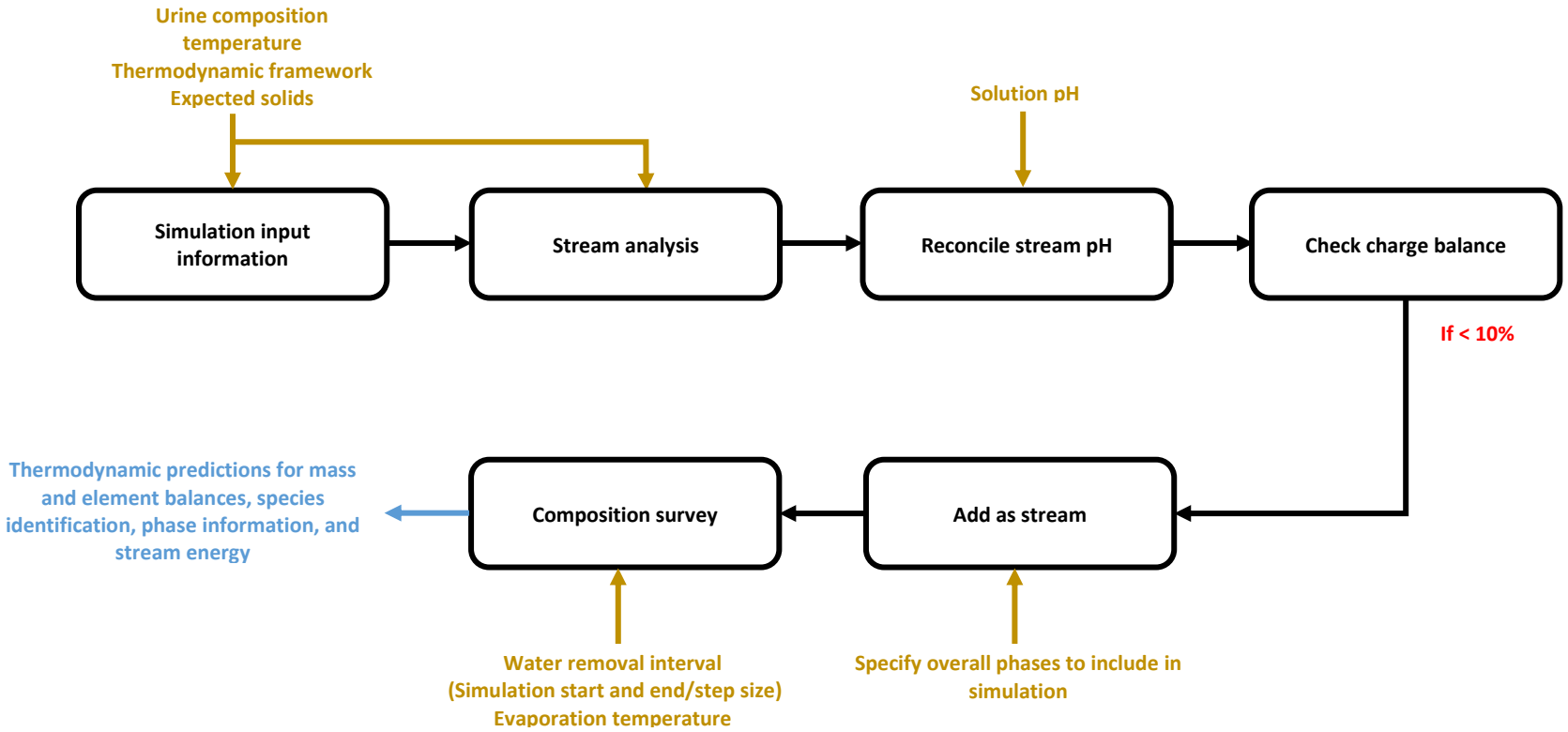

Figure 20. Simulation procedure steps followed to generate relevant OLI simulations for urine evaporation systems. Required input variables or specification steps, are indicated in golden text. Expected simulation output information is quoted in blue text. No $Ca(OH)_2$ stabilization has been included in this procedure. See below for stabilization procedure.

OLI simulation procedure and additional input information

Following the overall simulation procedure from Figure 20, the 'Stream Analysis' function was used to capture the determined input information into the OLI interface. This included the urine composition in terms of major ion concentrations, temperature at which this urine composition was determined (composition temperature), stream pH, and the OLI thermodynamic framework to be used for simulation calculations. Composition and temperatures associated with each urine composition used are available in Table 11, Table 12 and Table 22.

Additionally, the solids expected to form in the solid phase during evaporative processes were selected using the chemistry option in the OLI interface. In following this step, unrealistic solids are unselected and not considered in OLI thermodynamic calculations. Selected solids considered in simulations are presented and discussed in greater detail under in Table 25 below. The created urine stream was then reconciled to the required stream pH as quoted in Table 11, Table 12 and Table 22.

After reconciling stream pH, the charge balance error of this stream was determined before proceeding with the overall simulation process. Realistically a solution should be neutral i.e. have a charge balance error of 0%. However, in reality some ions cannot be measured in a laboratory. Additionally, there is also a precision error associated with the methods and equipment used when measuring the measurable major ion concentrations. As a result, experimentally determined urine compositions would have an associated charge balance error. As the created urine stream was based on this experimental laboratory analysis, it was also expected to have an associated charge balance error. However, to achieve the 0% charge balance error observed in reality, OLI will balance ionic charges to result in a neutral solution. This balancing is done through the addition of major anions or cations such as Na^+ or Cl^- respectively, to the created urine stream.

The charge balance error associated with urine streams created in OLI simulations is calculated using Equation (**10**.

$$Charge\ balance\ error\ (\%) = \frac{\sum cations - |\sum anions|}{\sum cations + |\sum anions|} \times 100 \qquad \textbf{(10)}$$

The required cation and anion concentrations for the above calculation, without the consideration of the additional balancing anion or cation quantity, was available as a simulation output after reconciling the pH of the stream. If the calculated charge balance error was below 10%, the composition of that urine stream was then used in the required composition surveys.

A charge imbalance greater than 10% deemed the stream unusable as this higher charge imbalance would result in simulation inaccuracies.

After determining the charge balance error, if applicable the resulting urine stream was added as a complete stream, including all phases. This added stream was to be used in the subsequent composition surveys.

The use of composition surveys simulated water removal from the complete urine stream. This water removal was synonymous with the evaporation processes. Composition surveys allowed for the amount of water remaining in the urine solution to be varied between a specified starting and end point. Additionally, surveys could be run over a range of water removal intervals, with a user-specified step size. Remaining water in solution could be varied between 1000 g and 0 g water. These masses corresponded to water removal intervals between 0% and 100% water removal from the urine solution respectively.

A composition survey was created in the required OLI simulation file by adding a survey and selecting the composition survey option. Under the composition survey specifications, the compound to be varied was selected. In the case of urine evaporation simulations, this compound was water [12]. The start and end point, as well as step size of the composition survey calculation were then specified also using the survey specifications option.

However, before the abovementioned composition surveys could be run, simulation input variables needed to be determined and specified. Required input variables are discussed below.

Simulation input information

OLI Stream Analyzer thermodynamic framework

When using OLI, there were three potential thermodynamic frameworks. These frameworks form the basis upon which thermodynamic predictions were calculated. One out of the three frameworks needed to be selected prior to executing the overall simulation procedure described in Figure 20.

The three available thermodynamic frameworks are listed below:

- Aqueous (AQ) model
- Mixed Solvent Electrolyte (MSE) model
- Mixed Solvent Electrolyte and Soave-Redlich Kwong (MSE-SRK) model

Each of the abovementioned thermodynamic frameworks differs slightly from each other. The MSE-SRK model is applicable to a high-pressure hydrocarbon system (OLI Systems, 2018). However, in the case of human urine evaporation this thermodynamic framework was less applicable. The AQ framework, which was the first thermodynamic framework to be available for use in OLI software, can be applied to most water-based multi-component solutions. This model holds for a variety of temperature, pressure and concentration conditions (OLI Systems, 2018).

Although the AQ framework could have been applied to urine evaporation simulations, the MSE database with H_3O^+ ion is the most recently updated framework out of these two thermodynamic frameworks. The MSE database is applicable to systems containing water, organic and salt mixtures. This model is able to predict speciation, chemical and phase equilibria in the abovementioned systems. Similar to that of the AQ model, the MSE model can applied in a wide range of operating conditions.

[12] When selecting the amount of water to be varied, the units of the stream needed to be in the correct units to allow for the selection of this compound. The required units of the overall stream were grams

As the MSE database with the H_3O^+ ion is the most updated and comprehensive thermodynamic database for water-organic-salt systems, this was the chosen framework for all OLI thermodynamic modelling conducted throughout this thesis. These simulations are expanded further in Chapters 3 and 4. The MSE database was selected as a simulation input variable on the OLI interface, before the required simulations were run. Additional input variables are discussed below.

Additional information on water removal boundaries

Two input variables for OLI simulations included the water removal intervals and calculation step size to be specified. These variables were specified in OLI when using a composition survey. The upper and lower water removal boundaries needed to be specified. Specified boundaries corresponded to the mass of water remaining in the urine solution. This could be varied between 0 g and 1000 g of water in solution (100% to 0% water removal). Additionally, the step size between these two specified boundaries needed to be specified.

All simulations created and used in this thesis were run using boundaries of 0 to 1000 g water in solution. Calculations were performed over a series of 50 steps (increments of 20 g water). This simulation range looked at the entire water removal interval from 100 to 0% water in solution and gave a good overview of the major solids forming and when these solids were expected to form.

As some solids, such as urea for example, were only predicted to form at water removal intervals much closer to 99.5 to 100%, further simulations 'zooming in' on higher water removal intervals were run. These simulations were run using boundaries of 0 to 25 g water remaining in solution (100 to 97.5% water removal). A series of 50 steps was also used in these additional simulations (increments of 0.5 g water). The results from these simulations were able to give a better indication of when compounds like urea, were crystallized from solution.

To generate a urine stream in OLI simulations, the required input information shown Figure 20 was specified using the 'Stream Analysis' function. Using the chemistry tab in the OLI interface, the individual solids expected to form in solution were selected. This selection was based on the findings of previous experimental work. These findings presented the individual solids formed when evaporating $Ca(OH)_2$ stabilized human urine (Randall et al., 2016). These solids are listed in Table 25. The created urine stream was then reconciled to the pH of relevant fresh urine (Table 11).

Once the pH of the fresh urine stream was reconciled, the charge balance of this stream was determined. The charge balance error associated with urine streams created in OLI simulations is calculated using Equation (**11**.

$$Charge\ balance\ error\ (\%) = \frac{\sum cations - |\sum anions|}{\sum cations + |\sum anions|} \times 100 \qquad \textbf{(11)}$$

The charge balance error is discussed in greater detail in Appendix A. All charge balance results for each urine stream used in this thesis are also available in Appendix A. If the

calculated charge balance error was below 10%, the created fresh urine stream could be used in OLI simulations. The created urine stream was added as a complete stream, including all phases. This stream was then used in composition surveys.

Composition surveys simulated the water removal process during evaporation in OLI. Surveys varied the amount of water in solution between a start and end point. Additionally, a user-specified step size could be used between the defined start and end points of each survey. Remaining water in solution could be varied between 1000 g and 0 g water. These masses corresponded to water removal intervals of 0% and 100%. Before composition surveys could be run, simulation input variables needed to be determined and specified. Required input variables are discussed below.

Urine composition input information

Urine composition: Fresh urine (a) composition

Urine composition was the first major input variable to be specified in simulations. In this thesis, three types of urine were studied. These included fresh urine (a), $Ca(OH)_2$ stabilized urine (b) and hydrolyzed urine (h). Furthermore, five different fresh urine compositions for each type of urine, were required to study the effect of urine composition on the evaporation process (See Figure 21).

Example calculations used for fresh urine input composition

For each fresh urine composition presented in Table 11, the urea content in the urine was measured in the units g-N m^{-3}. For simulation purposes, these values were converted into g-urea m^{-3} using stoichiometric conversions. Similarly, the amount of ammonia (NH_3) in U1-5a was converted into ammonium (NH_4^+) ions to be consistent with current wastewater conventions. Example calculations for these stochiometric conversions can be found below. After such conversions, collected fresh urine compositions were used in OLI simulations and the charge balance associated with each composition was determined. A low charge imbalance ensured suitability and consistency between results.

Urea in U1a unit conversion example calculation

The urea concentration in fresh urine solutions was taken as gN m^{-3} in urea when relevant. These units were converted to the units g urea m^{-3} :

$$Urea: CH_4N_2O$$

$$\therefore 2\ mols\ N\ for\ 1\ mol\ urea$$

$$5420\ \frac{gN}{m^3} \times \frac{1\ mol\ N}{14\ g\ N} \times \frac{1\ mol\ urea}{2\ mol\ N} \times \frac{60.06\ g\ urea}{1\ mol\ urea} = 11625.9\ \frac{g\ urea}{m^3}$$

Table 20. Urea conversion for fresh urine solution U1a to U5a using the above example calculation

Urine solution	Urea in solution (gN m^{-3})	(g urea m^{-3})

U1a	5420	11625.9
U2a	-	16300
U3a	-	16200
U4a	8750	18800
U5s	4450	9550

Ammonia in U1a converted to ammonium ions

The ammonia concentration in fresh urine compositions was taken as gN m^{-3} NH_3, excluding the abovementioned urea content. These units were converted to g NH_4^+ m^{-3} :

$$1\ mol\ N\ in\ 1\ mol\ NH_4^+$$

$$436\frac{gN}{m^3}\times\frac{1\ mol\ N}{14\ g\ N}\times\frac{1\ mol\ NH_4^+}{1\ mol\ N}\times\frac{18.089\ g\ NH_4^+}{1\ mol\ NH_4^+}=561.786\frac{g\ NH_4^+}{m^3}$$

Table 21. NH_4^+ conversion for fresh urine solution U1a to U5a using the above example calculation

Urine solution	NH_3 (gN m^{-3})	NH_4^+ (g NH_4^+ m^{-3})
U1a	436	561.8
U2a	465	599
U3a	476	613
U4a	386	497
U5s	-	564

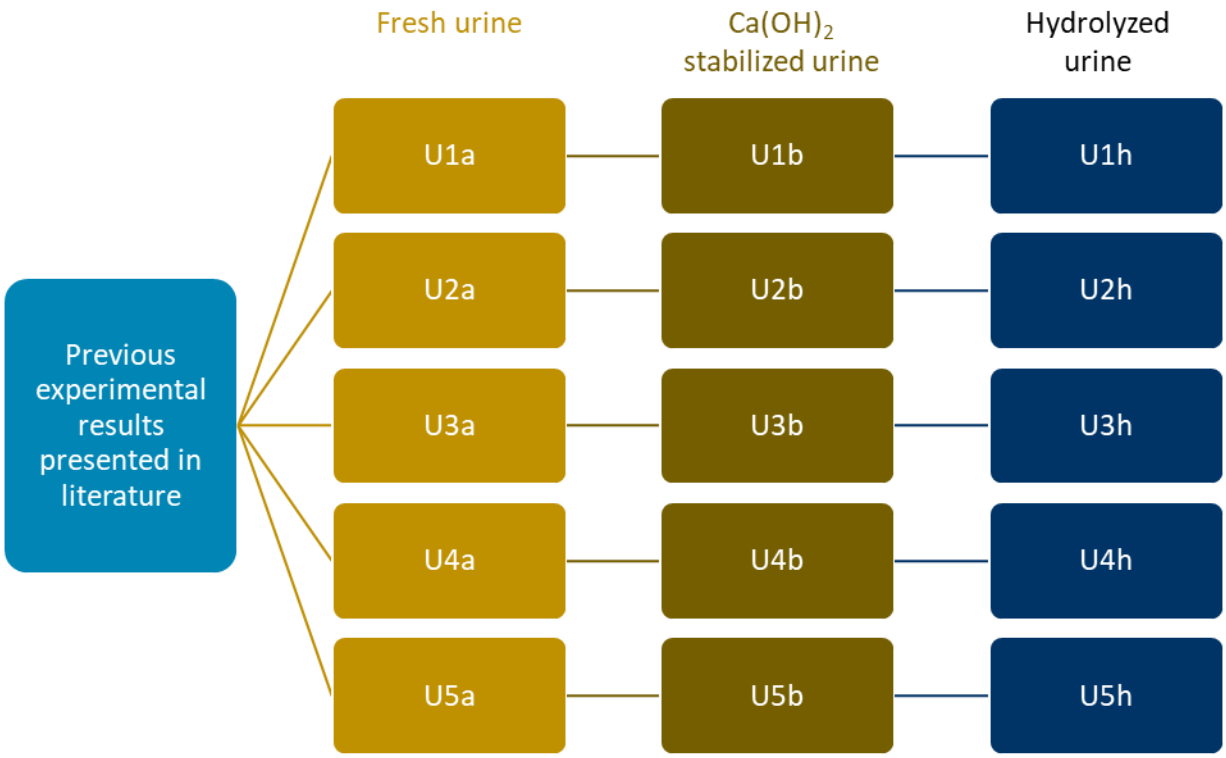

Figure 21. Fresh (a), $Ca(OH)_2$ stabilized (b) and hydrolyzed (h) urine composition flowchart from starting fresh urine composition. This fresh urine composition was taken from literature

Due to the climate created by the COVID-19 pandemic, fresh urine could not be collected and experimentally analyzed at the time. Instead, this data was compiled from previous experimental work presented in the literature. The five fresh urine compositions used in OLI simulations, as well as the literature from which these compositions were obtained, are presented in Table 11.

From Figure 21, each fresh urine composition was used as the basis for the two additional types of urine studied in this thesis. This assumption allowed for a better comparison to be drawn between simulation results as the composition of U1 for example, remained constant. Only the type of urine was varied i.e. U1a, U1b and U1h, when drawing comparisons between urine type.

Sections below describe the required calculations and additional simulations steps followed to derive the $Ca(OH)_2$ stabilized and hydrolyzed urine compositions from the five initial fresh urine composition.

Fresh urine $Ca(OH)_2$ stabilization process in OLI

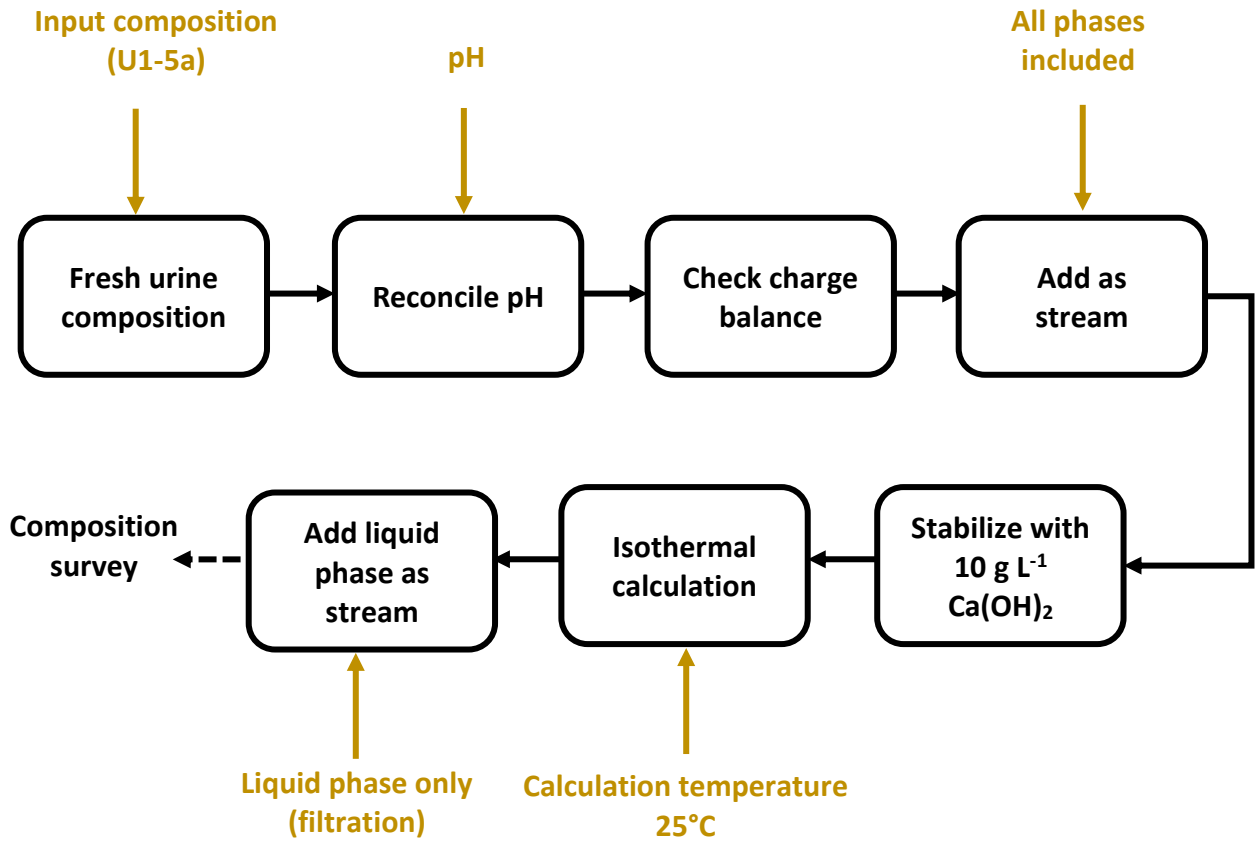

Figure 22. Simulation procedure steps followed to generate $Ca(OH)_2$ stabilized urine solutions from initial fresh urine compositions(U1-5a). Required input variables or specification steps, are indicated as golden text

An example whereby U1a was stabilized in OLI to create U1b is outlined in greater detail as follows:

1. As in Figure 22, the relevant fresh urine composition was entered OLI using the stream analysis function.
2. The pH of the U1a stream was reconciled, and the charge balance error was determined using Equation (**10**
3. Results added as a stream and named 'U1a.'
4. Single point isothermal calculation selected for the added U1a stream. The isothermal calculation was performed at a temperature of 25°C as it was assumed that the fresh urine would be stabilized and filtered at room temperature.
5. Under the description of the added U1a stream, a dosage of 10 g L^{-1} $Ca(OH)_2$ was added, and the isothermal calculation was run at 25°C. This isothermal calculation determined the speciation and phases of species at a constant temperature. This meant that the amount of $Ca(OH)_2$, in the solid and liquid phase was determined in the output results of this calculation.
6. Output from isothermal calculation added as a stream, excluding the solid phase as this represented the insoluble $Ca(OH)_2$ and other species which would have been

removed through physical filtration. This manually simulated the laboratory-based filtration step in OLI. Resulting stabilized stream was named 'U1b.'

7. U1b was used as the stabilized urine composition associated with U1a.

The above outline was repeated for the remaining four fresh urine compositions. The stabilized streams created in OLI were similar in composition to that of U1-5a, if these streams were to be experimentally stabilized with 10g L^{-1} $Ca(OH)_2$, filtered and measured experimentally. The corresponding unfiltered and filtered stabilized urine compositions obtained through OLI simulations can be found in Table 12. Only the filtered $Ca(OH)_2$ stabilized urine compositions were used in OLI simulations to remain consistent with laboratory work.

Hydrolyzed urine composition and calculations

Example calculations for U1a/U1h are shown below.

$$CON_2H_4 + 3H_2O \rightarrow 2NH_4^+ + CO_3^{-2} + H_2O \quad \textbf{(12)}$$

Example calculations to obtain U1h from U1a:

$$11.6\ g\ CON_2H_4\ (U1a) \times \frac{1\ mol\ urea}{60.1\ g\ CON_2H_4} = 0.194\ mol\ CON_2H_4$$

$$0.194\ mol\ CON_2H_4 \times \frac{2\ mol\ NH_4^+}{1\ mol\ CON_2H_4} \times \frac{18.0\ g\ NH_4^+}{1\ mol\ NH_4^+} = 7.55\ g\ NH_4^+\ (U1h)$$

$$0.194\ mol\ CON_2H_4 \times \frac{1\ mol\ CO_3^{-2}}{1\ mol\ CON_2H_4} \times \frac{61.0\ g\ CO_3^{-2}}{1\ mol\ CO_3^{-2}} = 11.8\ g\ {CO_3}^{-2}\ (U1h)$$

Following the above hydrolysis example calculations, Table 22 was populated with the corresponding hydrolyzed urine compositions required for OLI calculations. The pH of U1-5h could not be measured experimentally as hydrolyzed compositions were calculated from fresh urine compositions. As a result, the pH of each hydrolyzed stream was assumed to be at a pH of 9. This assumption was based on experimental pH values presented in the literature for hydrolyzed urine (Chipako and Randall, 2020b).

Table 22. Composition of hydrolyzed urine. All values represent the measured component, measured in g m^{-3}. In the case of nitrogen, measurements were converted to the relevant units and values as required for use in OLI simulations. These converted values are quoted in red text. Values used in OLI simulations are quoted in bold text.

Measurement	Units	U1h (Randall et al., 2016)	U2h (Rose et al., 2015)	U3h (K.M. Udert et al., 2003)	U4h (Kai M. Udert et al., 2003)	U5h (Etter et al., 2014)
TIC	g m^{-3}	28	-	-	-	-
Urea	**g urea m^{-3}**	**-**	**-**	**-**	**-**	**-**
PO_4-P	g m^{-3}	260	472	743	559	388
NH_3-N	g m^{-3}	436	465	476	386	-
NH_4^+	**g NH_4^+ m^{-3}**	**7550**	**10400**	**10400**	**11800**	**6300**
Dissolved COD	g m^{-3}	6400	8440	-	8150	7660
Cl^-	**g m^{-3}**	**4430**	**5140**	**3900**	**5230**	**6620**
SO_4^{-2}	**g m^{-3}**	**825**	**2075**	**1540**	**1350**	**878**
CO_3^{-2}	**g m^{-3}**	**11800**	**16600**	**16500**	**19070**	**9700**
Na^+	**g m^{-3}**	**2510**	**2780**	**2760**	**3730**	**3240**
K^+	**g m^{-3}**	**469**	**1680**	**2190**	**2250**	**1870**
Ca^{+2}	**g m^{-3}**	**132**	**111**	**184**	**168**	**89.2**
Mg^{+2}	**g m^{-3}**	**57**	**95.0**	**94.8**	**121**	**45.4**
Predicted pH	**-**	**9**	**9**	**9**	**9**	**9**
Temperature	**°C**	**25.0**	**25.0**	**25.0**	**25.0**	**25.0**
Charge imbalance	%	-0.92	-2.11	0.26	1.45	-1.77

Urine composition charge balances

Fresh urine composition charge balances

Table 23. Fresh urine charge balance information from OLI simulation output

		Fresh urine composition				
	Units	**U1a**	**U2a**	**U3a**	**U4a**	**U5a**
Cation concentration	eq L^{-1}	0.164	0.210	0.227	0.266	0.228
Anion concentration	eq L^{-1}	-0.167	-0.234	-0.214	-0.230	-0.243
Charge balance	%	-1.12	-5.24	2.95	7.25	-3.05
pH of stream without reconcile	-	8.52	9.05	9.46	9.27	9.02
Required to balance	-	Na^+	Na^+	Cl^-	Cl^-	Na^+
	mg L^{-1}	85.5	535	461	1270	330
True pH	-	6.3	6.2	6.2	6	5.6
Titrant added to reconcile	-	HCl	HCl	HCl	HCl	HCl
pH	mg L^{-1}	394	862	1340	1030	867

Stabilized urine composition charge balances

Same as that of fresh urine above. Fresh urine stream is manually saturated and this does not affect the concentration of anions and cations used in the charge balance error calculation.

Hydrolyzed urine composition charge balances

Table 24. Hydrolyzed urine charge balance information from OLI simulation output

		Hydrolyzed urine composition				
	Units	**U1h**	**U2h**	**U3h**	**U4h**	**U5h**
Cation concentration	eq L^{-1}	0.551	0.753	0.767	0.891	0.546
Anion concentration	eq L^{-1}	-0.561	-0.786	-0.763	-0.865	-0.566
Charge balance	%	-0.92%	-2.11%	0.26%	1.45%	-1.77%
pH of stream without reconcile	-	9.15	9.16	9.21	9.22	9.161
Required to balance	-	NH_4^+	NH_4^+	CO_3^{-2}	CO_3^{-2}	NH_4^+
	mg L^{-1}	184	585	118	763	355
Estimated pH	-	9	9	9	9	9
Titrant added to reconcile pH	-	HCl	HCl	HCl	HCl	HCl
	mg L^{-1}	1420	1980	2620	3020	1250

OLI selected solids input information

Table 25. Major solids expected to form in remaining $Ca(OH)_2$ stabilized urine solution when evaporating water from this solution. These solids were determined to be good estimates of the solids expected to form in solution through using the work presented in Table 1 Randall et al., 2016

Chemical formula		
$(NH_4)_2SO_4$	K_2SO_4	$MgCl_2{\cdot}6H_2O$
$CO(NH_2)_2$	$K_2Mg_2(SO_4)_3$	MgO
NH_4Cl	$K_2SO_4{\cdot}CaSO_4{\cdot}H_2O$	$MgSO_4$
$Ca(OH)_2$	$K_2SO_4{\cdot}MgSO_4{\cdot}2CaSO_4{\cdot}2H_2O$	$MgSO_4{\cdot}H_2O$
$Ca_3(PO_4)_2$	$K_2SO_4{\cdot}MgSO_4{\cdot}4H_2O$	$MgSO_4{\cdot}4H_2O$
$Ca_5(OH)(PO_4)_3$	$K_2SO_4{\cdot}MgSO_4{\cdot}6H_2O$	$MgSO_4{\cdot}5H_2O$
$CaCl_2$	K_3PO_4	$MgSO_4{\cdot}6H_2O$
$CaCl_2{\cdot}2H_2O$	KCl	$MgSO_4{\cdot}7H_2O$
$CaCl_2{\cdot}4H_2O$	KH_2PO_4	Na_2HPO_4
$CaCl_2{\cdot}6H_2O$	KOH	Na_2SO_4
$CaHPO_4$	$K_2Ca_5(SO_4)6{\cdot}H_2O$	$Na_2SO_4{\cdot}10H_2O$
$CaHPO_4{\cdot}2H_2O$	$KMgCl_3{\cdot}6H_2O$	$Na_2SO_4{\cdot}CaSO_4$
CaO	$KMgClSO_4{\cdot}3H_2O$	$Na_2SO_4{\cdot}MgSO_4{\cdot}4H_2O$
$CaSO_4$	$K_2SO_4{\cdot}KNaSO_4H_2O$	$Na_3H(SO_4)_2$
$CaSO4{\cdot}0.5H_2O$	$NH_4MgPO_4{\cdot}6H_2O$	$NaCl$
$CaSO_4{\cdot}2H_2O$	$Mg(OH)_2$	$NaOH$
K_2HPO_4	$MgCl_2{\cdot}4H_2O$	

OLI simulation paths followed

Fixed urine composition and varied temperature simulations (path one)

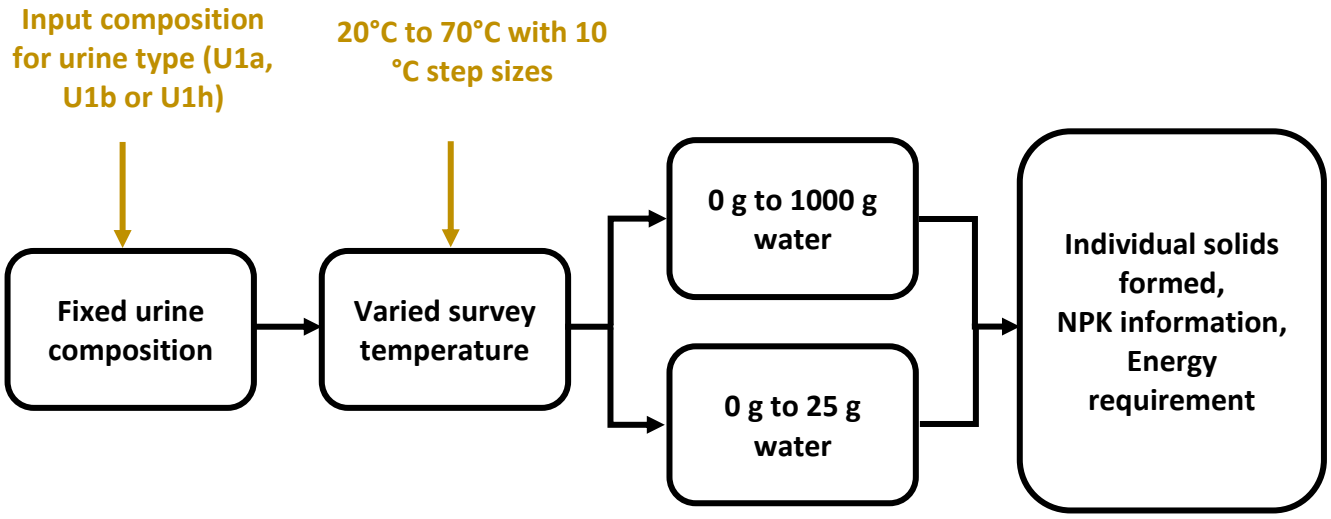

Figure 23. Overall simulation structure for simulation path one. This simulation path used a fixed urine composition for the chosen type of urine and varied the survey (evaporation) temperature. Simulations for path one were repeated for temperatures from 20°C to 70°C, every 10°C.

Fixed temperature and varied urine composition simulations (path two)

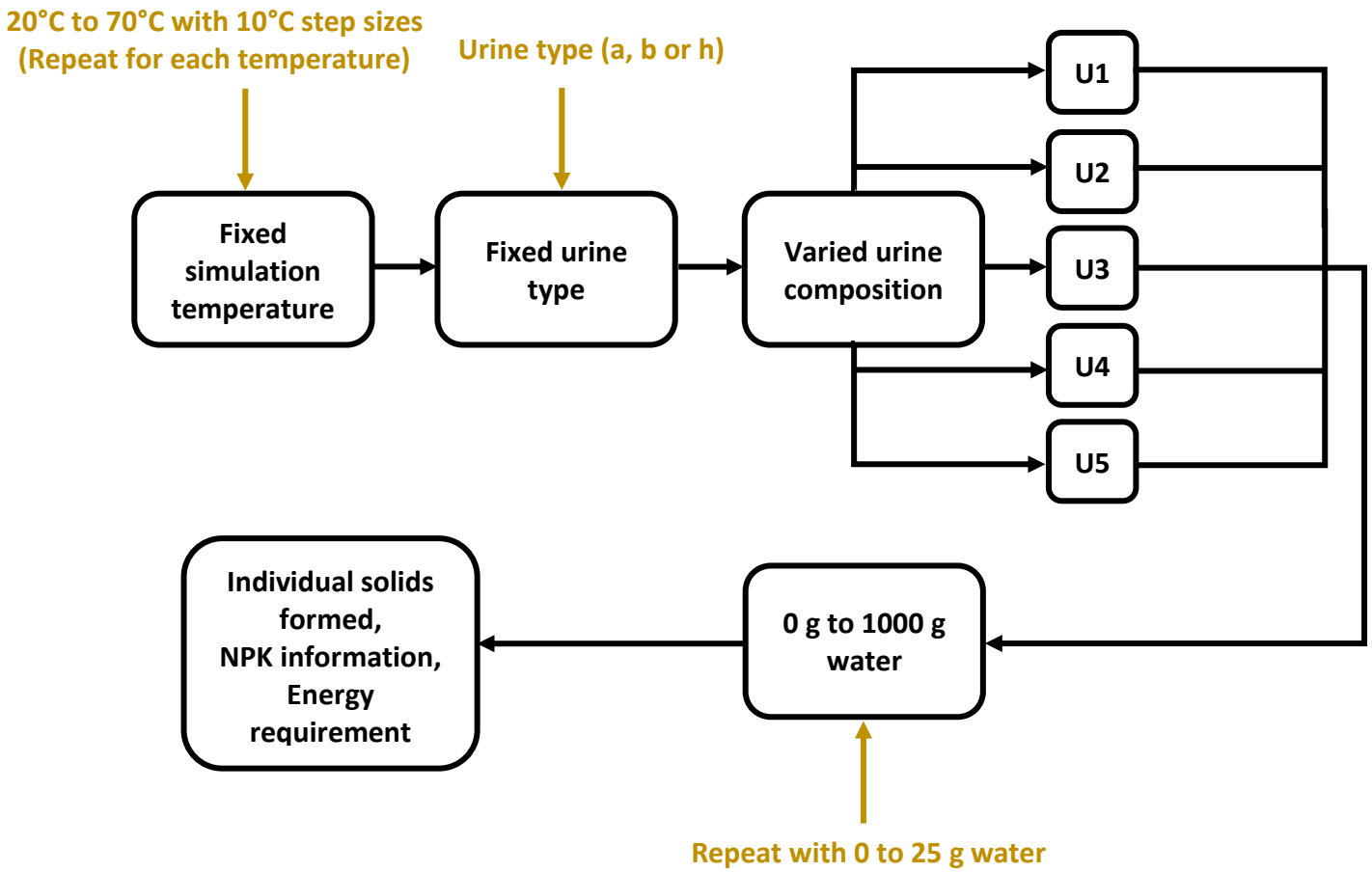

Figure 24. Overall simulation structure for simulation path two. This simulation path used a fixed survey (evaporation) temperature for the chosen type of urine. The composition of the chosen type of urine was varied by using five different urine compositions. Simulations for path two were repeated for a 'zoomed in' water removal interval of 0 g to 25 g of water remaining in the urine solution.

Appendix A.2: Supplementary experimental information and procedures

Experimental outline

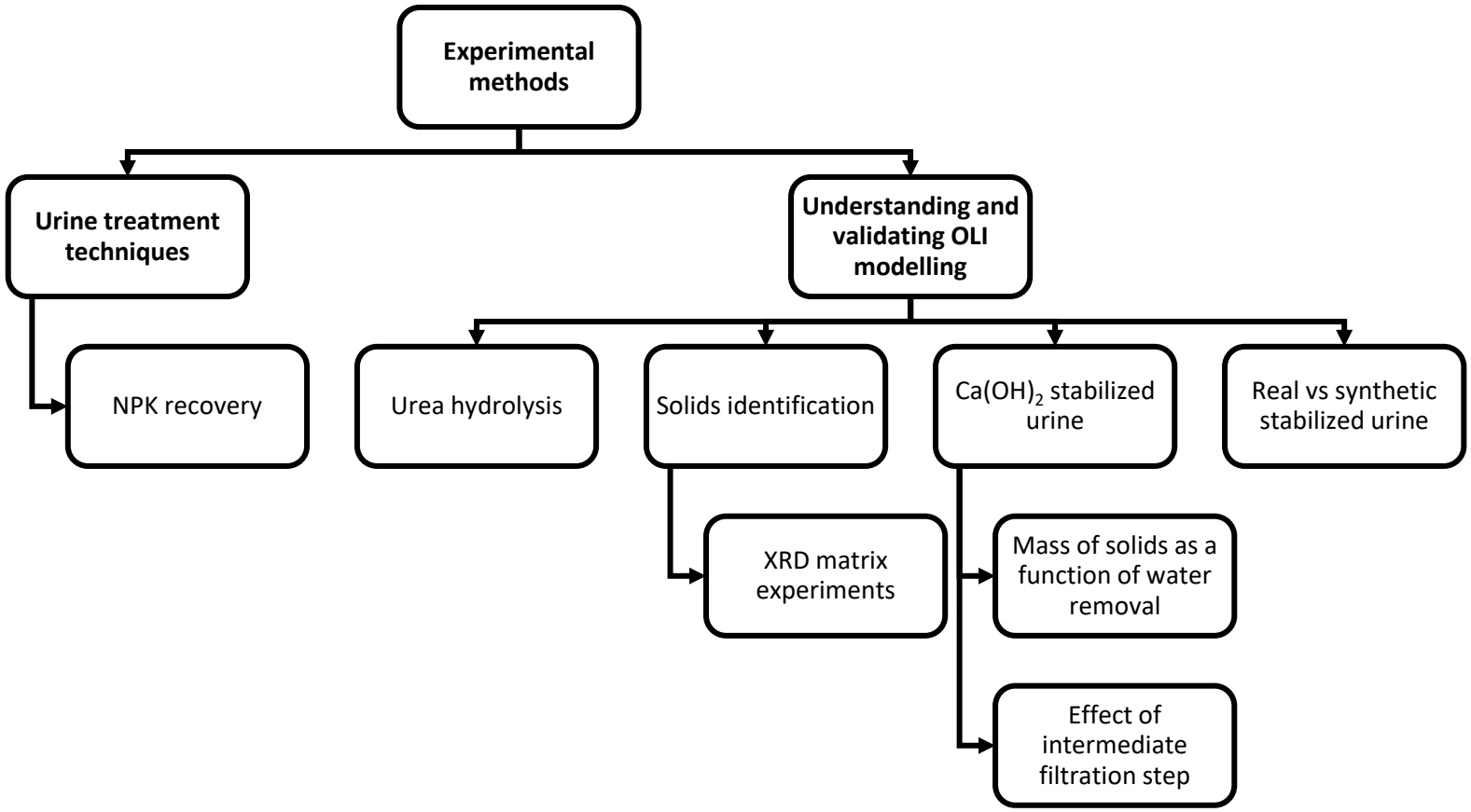

Figure 25. Schematic representation of experimental work conducted in this thesis. Experimental work was conducted over two main areas. One regarded the urine treatment methods and determining the best urine treatment method by considering the NPK recovery from each respective urine treatment method during evaporation. The second area of experimental work drew a comparison between the desktop-based OLI modelling and experimental work conducted in the laboratory.

Synthetic urine recipe and adjustment calculations

To develop the experimental fresh synthetic urine recipe, the suggested fresh urine recipe from the VUNA handbook was used as the basis for adjustment calculations. This suggested recipe is shown below.

The suggested recipe shows the masses of chemical salts suggested in the VUNA handbook, as well as the resulting major ion concentrations achieved through dissolving these suggested masses in one liter of deionized water. The masses of these suggested salts were stoichiometrically adjusted to match the major ion concentrations in U1a above. The adjusted recipe is shown below.

Some notable adjustments included an alternative calcium source to the suggested $CaCl_2$. Instead, $CaCl_2.2H_2O$ was used as this was the available in the laboratory. This adjustment was considered when performing stoichiometric calculations adjusting the VUNA recipe.

When adding the sodium source in the form of NaOH as suggested, a colloid was observed due to an increased pH. Hence, NaOH was not added to the synthetic urine recipe and the amount of NaCl was increased from adjusted 4.12 g to 5.22 g, to account for the additional sodium required in the adjusted solution. This resulted in the chloride concentration increasing from 4430 mg L^{-1} as in U1a, to 5094 mg L^{-1} in the suggested recipe. Full adjustment calculations can be found in below.

An additional consideration was the use of NaH_2PO_4 as suggested in the VUNA handbook recipe. Initially, Na_2HPO_4 was used as was NaH_2PO_4 unavailable. However, when NaH_2PO_4 was available, this salt was used as the phosphate salt as suggested. Through this it was seen that using this suggested phosphate source was an additional vital step to further avoid colloid formation observed.

Table 26. Suggested VUNA and adjusted fresh synthetic urine recipe (Etter et al., 2014). Quantity of salts to be dissolved in one liter deioinzed water to give resulting major ion concentrations of fresh urine.

Compounds dissolved in 1L water	**VUNA recipe Mass (g)**
$CO(NH_2)_2$	16
NH_4Cl	1.8
Na_2SO_4 (anhydrous)	2.3
NaH_2PO_4 (anhydrous)	2.9
KCl	4.2
$MgCl_2$	0.37
$CaCl_2$	0.51
$CaCl_2 \cdot 2H_2O$	-
NaCl	0.183
NaOH	0.23

Table 26 continued. Suggested VUNA and adjusted fresh synthetic urine recipe (Etter et al., 2014). Quantity of salts to be dissolved in one liter deioinzed water to give resulting major ion concentrations of fresh urine.

Major ion concentration (mg/L)		
	VUNA recipe	**Desired (U1a)**
$CO(NH_2)_2$	16200	11600
NH_3	574	436
PO_4^{-3}	2300	260
K^+	2201	469
SO_4^{-2}	1560	825
Cl^-	3903	5094
Na^+	1504	2510
Mg^{+2}	94,8	57
Ca^+	184	132
Na^+	2510	2510

In leaving out NaOH to avoid the formation of the colloid, the pH of the fresh urine was lower than required. The unadjusted pH ranged from 4.8 to 5.4 and hence needed to be adjusted to 6.3 to match that of U1a. Small amounts of NaOH were added incrementally to the synthetic solution. The mass of NaOH added was recorded. The solution was then well mixed, and the pH of the solution was re-measured. This procedure was repeated until the pH of the synthetic fresh urine was at the desired value of 6.3.

Adjustment calculations

$$Mass\ desired\ ion\ (g) = \ desired\ ion\ concentration\ \left(\frac{g}{L}\right) \times volume\ solution\ (L)$$

$$Mol\ desired\ ion = \frac{mass\ desired\ ion\ (g)}{molar\ mass\ desired\ ion\ \left(\frac{g}{mol}\right)}$$

Use the molar mass of the salt dissolved to determine the moles of the other ion, accompanying the desired ion, in solution. This is also done for the moles of the salt dissolved in solution:

$$Mol\ accompanying\ ion = mol\ desired\ ion\ \times mol\ ratio\ for\ accompnaying\ ion$$

$$Mol\ dissolved\ salt = mol\ desired\ ion\ \times mol\ ratio\ for\ dissolved\ salt$$

$$Adjusted\ mass\ dissolved\ salt = mol\ dissolved\ salt\ \times molar\ mass\ of\ salt$$

Each salt dissolved in solution is associated with both cations and anions when dissolved in water. The VUNA recipe is structured in such a way that each salt contributes one of the desired major ions to solution. In some cases, more than one salt contributes to the major ions, however there is one final salt that is added that makes up the final concentration of that specific desired ion. In the case of the major ion concentrations, the desired ions are shown below. Additionally, when dissolving the relevant salt to obtain the desired ion

concentrations, the associated anion or cation, which is not the desired ion, is tracked during calculations so that this concentration can be made up with a final salt.

NH_3/NH_4^+ adjustment calculation:

Salt dissolved: NH_4Cl

Concentrations in solution: NH_4^+, Cl^-

Desired NH_3 concentration: 436 mg L^{-1}

Calculation:

$$NH_4^+ = 0.436\ gN\ NH_3 \times \frac{1\ mol\ NH_3}{14\ g\ N} \times \frac{1\ mol\ N}{1\ mol\ NH_3} \times \frac{1\ mol\ NH_4^+}{1\ mol\ N} \times \frac{18.039\ g\ NH_4^+}{1\ mol\ NH_4^+}$$

$$= 0.561\ g\ NH_4^+\ L^{-1}$$

$$\frac{0.561\ g\ NH_4^+\ L^{-1}}{18.039\ g\ mol^{-1}} = 0.0311\ mol\ NH_4^+$$

$$0.0311\ mol\ NH_4^+ \times \frac{1\ mol\ Cl^-}{1\ mol\ NH_4^+} = 0.0311\ mol\ Cl^-$$

$$0.0311\ mol\ NH_4^+ \times \frac{1\ mol\ NH_4Cl}{1\ mol\ NH_4^+} = 0.0311\ mol\ NH_4Cl$$

$$0.0311\ mol\ NH_4Cl \times \frac{53.491\ g\ NH_4Cl}{1\ mol\ NH_4Cl} = 1.6658\ g\ NH_4Cl$$

K^+ adjustment calculation:

Salt dissolved: KCl

Concentrations in solution: K^+, Cl^-

Desired K^+ concentration: 469 mg L^{-1}

Calculation:

$$K^+ = 0.469\ g\ L^{-1}$$

$$\frac{0.469\ g\ L^{-1}}{39.0983\ g\ mol^{-1}} = 0.012\ mol\ K^+$$

$$0.012\ mol\ K^+ \times \frac{1\ mol\ Cl^-}{1\ mol\ K^+} = 0.012\ mol\ Cl^-$$

$$0.012\ mol\ K^+ \times \frac{1\ mol\ KCl}{1\ mol\ NH_4^+} = 0.012\ mol\ KCl$$

$$0.012\ mol\ KCl\ \times \frac{74.55\ g\ KCl}{1\ mol\ KCl} = 0.8943\ g\ KCl$$

SO_4^{-2} adjustment calculation:
Salt dissolved: Na_2SO_4
Concentrations in solution: Na^+, SO_4^{-2}
Desired SO_4^{-2} concentration: 825 mg L^{-1}

Calculation:

$$SO_4^{-2} = 0.825\ g\ L^{-1}$$

$$\frac{0.825\ g\ L^{-1}}{96.1\ g\ mol^{-1}} = 0.0089\ mol\ SO_4^{-2}$$

$$0.0089\ mol\ SO_4^{-2}\ \times \frac{2\ mol\ Na^+}{1\ mol\ SO_4^{-2}} = 0.0172\ mol\ Na^+$$

$$0.0089\ mol\ SO_4^{-2}\ \times \frac{1\ mol\ Na_2SO_4}{1\ mol\ SO_4^{-2}} = 0.0089\ mol\ Na_2SO_4$$

$$0.0089\ mol\ Na_2SO_4 \times \frac{142.04\ g\ Na_2SO_4}{1\ mol\ Na_2SO_4} = 1.2198\ g\ Na_2SO_4$$

Mg^{+2} adjustment calculation:
Salt dissolved: $MgCl_2$
Concentrations in solution: Mg^{+2}, Cl^-
Desired Mg^{+2} concentration: 57 mg L^{-1}
Calculation:

$$Mg^{+2} = 0.057\ g\ L^{-1}$$

$$\frac{0.057\ g\ L^{-1}}{24.305\ g\ mol^{-1}} = 0.0023\ mol\ Mg^{+2}$$

$$0.0023\ mol\ Mg^{+2}\ \times \frac{2\ mol\ Cl^-}{1\ mol\ Mg^{+2}} = 0.0047\ mol\ Cl^-$$

$$0.0023\ mol\ Mg^{+2}\ \times \frac{1\ mol\ MgCl_2}{1\ mol\ Mg^{+2}} = 0.0023\ mol\ MgCl_2$$

$$0.0023\ mol\ MgCl_2 \times \frac{95.21\ g\ MgCl_2}{1\ mol\ MgCl_2} = 0.2233\ g\ MgCl_2$$

Ca^{+2} adjustment calculation:
Salt dissolved: $CaCl_2 \cdot 2H_2O$
Concentrations in solution: Ca^{+2}, Cl^-
Desired Ca^{+2} concentration: 132 mg L^{-1}
Calculation:

$$Ca^{+2} = 0.132\ g\ L^{-1}$$

$$\frac{0.132\ g\ L^{-1}}{40.08\ g\ mol^{-1}} = 0.0033\ mol\ Ca^{+2}$$

$$0.0033\ mol\ Ca^{+2} \times \frac{2\ mol\ Cl^-}{1\ mol\ Ca^{+2}} = 0.0066\ mol\ Cl^-$$

$$0.0033\ mol\ Ca^{+2} \times \frac{1\ mol\ CaCl_2 \cdot 2H_2O}{1\ mol\ Ca^{+2}} = 0.0033\ mol\ CaCl_2 \cdot 2H_2O$$

$$0.0033\ mol\ CaCl_2 \cdot 2H_2O \times \frac{147.01\ g\ CaCl_2 \cdot 2H_2O}{1\ mol\ CaCl_2 \cdot 2H_2O} = 0.4841\ g\ CaCl_2 \cdot 2H_2O$$

PO_4^{-3} adjustment calculation:
Salt dissolved: NaH_2PO_4
Concentrations in solution: PO_4^{-3}, Na+
Desired PO_4^{-3} concentration: 260 mg L^{-1}
Calculation:

$$PO_4^{-3} = 0.260\ g\ L^{-1}$$

$$\frac{0.260\ g\ L^{-1}}{95\ g\ mol^{-1}} = 0.0027\ mol\ PO_4^{-3}$$

$$0.0027\ mol\ PO_4^{-3} \times \frac{1\ mol\ Na^+}{1\ mol\ PO_4^{-3}} = 0.0027\ mol\ Na^+$$

$$0.0027\ mol\ PO_4^{-3} \times \frac{1\ mol\ NaH_2PO_4}{1\ mol\ PO_4^{-3}} = 0.0027\ mol\ NaH_2PO_4$$

$$0.0027\ mol\ NaH_2PO_4 \times \frac{119.98\ g\ NaH_2PO_4}{1\ mol\ NaH_2PO_4} = 0.3285\ g\ NaH_2PO_4$$

Urea adjustment calculation:
Salt dissolved: Urea crystals
Concentrations in solution: urea
Desired urea concentration 11600 mg L^{-1}

Calculation:

$$\frac{11600\ mg\ L^{-1}}{1000\ \frac{mg}{g}} = 11.6\ g\ urea\ L^{-1}$$

Cl^- adjustment calculation:
Salt dissolved: NaCl
Concentrations in solution: Na^+, Cl^-
Desired Cl^- concentration: 4430 mg L^{-1}

$$NH_4Cl:\ 0.0311\ mol\ Cl^-$$
$$KCl:\ 0.012\ mol\ Cl^-$$
$$MgCl_2:\ 0.0047\ mol\ Cl^-$$
$$CaCl_2 \cdot 2H_2O:\ 0.0066\ mol\ Cl^-$$
$$Total\ Cl^-already\ in\ solution = 0.05441\ mol\ Cl^-$$
$$Remaining\ Cl^-required = \frac{4.43\ mol}{\frac{35.5g}{mol}} - 0.05441 = 0.0705\ mol\ Cl^-$$

Calculation:

$$remaining\ Cl^- = 0.0705\ mol\ Cl^-$$

$$0.0705\ mol\ Cl^- \times \frac{1\ mol\ Na^+}{1\ mol\ Cl^-} = 0.0705\ mol\ Na^+$$

$$0.0705\ mol\ Cl^- \times \frac{1\ mol\ NaCl}{1\ mol\ Cl^-} = 0.0705\ mol\ NaCl$$

$$0.0705\ mol\ NaCl \times \frac{58.44\ g\ NaCl}{1\ mol\ NaCl} = 4.122\ g\ NaCl$$

Na^+ adjustment calculation:
Salt dissolved: NaCl
Concentrations in solution: Na^+, Cl^-
Desired Cl^- concentration: 4430 mg L^{-1}

$$Na_2SO_4 : \ 0.0172\ mol\ Na^+$$
$$NaH_2PO_4 : \ 0.0027\ mol\ Na^+$$
$$NaCl: 0.0705\ mol\ Na^+$$
$$Total\ Na^+ already\ in\ solution = 0.0905\ mol\ Na^+$$
$$Remaining\ Na^+ required = \frac{2.51\ mol}{\frac{22.99 g}{mol}} - 0.0905 = 0.0187\ mol\ Na^+$$

Calculation:

$$remaining\ Na^+ = 0.0187\ mol\ Na^+$$

$$0.0187\ mol\ Na^+ \times \frac{1\ mol\ Cl^-}{1\ mol\ Na^+} = \ 0.0187\ mol\ Cl^-$$

$$0.0187\ mol\ Na^+ \times \frac{1\ mol\ NaCl}{1\ mol\ Na^+} = 0.1875\ mol\ NaCl$$

$$0.0187\ mol\ NaCl \times \frac{58.44\ g\ NaCl}{1\ mol\ NaCl} = 1.094\ g\ NaCl$$

Excess Cl- added:

$$Na^+ NaCl\ adds\ excess\ Cl^{-1} \therefore \ 0.0187\ mol\ Cl^-\ excess$$

Final Cl- in solution:

$$\left(0.0187\ mol\ Cl^- + \frac{4.43\ mol}{\frac{35.5 g}{mol}}\right) \times 35.5 \frac{g\ Cl^-}{mol\ Cl^-} = 5.094\ g\ Cl^-\ L^{-1}$$

Total mass of NaCl added:

$$1.094\ g + 4.122\ g = 5.2167\ g\ NaCl$$

Table 27. Adjusted fresh synthetic urine recipe (Etter et al., 2014). Quantity of salts to be dissolved in one liter deioinzed water to give resulting major ion concentrations of fresh urine presented above. The recipe has been adjusted to match the major ion concentrations used in OLI simulations for U1a.

Compounds dissolved in 1L water	**Adjusted recipe Mass (g)**
$CO(NH_2)_2$	11.6
NH_4Cl	1.67
Na_2SO_4 (anhydrous)	1.22
NaH_2PO_4 (anhydrous)	0.329
KCl	0.894
$MgCl_2$	0.223
$CaCl_2$	0.484
$CaCl_2 \cdot 2H_2O$	5.22

NPK general experimental set-up

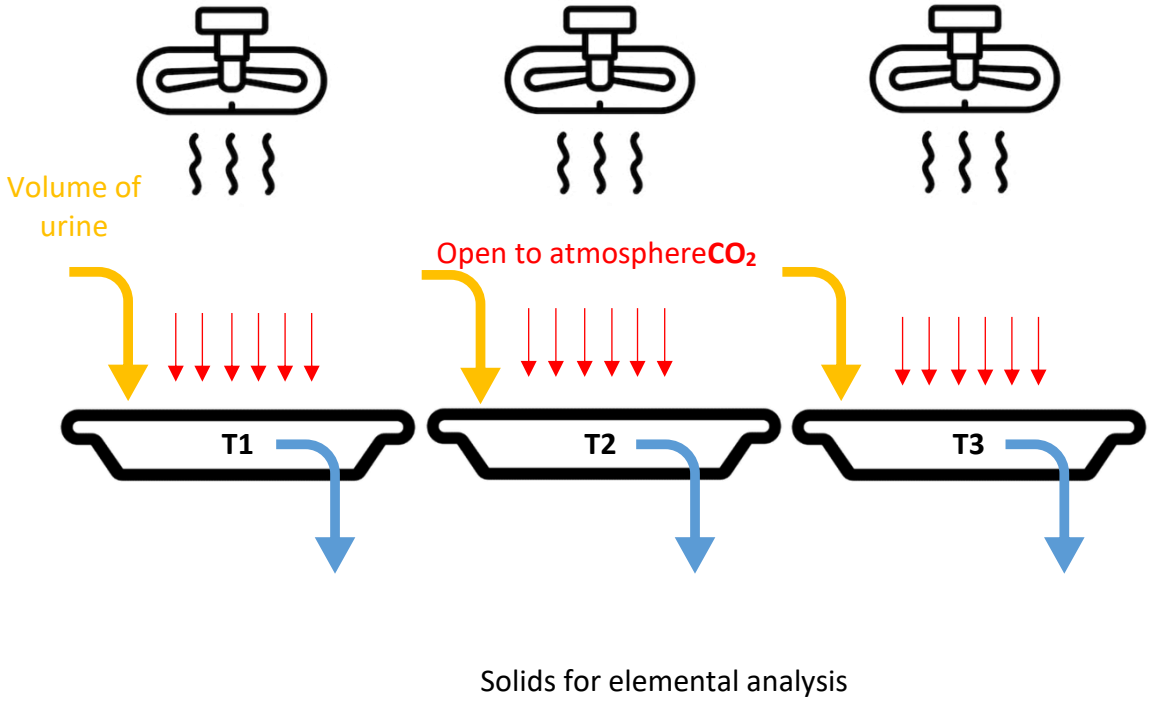

Figure 26. Experimental setup for NPK experiments. Experiments repeated in triplicate using three trays and overhead fans. Volumes added to each tray outlined in Table 14 for each urine treatment methodology studied.

The concentrated solids were scraped out of each tray and sent for elemental analysis (See analytical methods below). This determined the elemental composition of the remaining concentrated solids and any liquid phase present in each tray after water removal. Results from the initial composition analysis and final elemental analysis were used to determine the recovery for each major ion through Equation (**13** below. This in turn was used to determine the best urine treatment method.

$$Recovery\ (\%) = \frac{Final\ concentration\ of\ ion}{Initial\ concentration\ of\ ion} \times 100 \qquad \textbf{(13)}$$

Feasible operating regions for TH3 PE 100 climate chamber

When operating the TH3 PE 100 climate chamber, certain combinations of temperature and relative humidity were deemed as infeasible operating regions. Below, the regions which are both infeasible and feasible are shown.

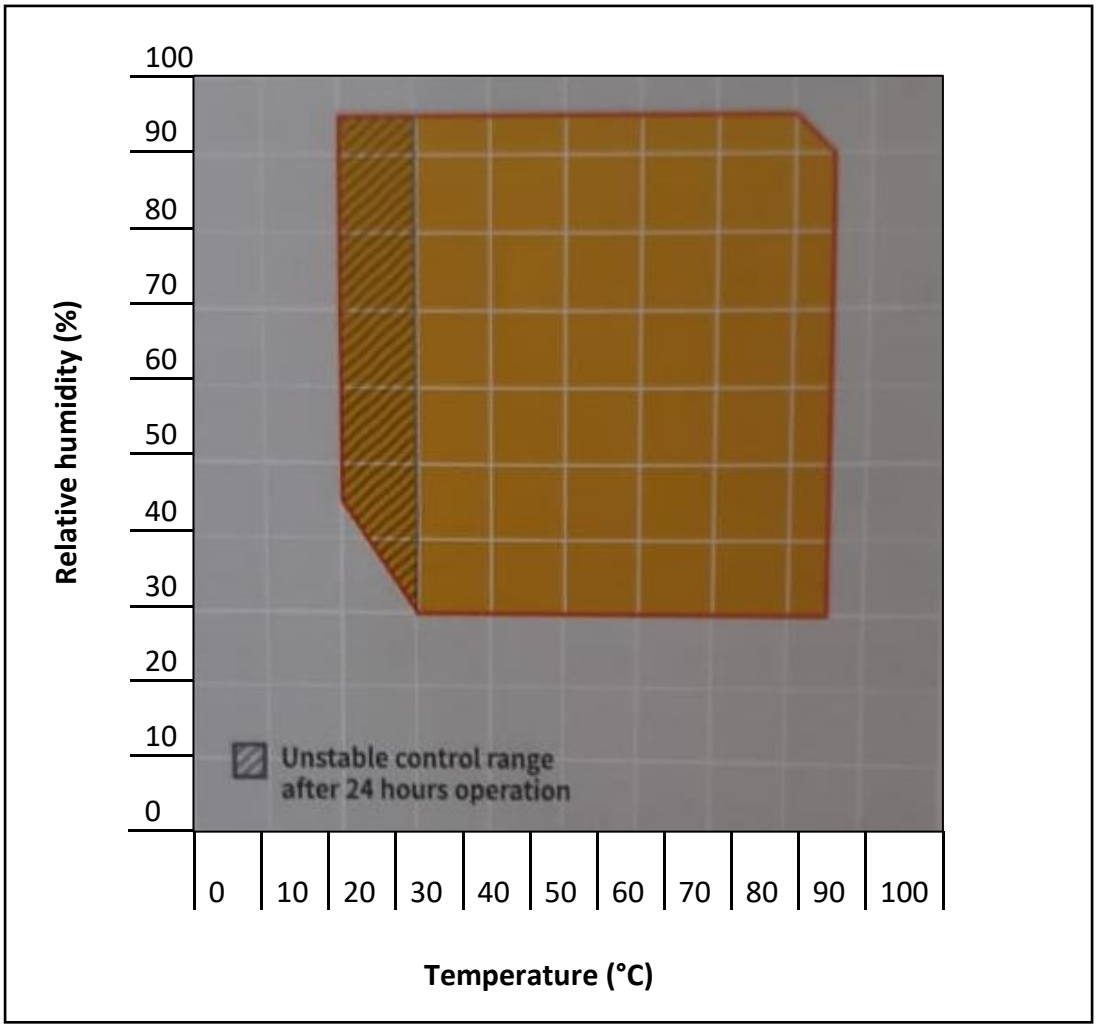

Figure 27. Operating temperature and relative humidity conditions for TH3 PE 100 climate chamber

From the feasible operating regions, an operating temperature of 40°C and a relative humidity of 40% was chosen for experimental conditions. The lowest temperature at which the chamber could be run was 30°C. However, this temperature fell in the region of unstable control. As a result, 40°C was chosen as the chamber operating temperature for experimental work. This temperature was low enough to avoid a high risk of urea hydrolysis. A low humidity of 40% was chosen as 30% humidity fell on the border of feasible operating regions.

ThermoScientific Gallery test limits

Before adding a sample to the gallery, the sample needed to be filtered to 0.45µm using micropore a syringe filter. This ensured that the gallery tubing was not blocked by small solid particles. The concentration of various species can then be determined when adding a sample to the ThermoScientific gallery. The gallery works like a spectrophotometer relating the absorbance of a chemical species to a concentration in solution, through the use of a calibration curve. For this reason, the various species tests available for use on the gallery, needed to be calibrated regularly. Calibrations were only accepted if a correlation value greater than 0.99 was obtained in the relevant calibration. The concentration of the relevant species needs to fall within the test limits for each species, as outlined below.

To ensure that the concentration of the relevant species fell within the allowable test limit, two types of dilutions were possible: human dilution and automatic gallery dilutions. A human dilution was used when the expected sample concentration was over the test limit. For example, the urea concentration was expected to be approximately 12000 mg L^{-1}. This sample was dilution 25 times, resulting in a concentration of 480 mg L^{-1}. Human dilutions were done before adding samples into the gallery to bring the sample's expected concentrations within range.

In most instances, a human dilution of 25 times was used for samples. This meant 1 mL of the initial sample was added to a new sample of 25 ml. The remaining 24 mL of this new sample was accounted for through the addition of deionized water, and 0.08 M HCl where applicable.

The human dilution needed to be considered when calculating the final concentration of tested species in solution. The definition of this human dilution can be demonstrated as follows:

$$25\ times\ dilution = \frac{total\ sample\ volume}{volume\ of\ initial\ sample}$$

$$= \frac{25\ ml}{1\ ml}$$

To consider the above manual dilution in experimental results the following step needed to be included in the data collection and processing step:

$$Final\ concentratoin = gallery\ concentration\ reading\ \times human\ dilution$$

After a human dilution if required, automatic gallery dilutions could be automatically implemented by the gallery when running sample analysis. However, to minimize reagent wastage, this dilution could be specified prior to any sample analysis. Unlike manual human dilutions, these gallery dilutions have already been incorporated into the concentration results obtained from the gallery.

To determine the required gallery dilution, one needed to use the gallery dilution series below, as well as the relevant calibration test results. The sample concentration for the relevant test, needed to be divided by the chosen gallery dilution, to ensure that the

concentration of the tested species, fell mid-region on the relevant calibration curve. If not specified, the gallery would run through the dilution series specified below, after reaching each specified concentration until a reading associated with the calibration curve, was obtained.

Using urea as an example, this could be specified as an additional five times dilution. Gallery dilutions ensured that the concentration of the species fell within a concentration/absorption range for each test as mentioned above.

$$Urea\ concentration = 12000\ \div human\ dilution \div gallery\ dilution$$

$$= 12000\ \div 25\ \div 5 = 96\ mg/L$$

Table 28. Gallery test limits and associated automatic gallery dilution series for each test available during sample analysis

Test	Test limit (mg/L)	Gallery dilution series	
Ammonia	125	Dilution 1 Dilution 2 Dilution 3 Dilution 4	4 times at 2.5 mg/L 14 times at 12.5 mg/L 29 times at 37.5 mg/L 49 times at 75 mg/L
Calcium	1000	Dilution 1	4 times at 200 mg/L
Chloride	1000	Dilution 1	4 times at 200 mg/L
Potassium	5-500	Dilution 1	4 times at 100 mg/L
Magnesium	300	Dilution 1 Dilution 2	4 times at 20 g/L 14 times at 100 mg/L
Phosphate	187.5	Dilution 1 Dilution 2 Dilution 3 Dilution 4	4 times at 2.5 mg/L 14 times at 12.5 mg/L 24 times at 37.5 mg/L 74 times at 62.6 mg/L
Sulfate	1600	Dilution 1 Dilution 2	4 times at 40 mg/L 39 times at 200 mg/L
Urea	10-720	Dilution 1	5 times at 120 mg/L

The urea test converts urea to ammonia and measures the total ammonia concentration. Hence, if ammonia is possibly present in solution, the urea and ammonia test should be run. The ammonia test results are given in the units mg N/L, compared to the urea test which is given in the units of mg urea/L. Hence, for calculation purposes, the urea results need to undergo the below unit conversion:

$$To\ convert\ urea\ \left(\frac{mg\ urea}{L}\right)\ to\ urea\ \left(\frac{mg\ N}{L}\right)$$

$$= \frac{mg\ urea}{L} \times \frac{g}{1000\ mg} \times \frac{mol\ urea}{60.06\ g\ urea} \times \frac{2\ mol\ N}{1\ mol\ urea} \times \frac{14\ g\ N}{mol\ N} = 0.466 \frac{mg\ N}{L}$$

The results obtained for urea and phosphate tests then needed to be converted through the following conversion calculations:

$$Urea\ \left(\frac{mg\ urea}{L}\right) = \frac{\left(\left[Urea\ \left(\frac{mg\ urea}{L}\right) \times 0.466 \left(\frac{mg\ N/L}{mgurea/L}\right)\right] - ammonia\ \left(\frac{mg\ N}{L}\right)\right)}{0.466\ \left(\frac{mgN/L}{mgurea/L}\right)}$$

$$Phosphate\ \left(\frac{mg\ PO_4}{L}\right) = gallery\ reading\ \left(\frac{mgP\ in\ PO4}{L}\right) \times \left(\frac{mol\ P}{30.97\ g\ P}\right) \times \left(\frac{1\ mol\ PO_4}{1\ mol\ P}\right) \times \left(\frac{94.97\ g\ PO_4}{mol\ PO_4}\right)$$

Sampling procedures

Pre-experimental sampling

Prior to beginning experimental work with fresh urine or undergoing any of the above treatment techniques, the composition of fresh urine both human and synthetic, was determined using the Gallery. Additionally, the pH of the initial solution and the temperature at which sampling was conducted, was recorded.

From the figure below, a portion of fresh urine was collected and filtered to 0.45 µm using a syringe filter. The filtrate was filtered into a beaker. A fixed volume of 1000 µL was pipetted into a 25 mL volumetric flask. As shown in sample 1, 50 µL 0.08 M HCl was then pipetted into the 25 mL flask. The flask was topped up with de-ionized water and sealed using a flask stopper. The sample 1 flask was well mixed and then ready for Gallery analysis. Sample 1 was manually diluted 25 times through this preparation.

As sample 2 tested for Ca^{2+} and Mg^{2+}, 1 mL dilute acid (0.08 M HCl) was added to 5 mL unfiltered urine sample, in a beaker and well mixed. This ensured any particulate Ca^{2+} and Mg^{2+} was solubilized before filtering to 0.45 µm. This acidification introduced a manual dilution factor of 1.2. A syringe filter was used to filter the acidified sample into a second beaker. This was sealed with parafilm and ready for the Gallery. No further manual dilution was required for sample 2.

Lastly, sample 3 tested for Cl^-. This meant that no additional HCl could be present in the sample. The preparation of sample 3 was identical to sample 1 above. However, as shown in Figure 28, the 50 µL 0.08 M HCl was omitted from sample 3.

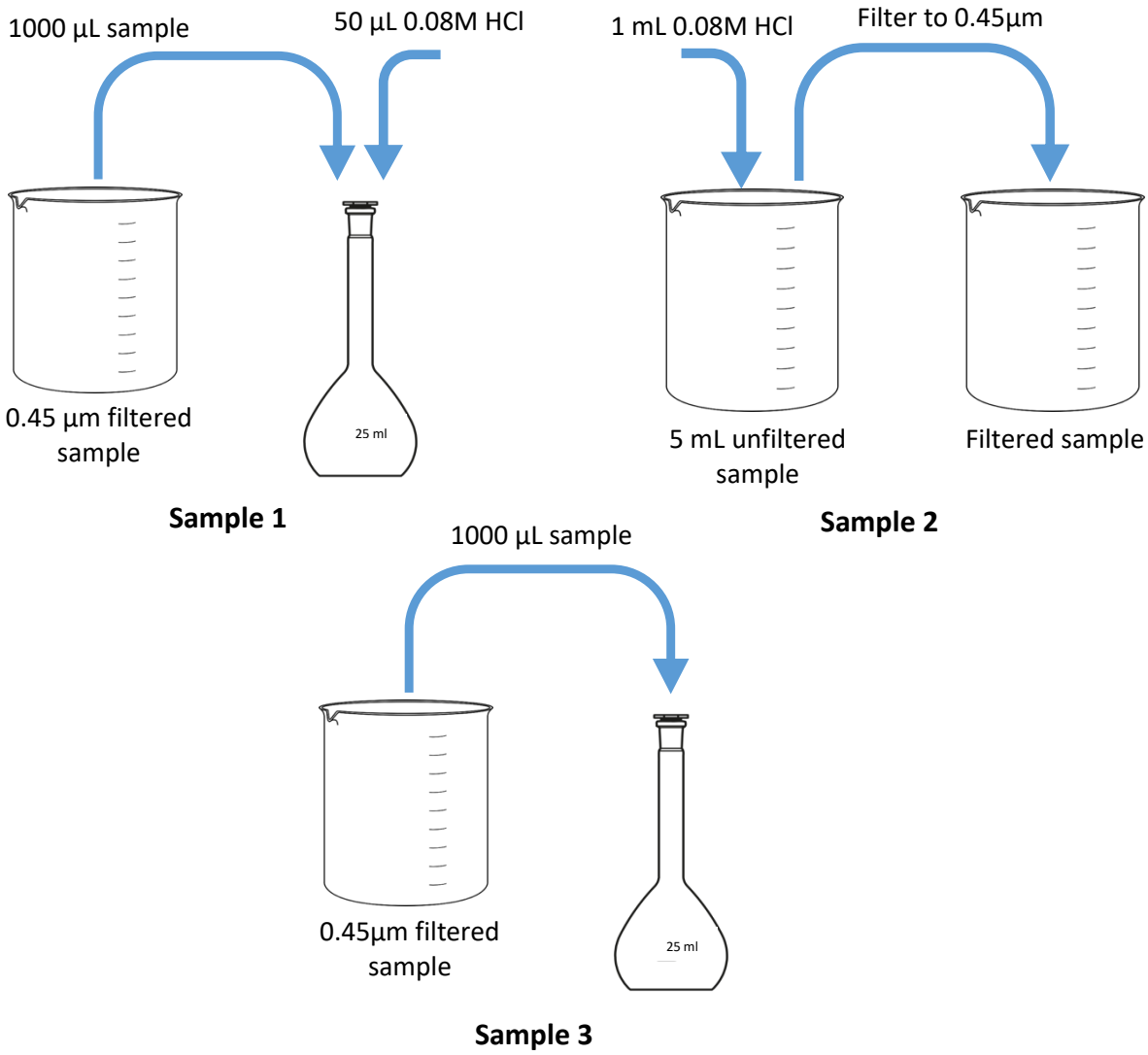

Figure 28. Pre-experimental sampling technique for analysis in ThermoScientific Gallery

The table below summarizes the samples from which each major ion concentration was determined. As well as this, the manual and Gallery performed dilutions are summarized for pre-experimental sampling.

Table 29. Manual and gallery dilutions for major ion concentrations measured using pre-experimental sampling procedure

Major ion	Dilution		Sample
	Manual	Gallery	
NH_4^+	25	14	1
$CO(NH_2)$		5	
SO_4^{-2}		1	
PO_4^{-3}		2	
K^+		-	
Ca^{+2}		-	3
Cl^-	1.2	-	2
Mg^{+2}		-	

Post experimental solids sampling procedure

After evaporating a urine solution, the final mass of the dried tray and solids was recorded. A sample of the formed solids was then harvested through scraping a dry tray with a clean spatula. The harvested solids were harvested in a clean beaker. It was desired to scrape and harvest as much of the formed solids as possible as this made calculations and dilution considerations easier as when re-dissolving solids back into solution. The mass of these solids was also recorded. These two mass measurements, along with the initial empty tray mass, were used as a mass correction factor (Equation (**14**)

$$Mass\ correction\ factor\ (\%) = \frac{Mass\ harvested\ solids}{Mass\ tray\ and\ solids - \ Mass\ empty\ tray} \times 100 \quad \textbf{(14)}$$

Deionized water was added to the beaker and solids. The beaker was swirled well and then emptied into a 1 L volumetric flask (post experimental solution volume). The beaker was washed with deionized water and emptied into the volumetric flask to ensure maximum transfer of solids. The volumetric flask was topped up to the 1 L mark. A magnetic stirrer bar was placed into the flask and the flask was sealed with parafilm. The flask was placed onto a magnetic stirrer and mixed vigorously for 15 minutes.

After mixing, post experimental sampling techniques below were used. The samples were prepared accordingly, and major ion concentrations were determined in the Gallery. The concentration for each major ion measured in the Gallery, was then adjusted using Equation (**15** below. This equation accounts for the difference in solution volumes as well as the mass correction factor from above.

(15)

$$Final\ concentration = A \times B \times C \times D$$

$$A = \ Gallery\ concentration$$

$$B = \ Manual\ dilution$$

$$C = \frac{1}{Mass\ correction\ factor}$$

$$D = \frac{Post\ experimental\ solution\ volume}{Initial\ urine\ solution\ volume}$$

Post experimental/stabilization sampling

After dissolving solids back into solution or stabilizing fresh urine with $Ca(OH)_2$ or MgO, Post experimental sampling techniques were used. These sampling techniques were similar to the pre-experimental sampling techniques above. The temperature and pH of the sample solution was also recorded in post experimental techniques.

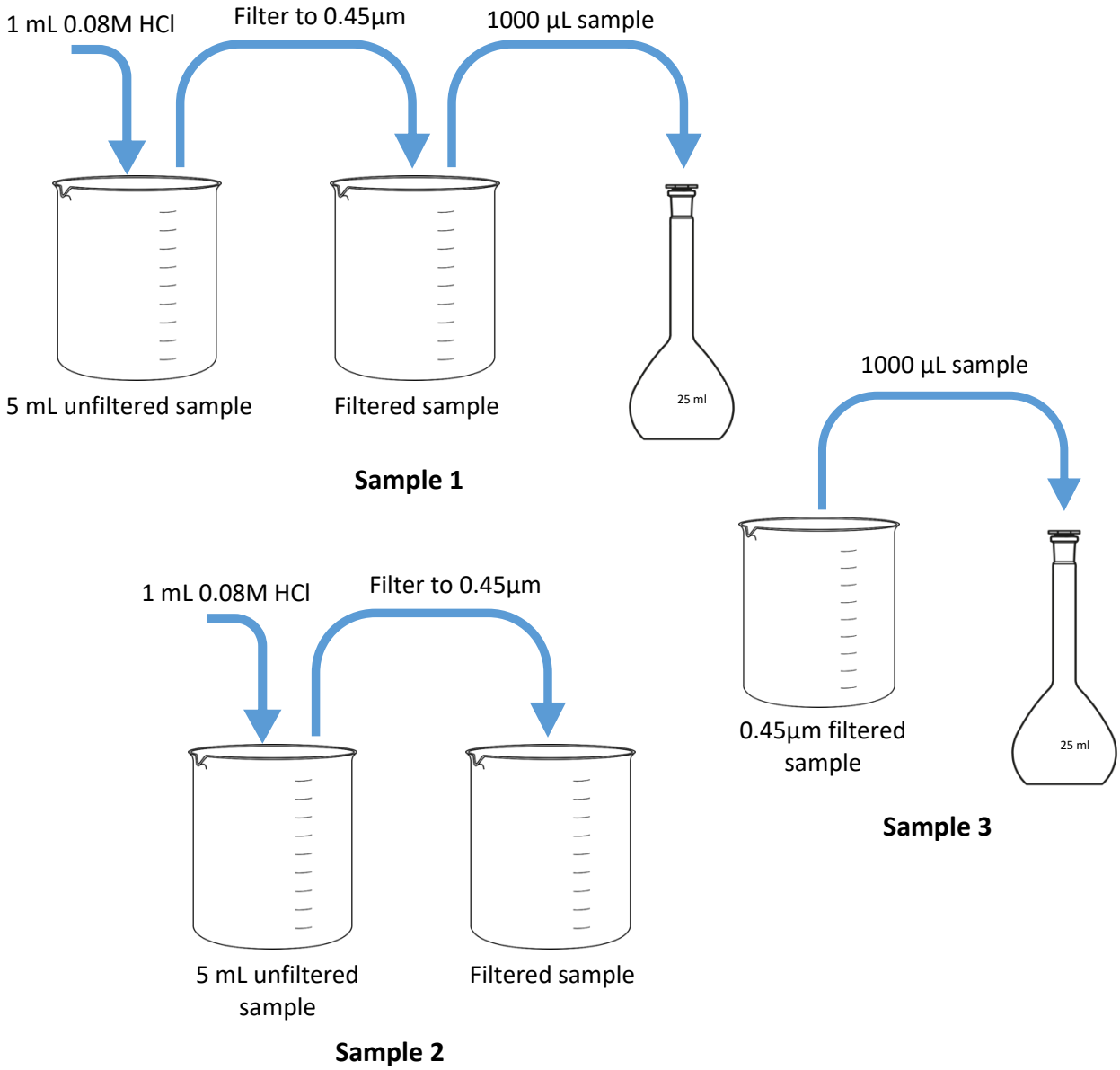

Figure 29. Post experimental/stabilization sampling technique for analysis in ThermoScientific Gallery

The main differences in this sampling technique include the Ca^{2+} concentration being determined from sample 1. Secondly, an acidification step also occurred in sample 1 prior to syringe filtration, as shown above. This meant that 50 µL HCl added during pre-experimental

sampling was no longer necessary. Lastly, when stabilizing with MgO, the Gallery dilution for Mg^{2+} was adjusted, as shown.

Table 30. Manual and gallery dilutions for major ion concentrations measured using post-experimental sampling procedure

Major ion	Dilution		Sample
	Manual	Gallery	
NH_4^+	30	14	1
$CO(NH_2)$		5	
SO_4^{-2}		1	
PO_4^{-3}		2	
K^+		-	
Ca^{+2}		-	
Cl^-	25	-	3
Mg^{+2}	30	2	2

Bemlabs sampling procedure

The sampling procedure for external analysis used a clean, dry sample cup. A volume of 50 mL of the required well mixed sample was added to the sample cup. The cup was clearly labelled with the sample number and well-sealed. Any manual dilutions on the sample and the experiment to which the sample belonged, were noted before the sample was taken for analysis. Samples were refrigerated between being collected and taken to Bemlab for external analysis.

Appendix B.1: Supporting results

$Ca(OH)_2$ and MgO saturation curves

When stabilizing urine with $Ca(OH)_2$ and MgO, the saturation pH curve for both basic salts is a useful guide in determining the correct mass dosage. When using $Ca(OH)_2$, a saturation pH of 12.5 is reached after 4 g or more $Ca(OH)_2$ is added to a fresh urine solution. When using MgO, a saturation pH of 9.80 is reached after 1 g or more MgO is added to the fresh urine solution. This saturation curve was generated using the composition of U1a in OLI (Randall et al., 2016). To ensure that the solutions were adequately stabilized, a $Ca(OH)_2$ and MgO dosage of 10 g L^{-1} and 1.5 g L^{-1} were used respectively.

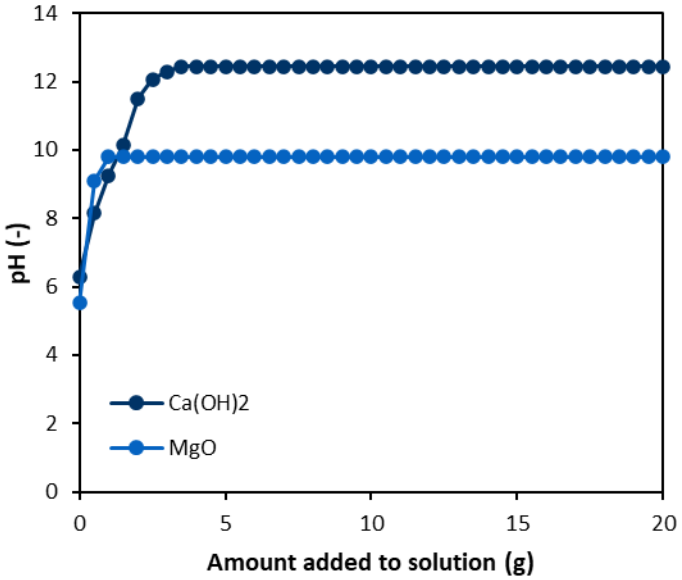

Figure 30. $Ca(OH)_2$ and MgO saturation pH curves used for NPK dosing method development. Saturation curves developed using U1a as the fresh urine composition.

Solubility graphs

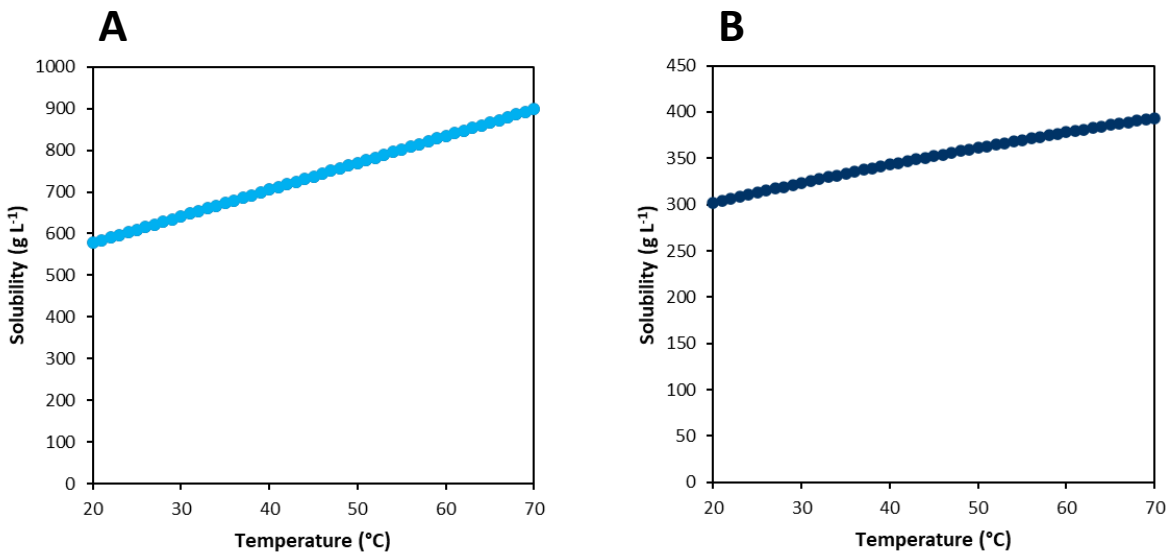

Figure 31. Solubility graphs. **(A)** shows the solubility of urea as a function of temperature as predicted using OLI software. **(B)** shows the solubility of KCl as a function of temperature. Both **(A)** and **(B)** were created using OLI simulations.

Appendix B.2: Costing guideline and supplementary costing results

When developing a preliminary cost associated with the evaporation process, basic mass and energy balances were conducted. Additionally, various unit conversions were applicable. The methodology and explanation for this costing is explained in greater detail below. Example calculations are also shown.

The costing methodology uses various nomenclature. Before explaining the costing methodology, this nomenclature is introduced.

Table 31. Nomenclature used during the costing associated with the evaporation process. The symbol, definition and units are outlined in the table below.

Symbol	Definition	Units
$\widehat{H}$	Specific enthalpy	kJ kg^{-1}
H^0	Standard enthalpy	kJ mol^{-1} K^{-1}
$\dot{m}$	Mass flow rate	kg $time^{-1}$
C_p	Specific heat capacity	kJ kg^{-1} $°C^{-1}$
T	Temperature	°C
H	Enthalpy	kJ
E_k	Kinetic energy	kJ
E_p	Potential energy	kJ
Q	Heat added /removed	kJ
W_s	Work done by/on the system	kJ
t	Temperature with conversion	K/1000

Preliminary costing of evaporative process

As evaporation is an endothermic process, the process requires an input of energy in the form of heat. The liquid molecules in the solution must absorb this heat to be able to vaporize. This energy input creating the required source of heat, corresponds to an operating cost.

As OLI is not able to determine the amount of water removed over time, the costing relationship cannot be determined in terms of the process power requirement but can be determined in terms of kWh which corresponds to the way municipal electricity is charged in South Africa.

As well as this, as the simulations are performed over a temperature range from 20°C to 70°C, in increments of 10°C. OLI is running the simulation at the specified operating temperature. This means that enthalpy information for each simulation does not account for the additional energy required to heat the initial solution from the assumed inlet temperature of 25°C, to the specified simulation temperature. A basic energy balance (See below) is done to correct for this additional energy cost.

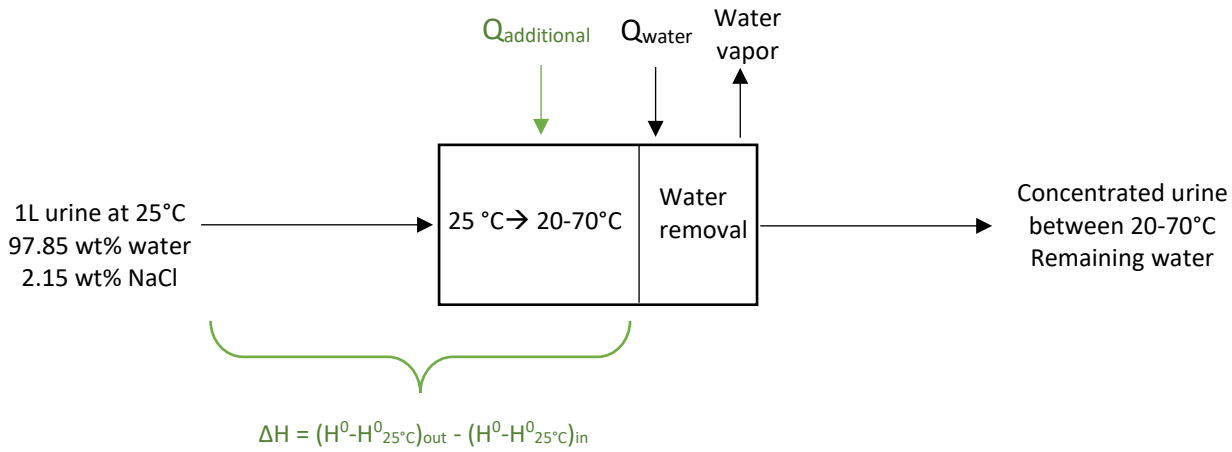

Figure 32. Schematic representation of the mass and energy balance over the urine evaporation process. One litre of human urine is feed into the process, this is 97.85 wt% water. Urine enters the process at 25°C. The urine is first heated to the chosen simulation temperature which lies between the range of 20 to 70°C, by adding an external source of heat ($Q_{additional}$). This is accompanied by a change in the enthalpy of the solution as indicated in the colour orange. Once heated, additional heat is added to the solution to remove water to the chosen water removal interval (Q_{water}). The water leaves the process in the form of water vapor and any remaining water that is not evaporated, will leave the process in the concentrated urine solution.

Basic mass balance

The below thermodynamic equations are used for a water/NaCl solution. To use these equations, U1 in OLI is used. This solution contains 97.85 wt% water. It is assumed that the remaining composition is attributed to NaCl (2.15 wt%). This assumption was made as urine is majority water and the major solid formed is NaCl.

Thermodynamic equations had to be done for water and NaCl independently using a weighted average of the total stream mass. Thermodynamic results are then added together to obtain one overall energy requirement for the water/NaCl system.

Basic energy balance equations

Overall energy balance

$$\Delta E_{system} = \Delta H + \Delta E_k + \Delta E_p + Q - W_s \quad \textbf{(16)}$$

$$\Delta E_{system} = \Delta H + Q_{additional} + \Delta H_{evaporation\ process}$$

(1) By determining the change in enthalpy of the solution by considering the change in enthalpy of the solution entering the process (25°C) and exiting the process (20-70°C), as well as (2)the heat generated (Q), the energy required to be added to the system (+) or removed from the system (-) can be determined. Energy added to the system correlates to a positive value and energy removed from the system corresponds to a negative value. This is relevant

in the case of the 20°C simulation as this temperature is lower than that of the assumed temperature at which the solution enters the process (Solution needs to be cooled in this case).

$\Delta H_{evaporation\ process}$ (3) is found using the change in the solution enthalpy during the evaporation process. This information is obtained from OLI considering the enthalpy at 0% and 100% water removal. This is explained below.

1. **Change in enthalpy when heating from initial to operating temperature (ΔH)**

$$\Delta H = \dot{m}\left(\widehat{H}_{out} - \widehat{H}_{in}\right) \tag{17}$$

As specific enthalpy cannot be determined in absolute terms, one has to specify a reference state:

$$\Delta H = \dot{m}\left(\left(\widehat{H}^{0}{}_{out,T_{out}} - \widehat{H}^{0}{}_{out,T_{ref}}\right) - \left(\widehat{H}^{0}{}_{in,T_{out}} - \widehat{H}^{0}{}_{in,T_{ref}}\right)\right) \tag{18}$$

The following equations were used to determine the change in enthalpy from a reference state as well as the heat capacity of both water and NaCl as a function of temperature. The thermodynamic constants for the below equation were used from the NIST database.

$$H^0 - H^0_{298.15} = At + \frac{Bt^2}{2} + \frac{Ct^3}{3} + \frac{Dt^4}{4} - \frac{E}{t} + F - H \tag{19}$$

$$Units: H^0: \left(\frac{kJ}{mol}\right)\ t: \frac{T(K)}{1000}$$

2. **Heat ($Q_{Additional}$)**

The heat added to the system to reach temperatures higher than the inlet temperature of 25°C, or removed to reach temperatures lower than the inlet temperature, the following equation with a species specific heat capacity, can be used. Specific heat capacity is a function of temperature, this is accounted for in the below equation using basic thermodynamic parameters from A to H in the table below.

$$Q\ (kJ) = mC_p\Delta T \tag{20}$$

$$Q(kWh) = Q(kJ)/3600 \tag{21}$$

$$C_p^0 = A + Bt + Ct^2 + Dt^3 + \frac{E}{t^2}$$

$$Units:\ C_p^0:\ \left(\frac{J}{mol\ K}\right)\ t:\frac{T(K)}{1000} \quad \textbf{(22)}$$

Table 32. NIST thermodynamic constants for water and NaCl

Basic thermodynamic data	
Water	
A	-203.606
B	1523.29
C	-3196.41
D	2474.455
E	3.855326
F	-256.548
G	-488.716
H	-285.83
NaCl	
A	50.72389
B	6.672268
C	-2.51717
D	10.15934
E	-0.20068
F	-472.212
G	130.3973
H	-411.12

https://webbook.nist.gov/cgi/cbook.cgi?ID=C7647145&Units=SI&Mask=2#Thermo-Condensed

3. Solution evaporation

The final energy consideration required is the change in enthalpy associated with the water removal process. There is no Q (heat requirement) associated with the water removal process as this process is occurring at a fixed temperature.

The change in enthalpy of the solution is determined using the solution enthalpy information from OLI water removal simulations. The required information is the total enthalpy and total mass and moles at each water removal interval. The enthalpy information from OLI needed to be adjusted as this information was the absolute enthalpy. To do this adjustment, the triple point of water needed to be considered as discussed below.

OLI enthalpy adjustment calculations and comparison to manually calculated values

The output enthalpy calculated in OLI simulations refers to the absolute enthalpy, referenced at 0 K, and has the units kJ/mol. This meant that to be comparable to basic manual thermodynamic calculations, as well as to be used in costing calculations, output enthalpies from OLI needed to be adjusted from absolute enthalpies at 0 K (Equation (**23)**), to an

enthalpy refenced at 298.15 K (Equation (**24)**) . This is summarized in Equations (**23)** and (**24)** below.

$$\Delta_{absolute}H = H_{triple\ point} - (H^0 - H^0_{298}) \quad \textbf{(23)}$$

$$(H^0 - H^0_{298}) = \Delta_{absolute}H - H_{triple\ point} \quad \textbf{(24)}$$

For the purposes of this thesis, it was assumed that the enthalpy of the triple point of a human urine solution could be approximated by the triple point of water. A value of -16.448 kJ/mol was hence used in enthalpy adjustments. As an example of this, OLI predicts an enthalpy of 285.83 kJ for water at 40°C.

From the above, this is the absolute enthalpy of water and hence is the enthalpy of 1 mole of water, hence 285.83 kJ/mol. Using Equation B with the triple point of water, a change in enthalpy of -269.38 kJ/mol is calculated.

$$(H^0 - H^0_{298}) = 285.83 - (-16.448) = \ -269.38\ kJ/mol$$

Using the molar mass of water, this was converted to -14972 kJ/kg.

For comparison, if the thermodynamic equation (Equation (**25)**) for water from the NSIT handbook was used to determine the enthalpy of pure water.

$$H^0 - H^0_{298.15} = At + \frac{Bt^2}{2} + \frac{Ct^3}{3} + \frac{Dt^4}{4} - \frac{E}{t} + F\ - H \quad \textbf{(25)}$$

$$Units\ H^0: \left(\frac{kJ}{mol}\right)\ t: \frac{T(K)}{1000}$$

Equation C above, required the following thermodynamic constants and temperature relationship. As well as this, the reference enthalpy for pure water at 298.15 K (H^0_{298}) was taken as -285.83 kJ/mol[13]

Table 33. Water thermodynamic constants from NIST database

	Water
A	-203,606
B	1523,29
C	-3196,41
D	2474,455
E	3,855326
F	-256,548
G	-488,716
H	-285,83

[13] https://webbook.nist.gov/cgi/cbook.cgi?ID=C7732185&Mask=2#Thermo-Condensed

$$t = \frac{40 + 273.15}{1000} = 0.313\ K/1000$$

Using this information, the enthalpy of water at 40°C was determined as follows:

$$H^0 - H^0_{298.15} = 12.235\ kJ/mol$$

$$H^0 = 12.235 - H^0_{298.15}$$

$$H^0 = 12.235 + (-285.83) = -273.594\ kJ/mol$$

This value was then compared to the OLI determined value of -269.38 kJ/mol. As seen, the values obtained from the manual calculations are similar and approximate of that of the OLI values.

Costing example calculations

A basis of treating 1000 L (1 m^3) urine via evaporative processes per day was used. This basis was used when determining the initial input heat requirement for water and NaCl. These results for 1000 L are shown in Table 35 and Table 36 and used to determine the initial heat associated with each operating temperature in Table 37.

To determine the change in enthalpy associated with water, the enthalpy obtained from OLI was first converted from absolute enthalpy, to the form of $H^0 - H^0_{298}$ as discussed above. This enthalpy was multiplied by the molar mass of the solution at the relevant water removal interval to obtain an enthalpy in the units kJ. An example is shown below for 60 g water remaining in solution (94% water removal in U1b) at 40°C.

Table 34. Sample data from OLI simulations used for OLI enthalpy costing

Absolute enthalpy from OLI					**Molar mass of solution**		
H_2O	**Total**	**Liquid**	**Solid**		**Total**	**Liquid**	**Solid**
g	**kJ/mol**	**kJ/mol**	**kJ/mol**		**mol**	**mol**	**mol**
0	-150.57	-21.48	-128.44		0.398646	0.082081	0.302316
20	-466.70	-432.81	-33.89		1.59749	1.5669	3.06E-02
40	-782.70	-750.11	-32.59		2.70582	2.67626	2.96E-02
60	-1098.72	-1067.60	-31.12		3.81632	3.78792	2.84E-02
80	-1414.76	-1385.02	-29.74		4.92729	4.89999	2.73E-02
100	-1730.81	-1702.36	-28.45		6.0384	6.01214	2.63E-02
1000	-15954.00	-15951.70	-2.31		56.0297	56.0274	2.35E-03

A reference state was needed for the solution, as used in the manual calculations shown for water above. As this could not easily be looked up in a handbook, due to the nature of the solution, the enthalpy of the solution at 0% water removal was used. This reference state was determined from the information above, as follows:

$$Adjusted\ enthalpy_i(kJ/mol) - adjusted\ enthalpy_{0\%\ water\ removal}(kJ/mol) = energy\ input_i(kJ/mol) \quad \textbf{(26)}$$

$$Energy\ inout_i(kJ/mol) \times molar\ mass\ solution_i\ (mol) = enthalpy_i\ (kJ) \quad \textbf{(27)}$$

$$energy\ input\ (kWh) = enthalpy_i(kJ)/3600 \quad \textbf{(28)}$$

$$\begin{aligned} Adjusted\ enthalpy &= total\ absolute\ enthalpy - triple\ point\ enthalpy \\ &= -15954 - (-16.448) \\ &= -16402\ kJ/mol \end{aligned} \quad \textbf{(29)}$$

$$-16402\frac{kJ}{mol} \times 56.0297\ mol = -892976\ kJ$$

This reference enthalpy was used in each calculation as shown in the following example for 94% water removal in U1b at 40°C:

$$\begin{aligned} &Total\ absolute\ enthalpy - Triple\ point\ enthalpy \\ &= -1098.72 - (-16.448) \\ &= -1115.17\ kJ/mol \end{aligned}$$

$$-1115.17\frac{kJ}{mol} \times 3.81632\ mol = -4255.84\ kJ$$
$$-4255.84\ kJ - (-892976\ kJ) = 888846\ kJ$$
$$888846\ kJ \times \frac{1\ kWh}{3600\ kJ\ 24h} = 10.29\ kWh$$

This value does not however consider the change in enthalpy due to initial heating (1) and initial heating requirement (2) of the solution (2). At 20°C, this was determined to be 1.58 kWh at 40°C for 1000L urine.

$$10.29\ kWh + (1.58\ kWh) = 11.83\ kWh$$

This example calculation procedure was followed for each set of information obtained at each water removal. This was extended to all the simulation results for all three types of urine at a range of temperatures from 20°C to 70°C.

Additional input energy requirement calculation results

Table 35. Additional heating requirements for water in water-NaCl solution. Results obtained from basic thermodynamic and mass balance calculations. Results include heat capacity determined as a function of temperature.

Temperature		Additional heat requirement per litre of urine				
Inlet (°C)	**Outlet (°C)**	**C_p (kJ kg^{-1} K^{-1})**	**Q (kJ)**	**ΔH (kJ)**	**(kJ)**	**(kWh m^{-3})**
25	20	4.19	-20492	-20480	-40972	-0.47
25	30	4.18	20454	20462	40916	0.47
25	40	4.18	61320	61352	122672	1.42
25	50	4.18	102217	102233	204450	2.37
25	60	4.18	143229	143137	286365	3.31
25	70	4.19	184419	184086	368505	4.27

Table 36. Additional heating requirements for NaCl in water-NaCl solution. Results obtained from basic thermodynamic and mass balance calculations. Results include heat capacity determined as a function of temperature.

Temperature		Additional heat requirement per litre of urine				
Inlet (°C)	**Outlet (°C)**	**C_p (kJ kg^{-1} K^{-1})**	**Q (kJ)**	**ΔH (kJ)**	**(kJ)**	**(kWh m^{-3})**
25	20	0.862	-92.7	-92.8	-185	-0.052
25	30	0.866	93.1	93.0	186	0.052
25	40	0.870	281	280	560	0.156
25	50	0.873	469	467	936	0.260
25	60	0.877	660	655	1315	0.365
25	70	0.880	851	844	1695	0.471

Table 37. Total additional heating requirement from NaCl and water solution

Temperature (°C)	Additional heating requirement (kWh m^{-3} urine)
20	-0.526
30	0.525
40	1.575
50	2.626
60	3.680
70	4.736

Appendix C: NPK raw data

Experimental adjustment factor in tables below refers to a mass ratio of the solids recovered and the solids present in the tray after evaporation. This adjustment factor considers the total solids in the tray after evaporation and the amount of solids scraped from the tray and added into one litre of deionized water, as not all the solids formed could be scrapped, naturally some would remain in the tray. However, the concentration achieved in a one litre solution hence needs to be adjusted for as the measured concentration will be lower than the actual concentration, should all of the solids be scraped and dissolved.

$$Experimental\ adjustment\ factor = \frac{Mass\ of\ scraped\ solids}{Mass\ of\ tray\ after\ evaporation - mass\ empty\ tray} \quad \textbf{(30)}$$

Fresh synthetic urine

Initial fresh urine results									
	Dilution		Gallery measurement (mg L^{-1})			Concentration (mg L^{-1})			Average
	Gallery	Manual							
Ammonia	14	25	16.95	16.97	16.59	423.75	424.25	414.75	420.92
Urea	5	25	491.89	483.35	476.86	12297.19	12083.87	11921.45	12100.84
N						6154.24	6055.33	5970.15	6059.91
PO4	4	25	3.84	3.18	3.59	294.05	244.07	275.27	271.13
K						444.00	444.00	444.00	444.00

Final fresh urine results										
	Dilution		Gallery measurement (mg L^{-1})			Concentration (mg L^{-1})			Average	Experimental adjustment factor
	Gallery	Manual								
Ammonia	14	25	20.18	20.37	19.88	557.27	562.52	548.99	556.26	
Urea	5	25	390.41	396.59	393.05	10781.11	10951.94	10854.17	10862.41	
N						5581.27	5666.12	5607.03	5618.14	0.91
PO4	4	25	3.20	2.53	3.10	270.95	214.31	262.49	249.25	
K						490.44			490.44	

Recovery (%)				
				Average
N	90.69	93.57	93.92	92.73
P	92.15	87.81	95.36	91.77
K	110.46			110.46

Hydrolyzed synthetic urine

Initial hydrolyzed urine results									
	Dilution		Gallery measurement (mg L^{-1})			Concentration (mg L^{-1})			Average
	Gallery	Manual							
Ammonia	49	25	67.08	65.74	70.21	1677.00	1643.50	1755.25	1691.9
Urea	5	25	401.43	406.70	391.67	10035.71	10167.48	9791.77	9998.3
N						6353.64	6381.54	6318.21	6351.1
PO4	4	25	1.38	1.31	1.34	105.48	100.19	103.02	102.9
K						444.00			444.0

Final hydrolyzed urine results										
	Dilution		Gallery measurement (mg L^{-1})			Concentration (mg L^{-1})			Average	Adjustment factor
	Gallery	Manual								
Ammonia	49	25	21.56	21.84	22.66	826.33	837.06	868.49	843.96	
Urea	5	25	222.26	272.07	283.50	8518.37	10427.44	10865.78	9937.20	
N						4795.89	5696.25	5931.94	5474.69	0.65
PO4	4	25	0.93	0.94	0.97	108.70	110.11	114.46	111.09	
K						411.76			411.76	

Recovery (%)				
				Average
N	75.48	89.26	93.89	86.21
P	103.06	109.91	111.10	108.02
K	92.74			92.74

$Ca(OH)_2$ stabilized synthetic urine

Initial $Ca(OH)_2$ stabilized urine results									
	Dilution		Gallery measurement (mg L^{-1})			Concentration (mg L^{-1})			Average
	Gallery	Manual							
Ammonia	14	25	17.10	15.90	15.84	427.50	397.50	395.97	406.99
Urea	5	25	487.71	493.07	506.21	12192.84	12326.70	12655.35	12391.63
N						6109.36	6141.74	6293.36	6181.49
PO4	4	25	0.22	0.21	0.21	16.48	16.02	15.79	16.10
K			19.13	20.17	18.88	478.13	504.22	471.88	484.74

Final $Ca(OH)_2$ stabilized urine results										
	Dilution		Gallery measurement (mg L^{-1})			Concentration (mg L^{-1})			Average	Adjustment factor
	Gallery	Manual								
Ammonia	14	25	0.02	0.00	0.00	0.61	0.00	0.00	0.20	
Urea	5	25	384.96	391.00	395.60	11679.87	11863.21	12002.78	11848.62	
N						5443.42	5528.26	5593.30	5521.66	0.82
PO4	4	25	0.20	0.20	0.20	18.79	18.79	18.23	18.61	
K	-	25	15.96	15.71	17.12	484.28	476.58	519.29	493.39	

Recovery (%)				
				Average
N	89.10	90.01	88.88	89.33
P	114.02	117.30	115.47	115.60
K	101.29	94.52	110.05	101.95

MgO stabilized synthetic urine

Initial MgO stabilized urine results									
	Dilution		Gallery measurement (mg L^{-1})			Concentration (mg L^{-1})			Average
	Gallery	Manual							
Ammonia	14	30	13.50	13.68	13.50	405.00	410.40	405.00	406.80
Urea	5	30	355.16	366.68	363.85	10654.83	11000.39	10915.50	10856.91
N						5370.15	5536.58	5491.62	5466.12
PO4	4	30	0.17	0.19	0.18	15.45	17.20	16.93	16.53
K	-	25	18.73	20.38	18.98	468.30	509.43	474.55	484.09

Final MgO stabilized urine results										
	Dilution		Gallery measurement (mg L^{-1})			Concentration (mg L^{-1})			Average	Adjustment factor
	Gallery	Manual								
Ammonia	14	25	1.72	0.98	0.65	49.40	28.15	18.67	32.07	
Urea	5	25	402.07	391.75	398.41	11547.80	11251.49	11442.79	11414.03	
N						5430.68	5271.34	5351.01	5351.01	0.87
PO4	10	30	0.12	0.16	0.14	13.10	17.12	14.37	15.75	
K	-	25	18.26	18.17	18.11	524.45	521.86	520.14	522.15	

Recovery (%)				
				Average
N	101.13	95.21	97.44	97.93
P	84.80	99.53	84.91	89.74
K	111.99	102.44	109.61	108.01

Acetic acid stabilized synthetic urine

Initial acetic acid stabilized urine results									
	Dilution		Gallery measurement (mg L^{-1})			Concentration (mg L^{-1})			Average
	Gallery	Manual							
Ammonia	14	25	16.16	16.85	16.77	404.00	421.13	419.25	414.79
Urea	5	25	415.48	432.92	435.34	10386.95	10822.90	10883.47	10697.77
N						5244.32	5464.60	5490.95	5399.95
PO4	4	25	3.12	3.28	3.32	239.01	251.43	254.19	248.21
K		1			444.00			444.00	444.00

Final acetic acid stabilized urine results										
	Dilution		Gallery measurement (mg L^{-1})			Concentration (mg L^{-1})			Average	Adjustment factor
	Gallery	Manual								
Ammonia	14	25	14.54	15.20	13.99	380.67	397.82	366.14	381.55	
Urea	5	25	432.96	420.85	415.81	11335.34	11018.32	10886.49	11080.05	
N						5662.94	5532.36	5439.25	5544.85	0.95
PO4	4	25	2.62	2.58	2.55	210.40	206.87	204.78	207.35	
K								411.00	411.00	

Recovery (%)				
				Average
N	107.98	101.24	99.06	102.76
P	88.03	82.28	80.56	83.63
K			92.57	92.57

Citric acid stabilized synthetic urine

Initial citric acid stabilized urine results									
	Dilution		Gallery measurement (mg L^{-1})			Concentration (mg L^{-1})			Average
	Gallery	Manual							
Ammonia	14	25	17.64	18.11	17.92	441.00	452.75	448.00	447.25
Urea	5	25	462.59	468.49	464.30	11564.72	11712.13	11607.45	11628.10
N						5830.16	5910.60	5857.07	5865.95
PO4	4	25	3.24	3.08	3.22	248.51	235.87	246.44	243.61
K			444.00			444.00			444.00

Final citric acid stabilized urine results										
	Dilution		Gallery measurement (mg L^{-1})			Concentration (mg L^{-1})			Average	Adjustment factor
	Gallery	Manual								
Ammonia	14	25	15.42	15.89	16.37	399.02	411.18	423.61	411.27	
Urea	8	25	403.61	428.14	431.49	10444.15	11078.92	11165.71	10896.26	
N						5265.99	5573.96	5626.83	5488.93	0.97
PO4	8	25	2.88	2.91	3.02	228.27	230.81	239.93	233.00	
K		1	411.00			425.42			425.42	

Recovery (%)				
				Average
N	90.32	94.30	96.07	93.57
P	91.85	97.86	97.36	95.69
K	95.81			95.81

Fresh human urine

Initial fresh urine results									
	Dilution		Gallery measurement (mg L^{-1})			Concentration (mg L^{-1})			Average
	Gallery	Manual							
Ammonia	14	25	9.59	9.59	9.80	239.75	239.75	245.00	241.50
Urea	5	25	360.56	360.56	366.17	9013.99	9013.99	9154.15	9060.71
N						4440.27	4440.27	4510.83	4463.79
PO4	2	25	4.37	4.37	4.91	334.67	334.67	376.53	348.62
K	-	20	51.50	51.50	51.50	1030.00	1030.00	1030.00	1030.00

Final fresh urine results										
	Dilution		Gallery measurement (mg L^{-1})			Concentration (mg L^{-1})			Average	Adjustment factor
	Gallery	Manual								
Ammonia	4	25	1.07	2.05	1.75	26.84	51.17	43.70	40.57	1.00
Urea	1	50	185.76	186.64	344.25	9287.84	9331.95	8606.32	9075.37	
N						4354.98	4399.86	4054.24	4269.69	
PO4	2	30	3.87	3.35	4.27	355.78	308.07	392.52	352.12	
K	0	30	38.18	39.03	37.70	1145.40	1170.78	1131.09	1149.09	

Recovery (%)				
				Average
N	98.08	99.09	89.88	95.68
P	106.31	92.05	104.25	100.87
K	111.20	113.67	109.81	111.56

Hydrolyzed human urine

Initial hydrolyzed human urine results									
	Dilution		Gallery measurement (mg L^{-1})			Concentration (mg L^{-1})			Average
	Gallery	Manual							
Ammonia	35	100	35.14	30.24	32.35	3514.00	3024.00	3235.00	3257.67
Urea	5	25	223.86	239.29	233.36	5596.56	5982.21	5834.01	5804.26
N						6122.00	5811.71	5953.65	5962.45
PO4	2	33	3.34	3.20	3.11	337.45	323.28	314.88	325.20
K	-	22	46.30			1018.60			1018.60

Final hydrolyzed human urine results										
	Dilution		Gallery measurement (mg L^{-1})			Concentration (mg L^{-1})			Average	Adjustment factor
	Gallery	Manual								
Ammonia	4	25	6.17	7.00	7.00	258.85	293.88	293.88	282.20	
Urea	1	25	4.74	10.62	6.71	198.86	445.73	281.63	308.74	
N						351.52	501.58	425.11	426.07	0.60
PO4	2	25	2.35	2.55	2.47	302.82	328.24	317.71	316.26	
K	-	20	32.93			1105.84			1105.84	

Recovery (%)				
				Average
N	5.74	8.63	7.14	7.17
P	89.74	101.53	100.90	97.39
K	108.56			108.56

$Ca(OH)_2$ stabilized human urine

Initial $Ca(OH)_2$ stabilized urine results									
	Dilution		Gallery measurement (mg L^{-1})			Concentration (mg L^{-1})			Average
	Gallery	Manual							
Ammonia	14	25	8.69	7.84	7.96	217.25	196.00	199.00	204.08
Urea	5	25	427.02	426.73	440.26	10675.55	10668.37	11006.46	10783.46
N						5192.06	5167.46	5328.01	5229.18
PO4	-	25	0.11	0.11	0.10	8.28	8.13	7.97	8.13
K	-	20	62.60	62.60	62.60	1252.00	1252.00	1252.00	1252.00

Final $Ca(OH)_2$ stabilized urine results										
	Dilution		Gallery measurement (mg L^{-1})			Concentration (mg L^{-1})			Average	Adjustment factor
	Gallery	Manual								
Ammonia	14	25	1.23	0.48	0.93	52.78	20.37	40.04	37.73	
Urea	5	25	250.56	295.30	305.44	10735.01	12651.51	13086.26	12157.59	
N						5055.29	5915.97	6138.24	5703.17	0.58
PO4	-	30	0.05	0.04	0.05	7.94	6.69	8.32	7.65	
K									1172.79	

Recovery (%)				
				Average
N	97.37	114.48	115.21	109.02
P	95.96	82.34	104.33	94.21
K	93.67			93.67

Average experimental recovery and standard deviation results

Recoveries, average and standard deviation for graphs in report															
Urine	**Fresh (S)**			**Average**	**STD**	**Hydrolyzed (S)**			**Average**	**STD**	**$Ca(OH)_2$ stabilized (S)**			**Average**	**STD**
N	90.69	93.57	93.92	92.73	1.45	75.48	89.26	93.89	86.21	7.82	89.10	90.01	88.88	89.33	0.49
P	92.15	87.81	95.36	91.77	3.09	103.06	109.91	111.10	108.02	3.54	114.02	117.30	115.47	115.60	1.34
K	110.46			110.46	0.00	92.74			92.74	0.00	101.29	94.52	110.05	101.95	6.36

Recoveries, average and standard deviation for graphs in report continued															
Urine	**MgO stabilized (S)**			**Average**	**STD**	**Acetic acid stabilized (S)**			**Average**	**STD**	**Citric acid stabilized (S)**			**Average**	**STD**
N	101.13	95.21	97.44	97.93	2.44	107.98	101.24	99.06	102.76	3.80	90.32	94.30	96.07	93.57	2.40
P	84.80	99.53	84.91	89.74	6.92	88.03	82.28	80.56	83.63	3.19	91.85	97.86	97.36	95.69	2.72
K	111.99	102.44	109.61	108.01	4.06			92.57	92.57	0.00	95.81			95.81	0.00

Recoveries, average and standard deviation for graphs in report continued															
Urine	**Fresh (H)**			**Average**	**STD**	**Hydrolyzed (H)**			**Average**	**STD**	**Ca(OH)2 stabilized (H)**			**Average**	**STD**
N	98.08	99.09	89.88	95.68	4.13	5.74	8.63	7.14	7.17	1.18	97.37	114.48	115.21	109.02	8.25
P	106.31	92.05	104.25	100.87	6.29	89.74	101.53	100.90	97.39	5.42	95.96	82.34	104.33	94.21	9.06
K	111.20	113.67	109.81	111.56	1.59	108.56			108.56	0.00	93.67			93.67	0.00

Theoretical recoveries from OLI

Synthetic urine solution	Initial concentration (g L^{-1})					Final concentration (g L^{-1})					Recovery (%)		
	Ammonia	Urea	N	P	K	Ammonia	Urea	N	P	K	N	P	K
Fresh	0.4362	11.6259	5.8539	0.1265	0.4690	0.0144	10.1242	4.7323	0.1259	0.4676	80.8404	99.5060	99.7000
Hydrolyzed			5.9640	0.1265	0.4690			5.7876	0.1259	0.4682	97.0423	99.5060	99.8350
$Ca(OH)_2$ stabilized	0.4362	11.6259	5.8539	0.0000	0.4690	0.0000	9.5624	5.7876	0.0000	0.4683	98.8680	100.0000	99.8469
MgO stabilized	0.4362	11.6259	5.8539	0.0001	0.4690	0.3555	10.9505	5.4585	0.0001	0.4650	93.2453	100.0000	99.1441
Acetic acid stabilized	0.4362	11.6259	5.8539	0.1265	0.4690	0.3793	9.8857	4.9860	0.1239	0.4358	85.1745	97.9053	92.9217
Citric acid stabilized	0.4362	11.6259	5.8539	0.1265	0.4690	0.4044	10.6348	5.3602	0.1248	0.4388	91.5666	98.6104	93.5635

Real urine solution	Initial concentration (g L^{-1})					Final concentration (g L^{-1})					Recovery (%)		
	Ammonia	Urea	N	P	K	Ammonia	Urea	N	P	K	N	P	K
Fresh	0.24162	10.976	5.3564	0.25327	1.321	0.24085	10.9523	5.3446	0.25212	1.31952	99.7793	99.5432	99.8880
Hydrolyzed			5.82572	0.16168	1.321			5.72736	0.16168	1.3205	98.3116	100.0000	99.9621
$Ca(OH)_2$ stabilized	0.41621	10.976	5.5310	1.72E-12	1.321	0.0000	10.8754	5.0679	1.72E-12	1.32096	91.6274	100.0000	99.9970

NPK sample of pH data

Sample of NPK pH data for the first 6 hours of data collection for both synthetic and human urine solutions

Time (h)	Synthetic urine solutions pH					
	Fresh	**Hydrolyzed**	**$Ca(OH)_2$**	**MgO**	**Acetic acid**	**Citric acid**
0.00	6.35	8.46	12.50	10.28	3.00	3.08
0.17	6.31	8.48	12.59	10.23	3.02	3.11
0.33	6.31	8.50	12.56	10.22	3.02	3.13
0.50	6.32	8.48	12.54	10.26	3.03	3.14
0.67	6.32	8.45	12.51	10.25	3.03	3.15
0.83	6.32	8.42	12.49	10.23	3.03	3.16
1.00	6.32	8.39	12.46	10.21	3.03	3.16
1.17	6.32	8.36	12.45	10.20	3.04	3.16
1.33	6.32	8.32	12.42	10.18	3.04	3.16
1.50	6.32	8.29	12.40	10.16	3.05	3.16
1.67	6.32	8.25	12.37	10.13	3.05	3.16
1.83	6.32	8.22	12.34	10.11	3.04	3.16
2.00	6.32	8.19	12.30	10.09	3.05	3.16
2.17	6.32	8.16	12.26	10.07	3.05	3.16
2.33	6.32	8.13	12.21	10.04	3.05	3.16
2.50	6.32	8.12	12.17	10.01	3.05	3.17
2.67	6.32	8.10	12.13	9.98	3.05	3.17
2.83	6.32	8.09	12.08	9.96	3.05	3.17
3.00	6.32	8.08	12.01	9.94	3.05	3.17
3.17	6.31	8.07	11.99	9.92	3.06	3.17
3.33	6.31	8.06	12.01	9.91	3.06	3.17
3.50	6.31	8.05	12.01	9.88	3.06	3.17
3.67	6.31	8.04	12.00	9.85	3.06	3.16
3.83	6.31	8.03	12.01	9.83	3.06	3.16
4.00	6.31	8.01	12.01	9.81	3.06	3.17
4.17	6.31	8.01	12.01	9.79	3.06	3.17
4.33	6.31	8.00	12.03	9.79	3.06	3.17
4.50	6.31	7.99	12.03	9.78	3.06	3.16
4.67	6.31	7.97	12.03	9.74	3.06	3.16
4.83	6.31	7.97	12.02	9.70	3.07	3.16
5.00	6.31	7.96	12.03	9.67	3.07	3.16
5.17	6.31	7.95	12.01	9.63	3.07	3.16
5.33	6.31	7.94	11.98	9.60	3.07	3.16
5.50	6.31	7.93	11.97	9.59	3.07	3.16
5.67	6.31	7.92	11.96	9.56	3.07	3.16
5.83	6.31	7.92	11.96	9.54	3.07	3.16
6.00	6.31	7.91	11.94	9.52	3.07	3.16

Time (h)	Human urine solutions pH		
	Fresh	Hydrolyzed	$Ca(OH)_2$
0.00	6.88	9.01	12.33
0.17	6.85	9.03	12.23
0.33	6.88	9.00	12.11
0.50	6.90	8.95	12.07
0.67	6.92	8.89	12.11
0.83	6.94	8.81	12.10
1.00	6.95	8.74	12.08
1.17	6.96	8.67	12.08
1.33	6.98	8.67	12.09
1.50	6.99	8.64	12.10
1.67	7.00	8.60	12.10
1.83	7.02	8.50	12.10
2.00	7.03	8.47	12.09
2.17	7.04	8.43	12.09
2.33	7.05	8.37	12.08
2.50	7.06	8.36	12.08
2.67	7.06	8.33	12.08
2.83	7.07	8.29	12.08
3.00	7.07	8.24	12.07
3.17	7.08	8.20	12.07
3.33	7.08	8.19	12.07
3.50	7.09	8.17	12.06
3.67	7.09	8.16	12.05
3.83	7.10	8.15	12.04
4.00	7.10	8.13	12.05
4.17	7.10	8.12	12.04
4.33	7.10	8.11	12.03
4.50	7.10	8.10	12.02
4.67	7.10	8.09	12.02
4.83	7.10	8.09	12.01
5.00	7.10	8.09	12.01
5.17	7.10	8.08	12.01
5.33	7.09	8.07	12.02
5.50	7.09	8.07	12.02
5.67	7.09	8.06	12.02
5.83	7.09	8.06	12.03
6.00	7.08	8.06	12.03

Appendix D: Water removal and solids raw data

Effect of water removal on solids formed- OLI and experimental comparison raw data

50% water removal

Initial stabilized urine composition

Sample conditions		**Synthetic stabilized urine**						
Temperature	23.6							
ion	**units**	**Gallery dilution**	**Manual dilution**	**1**	**2**	**3**	**Average**	**Concentration (mg/L)**
Ammonia	mg N/l	14	30	14.1	13.9	14.0	14.0	419.6
Urea (ammonia)	mg urea/l	5	30	429.5	432.2	430.9	430.9	12926.1
	mg N/l	-	-	200.1	201.4	200.8	200.8	6023.5
Urea	mg Urea/l	-	-	399.3	402.4	400.9	400.9	12025.7
SO4	mg SO4/l	-	30	26.4	23.4	24.9	24.9	748.2
PO4	mg PO4/l	4	30	0.1	0.1	0.1	0.1	3.2
							0.1	9.8
K	mg/l	-	30					444.0
Cl	mg/l	1	25	193.5	192.3	192.9	192.9	4822.1
Ca	mg/l	-	25	59	56.8	57.9	57.9	1447.6
Mg	mg/l	4	1	15.7	13.8	14.7	14.7	17.7

Final solid phase composition

Sample conditions		Solids formed after evaporating Ca(OH)2 stabilized urine, testing using acid digestion method												
Temperature	22.4													
ion	**units**	**Gallery dilution**	**Manual dilution**	**1**	**0.856502644**	**2**	**0.892318788**	**3**	**0.292372063**	**Average**	**C1: Concentration in solids solution (mg/L)**	**V1: Volume remaining solution (mL)**	**V2: Volume of initial solution (mL)**	**C2: Concentration in initial solution (mg/L)**
Ammonia	mg/l	14	25	0.0	0.0	0.0	0.0	0	0.0	0.0	0.0	450.91	1000.00	0.00
Urea (ammonia)	mg urea/l	1	25	7.1	207.2	6.9	193.0	7.025	196.8	199.0	199.0	450.91	1000.00	89.73
	mg N/l			3.3	0.0	3.2	90.0	3.3	0.0	30.0	30.0	450.91	1000.00	13.52
Urea	mg Urea/l			7.1	0.0	6.9	193.0	7.0	0.0	64.3	64.3	450.91	1000.00	29.01
SO4	mg SO4/l	6	1	9.2	10.7	7.3	8.2	7.939	8.9	9.2	9.2	450.91	1000.00	4.17
PO4	mg PO4/l	4	30	0.0	0.0	0.0	0.0	0	0.0	0.0	0.0	450.91	1000.00	0.00
			25								0.0	450.91	1000.00	0.00
K	mg/l	10	1	18.1	21.1	18.2	20.4	18.06	20.2	20.6	20.6	450.91	1000.00	9.28
Cl	mg/l	4	25	294.0	8582.6	290.8	8147.0	298.3	8357.4	8362.3	8362.3	450.91	1000.00	149.66
Ca	mg/l	4	1	344.9	402.7	432.6	484.8	90.59444444	309.9	399.1	399.1	450.91	1000.00	179.97
Mg	mg/l	1	1	4.0	5.6	5.3	7.2	0.22	0.9	6.4	6.4	450.91	1000.00	2.87

Experimental solids

		1	2	3	
Initial mass	Petri dish	24.0573	24.1275	24.8433	
	Filter paper	0.0666	0.0673	0.0675	
	Tray	**1**	**2**	**3**	
Before drying	Initial mass	**222.35**	**278.8**	**278.34**	
	Full tray	644.2	754.66	731.3	
	Emptied tray	225.92	283.79	284.72	
	Filter paper and Petri dish	25.5517	26.27435	25.6565	
After drying	Emptied tray	222.83	279.61	279.71	
	Filter paper and Petri dish	24.7596	24.7713	25.0943	
Solids formed	FP	0.6357	0.5765	0.1835	
	Tray	0.48	0.81	1.37	
	Total	1.1157	1.3865	1.5535	1.3519
	Water removed	56%	50%	53%	53%
	OLI experimental solids	1.00	0.91	0.94	0.95

75% water removal

Initial stabilized urine composition

Sample conditions		**Synthetic stabilized urine**						
Temperature	20.2							
Measured pH	6.33							
stabilized pH	12.51							
ion	**units**	**Gallery dilution**	**Manual dilution**	**1**	**2**	**3**	**Average**	**Concentration (mg/L)**
Ammonia	mg N/l	14	30	13.2	13.0		13.1	393.8
Urea (ammonia)	mg urea/l	5	30	399.4	394.6		397.0	11909.8
	mg N/l	-	-	186.1	183.9	0.0	123.3	5550.0
Urea	mg Urea/l	-	-	371.0	366.6	0.0	245.9	11064.9
SO4	mg SO4/l	-	25	32.3			32.3	808.3
PO4	mg PO4/l	4	30	0.2	0.2		0.2	6.4
							0.2	19.7
K	mg/l	-	30	38.2	39.5		16.9	444.0
Cl	mg/l	1	25	204.4	204.4		204.4	5110.1
Ca	mg/l	-	25	56.2	60.3		58.2	1456.0
Mg	mg/l	4	1	9.5	9.9		9.7	11.6

Final solids composition

Temperature	22.4	Solids formed after evaporating Ca(OH)2 stabilized urine, testing using acid digestion method						
ion	units	Gallery dilution	Manual dilution	1	2	3	Average	Concentration from mixed solution (mg/L)
Ammonia	mg/l	4	25	0.1	0.1	0.21	0.1	2.8
Urea (ammonia)	mg urea/l	5	25	15.1	14.9	13.05	14.4	358.9
	mg N/l			7.0	7.0	6.1	6.7	6.7
Urea	mg Urea/l			15.0	14.8	12.6	14.1	14.1
SO4	mg SO4/l	2	1	50.9	52.3	51.06	51.4	51.4
PO4	mg PO4/l	1	25	0.1	0.1	0.065	0.1	2.4
			25				0.1	7.3
K	mg/l	10	1	22.1	22.1	25.62	23.3	23.3
Cl	mg/l	3	25	265.9	266.0	267.58	266.5	79.1
Ca	mg/l	1	25	21.8	22.3	20.54	21.6	539.0
Mg	mg/l	1	1	6.1	7.5	6.83	6.8	6.8

Experimental solids

		1	2	3	
Initial mass	Petri dish	-	-	-	
	Filter paper	-	-	-	
	Tray	**1**	**2**	**3**	
Before drying	Initial mass	**222.43**	**279.11**	**278.88**	
	Emptied tray	272.57	308.89	319.12	
After drying	Emptied tray	224.5	281.1	280.49	
Solids formed	Tray	2.07	1.99	1.61	
	Total	1.479	1.346	1.072	1.298996
	Water removed	71.4%	67.6%	66.6%	69%
	OLI experimental solids	1.60	1.29968	1.20	1.37

100% water removal

Initial stabilized urine composition

Sample conditions		Synthetic stabilized urine						
Temperature	20.2							
Measured pH	6.33							
stabilized pH	12.51							
ion	**units**	**Gallery dilution**	**Manual dilution**	**1**	**2**	**3**	**Average**	**Concentration (mg/L)**
Ammonia	mg N/l	14	25	30.8	28.6	28.5	16.3	407.0
Urea (ammonia)	mg urea/l	5	25	524.4	527.2	540.2	530.6	13265.0
	mg N/l	-	-	244.4	245.7	251.7	247.3	6181.5
Urea	mg Urea/l	-	-	458.4	465.8	479.0	467.7	12391.6
SO4	mg SO4/l	-	25	34.8	33.4	33.1	33.8	844.1
PO4	mg PO4/l	4	25	0.2	0.2	0.2	0.2	5.3
							0.2	16.1
K	mg/l	-	25	30.6	32.3	30.2	19.4	444.0
Cl	mg/l	1	25	201.9	205.9	198.4	202.1	5051.3
Ca	mg/l	-	30	51.5	51.3	49.2	50.6	1519.1
Mg	mg/l	4	1	7.0	6.9	6.4	6.8	8.1

Final stabilized urine solids composition

Sample conditions		Solids formed after evaporating Ca(OH)2 stabilized urine, testing using acid digestion method						
Temperature	23.6							
ion	**units**	**Gallery dilution**	**Manual dilution**	**1**	**2**	**3**	**Average**	**Concentration from mixed solution (mg/L)**
Ammonia	mg/l	14	25	0.0	0.0	0.0	0.0	0.2
Urea (ammonia)	mg urea/l	5	25	385.0	391.0	395.6	390.5	9763.3
	mg N/l			179.4	182.2	184.3	182.0	4549.7
Urea	mg Urea/l			385.0	391.0	395.6	390.5	9763.0
SO4	mg SO4/l	4	25	22.4	24.4	23.1	23.3	582.9
PO4	mg PO4/l	4	25	0.2	0.2	0.2	0.2	4.9
							0.2	15.1
K	mg/l	-	25	16.0	15.7	17.9	16.5	412.9
Cl	mg/l	4	25	463.5	465.3	472.8	467.2	4437.8
Ca	mg/l	-	25	52.5	49.5	49.2	50.4	1259.9
Mg	mg/l	4	1	8.3	6.5	6.9	7.2	7.2

Ion	Measured AD results mg/L	Adjusted AD results mg/L
Ammonia	0.2	0.2
Urea	9763.3	11849.1
SO4	582.9	707.4
PO4	15.1	18.3
K	412.9	501.2
Cl	4437.8	5385.9
Ca	1259.9	1529.1
Mg	7.2	8.8
Na	1908.8	2316.5

Experimental solids

		1	2	3	
Initial mass	Petri dish	-	-	-	
	Filter paper	-	-	-	
	Tray	**1**	**2**	**3**	
Before drying	Initial mass	**222.833**	**279.35**	**278.92**	
	Emptied tray	244.86	301.88	301.95	
After drying	Emptied tray	244.86	301.88	301.95	
Solids formed	Tray	22.027	22.53	23.03	
	Total	21.51445	21.99377	22.4697	21.99264
	Water removed	97.7%	97.6%	97.6%	98%
	OLI experimental solids	18.81	18.81	18.81	18.81

Raw mass data recorded over time for 50%, 75% and 100% water removal from $Ca(OH)_2$ stabilized urine solutions

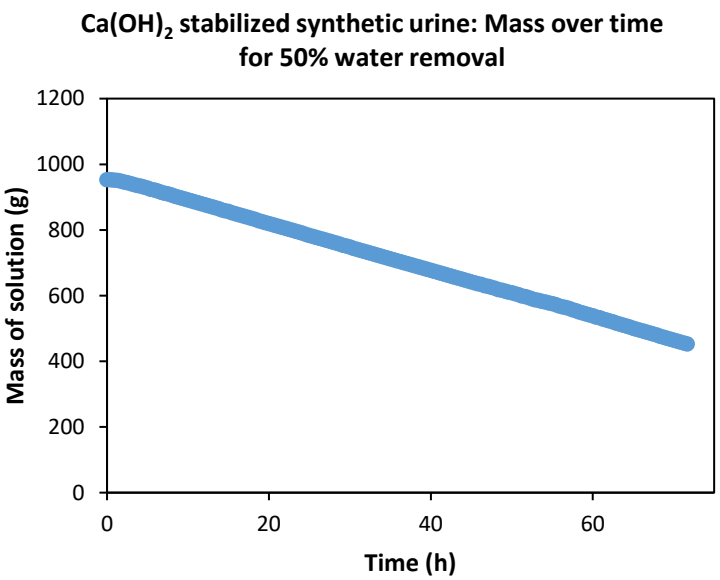

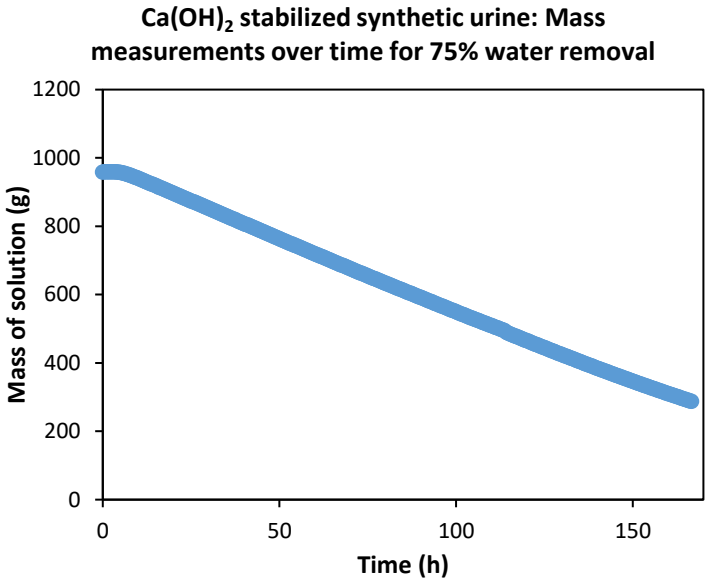

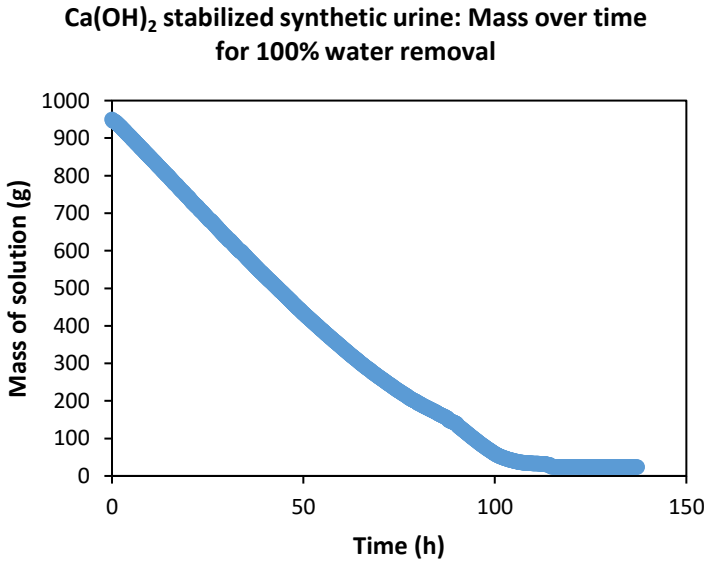

pH data collected for 100% water removal

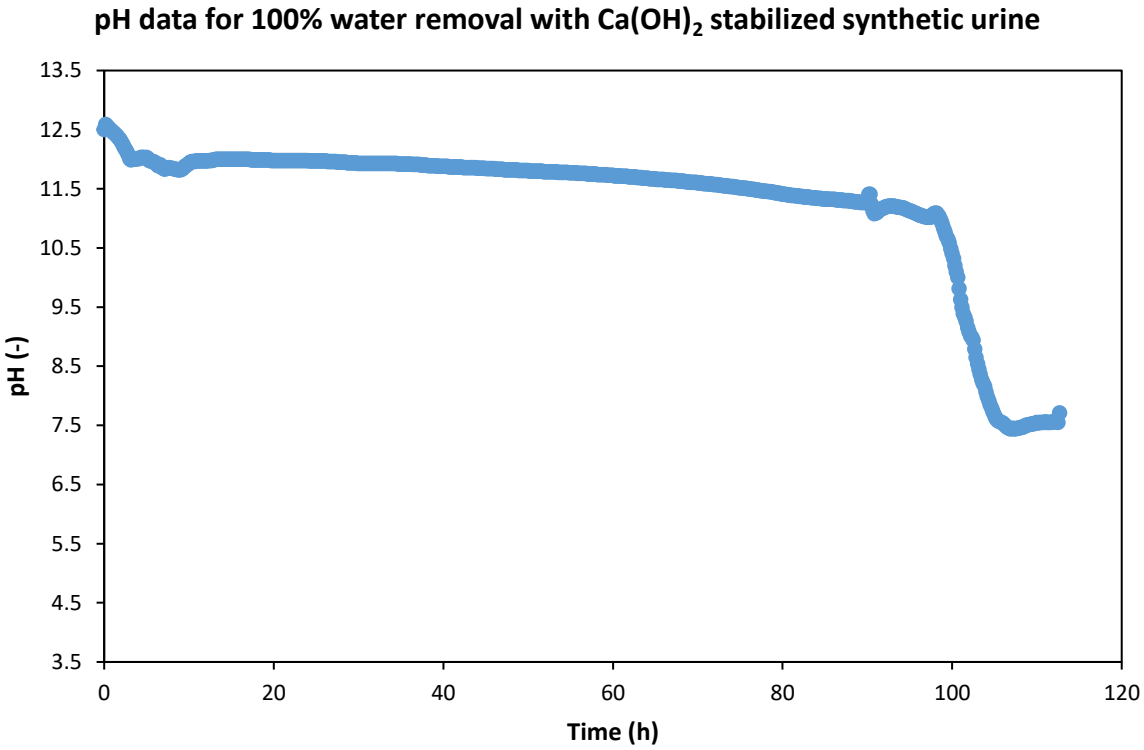

OLI raw data for 50%, 75% and 100% water removal

Water removal %	Solid g
100	18.8058
90	2.3043
80	1.81716
75	1.60255
70	1.39863
60	1.05714
50	0.905639
40	0.756269
30	0.608659
20	0.462522
10	0.317633
0	0.173814

OLI recovery in solids (%)			
Water removal (%)	**N**	**P**	**K**
50	0	0	0
75	0	19	0
100	92.55168	98	99

Appendix E: Urea hydrolysis raw data

Urea hydrolysis raw OLI data

Water removal	40°C		50 °C		60 °C		70°C	
	Urea mass by phase							
	Liquid	Solid	Liquid	Solid	Liquid	Solid	Liquid	Solid
%	g	g	g	g	g	g	g	g
100.0	0.000	10.000	0.000	10.000	0.000	10.000	0.000	10.000
100.0	0.156	9.844	0.192	9.808	0.241	9.759	0.308	9.692
100.0	0.311	9.689	0.385	9.615	0.483	9.517	0.617	9.383
100.0	0.467	9.533	0.577	9.423	0.724	9.276	0.925	9.075
100.0	0.622	9.378	0.770	9.230	0.965	9.035	1.234	8.766
100.0	0.778	9.222	0.962	9.038	1.207	8.793	1.542	8.458
99.9	0.933	9.067	1.155	8.845	1.448	8.552	1.851	8.149
99.9	1.089	8.911	1.347	8.653	1.690	8.311	2.159	7.841
99.9	1.244	8.756	1.540	8.460	1.931	8.069	2.468	7.532
99.9	1.400	8.600	1.732	8.268	2.172	7.828	2.776	7.224
99.9	1.555	8.445	1.925	8.075	2.414	7.586	3.085	6.915
99.9	1.711	8.289	2.117	7.883	2.655	7.345	3.393	6.607
99.9	1.866	8.134	2.310	7.690	2.896	7.104	3.701	6.299
99.9	2.022	7.978	2.502	7.498	3.138	6.862	4.010	5.990
99.9	2.177	7.823	2.694	7.306	3.379	6.621	4.318	5.682
99.9	2.333	7.667	2.887	7.113	3.620	6.380	4.627	5.373
99.8	2.488	7.512	3.079	6.921	3.862	6.138	4.935	5.065
99.8	2.644	7.356	3.272	6.728	4.103	5.897	5.244	4.756
99.8	2.800	7.201	3.464	6.536	4.344	5.656	5.552	4.448
99.8	2.955	7.045	3.657	6.343	4.586	5.414	5.861	4.139
99.8	3.111	6.889	3.849	6.151	4.827	5.173	6.169	3.831
99.8	3.266	6.734	4.042	5.958	5.068	4.932	6.478	3.522
99.8	3.422	6.578	4.234	5.766	5.310	4.690	6.786	3.214
99.8	3.577	6.423	4.427	5.573	5.551	4.449	7.094	2.906
99.8	3.733	6.267	4.619	5.381	5.793	4.207	7.403	2.597
99.8	3.888	6.112	4.812	5.188	6.034	3.966	7.711	2.289
99.7	4.044	5.956	5.004	4.996	6.275	3.725	8.020	1.980
99.7	4.199	5.801	5.196	4.804	6.517	3.483	8.328	1.672
99.7	4.355	5.645	5.389	4.611	6.758	3.242	8.637	1.363
99.7	4.510	5.490	5.581	4.419	6.999	3.001	8.945	1.055
99.7	4.666	5.334	5.774	4.226	7.241	2.759	9.254	0.746
99.7	4.821	5.179	5.966	4.034	7.482	2.518	9.562	0.438
99.7	4.977	5.023	6.159	3.841	7.723	2.277	9.871	0.129
99.7	5.132	4.868	6.351	3.649	7.965	2.035	10.000	0.000
99.7	5.288	4.712	6.544	3.456	8.206	1.794	10.000	0.000
99.7	5.443	4.557	6.736	3.264	8.447	1.553	10.000	0.000
99.6	5.599	4.401	6.929	3.071	8.689	1.311	10.000	0.000
99.6	5.755	4.245	7.121	2.879	8.930	1.070	10.000	0.000
99.6	5.910	4.090	7.314	2.686	9.172	0.828	10.000	0.000
99.6	6.066	3.934	7.506	2.494	9.413	0.587	10.000	0.000

99.6	6.221	3.779	7.698	2.302	9.654	0.346	10.000	0.000
99.6	6.377	3.623	7.891	2.109	9.896	0.104	10.000	0.000
99.6	6.532	3.468	8.083	1.917	10.000	0.000	10.000	0.000
99.6	6.688	3.312	8.276	1.724	10.000	0.000	10.000	0.000
99.6	6.843	3.157	8.468	1.532	10.000	0.000	10.000	0.000
99.6	6.999	3.001	8.661	1.339	10.000	0.000	10.000	0.000
99.5	7.154	2.846	8.853	1.147	10.000	0.000	10.000	0.000
99.5	7.310	2.690	9.046	0.954	10.000	0.000	10.000	0.000
99.5	7.465	2.535	9.238	0.762	10.000	0.000	10.000	0.000
99.5	7.621	2.379	9.431	0.569	10.000	0.000	10.000	0.000
99.5	7.776	2.224	9.623	0.377	10.000	0.000	10.000	0.000
99.5	7.932	2.068	9.816	0.184	10.000	0.000	10.000	0.000
99.5	8.087	1.913	10.000	0.000	10.000	0.000	10.000	0.000
99.5	8.243	1.757	10.000	0.000	10.000	0.000	10.000	0.000
99.5	8.398	1.602	10.000	0.000	10.000	0.000	10.000	0.000
99.5	8.554	1.446	10.000	0.000	10.000	0.000	10.000	0.000
99.4	8.710	1.290	10.000	0.000	10.000	0.000	10.000	0.000
99.4	8.865	1.135	10.000	0.000	10.000	0.000	10.000	0.000
99.4	9.021	0.979	10.000	0.000	10.000	0.000	10.000	0.000
99.4	9.176	0.824	10.000	0.000	10.000	0.000	10.000	0.000
99.4	9.332	0.668	10.000	0.000	10.000	0.000	10.000	0.000
99.4	9.487	0.513	10.000	0.000	10.000	0.000	10.000	0.000
99.4	9.643	0.357	10.000	0.000	10.000	0.000	10.000	0.000
99.4	9.798	0.202	10.000	0.000	10.000	0.000	10.000	0.000
99.4	9.954	0.046	10.000	0.000	10.000	0.000	10.000	0.000
99.4	10.000	0.000	10.000	0.000	10.000	0.000	10.000	0.000
99.3	10.000	0.000	10.000	0.000	10.000	0.000	10.000	0.000
99.3	10.000	0.000	10.000	0.000	10.000	0.000	10.000	0.000
99.3	10.000	0.000	10.000	0.000	10.000	0.000	10.000	0.000
99.3	10.000	0.000	10.000	0.000	10.000	0.000	10.000	0.000
99.3	10.000	0.000	10.000	0.000	10.000	0.000	10.000	0.000
99.3	10.000	0.000	10.000	0.000	10.000	0.000	10.000	0.000
99.3	10.000	0.000	10.000	0.000	10.000	0.000	10.000	0.000
99.3	10.000	0.000	10.000	0.000	10.000	0.000	10.000	0.000
99.3	10.000	0.000	10.000	0.000	10.000	0.000	10.000	0.000
99.3	10.000	0.000	10.000	0.000	10.000	0.000	10.000	0.000
99.2	10.000	0.000	10.000	0.000	10.000	0.000	10.000	0.000
99.2	10.000	0.000	10.000	0.000	10.000	0.000	10.000	0.000
99.2	10.000	0.000	10.000	0.000	10.000	0.000	10.000	0.000
99.2	10.000	0.000	10.000	0.000	10.000	0.000	10.000	0.000
99.2	10.000	0.000	10.000	0.000	10.000	0.000	10.000	0.000
99.2	10.000	0.000	10.000	0.000	10.000	0.000	10.000	0.000
99.2	10.000	0.000	10.000	0.000	10.000	0.000	10.000	0.000
99.2	10.000	0.000	10.000	0.000	10.000	0.000	10.000	0.000
99.2	10.000	0.000	10.000	0.000	10.000	0.000	10.000	0.000
99.2	10.000	0.000	10.000	0.000	10.000	0.000	10.000	0.000
99.1	10.000	0.000	10.000	0.000	10.000	0.000	10.000	0.000

99.1	10.000	0.000	10.000	0.000	10.000	0.000	10.000	0.000
99.1	10.000	0.000	10.000	0.000	10.000	0.000	10.000	0.000
99.1	10.000	0.000	10.000	0.000	10.000	0.000	10.000	0.000
99.1	10.000	0.000	10.000	0.000	10.000	0.000	10.000	0.000
99.1	10.000	0.000	10.000	0.000	10.000	0.000	10.000	0.000
99.1	10.000	0.000	10.000	0.000	10.000	0.000	10.000	0.000
99.1	10.000	0.000	10.000	0.000	10.000	0.000	10.000	0.000
99.1	10.000	0.000	10.000	0.000	10.000	0.000	10.000	0.000
99.1	10.000	0.000	10.000	0.000	10.000	0.000	10.000	0.000
99.0	10.000	0.000	10.000	0.000	10.000	0.000	10.000	0.000
99.0	10.000	0.000	10.000	0.000	10.000	0.000	10.000	0.000
99.0	10.000	0.000	10.000	0.000	10.000	0.000	10.000	0.000
99.0	10.000	0.000	10.000	0.000	10.000	0.000	10.000	0.000
99.0	10.000	0.000	10.000	0.000	10.000	0.000	10.000	0.000

Urea hydrolysis raw experimental data

40°C

Before evaporation				
Tray	**Mass tray (g)**	**Mass urea added (g)**	**Mass tray and solution (g)**	**Mass solution (g)**
1	12.45	10.001	511.85	499.4
2	12.35	10.0033	511.89	499.54
3	12.32	10.0092	512.99	500.67
Average urea added (g)			10.0045	

After evaporation			
Tray	**Initial mass of tray (g)**	**Remaining mass (g)**	**Remaining urea (g)**
1	12.45	22.5	10.05
2	12.35	22.41	10.06
3	12.32	22.39	10.07
Mass (g)			10.06
Average remaining urea for experiment (%)			100.55%

50°C

Before evaporation				
Tray	**Mass of tray (g)**	**Mass urea added (g)**	**Mass tray (g)**	**Mass solution (g)**
1	12.41	10.0038	513.01	500.6
2	12.35	10.0044	512.21	499.86
3	12.31	10.0061	512.6	500.29
Average urea added (g)		10.0048		

After evaporation			
Tray	**Initial mass of tray (g)**	**Remaining mass (g)**	**Remaining urea (g)**
1	12.41	22.375	9.965
2	12.35	22.315	9.965
3	12.31	22.29	9.98
Mass (g)			9.970
Average remaining urea for experiment (%)			99.65%

60°C

Before evaporation				
Tray	**Mass of tray (g)**	**Mass urea added (g)**	**Mass tray (g)**	**Mass solution (g)**
1	12.415	10.002	512.715	500.3
2	12.39	10.0035	512.555	500.165
3	12.32	10.0028	512.715	500.395
Average urea added			10.0028	

After evaporation			
Tray	**Initial mass of tray (g)**	**Remaining mass (g)**	**Remaining urea (g)**
1	12.415	22.29	9.875
2	12.39	22.22	9.83
3	12.32	22.18	9.86
Mass (g)			9.855
Average remaining urea for experiment (%)			98.52%

70°C

Before evaporation				
Tray	**Mass of tray (g)**	**Mass urea added (g)**	**Mass tray (g)**	**Mass solution (g)**
1	12.415	10.0064	512.34	499.925
2	12.38	10.0117	512.18	499.8
3	12.35	10.0089	512.3	499.95
Average urea added		10.0090		

After evaporation			
Tray	**Initial mass of tray (g)**	**Remaining mass (g)**	**Remaining urea (g)**
1	12.415	22.04	9.625
2	12.38	21.53	9.15
3	12.35	21.68	9.33
Mass (g)			9.3683
Average remaining urea for experiment (%)			93.60%

Urea hydrolysis rate raw experimental data

40°C

Before evaporation				
Tray	**Mass of tray (g)**	**Mass urea added (g)**	**Mass tray (g)**	**Mass solution (g)**
1	12.54	9.9992	512.75	500.21
2	12.41	10.008	512.41	500
3	12.58	10.0084	512	499.42
Average urea added (g)		10.0052		

After evaporation				
Tray	**Initial mass of tray (g)**		**Remaining mass (g)**	**Remaining urea (g)**
1	12.54		22.5	9.96
2	12.41		22.47	10.06
3	12.58		22.65	10.07
Average remaining urea for experiment			**Mass (g)**	10.03
			%	100.25%

Sample of raw mass data for 40°C urea hydrolysis rate experiment

Measurement				
Id	Date	Time (h)	Mass	Mass adjusted
3673	######	0.00	511.56	499.02
3674	######	0.17	511.42	498.88
3675	######	0.33	511.17	498.63
3676	######	0.50	510.41	497.87
3677	######	0.67	509.38	496.84
3678	######	0.83	508.12	495.58
3679	######	1.00	506.88	494.34
3680	######	1.17	505.54	493.00
3681	######	1.33	504.28	491.74
3682	######	1.50	502.7	490.16
3683	######	1.67	501.24	488.70
3684	######	1.83	500.02	487.48
3685	######	2.00	498.65	486.11

70°C

Before evaporation				
Tray	**Mass of tray (g)**	**Mass urea added (g)**	**Mass tray (g)**	**Mass solution (g)**
1	12.54	10.0071	512.62	500.08
2	12.41	10.0108	511.6	499.19
3	12.62	10.0109	512.52	499.9
Average urea added (g)		10.0096		

After evaporation				
Tray	**Initial mass of tray (g)**		**Remaining mass (g)**	**Remaining urea (g)**
1	12.54		21.58	9.04
2	12.41		21.65	9.24
3	12.62		21.93	9.31
Average remaining urea for experiment			**Mass (g)**	9.196667
			%	91.88%

Sample of raw mass data for 70°C urea hydrolysis rate experiment

Measurement					
Id	Date		Mass		Unit
4363	2020.11.17 09:07:08 .811	0.00	514.56	502.02	g
4364	2020.11.17 09:17:08 .820	0.17	514.36	501.82	g
4365	2020.11.17 09:27:08 .821	0.33	520.02	507.48	g
4366	2020.11.17 09:37:08 .822	0.50	523.35	510.81	g
4367	2020.11.17 09:47:08 .826	0.67	520.83	508.29	g
4368	2020.11.17 09:57:08 .842	0.83	519.12	506.58	g
4369	2020.11.17 10:07:08 .824	1.00	516.44	503.90	g
4370	2020.11.17 10:17:08 .825	1.17	513.85	501.31	g
4371	2020.11.17 10:27:08 .825	1.33	512.24	499.70	g
4372	2020.11.17 10:37:08 .827	1.50	509.76	497.22	g
4373	2020.11.17 10:47:08 .828	1.67	507.12	494.58	g
4374	2020.11.17 10:57:08 .839	1.83	503.79	491.25	g